UNIVERSITY OF SOUTHAMPTON

FACULTY OF NATURAL AND ENVIRONMENTAL SCIENCES

Institute for Life Sciences
Centre for Biological Sciences

Fcγ receptors and immune complex-mediated inflammation in age-related macular degeneration

by

Salomé Murinello, BSc

Thesis for the degree of Doctor of Philosophy

February 2014

UNIVERSITY OF SOUTHAMPTON

ABSTRACT

FACULTY OF NATURAL AND ENVIRONMENTAL SCIENCES, INSTITUTE FOR LIFE SCIENCES, CENTRE FOR BIOLOGICAL SCIENCES

Doctor of Philosophy

Fcγ RECEPTORS AND IMMUNE COMPLEX-MEDIATED INFLAMMATION IN AGE-RELATED MACULAR DEGENERATION

Salomé Magalhães Cardoso Murinello

Age-related macular degeneration (AMD) is the leading cause of irreversible blindness in the developed world, but the mechanisms leading to AMD are poorly understood. Circulating retinal autoantibodies and antibody deposits in the retina are associated with AMD but despite this relationship, immune complex (IC)-mediated responses and underlying mechanisms of inflammation in the retina have not been characterised. IgG antibodies can activate immune effector function through formation of IC and their interaction with Fcγ receptors (FcγR) expressed by immune cells. This study aims to test the hypothesis that IC formed in the retina induce an inflammatory response following interaction with activating FcγRs expressed on microglia and/or macrophages, which may contribute to the pathogenesis of AMD.

To study the biological effect of IC formation in the retina a model of IC injury was developed and fully characterised. The involvement of mouse FcγRs (mFcγRs) was first studied using Fc gamma chain deficient ($\gamma^{-/-}$) mice, lacking cellular expression of activating mFcγRs, and further characterised using *FcγRI*$^{-/-}$, *FcγRIII*$^{-/-}$ and *FcγRIV*$^{-/-}$ mice. The presence of IC and human FcγR (hFcγR) expression was investigated in human donor eyes from early and wet AMD patients and healthy controls. Finally the effect of inflammatory mediators on human retinal pigmented epithelium (RPE) function was investigated by direct stimulation with cytokines or indirect stimulation using conditioned medium of polarised human macrophages.

IC deposition in the mouse retina led to an inflammatory response that depended on the presence of activating mFcγRs, particularly mFcγRI and mFcγRIII, but not on mFcγRIV. Immune complex deposition and increased numbers of immune cells expressing hFcγRIIa and hFcγRIIb were found in the choroid of early AMD donors and microglia in the retina of wet AMD donor eyes. Finally, macrophage activation differentially impacted on RPE cell function, with regards to barrier function and VEGF secretion.

The results in this thesis support the hypothesis that immune complex-mediated inflammation could play a role in the pathogenesis of AMD.

Table of Contents

List of tables

List of figures

DECLARATION OF AUTHORSHIP

I, Salome Murinello

declare that this thesis and the work presented in it are my own and has been generated by me as the result of my own original research.

Fcγ receptors and immune complex-mediated inflammation in age-related macular degeneration

I confirm that:

1. This work was done wholly or mainly while in candidature for a research degree at this University;
2. Where any part of this thesis has previously been submitted for a degree or any other qualification at this University or any other institution, this has been clearly stated;
3. Where I have consulted the published work of others, this is always clearly attributed;
4. Where I have quoted from the work of others, the source is always given. With the exception of such quotations, this thesis is entirely my own work;
5. I have acknowledged all main sources of help;
6. Where the thesis is based on work done by myself jointly with others, I have made clear exactly what was done by others and what I have contributed myself;
7. Parts of this work have been published as:

Murinello, S., Mullins, R.F., Lotery, A.J., Perry, V.H., Teeling, J.L. Fcγ receptor upregulation is associated with immune complex inflammation in the mouse retina and early age-related macular degeneration. *Invest Ophthalmol Vis Sci*. 2014

Signed:.....

Date:.....

Acknowledgements

I would like to thank my supervisors, Jessica Teeling, Hugh Perry and Andrew Lotery, for the excellent supervision and for all the guidance and support throughout the development of the present work and my career as a young investigator.

I would like to give a big thank you to Rob Mullins, who very kindly welcomed me in his lab and has since been very helpful with interpretation of the human data in this thesis. I would like to thank Steve Booth for the excellent technical support and assistance with intravitreous injections but also for the good humour and the awful musical taste; Heather Thomson for answering countless questions on ARPE19 cell culture and for the great advice this past year; all of the BRF staff, in particular Miriam Atkinson, Mike Broome and Leslie Lawes who have been extremely helpful and have taken excellent care of all the mice used in these experiments; Steve Beers for kindly providing human macrophages and clodronate liposomes; Lehk Dahal for isolating and preparing the human macrophages used in Chapter 6; Aditi Khanna and Miles Flamme-Wiese for technical support in Iowa and for cutting the human sections used in this thesis and all those in level D who have at some point helped me with experimental issues, in particular Jenny Scott, Maureen Gatherer and Steph Smith. I would also like to thank Angela Cree and Lorraine Williams for making sure everything always ran smoothly.

Thanks to all of those who have helped me through the very emotional journey that has been my PhD. The two other members of the early morning coffee triad, Olivia now Dr. Larsson and Ursula Puentener; past and present members of the CNS inflammation group, in particular, Adam Hart, James Fuller, Nash Matinyarare, Matt Davies, Diego Gomez-Nicola and Patrick Garland for the friendship and Friday night drinks; past and present members of the Vision Sciences group and colleagues from B85. Thanks also to Neil Smyth who has provided constant guidance and support throughout my undergraduate and postgraduate studies. Thank you also to my family and friends who have always made their best to support me, despite the distance.

Finally, a big thank you to Fight for Sight for sponsoring my PhD and for the personal interest they have taken in my progression. It has been a wonderful experience!

Definitions and Abbreviations

ACAID	Anterior chamber associated immune deviation
ADCC	Antibody dependent cell cytotoxicity
AGEs	Advanced glycation end products
AHA	Autoimmune haemolytic anaemia
AMD	Age-related macular degeneration
APC	Antigen presenting cell
APES	3'Aminopropyltriethoxysilane
ApoE	Apolipoprotein E
ATCC	American Tissue Culture Collection
BBB	Blood retina barrier
BCR	B-cell receptor
BLamD	Basal laminar deposits
BLinD	Basal linear deposits
BRB	Blood retina barrier
BrM	Bruch's membrane
BSA	Bovine serum albumin
C1r	Protease R
C1s	Protease S
Calu3	Cultured Human Airway Epithelial Cells
CCL	Chemokine (C-C motif) ligand
CD	Cluster of differentiation

CEP	Carboxyethylpyrrole
CFH	Complement factor H
cGMP	Cyclic guanosine monophosphate
CNS	Central nervous system
CNV	Choroidal neovascularisation
CNVM	Choroidal neovascular membrane
CR1	Complement receptor 1
CRP	C-reactive protein
CX3CL1	C-X3-C motif ligand 1
CX3CR1	C-X3-C motif receptor 1
DAPI	4’,6-diamidine2-phenylindole
DC	Dendritic cell
DHA	Docosahexaenoic acid
DMEM	Dulbecco’s modified Eagle’s medium
DMSO	Dimethyl sulfoxide
DNA	Deoxyribonucleic acid
dNTP	Deoxyribonucleotide triphosphate
ERG	Electroretinogram
ERK	Extracellular signal-regulated kinases
FasL	Fas Ligand
FBS	Foetal bovine serum
FcRs	Fc receptors

FcγRs	Fcγ receptors
FDA	Food and Drug Administration
GA	Geographic atrophy
GAPDH	Glyceraldehyde-3-phosphate dehydrogenase
GCL	Ganglion cell layer
G-CSF	Granulocyte colony-stimulating factor
GFAP	Glial fibrillary acidic protein
GoI	Gene of interest
GPI	Glycophosphatidylinositol
GST	glutathione S-transferase
HAR	Hyperacute rejection
HBSS	Hanks' Balanced Salt solution
HLA	Human leukocyte antigen
HO-1	haeme oxygenase 1
HAS	Human serum albumin
HUVEC	Human umbilical vein endothelial cell
i.p.	Intraperitoneal
IC	Immune complex
IFN	Interferon
IgG	Immunoglobulin G
IL	Interleukin
IL1-RA	Interleukin 1 receptor antagonist

INL	Inner nuclear layer
iNOS	Inducible nitric oxide synthase
IPL	Inner plexiform layer
ITAM	Immunoreceptor tyrosine-based activation motif
ITIM	Immunoreceptor tyrosine-based inhibitory motif
LPS	Lipopolysaccharide
mAb	Monoclonal antibody
MAC	Membrane-attack complex
MACRO	Macrophage receptor with collagenous domain
MASP	MBL- associated serinase protease
MBL	Mannose-binding lectin
MHC	Major histocompatibility complex
MIP	Macrophage inflammatory protein
MMP	Metalloproteinase
MPGN	Membranoproliferative glomerulonephritis
MR	Mannose receptor
MSA	Mouse serum albumin
MΦ	Macrophage
NE	Neutrophil elastase
NFL	Nerve fibre layer
NK	Natural killer
NKT	Natural killer T

NO	Nitric oxide
Nrf2	Nuclear factor erythoid 2-related factor 2
OCT	Optimal cutting temperature
OD	Optic disk
ONL	Outer nuclear layer
OPL	Outer plexiform layer
OVA	Ovalbumin
PBS	Phosphate buffered saline
PCR	Polymerase chain reaction
PDE	Phosphodiesterase
PEDF	Pigmented epithelium derived factor
PFA	Paraformaldehyde
PGE_2	Prostaglandin E2
PIP2	Phosphatidylinositol 4,5-bisphosphate
PIP3	Phosphatidylinositol (3,4,5)-trisphosphate
PKC	Protein kinase C
PLC	Phospholipase C
POS	Photoreceptor outer segments
PR	Photoreceptors
PTP	Protein tyrosine phosphatase
PTX3	Pentraxin 3
RAP	Retinal angiomatous proliferation

RG	Reference gene
RNA	Ribonucleic acid
ROS	Reactive oxygen species
RPE	Retinal pigmented epithelium
RT	Real time
SERPING1	Serpin peptidase, clade G (C1 inhibitor) 1
SH	Src homology domain-2
SHIP	SG2 domain containing inositol phosphate
SHP	Src-homology-2-domain-containing protein tyrosine phosphatase
SLAM	Signalling lymphocyte activation molecule
SLE	Systemic Lupus Erythematous
SOD1	Superoxide dismutase
SR	Subretinal space
SRA	Scavenger receptor A
TEER	Transepithelial electrical resistance
TGF	Tumour growth factor
TIMP3	Tissue inhibitor of metalloproteinases-3
TLR	Toll-like receptor
TMB	3,3’,5,5’–Tetramethylbenzidine
TMB	3,3',5,5'-tetramethylbenzidine
TNF	Tumour necrosis factor
Txnrd1	thioredoxin-1 reductase

UEA	Ulex Europaeus Agglutinin 1
VCAID	Vitreous chamber associated immune deviation
VEGF	Vascular endothelial growth factor
VEGFR	Vascular endothelial growth factor receptor
ZAP	Zeta-chain-associated protein kinase
ZO	Zonula occludens

Chapter 1:

Introduction

1.1 General Introduction

Vision has evolved as a vital function for most animals. The eye, an organ that is central to vision, is an extremely specialised and complex organ, allowing vision to be shaped to an animal's needs. Remarkably there are several species-specific specialisations of the eye which are adapted to a species way of life.[1] The human retina, for example, contains a specialised area, the macula, which allows for high acuity vision. Without the macula, tasks such as recognising faces or reading would not be possible.[2] The human eye has thus evolved to facilitate basic human behaviours such as social interactions and learning through reading.[2] Despite the notable adaptations of the eye allowing us to see our surroundings in detail, visual function can be greatly decreased with age.

Age-related macular degeneration (AMD) is a serious condition leading to loss of central vision, most commonly in the elderly and affecting 25 million people worldwide.[3] In spite of this, existent therapies for this disease are only effective in less than 10% of all cases of AMD and a lot remains to be understood about the aetiology of this disease.[4] Several risk factors including ageing, family history, smoking and obesity have been associated with the pathogenesis of AMD,[5] but the mechanisms leading to AMD are poorly understood. Ageing, the biggest risk factor for developing AMD, leads to several physiological and structural changes to the body, including the eye,[6] which could contribute to pathogenesis of the disease. In particular, the immune system, which is essential for fighting infections and maintaining homeostasis, undergoes several changes as we age.[7-9] Curiously, exaggerated inflammation has been associated with the development of AMD.[10]

In AMD there are increased levels of circulating autoantibodies and antibody deposits in the retina.[11-16] Antibodies activate immune effector function through interaction with their receptors, Fc receptors, which are expressed by immune cells.[17] The expression of Fc receptors by immune cells of the retina has been previously described.[18] However, antibody-mediated responses in the retina have not been characterised. Understanding the mechanisms by which the retina deals with immune complexes may help understand the contribution of autoantibodies and IgG deposits for AMD pathology. Additionally they may help designing new and/or improved antibody therapies.

1.2 The eye – an extension of the brain

To understand the pathological mechanisms involved in AMD, it is essential to understand how vision is achieved. The process of vision can be coarsely divided into three steps; firstly, the focusing of an image on the retina, secondly, the transduction of light into electrical stimuli (phototransduction) and thirdly, the processing of the electrical stimuli into something that can be perceived as an image. These three steps depend on the optics of the eye, the retina and the brain, respectively.[19] Processing of images in higher centres in the brain is a complex phenomenon which remains incompletely understood and is out of the scope of this thesis and therefore will not be discussed (for a review see T. Pasternak et al[20]). In AMD, degeneration of the retina, and in particular of the photoreceptors, leads to loss of central vision. In this section the anatomy of the eye and the mechanisms involved in vision are discussed with a focus on the retina and phototransduction.

1.2.1 Anatomy of the eye

Integrity of the eye structure is essential to allow appropriate light refraction and, consequently, focusing of images on the retina. Structurally the eye can be seen as a fluid filled sphere enclosed by three layers of tissue (retina, uveal tract and sclera), as illustrated in Figure 1.1. The front of the eye, or anterior chamber, is filled with a clear liquid, the aqueous humour, produced by the cilliary body.[19] Drainage of the aqueous humour occurs by a specialised meshwork of cells that lies at the junction of the iris and the cornea (limbus), the trabecular meshwork. This drainage system is of particular interest as it may allow antigen presenting cells or antigens themselves to escape the eye, otherwise devoid of a lymphatic system.[21-24] About 80% of the volume of the eye is accounted for by the vitreous humour, a similarly clear but viscous fluid that fills the posterior chamber of the eye. The vitreous contributes to appropriate focusing of images in the retina. Apart from maintaining the shape of the eye, it contains hyalocytes, cells of myeloid origin that phagocytose plasma proteins and other debris, keeping the light path clear (for a review see T. Sakamoto et al 2011) [25] . The architecture of the eye, similarly to a camera allows light to pass through and images to be visualised as they are focused on the retina. Defects in the optics of the eye can lead to mild visual disturbances such as myopia, where distant objects appear out of focus. This is due to images not focusing appropriately on the retina.[19]

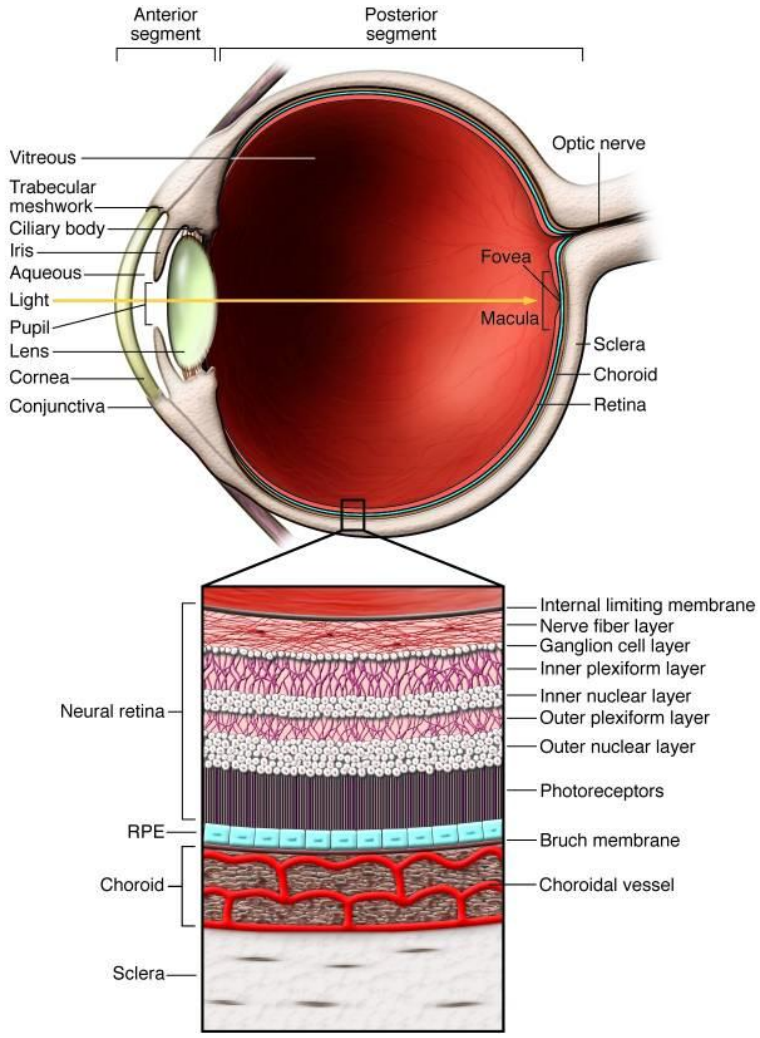

Figure 1.1. Schematic of the human eye.

The innermost layer of the eye, the retina, contains the neurons that are capable of sensing light, translating visual signals into electrical ones and transmitting them to the central targets in the brain. The immediately adjacent layer, the uveal tract, is made up of three layers; the choroid, the cilliary body and the pupil. The choroid is a layer rich in blood vessels and responsible for nourishing the photoreceptors of the retina and the adjacent epithelial cell layer, the retinal pigmented epithelium (RPE). The cilliary body extends from the choroid in the front of the eye. It is a ring of muscle tissue surrounding the lens, important to adjust its refractive power. It also contains a vascular component responsible for the production of the aqueous humour that fills the anterior chamber of the eye. The final component of the uveal tract is the pupil, the aperture at the front of the eye through which light passes. It contains two sets of muscles with opposing actions which allow the size of its aperture to be adjusted under neural control, hence allowing control of the amount of light entering the eye. The outermost tissue layer is made of a tough fibrous white tissue, the sclera. At the front of the eye this layer transforms into the cornea, a specialised transparent tissue that permits light to enter the eye. *Figure from Caspi et al 2010.*[26]

1.2.2 The Retina

The second step of vision, phototransduction, is performed by the retina. The retina is a part of the central nervous system (CNS) that allows us to directly receive information from our surroundings so that within a fraction of a second we can visually assess our environment. Two key aspects of the retina are essential to allow us to see in such impressive short times. First the specialised nature of the neurons of the retina, secondly the spacial organisation of the retinal cells.

1.2.3 Anatomy of the retina

The human retina is approximately 0.5 mm thick and contains six major classes of neurons organised in three nuclear layers and two layers of synaptic connections[27] (Figure 1.2.). Closest to the back of the eye, separating the retina from the choroid blood supply, is the retinal pigmented epithelium (RPE). Just below the RPE, separated by the subretinal space, are the photoreceptors, whose cell bodies are distributed across the outer nuclear layer (ONL). The photoreceptors synapse with bipolar cells, whose cell bodies are distributed across the inner nuclear layer (INL). In turn, the bipolar cells synapse with ganglion cells, distributed across the ganglion cell layer (GCL). The axons of the ganglion cells run along the nerve fibre layer (NFL) and make up the optic nerve in the centre of the retina from where the retinal blood vessels radiate.[27] At the synaptic layers there are laterally extending feedback neurons, the horizontal cells at the photoreceptor-bipolar synapses (outer plexiform layer, OPL) and the amacrine cells at the bipolar-ganglion cell synapses (inner plexiform layer, IPL; Figure 1.2.).

The mammalian retina has two main blood supplies: the blood vessels of the choroid and the major retinal blood vessels (Figure 1.2). The choroid is made up of three capillary layers: the outer capillary layer, closest to the sclera; the medial capillary layer; and the inner capillary layer, closest to the RPE. It receives 80% of the ocular blood flow and it supplies the outer retina. Accordingly, photoreceptor function is highly dependent on the integrity of the choroid. The retinal blood vessels radiate from the optic disc to nourish the inner retina and they receive the remaining 20% of the ocular blood flow. Four major arterial branches at the NFL give rise to three capillary beds: the radial peripapillary capillaries at the NFL, the inner capillaries at the GCL and the outer capillaries that run from the IPL through to the OPL (Figure 1.2).[28]

Photons reaching the eye are sensed by the photoreceptors which convert the light information into an electrical signal which, in turn, is transmitted to bipolar cells and from these, to ganglion cells, whose axons project to higher processing centres in the brain. Horizontal cells integrate and modulate signals from several photoreceptors (through glutamate signalling), and from other horizontal cells (through gap junctions),[29] while amacrine cells integrate and modulate information from bipolar to ganglion cells.[30] It is believed that over 40 different amacrine cell subtypes exist, varying in location and neurotransmitter used and all performing specific roles. This description is a rather simplified portrayal of the extremely complex neuronal circuitry in the retina, for a review see H. Kolb et al 1995.[29]

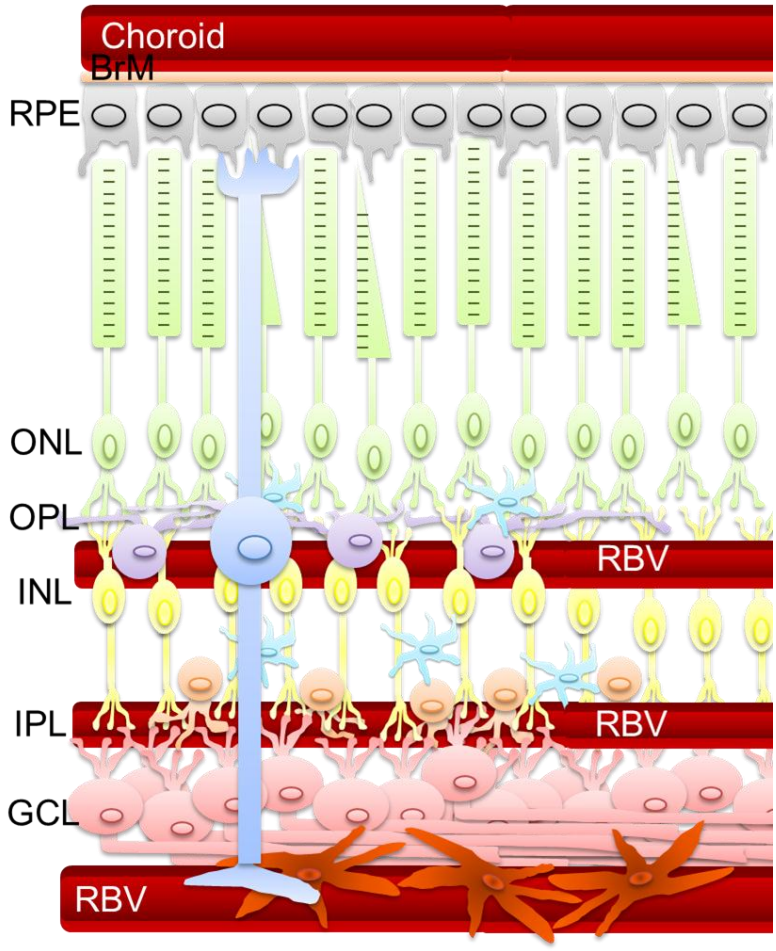

Figure 1.2. Schematic of the retina and its major cell types.
The ganglion cells (pink) lie in the innermost layer in the retina, closest to the vitreous and the front of the eye, while the photoreceptors (green) lie on the outermost layer in the retina, closest to the RPE (gray). The RPE and photoreceptors are separated by the subretinal space. In the outer plexiform layer, horizontal cells (purple) interconnect photoreceptors laterally. In the inner plexiform layer, the different varieties of amacrine cells (light orange) interact to influence and integrate the signals from bipolar to ganglion cells.

The Muller cells (darker blue) stretch across the whole width of the retina and astrocytes (dark orange) reside in the ganglion cell layer. Both Muller cells and astrocytes have processes, endfeet, that ensheath the retinal blood vessels. In the normal retina microglia (light blue) reside in the inner and outer plexiform layers of the retina. The outer retina is supplied by the blood vessels of the choroid, whilst the inner retina is supplied by the retinal blood vessels (RBV). BrM – Bruch's membrane, SR- subretinal space, ONL – outer nuclear layer, OPL – outer plexiform layer, INL – inner nuclear layer, IPL – inner plexiform layer, GCL – ganglion cell layer, RBV- retinal blood vessels.

The retina contains three basic types of glial cells, the Müller cells, astrocytes and microglia (Figure 1.2.). Müller cells are retina-specific glia and perform a variety of functions.[28] These cells stretch radially across the retina, with processes interacting with the RPE and photoreceptors in the outer layers and surrounding the retinal blood vessels (end-feet) in the inner layers. Therefore Müller cells are thought to provide architectural support and also to help maintain the blood-retina-barrier (BRB). In addition, Müller cells serve several homeostatic functions such as supplying end products of anaerobic metabolism to the retina's neurons, maintain microenvironment by "mopping up" waste products (e.g. ammonia) and neurotransmitters (e.g. glutamate, GABA and dopamine), maintain ionic balance by taking up extracellular K^+ ions and recycling glutamate.[28] Astrocytes reside almost exclusively in the nerve fibre layer. They are known to serve similar functions to those of Müller cells in maintaining homeostasis and BRB integrity. In addition to forming vascular sheaths, astrocyte end feet have also been shown to surround axons in the nerve fibre layer, likely contributing to ganglion cell function.[28] Finally, three main types of resident immune cells exist in the retina: microglia, perivascular macrophages and dendritic cells (DCs).[31-34] Microglia are the specialised tissue resident macrophage population of the CNS[35] and are discussed in detail in section 1.2.4.6. Phenotypically perivascular macrophages resemble microglia in their expression of cell-surface molecules such as F4/80 and CD11b, but differ in that they reside in the perivascular space and constitutively express high levels of scavenger receptor class A.[32] Perivascular macrophages likely contribute to the immune privilege of the retina by scavenging debris in the perivascular space.[36] Additionally, these macrophages have been shown to migrate to injury sites in the retina, where they may have a role in the immune response, similar to microglia.[31, 32] Although the presence of DCs in the resting retina is controversial, cells expressing the DC marker CD11c have been shown in the retina in response to injury such as optic nerve crush, light injury[34] and in a model of experimental autoimmune uveitis.[33]

These cells have been shown to quickly migrate to sites of injury but whether they can then migrate to lymphoid organs and/or perform antigen presentation has not been investigated and the function of these cells in the retina remains poorly understood.[33, 34]

1.2.3.1 Photoreceptors and phototransduction

Photoreceptors are specialised neurons of the retina that allow conversion of light into electrical stimuli. There are two types of photoreceptors: rods and cones. Rod photoreceptors are very sensitive and can be activated by a single photon of light, thus they are the photoreceptors allowing for vision in dim-light conditions. Cone photoreceptors are less sensitive to light but are tuned for different wave-lengths, allowing for high acuity colour vision.[1] Bright light conditions are required to activate cones. Accordingly, the retinae of nocturnal animals, such as mice, contain mostly rods. All photoreceptors contain light sensitive pigments which allow the process of phototransduction to occur. The visual pigments consist of a protein moiety, opsin, and a chromophore, 11-cis retinal. Small amino acid differences in the opsin sequence and different chromophores in the photopigment determine the light wave to which it is most sensistive.[27] Most of what is known about the mechanisms of phototransduction has been studied in rod photoreceptors, containing the visual pigment rhodopsin and is summarised in Figure 1.3.[1]

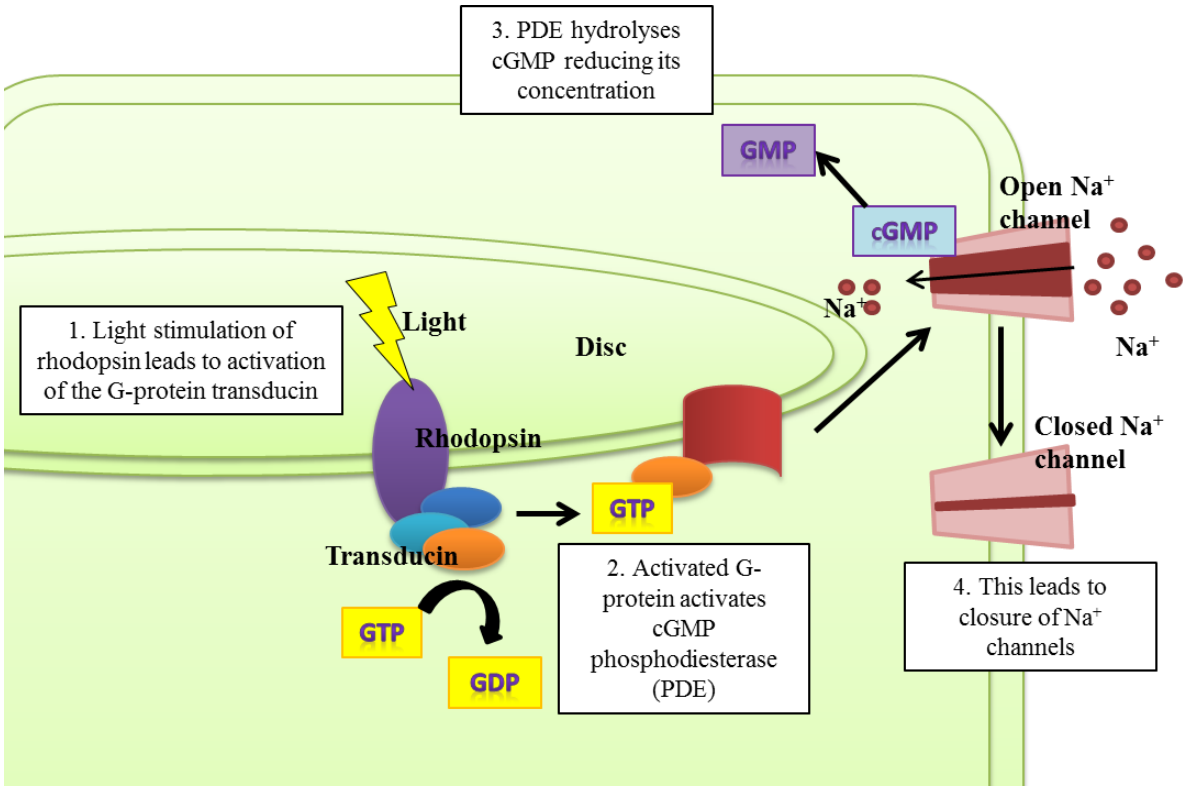

Figure 1.3. Schematic of phototransduction cascade.
In the dark the outer segment of the photoreceptors is depolarised due to influx of Ca^{2+} and Na^{+} ions through guanosine-monophosphate cGMP-gated ion channels. **(1)** As light hits the photoreceptors it causes the chromophore in rhodopsin, 11-cis retinal, to change into all-trans retinal, which in turn causes a conformational change in the protein moiety of rhodopsin. **(2)** This activates a coupled G-protein, transducin which in turn activates cGMP phosphodiesterase (PDE). **(3)** PDE hydrolizes cGMP **(4)** causing the cGMP-gated ion channels to close and hence causing the photoreceptors to hyperpolarise. This hyperpolarisation in turn causes a reduction in glutamate release by the photoreceptors, which is sensed by the bipolar cells.[1] *Modified from Purves D. et al Neuroscience,4th edition.*

The ability to convert light into an electrical stimulus that can then be processed by the brain renders photoreceptors essential for vision, without them vision simply would not be possible. Supporting the important role of photoreceptors in vision are, for example, conditions such as colour blindness, where changes in photoreceptor photopigments lead to disturbed perception of colour, or AMD where loss of photoreceptors leads to blindness.[1]

1.2.3.2 The RPE and the visual cycle

The RPE is a monolayer of polarised melanin-pigmented cells of neuroectoderm origin. The RPE differentiates in parallel with photoreceptors and interactions between the two

have been shown to be crucial for appropriate differentiation of both cell types during development.[37] In the adult retina the RPE performs a plethora of functions (Figure 1.4.), including light absorption, maintaining of the BRB (discussed in section 1.2.4.1), transepithelial transport of ion and nutrients between the choroid and the photoreceptors, maintaining of ionic balance in the subretinal space and secretion of cytokines and growth factors (discussed in section 1.2.4.4). Of particular relevance for understanding vision and how it may be disturbed in AMD, is the role of the RPE in the phagocytosis of photoreceptor outer segments (POS) and the visual cycle.[37]

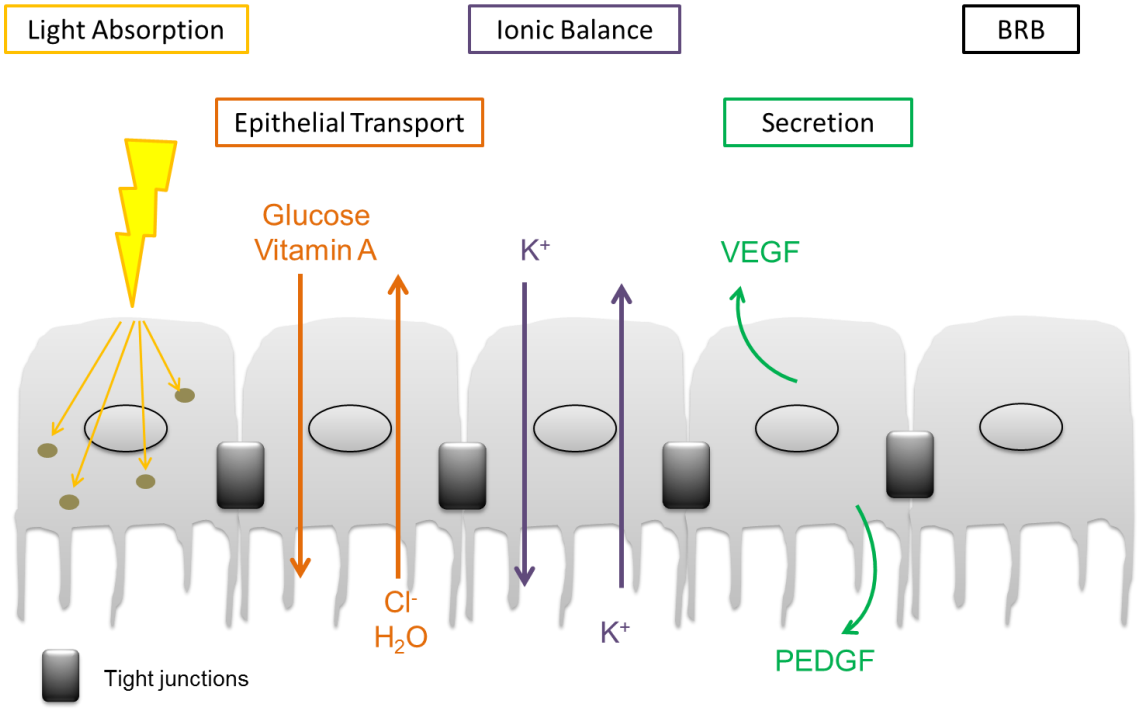

Figure 1.4. Schematic of RPE functions excluding POS phagocytosis and visual cycle.
Light absorption by melanin-containing melanosomes in the RPE reduces photo-oxidative injury to the retina and improves visual function by reducing light scattering. The RPE also plays an important role in allowing the transport of substances such as nutrients and fluids between the photoreceptors and choroid; maintaining the ionic balance in the subretinal space thus allowing appropriate photoreceptor excitability; secreting growth factors essential for homeostasis of the choroid and retina; and maintaining the outer BRB. *Adapted from O. Strauss 2005.*[37]

The light sensitive pigment molecules are contained in the POS, in double membrane structures, the photoreceptor discs. These discs are constantly renewed.[37, 38] Daily 10% of the length of the POS is shed and it is estimated that over a life-time a single RPE cell phagocytoses hundreds of thousands of discs.[38] As new discs are added at the base of the outer segment, old discs move up, are pinched off at the tips and engulfed by

apical processes of the RPE, where they are degraded (Figure 1.5.). In the RPE all-trans retinal is converted to 11-cis-retinal and then shuttled back into the retina, in a process known as the visual cycle.[37] The RPE has been thought of as the only cell type capable of performing the visual cycle. However, recently, it has been found that Müller cells may provide an alternative cone-specific pathway.[39] Nevertheless, the RPE is still accepted as the major cell type involved in the visual cycle. Accordingly, dysfunction of the RPE leads to a depletion of 11-cis-retinal and thus could lead to abnormalities in vision. Further, upon phagocytosis of POS, the RPE can degrade photoreceptor disc material and clear products of the visual cascade, which could otherwise build up in the retina and become toxic. It is clear that the integrity of the RPE is essential for photoreceptor functioning and hence, vision. In fact, it has been proposed that in AMD dysfunction of the RPE leads to build-up of debris, resulting in toxicity and degeneration of the photoreceptors.[40]

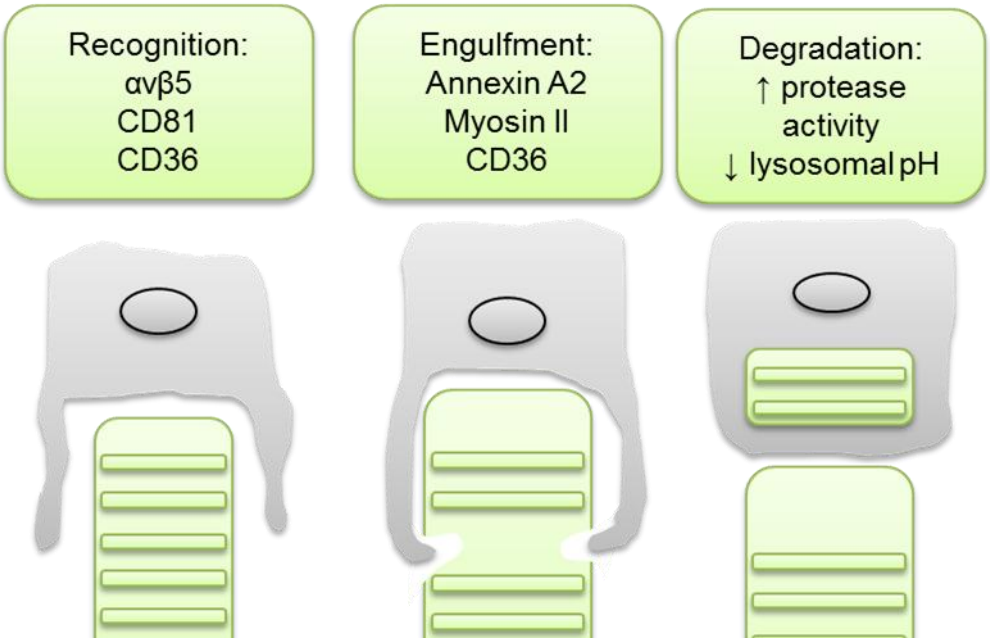

Figure 1.5. Phagocytosis of the photoreceptor discs by the RPE.
Recognition of the photoreceptor is made through the vitronectin receptor αvβ5, CD81 and CD36. The RPE then engulfs the tip of the photoreceptor. This process requires annexin A2, Myosin II and CD36. The tip of the receptor is then pinched off and degraded by in the RPE. Retinal is recycled and shuttled back to the photoreceptors. Photoreceptor disc material is degraded in lysosomes on the basal side of the RPE, closer to the choroid. *Adapted from Kevany B.M. et al 2010*[38]

1.2.3.3 The Macula

The macula is a specialised region responsible for high acuity central vision, which allows us to perform tasks such as reading and object recognition.[27] Therefore, small defects in this area can greatly impair central vision.[2, 27] Damage to the macula occurs in rare genetic disorders such as Best's disease but also in the common disease AMD, affecting one third of individuals aged ≥80 years of age.[41] It is thus important to understand the characteristics of the macula and how these are altered in disease and/or ageing.

In the human retina, the macula is located 4.5-5.5mm to the left of the optic disc. It is 5-6mm in diameter with a 0.35mm depression (the foveola). The foveola is surrounded by an area of 1.5-2.0mm in diameter, the fovea[27] (Figure 1.6.). In the fovea, the ratio of cone to rod photoreceptors is increased (Figure 1.7.). This allows for better colour and detailed light perception. In addition, in this area the neural retina is composed of only photoreceptors and their projections. This specialisation reduces light scattering and increases sensitivity as photons of light can directly reach the photoreceptors and do not need to travel through the whole length of the retina. The lack of retinal blood vessels in this area further reduces light scattering, hence contributing to high acuity vision.[27] Furthermore, throughout the macular region there is an increased concentration of the pigments lutein and zeaxanthin in the RPE. These pigments absorb short-wave-length visible and UV light and hence serve as a protective filter. In addition, these pigments have the potential to act as free radical scavengers, although it has not been confirmed if they act as such in the retina.[27]

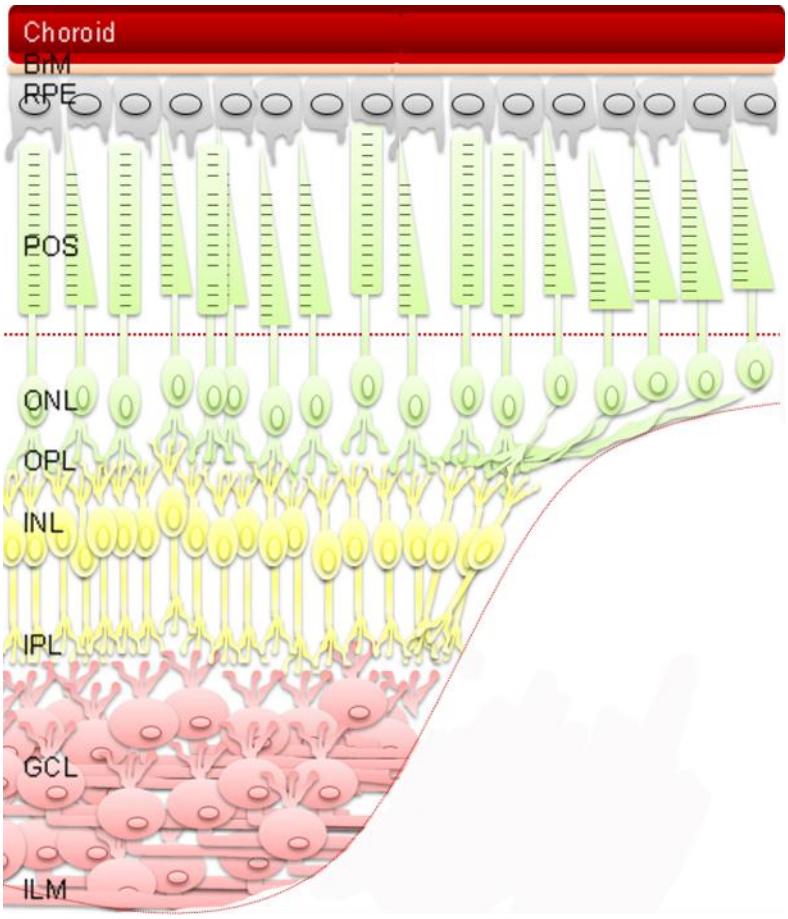

Figure 1.6. Schematic of the macula.

The macula is a specialised area of the retina allowing for sharp central vision. A higher ratio of cone photoreceptors to rod photoreceptors can be seen in the macula. In the central fovea only cone photoreceptor are present. In addition, a decreased ratio of bipolar cells to photoreceptors (allowing better tuning of information from individual photoreceptors) and an increased number of ganglion cells, ensures increased sharpness of the central field of vision. The centre of the macula, the fovea is further specialised and in this area the retina is only composed of photoreceptors, photoreceptor projections (Henle fibre layer) and the inner limiting layer. The central area of the fovea is virtually absent of blood vessels, preventing light scattering.[27] BrM- Bruch's membrane, RPE-retinal pigmented epithelium, POS-photoreceptor outer segments, ONL-outer nuclear layer, OPL-outer plexiform layer, INL- inner nuclear layer, IPL-inner plexiform layer, GCL-ganglion cell layer, ILM-inner limiting membrane.

High acuity vision is essential for our daily lives, where being able to read, recognise faces or drive a vehicle has become indispensable. Although the anatomical features of the macula allow for better vision, some of them may render this area of the retina more susceptible to damage. In particular, the lack of retinal blood vessels makes the macula completely dependent on the choroid for oxygen and nutrient supply.[2] Therefore,

changes to the choroid such as decreased thickness (as seen with age) or damage due to oxidative stress or obesity could severely impact the macula's oxygen supply, possibly contributing to pathogenesis of diseases such as AMD.

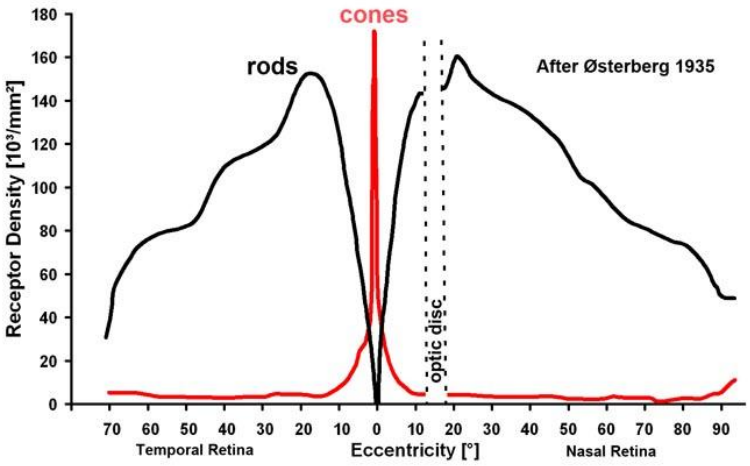

Figure 1.7. Rod and cone photoreceptor density in the human retina.
In most of the human retina the density of rod photoreceptors is 40-150 times higher than that of cone photoreceptors. In the macula, the ratio of cone:rod photoreceptor dramatically changes, as cone density becomes higher than that of rods. In the fovea only cone photoreceptors are present. *Figure from Kolb. H et al 1995.*[2]

1.2.4 The eye's immune system

The eye is an immune privileged site, which is formally described as an organ in which a graft can be introduced without rejection.[21, 37] Immune privilege is achieved by the local environment keeping the local immune system in a quiescent, downregulated state. In organs such as the retina and the brain where there is limited regenerative capacity this can act as a protective mechanism, as inflammation could lead to irreversible bystander damage to neurons.[21] In the retina an intact BRB, a suppressive microenvironment and tight regulation of the complement cascade and microglia all contribute to maintaining of the immune-privilege.

1.2.4.1 Immune privilege in the retina

The identification of the eye as an immune privileged site first came from the studies by Dooremal who showed human tumours grew in the anterior chamber of rabbit eyes.[42] The concept of immune privilege in the eye was then experimentally formalised by

Medawar in the 1950's and expanded by Maumenee who demonstrated the success of orthotopic corneal transplants due to the privileged nature of the cornea. Experiments by Streilen and colleagues showed that immune privilege in the eye was not due to immune ignorance, but due to an active regulation of immunity.[42, 43] In his experiments, he demonstrated that skin and thyroid allografts survived in the anterior chamber of rat eyes. However, the immune system responded to the alloantigens by producing antibodies, while limiting cell-mediated responses against those alloantigens.[22, 42-45] These experiments led to the understanding that, despite the existence of an blood-ocular-barrier[21-24, 42-45] and the lack of lymphatic drainage,[23] antigens could still escape the eye. Although most experiments on immune privilege have used the anterior chamber of the eye, many of the same principles have been demonstrated in the posterior chamber of the eye, including the retina, where allografts also experience prolonged survival.[21, 46] The immune privilege in the retina is maintained by lack of lymphatic drainage,[21, 23] a BRB,[22, 43] and an immunosuppressive microenvironment.[24, 26, 47] Loss of ocular immune privilege, as may occur by breach of the BRB due to infection or age-related changes, can lead to transplant rejection, damaging inflammation and most importantly to auto-immune disease.[26, 48]

1.2.4.2 Blood-Retina-Barrier

The retina has two areas of interaction with the blood circulation, accordingly the BRB is divided in two parts; an inner barrier separating the retina and the retinal blood vessels and an outer barrier separating the retina and the choroid.[23] The two barriers have different properties and it has been suggested that the inner BRB provides an absolute barrier, much like the blood brain barrier (BBB), while the outer BRB provides an educational gate, where the activation state of infiltrating leukocytes is modulated by interaction with soluble (e.g. TGF-β and IL-10) and cell-surface molecules (FasL).[31]

The inner BRB consists of tight junctions between the endothelial cells of the retinal vasculature, the surrounding basement membrane and pericytes.[31, 49, 50] Tight junctions are protein complexes that allow the restriction of solute passage from the blood circulation. In the inner BRB some of the main components of tight junctions are occludin, proteins of the claudin family (particularly claudin-11 and claudin-12), and zonula occludens (ZO)-1, -2 and -3, [51, 52] and breakdown of the BRB is often associated with disrupted tight junctions.[52-55] Pericytes surround blood vessels capillaries. In the

retinal blood vessels pericytes exist in a 1:1 ratio to endothelial cells, contrasting to other blood vessel systems where they exist at a 1:10 ratio.[56] They perform a variety of functions, such as providing structural support for the capillaries, contractile regulation of blood flow and regulation of tight junction protein expression, all of which contribute to maintaining of the inner BRB.[49, 50, 57] The important role of pericytes in the inner BRB is highlighted by the fact that loss of pericytes in diabetic retinopathy,[58] ageing,[59] or genetic depletion[60] leads to destabilisation of the capillaries and break down of the blood barrier.[58-60] In addition to tight junctions and pericytes, the retinal blood vessels are surrounded by a sheath of cellular processes, the *glia limitans*, which separates the blood vessels from the neuronal environment, thus forming a physical barrier between the blood vessels and the neuronal retina.[61] At least four cell types contribute to this sheath: Müller cells, astrocytes, microglia, and some types of amacrine cells.[62]

The blood vessels of the choroid are fenestrated, thus, the outer retina barrier is mostly composed of tight junctions between the RPE, and the BrM. [23, 61] An important component of the outer BRB is the maintenance of an "anti-inflammatory" microenvironment, which restricts activation of infiltrating cells.[31] This is discussed in more detail in section 1.2.4.4. The function of the BRB is highly dependent on integrity of the RPE, blood vessel tight junctions, pericytes and components of the *glia limitans*.[50]

Table 1.1 Summary of differences between the retina's two blood retina barriers

	Outer Barrier	**Inner Barrier**
Blood Supply	Choroid	Retinal blood vessels
Endothelial cells	Fenestrated	Connected by tight junctions
Other components of BRB		Pericytes
	Bruch's Membrane	Blood vessel's basement membrane
	RPE tight junctions	*Glia limitans* ensheathing the blood vessels

The BRB helps maintain the physiological environment of the retina while limiting inflammatory responses by blocking free passage of large molecules such as serum proteins (e.g. albumin and antibodies) and cells (e.g. lymphocytes) into this tissue.[26] However, the BRB is not an absolute barrier and especially under inflammatory

conditions influx of plasma proteins and activated lymphocytes into the retina may not be prevented.[48, 62] In spite of their anatomical differences, it is not yet clear whether the outer and inner BRB respond differently to inflammatory stimuli.[63] Although the BRB limits the risk of inflammatory damage it also limits appropriate development of tolerance against self-retinal antigens. Hence, in situations where the BRB is breached (e.g. due to infection, blood vessel damage or age-related changes) autoimmunity may ensue.[21, 26, 48]

1.2.4.3 Anterior chamber-associated immune deviation (ACAID)

Despite the BRB, it is believed that eye-derived antigens can induce systemic immune deviation, i.e. tolerance. The best studied mechanism by which tolerance to eye-derived antigen is induced is the anterior chamber-associated immune deviation (ACAID), a non-physiological phenomenon. It has been induced in rodents and non-human primates and some authors believe that similar mechanisms may occur in humans to induce tolerance to eye antigens.[21, 44, 48] ACAID refers to the process by which antigenic material; placed on or arising in the anterior chamber of the eye, elicit a deviant form of systemic immunity which includes regulatory T and B lymphocytes (producing non-complement fixing antibodies) in the absence of inflammation.[42, 44] This process appears to be dependent on antigen presentation in the spleen as ACAID cannot be induced in animals lacking a spleen.[22, 44] In addition, if the eye in which foreign antigen has been introduced is removed within 4-5 days of antigen exposure, ACAID is also suppressed. [22, 44] Hence, ACAID is dependent on the presence of an intact spleen and the antigen-bearing eye. When blood is collected 48h after introduction of antigen in the anterior chamber of an animal and injected intravenously into a naive animal, the latter develops ACAID to the original antigen. Analysis of this blood has identified $F4/80^+$ monocytes bearing the antigenic epitopes to be the ACAID-inducing signal. In addition, $F4/80^+$ cells harvested from eyes injected with antigen were able to induce ACAID when injected into naive mice. These cells are thought to then perform antigen presentation in the spleen, leading to the formation of immune suppressive Treg cells[22, 64] (Figure 1.8.). Assuming the process of introducing antigen in the eye (by injection) does not affect the integrity of the blood-ocular barrier, these results imply the presence of a camero-splenic axis[26] for the transfer of immunological information.

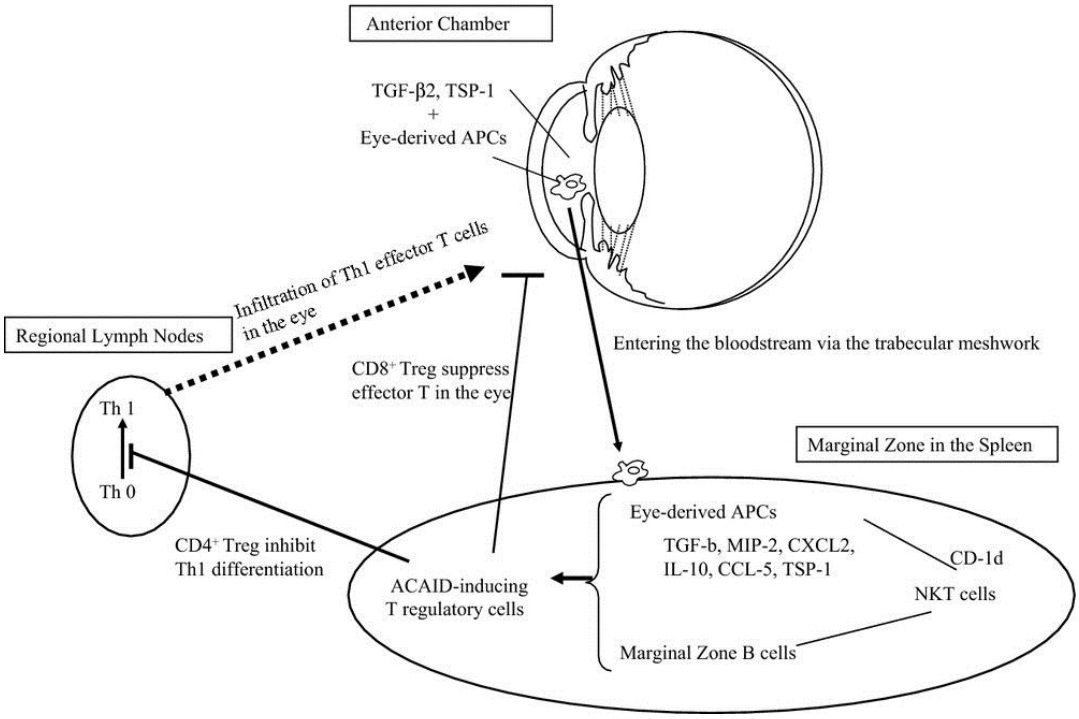

Figure 1.8. Schematic of the mechanisms involved in ACAID.

Antigen-bearing F4/80$^+$ antigen presenting cells (APC) exit the anterior chamber and move to the spleen. Here they recruit natural killer T cells (NKT cells) through a process requiring CD1d and macrophage inflammatory protein 2 (MIP-2) as well as marginal zone B cells. This multicellular process culminates in the induction of CD4$^+$ and CD8$^+$ T regs. CD4$^+$ Treg cells inhibit acquisition of immunity (afferent acting) by inhibiting Th1 cell differentiation, while CD8$^+$ Treg cells suppress expression of immunity (efferent acting) by suppressing effector T cells in the eye. In addition, soluble factors present in the eye, in particular TGF-β, also contribute to induction of ACAID. *Figure from Hori et al 2008*[64]

Although less extensively studied, immune deviation has also been experimentally shown in the posterior chamber.[65-67] It was shown that ovalbumin (OVA) introduced in the subretinal space induced immune deviation. This was, however, dependent on the integrity of the immune privilege of the anterior chamber.[66] A possible explanation for this is that a small fraction of the aqueous humour can be drained through the retina.[23] If immune privilege is removed from the anterior chamber, then molecules and even cells that are normally not allowed in the eye may be in contact with the subretinal space, due to this aqueous humour drainage pathway. The name vitreous chamber associated immune deviation (VCAID) was suggested for this process. VCAID was shown to require NKT cells and not to develop in the presence of inflammation in the eye.[68]

ACAID, VCAID and related phenomena, even if experimental, are of particular interest for eye diseases with an autoimmune component, such as uveitis[26] and possibly AMD, as they represent mechanisms by which eye-derived-antigens can escape the eye and be presented in lymphoid organs, hence leading to the formation of autoantibodies by antigen-specific B cells.

1.2.4.4 Immunosuppressant microenvironment of the eye

Immune privilege in the retina is also maintained via tight control of its microenvironment. Immunosuppressant molecules, such as pigment epithelial-derived factor (PEDF), transforming growth factor-β (TGF-β), α-melanocyte-stimulating hormone and vasoactive intestinal peptide are constitutively expressed in the retina under normal physiological conditions. This keeps the tissue resident macrophages, the microglia, in a downregulated state.[48, 69] The RPE is thought to play an important role in the maintenance of this immunosuppressive environment as it has the capacity to secrete many soluble factors. [47, 70-72] Zamiri et al showed that PEDF secreted by the RPE is able to suppress IL-12 expression while substantially increasing production of IL-10 by LPS-stimulated mouse macrophages *in vitro.* This effect was blocked by neutralizing anti-PEDF antibodies. In addition, PEDF was shown to reduce inflammation *in vivo*. Following intradermal injection of LPS in mouse ears, PEDF was injected intradermally and ear thickness (swelling) was taken as a measure of inflammation. In this study PEDF was shown to substantially reduce the LPS induced swelling of the ear pinae.[71] These results suggest that PEDF, produced by the RPE, has the potential to suppress inflammation.[71] Finally, control of cell-surface molecule expression in the retina and RPE also contributes to maintenance of immune privilege. For example, MHC I and II expression is virtually absent in ocular cells, preventing antigen presentation and consequently T cell activation.[26] In addition, the pro-apoptotic molecule FasL is highly expressed by the RPE. When bound to its receptor, Fas receptor, FasL promotes apoptosis. Fas receptor is expressed, for example, by T cells. In this way, retinal FasL can prevent survival of T cells in this tissue.[48] However, upon insult, expression of these cell-surface molecules, as well as soluble cytokines and growth factors can change, allowing inflammatory responses, antigen-presentation and infiltration of circulating cells into the retina to occur.[69] In addition, age-related changes to the retina and to the

immune system (discussed in 1.3) could similarly lead to changes to the microenvironment, contributing to pathogenesis of AMD.

1.2.4.5 Regulation of the complement system

Evidence of reduced adaptive immunity is widely available, but more recently, regulation of the innate immune system has been implicated in the homeostasis of the retina.[73] The complement system is part of the innate immune system and made up of over 30 proteins in the plasma and on cell surfaces.[74-76] Complement activation results in a proteolytic cascade that can be initiated via three pathways: the classic, lectin or alternative pathway. When complement components are activated they acquire proteolytic activity and are then able to activate the next component in the cascade. The three pathways differ in their initiation and all converge at the generation of C3 convertase. The complement cascade culminates with the formation of membrane-attack complex (MAC;[74-77] Figure 1.9.). In summary, activation of the complement cascade can result in MAC-mediated cell lysis, opsonisation of pathogens, release of anaphylatoxins (C5a/C3a) to recruit inflammatory cells and increased blood vessel permeability.[74-77] While normal function of the complement system is essential for protection of the host against invading organisms, its dysregulation may result in damage to the host and/or disease[74] and hence regulatory mechanism are in place to control complement activation.[74-76] In the healthy eye, the RPE expresses complement inhibitors such as CD55, CD59 and CD46[78] to prevent complement overactivation. Dysregulation of expression of these molecules in the retina, e.g. by genetic predisposition, chronic inflammation or oxidative stress, could lead to overactivation of the complement system, contributing to damage to the retina.[78, 79]

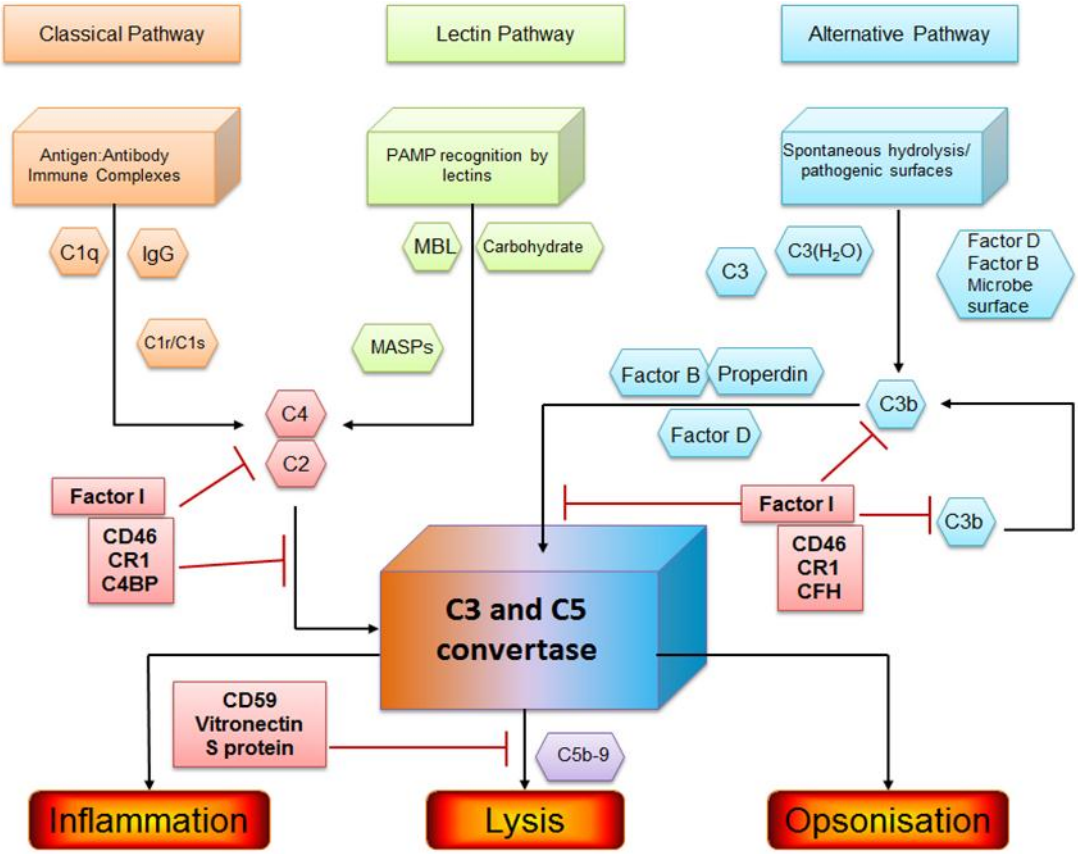

Figure 1.9. Diagram showing the three complement cascade activating pathways.

Classical Pathway: The classical pathway is activated by binding of C1q to two molecules of IgG or one molecule of IgM complexed with the target antigen (immune complexes). This activates the proteases R (C1r) and S (C1s) which in turn cleave the complement components C4 and C2 into small fragments (C4a and C2b) and larger fragments (C4b and C2a) which form a complex and generate the C3 convertase. C3 convertase cleaves C3 into soluble C3a and C3b. C3b can then complex with C4bC2a, forming the C5 convertase, which in turn cleaves the C5 component, culminating in the formation of the MAC (C5b-9) complex. Regulation of the classical pathway is achieved by Factor I in conjunction with the co-factors CD46, complement receptor 1 (CR1) and complement 4 binding-protein, which cleave C4b into a non-active fragment. Lectin Pathway: The lectin pathway is activated by recognition of mannose on the surface of invading microorganisms by mannose-binding lectin (MBL), which then results in activation of MBL-associated serine proteases (MASPs) and cleavage of C4 and C2. The lectin pathway then proceeds in a similar way to the classical pathway. Alternative Pathway: the alternative pathway begins with spontaneous hydrolysis of C3 component into C3a and C3b components. C3b can then bind to Factor B allowing cleavage into Ba and Bb by Factor D, leading to the formation of the C3bBb complex (alternative pathway C3 convertase) stabilized by properdin. This complex then hydrolyses C3, leading to an amplification cascade and to the formation of the C3bBbC3b complex, which is able to hydrolyse C5. The alternative pathway, similarly to the classical pathway is regulated by factor I and the co-factors CD46, CR1 and complement factor H (CFH), which hydrolyze C3b into inactive fragments. Formation of the MAC complex, and hence cell lysis, is also regulated by CD59, vitronectin and S protein which

inhibit MAC formation by preventing complement 9 binding. *Modified from Dunkelberger J.R. et al 2010.*[75]

1.2.4.6 Microglia: the macrophages of the CNS

Microglia are the tissue resident macrophages of the central nervous system (CNS).[80] During development, microglia differentiate from progenitor cells in the embryonic yolk-sac and migrate into the brain and retina.[81] Microglia populations in the CNS are then established by local proliferation of the embryonic microglia.[82] It is not clear whether in adulthood microglia in the retina are replenished by blood circulating precursors, whether they replicate locally and/or if age-related changes or systemic insults contribute to the microglial population over time. Using radiation chimeras it has been shown that bone-marrow precursors can replenish microglia populations.[83-85] However, radiation was shown to induce damage to the blood-barrier[80] and in the absence of injury to the retina, microglia replenishment appears to be limited.[83] Independently of microglia turnover, it is accepted that under certain conditions, such as inflammation, circulating myeloid cells are able to infiltrate the retina and adopt a microglia-like phenotype,[86] consistent with findings in the brain.[82]

Microglia perform a variety of functions to ensure tissue homeostasis, including providing neurotrophic support to retinal neurons.[87, 88] During retinal development microglia play a major role in guiding blood vessel growth,[89] eliminating cellular debris from apoptotic neurons, and removing excess blood vessels.[84] In the adult retina, one of the main functions of microglia is immune-surveillance.[86] In a normal retina non-stimulated microglia, so called "resting" microglia, reside in the inner and outer plexiform layers (Figure 1.10.). They have a ramified morphology characterised by a small round cell body and long thin processes radiating from it.[86] These processes are highly motile and scan their environment for disturbances, without overt cellular migration.[90] However, when presented with activating stimuli, such as neuronal damage, microglia quickly migrate towards the site of injury, acquiring a more amoeboid morphology.[86, 91] Additionally, under severe inflammatory conditions, circulating monocytes/macrophages can be recruited from the circulation into the retina[86] (Figure 1.10.).

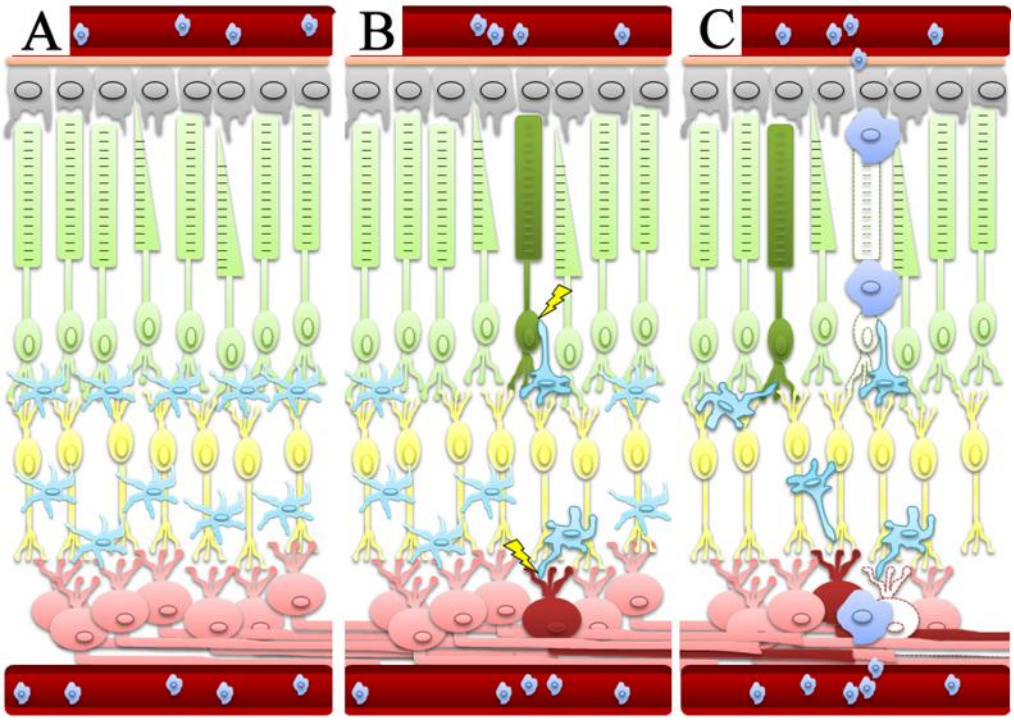

Figure 1.10. Schematic of microglia distribution on the retina.

(A) Under normal physiological conditions microglia (ramified light blue) reside in the outer and inner plexiform layers (OPL and IPL). **(B)** Upon activating stimuli, such as damage to photoreceptors or other neurons in the retina, microglia acquire an activated phenotype, characterised by morphological and cell-surface marker changes, and migrate to the site of injury, returning to the plexiform layers after the insult has been removed. **(C)** Under severe inflammatory conditions, more microglia are activated, chemokines are released and circulating monocytes/macrophages (rounded dark blue) can cross the BRB and infiltrate the retina. *Modified from Karlstetter 2010*[86]

Retinal microglia are kept under tight control; they have a down-regulated phenotype.[22, 24, 42] Control of microglia is achieved via the retina's immunosuppressive microenvironment[72, 92] (see section 1.2.4.4.), and via interaction with cell-surface molecules expressed by neurons (e.g. CX3CL1 and CD200). Resting microglia express receptors for these ligands (e.g. CX3CR1 and CD200R) which contain immunoreceptor tyrosine-based inhibitory motifs (ITIMs); crosslinking of these receptors leads to inhibition of microglia activation.[93] Disturbances such as RPE or photoreceptor damage, can lead to changes in the microenvironment and expression of microglia regulators, which in turn could lead to overactivation of microglia.[93] Moreover, when presented with specific stimuli, microglia can change their phenotype much like other macrophages.[86, 94]

Macrophage activation has been typically divided into two broad phenotypes: classically activated M1, pro-inflammatory phenotype, and alternatively activated M2, anti-inflammatory phenotype.[95, 96] The M2 phenotype can be further divided into three subtypes: IL-4 and IL-13 activated M2a, immune complex and TLR4 activated M2b and IL-10 activated M2c [95] (Figure 1.11.). Upon activation, macrophages and microglia can change expression of cell surface-markers and secretion of chemokines and cytokines[96] (Table 1.2.), the combination of which determines effector function. Dividing macrophage phenotype into four types of activation is a rather simplistic view of a very complex system. In addition to the well characterised M1 and M2a-c macrophages, other macrophage phenotypes such as M2d, Mox and M4 have been recently described (Table1.3.). Further adding complexity to understanding this system, it is unlikely that *in vivo* a population of microglia or macrophages will present with a "pure" phenotype. For example, in the retina, even in the presence of pro-inflammatory stimulation, microglia will also be interacting with their immunosuppressant microenvironment, therefore it would be unlikely they develop into a full M1 phenotype. Nevertheless, categorisation of macrophage phenotypes is a helpful tool to begin understanding macrophage function in response to specific stimuli. In AMD microglia and macrophages are recruited to lesion sites,[10] suggesting activation of these cells. If this is the case, these cells could change the microenvironment due to chemokine and cytokine secretion, thus contributing to pathology. Currently no convincing evidence exists for the presence of a dominant polarization state of retinal macrophages or microglia in AMD.

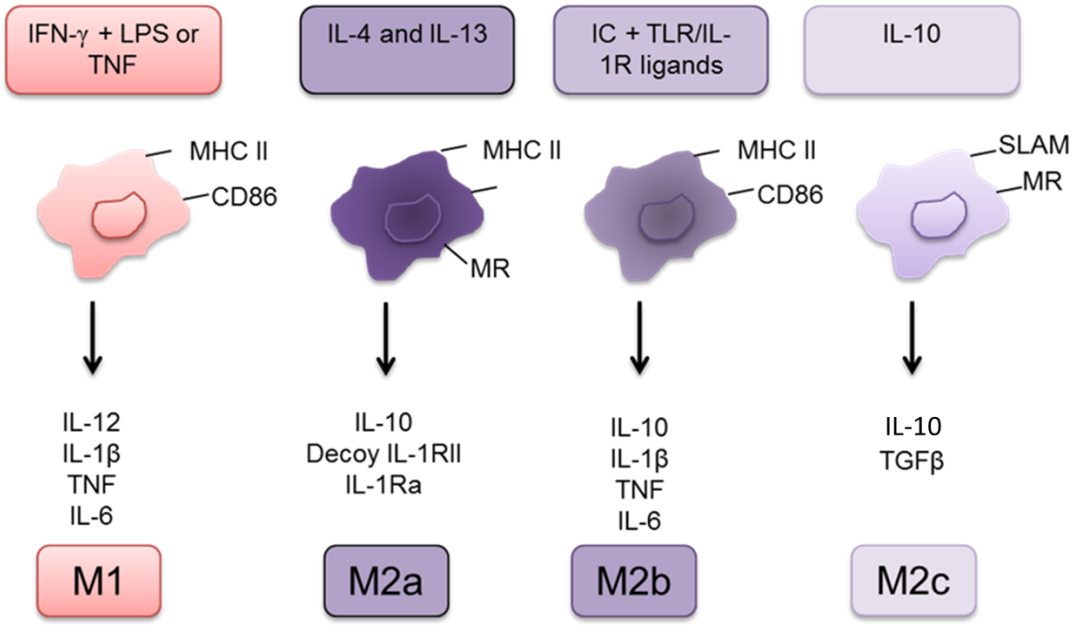

Figure 1.11. Diagram showing some characterised modes of macrophage activation.
(M1) Classically activated macrophages require two stimuli: INF-γ, usually transiently produced by NK cells but also by macrophages themselves, or by Th1 cells in a more sustained fashion; and TNF-α produced by antigen-presenting cells such as macrophages. Classically activated macrophages have increased microbicidal activity due to increased secretion of pro-inflammatory cytokines such as TNF-α, IL-12, IL-1β and IL-6, upregulation of MHC class II receptors and co-stimulatory molecules, such as CD86, providing the signal for activation following recognition of antigen. **(M2a)** Alternatively activated (wound-healing) macrophages are activated by IL-4 and IL-13 or glucocorticoids. They have an "anti-inflammatory" phenotype characterised by secretion of IL-1 receptor antagonist (IL-1Ra) and IL-10. These macrophages are involved in tissue repair and hence can promote wound healing and new blood vessel formation. However, inadequate stimulation of M2 macrophages can lead to allergy **(M2b)** Immune complex and LPS activated macrophages have characteristics of both M1 and M2 macrophages. Accordingly they produce the anti-inflammatory cytokine IL-10, often associated with neovascularisation, but also the pro-inflammatory cytokines TNF-α and IL-6. This type of macrophage can also upregulate expression of MHC II and CD86 molecules, promoting antigen presentation and T cell activation. Finally, IC activated macrophages can also produce NO and oxygen free radicals. **(M2c)** Regulatory macrophages are activated by IL-10. This type of macrophage secretes the anti-inflammatory cytokines IL-10 and TGF-β and is involved in immunoregulation and tissue remodeling. *Modified from Mosser and Edwards 2008*[96]

Table 1.2. Phenotypic changes in the main modes of macrophage activation

	M1[96-98]	M2a[96-98]	M2b[96-98]	M2c[96-98]
Activating Signals	IFN-γ, TNFα, LPS	IL-4, IL-13	IC, TLR agonists	IL-10
Secretory Products	TNFα, IL-12, IL-1β, IL-6, IL-23	IL-10, IL-1RA, Decoy IL-1RII	IL-10, TNFα, IL-1β, IL-6	IL-10, TGF-β
Biological Markers	MHC II CD86	MHC II Mannose Receptor Scavenger Receptor CD23	MHC II CD86	Mannose Receptor Signalling Lymphocytic Activation Molecule
Other	NO, O_2-	Polyamine	NO, O_2-	Versican PTX3 α antitrypsin
Chemokine	CX3CL1 CCL5 CXCL16 CXCL9 CXCL10 CXCL11	CCL24 CCL22 CCL17 CCL18	CCL1	CCL18 CCL16 CXCL13
Function(s)	Killing of intracellular pathogens Tumour resistance Support T_H1 responses	Allergy Killing and encapsulation of parasites Support T_H2 responses	Immunoregulation Support T_H2 responses Stronger induction of humoral response	Immunoregulation Matrix deposition Tissue remodelling Support T_H2 responses

Table 1.3. Phenotypic changes in newly characterised modes of macrophage activation

	M2d[99]	Mox[100]	M4[101]
Activating Signals	Adenosine A_{2A} receptor agonists, TLR2/4/7/9 agonists	Oxidised phospholipids	CXCL4
Secretory Products	IL-10 G-CSF VEGF IL-10	IL-10 IL-1 β	TNF-α, IL-6
Biological Markers	A_{2A} receptors	Nrf2 HO-1 GST Txnrd1	CD86 Mannose Receptor MHC-II MMP7 MMP12
Chemokine	-	THP1	CCL18 CCL22
Function	Hypoxia induced angiogenesis	Artherosclerotic lesion development	Artherosclerotic lesion development

1.3 The ageing retina

As illustrated in the previous sections, the eye is an extremely complex organ, where several specialised cells interact to allow vision to occur. In addition to its inherent complexity, the eye is an extremely active organ. In fact, the retina is thought to be one of the most metabolically active tissues in the body. Ageing is associated with the development of a variety of diseases, including rheumatoid arthritis, Alzheimer's disease and AMD.[102] It has been suggested that over time products of metabolism such as reactive oxygen species (ROS), advanced glycation endproducts (AGEs) and toxins accumulate in ageing tissues. Eventually the aged body cannot cope with these metabolic products resulting in disease.[103] Several changes in the ageing eye have been reported, both structural (e.g. blood vessel and BrM thickness) and functional (e.g. autophagy, mitochondrial dysfunction, abnormal signalling, inflammation), all of which are likely to affect eye function.[6] In this section the focus is directed towards structural changes in the eye and the immune system which could lead to inflammation and thus contribute to AMD pathology, for a comprehensive review on age-related changes to the retina see D. Arldejan and C.C. Chan 2013.[6]

1.3.1 Structural changes to the posterior chamber

1.3.1.1 The choroid and choriocapillaris

Progressive changes to choroid, the vascular network that nourishes the outer retina, are observed from the age of 50 and include decrease in density and lumen diameter of the choriocapillaris, the capillary bed of the choroid, as well as decrease of overall choroidal thickness from 200µm to about 80µm by the age of 80.[104] With the development of optical coherence tomography this has been confirmed by several groups.[105] However, choroidal thickness does not appear to be significantly different between healthy aged and AMD patients.[105] It is thus unclear what the relationship between changes in the choroid and AMD may be. Nevertheless, changes to the choroid are likely to affect retina function. The outer retina (RPE and photoreceptors) depend on the choriocapillaris for nutrient and oxygen supply[106] and hence these age-related changes in the choroid may cause a certain degree of oxygen deprivation. Ischaemic

conditions can lead to damage and dysfunction of the RPE, which in turn can lead to secondary degeneration of the photoreceptors. Together with other risk factors, (discussed in 1.4.1.) this could lead to oxidative stress and/or inflammation and, in turn, could further trigger degradation of the RPE and photoreceptors.[61] The products of photoreceptor degradation are thought to be shed from the RPE into the choroid.[37] It has been suggested that they can get trapped between the RPE and BrM, due to age-related changes in the BrM, where they could form the basis for subsequent drusen formation.[61]

1.3.1.2 Bruch's membrane

Bruch's membrane (BrM) is a basement membrane complex located between the RPE and the choriocapillaris, which functions as a barrier between these two compartments. It is a 5 layer membrane consisting of a central elastin layer, with an adjacent layer rich in collagen on both sides and the basal lamina of the RPE and choriocapillaris basement membranes.[40] Under normal conditions the BrM allows efflux of waste material through the RPE into the choroid and influx of nutrients from the choroid to the RPE and photoreceptors.[61] BrM thickness increases, from 2.0 to 4.7μm between birth and 90 years of age.[104] Although it is not clear if and how these changes in BrM thickness relate to pathogenesis of AMD,[61] it is possible that structural abnormalities in this membrane affect exchange of waste products from the RPE to the choroid,[40] causing them to be trapped between the RPE and BrM. Supporting this, studies using human donor BrM, have shown a time-dependent decrease in permeability to 21KDa-dextran complexes. By 90 years of age diffusion of these complexes is reduced to 9% of that achieved at 10 years of age.[107] Small lipid debris, only detectable by electron microscopy, starts accumulating adjacent to the elastin layer from age 20. This debris increases in frequency and number with age.[108, 109] Additionally, the tissue inhibitor of metalloproteinase-3 (TIMP3),[110] AGEs[111] and other proteins (e.g. collagen I, elastin and α-crystallin)[111] have also been shown to accumulate in the aged BrM, further suggesting changes in permeability of the BrM. With an increase in cell debris from age-related damage to the retina, a decrease in BrM permeability could allow drusen formation.

1.3.1.3 Drusen

Drusen are localised deposits that form between the RPE and the BrM. These deposits have different characteristics and are accordingly divided into different types such as diffuse, hard (nodular), soft, small, large, calcified, cuticular and semisolid.[112] Drusen formation can occur in normal ageing eyes, not necessarily developing into pathology-related drusen. Non-pathological drusen tends to be of the hard type only.[41] Accordingly, the incidence of hard drusen has not been associated with an increased risk of developing AMD or with the disease itself.[41, 113-115] Much of this hard drusen material has been identified as products of RPE degradation, containing traces of melanin granules, lipofuscin, membranous material and organelles.[74] Drusen specific components have been identified in the cytoplasm of specific retinal pigmented epithelial cells, which suggests that some cells of the RPE may be more important than others in drusen biogenesis.[74] These cells have been described as having a "compromised RPE phenotype".[74] It has been hypothesised that cellular debris from "compromised" retinal pigmented epithelial cells is shunted away from the RPE but cannot cross the BrM and so it accumulates, eventually leading to the formation of drusen. Changes to the choroid could alter oxygen and nutrient supply to the RPE, potentially leading to this "compromised" RPE phenotype. If debris from these dead retinal pigmented epithelial cells then accumulates in the BrM this could lead to oxidative stress and/or inflammation, possibly contributing to the progression of this "age-related" drusen into "AMD-related" drusen.[61] It is unclear whether drusen contributes to or is merely a consequence of AMD pathology. However, the presence of inflammatory mediators in AMD-related drusen, but not hard drusen, suggests a relationship between drusen and inflammation, an accepted component of AMD pathology.

1.3.2 The aged immune system and parainflammation

It has been recognized that with ageing, changes to the immune system occur. Healthy aged individuals present with a "hyperinflammatory" state when compared to young and healthy individuals, characterised by increased circulating levels of the pro-inflammatory cytokine IL-6,[116] and prolonged and exacerbated inflammatory responses after injury.[7] Changes to the immune system have been described in both the innate and adaptive branches of immunity. In the adaptive immune system T and B cell production

is thought to be reduced, limiting the availability of naïve T and B cells.[117] Functional changes have been best described for CD8 T cells. These undergo oligoclonal expansion skewing the antigen-specific CD8 T cell repertoire to previously encountered antigens.[118] It is possible that CD4 T cells and B cells both undergo similar changes.[119] Moreover B cells are thought to produce antibodies with reduced antigen specificity and to have impaired IgG class switching.[9] Together with reduced numbers of naïve T and B cells, this potentially limits the ability of aged individuals to respond to new pathogens.

Despite the "hyperinflammatory" state, *in vitro* studies on innate immune cell function show that cells such as monocytes/macrophages and neutrophils are less responsive to inflammatory stimuli with age, having reduced chemotaxic and phagocytic capacity and reduced capability of secreting reactive oxygen species.[102] These observations suggest aged cells of the innate immune system respond differently to inflammatory stimuli. The conflicting results from *in vivo* and *in vitro* data on age-related changes to the innate immune system could be due to differences in the environment and to interactions with an altered adaptive immune system. It could thus be that although in a controlled cell-culture environment aged cells are less reactive to inflammatory stimuli, when exposed to an aged tissue environment (e.g. elevated levels of IL-6),[116] or to a persistent pathogen due to impaired adaptive immunity, these cells are more prone to inflammation. Finally, some changes to microglia with ageing have also been reported. Increased numbers and altered distribution of microglia have been reported both in the brain and retina, with microglia accumulating in the subretinal space in aged eyes.[120] Functionally it is thought that aged microglia display higher levels of basal activation with increased expression of markers such as CD11b and MHC II, pro-inflammatory cytokine secretion and altered expression of complement proteins.[8, 121, 122]

Parainflammation refers to an immune response to noxious stress or tissue malfunction that has characteristics intermediate between basal and inflammatory states[123] and has been associated with pro-inflammatory damage to tissues like the eye during ageing.[73] It serves the purpose of restoring tissue homeostasis; however, parainflammation can become chronic (i.e. low grade chronic inflammation) or turn into full-grade inflammation, hence contributing to onset of disease.[123] In the ageing eye several triggers could contribute to retinal parainflammation; increase in oxidative stress and free radicals, accumulation of oxidated lipids and AGEs, changes to complement

regulation, altered microglia responses and distribution, and breakdown of the BRB.[8, 73, 111, 122] Although these responses may be triggered to restore tissue homeostasis in the ageing retina, environmental (e.g. smoking and high lipid intake)[3] and genetic factors may push this response towards uncontrolled inflammation leading to the development of retinopathies such as AMD.

1.4 Age-related macular degeneration (AMD)

AMD is among the most common causes of irreversible blindness in industrialised countries.[3, 113, 124, 125] It is estimated that 30-50 million individuals are affected by this disease.[3] With a rapidly increasing ageing population this number is likely to increase in the near future.[3] In an American study it has been estimated that the numbers of individuals suffering from AMD worldwide will increase by 50% in 2020.[126] This debilitating disease is generally characterised by the presence of extracellular deposits (drusen) between the RPE and BrM and by pigmentary changes to the RPE[41] and leads to progressive loss of central vision. In the late stages it can present itself in two forms; dry and wet AMD, both resulting in degeneration of the RPE and photoreceptors.[3, 127, 128] Several risk factors have been associated with AMD and it is accepted that this is a multifactorial disease. However, a lot still needs to be understood about the mechanisms of AMD.

1.4.1 Incidence and risk factors

Advanced age is the biggest risk factor associated with AMD, but several environmental and genetic risk factors are also associated with a higher incidence of the disease.[62, 127, 129] Cigarette smoking has been one of the strongest environmental factors associated with a higher risk of development of AMD.[5, 130-134] Accordingly, quitting to smoke results in decreased risk of developing AMD.[5, 130, 131, 135] In a European based study, subjects who quit smoking for 20 years or more had a similar risk of developing AMD as non-smokers.[135] Possible mechanisms by which smoking induces AMD could be a reduction in antioxidant production, changes in choroidal blood flow, hypoxia and oxidative damage to the RPE and retina.[115] Smoking has also been associated with increased inflammation[127] and increased vascular endothelial growth factor (VEGF) protein expression *in vitro*[132, 136] and *in vivo*[132] which, in turn, are thought to play a role in the pathogenesis of AMD.[61] Obesity, high fat intake diet[137, 138] and high β-

carotene[127] intake have also been linked to increased risk of development of AMD, although these risk factors have a weaker, less consistent relationship to development of the disease than cigarette smoke.[133] Conversely, a diet rich in omega-3 polysaccharide unsaturated fatty acids and the macular xantophylls lutein and zeaxanthin has shown some protection, with a decreased risk of AMD incidence.[127] In addition, supplementation of these diet components has shown to reduce the risk of progression from early to late AMD by 25%.[139] Zinc-antioxidant supplements have also been shown to prevent or delay progression of early AMD into late AMD.[127] Last but not least, several gene polymorphisms are associated with higher risk of development of AMD. Interestingly, most of these genes have a role in control of inflammatory responses, such as the complement cascade (cofactor H,[127, 140] SERPING1[141], C3[142]) and macrophage activity (CX3CR1,[141, 143] TLR4[144], HLA-I/II[145]). It is increasingly accepted that the increased risk of developing AMD is a result of gene and environment interactions. The role of inflammation in the pathogenesis of AMD is further discussed in section 1.5.

1.4.2 Early AMD

According to the International Classification and Grading System[41] early AMD is defined as a disorder of the macula, most often clinically apparent after the age of 50 and characterised by the presence of soft drusen,[41, 115] hyperpigmentation of the RPE in areas associated with drusen and/or smaller areas of hypopigmentation.[41] The earliest pathological changes are the appearance of basal laminar deposits (BLamD), clusters of membranogranular material and wide spread collagen between the RPE and BrM, and of basal linear deposits (BLinD), accumulations of vesicular material in the collagenous zone of the BrM which can further develop into drusen.[127]. However, basal deposits can only be detected with electron microscopy (hence post-mortem) and are thus not classified as drusen.[146] Clinically there are two main types of drusen, hard and soft drusen. Hard drusen are seen as round yellow-whitish deposits of less than 63µm in fundoscopy examination (Figure 1.12.) and are often present in eyes of patients with either early or late stage AMD but no association between the presence of this type of drusen and progression of macular pathology has been found.[41, 113-115] In fact, some studies have shown a decrease in incidence of hard drusen with development of early, as well as progression to late, macular degeneration.[112, 113] It has been hypothesized that

hard drusen appear originally and that they can become confluent and develop into soft drusen.[41, 147] Soft drusen are also seen as yellow-whitish deposits, but are bigger than 63µm and can be further classified into distinct and indistinct soft drusen.[41] Indistinct soft drusen have decreasing density from their centre to periphery and fuzzy borders, while distinct soft drusen appear with uniform density and sharp edges. Similarly to hard drusen, soft drusen can become confluent forming larger drusenoid deposits.[147-149] Drusen formation does not appear to be spatially random; in contrast, these deposits seem to preferentially form in intercapillary regions.[150, 151] A recent study confirmed that drusen formation is highly associated with areas of decreased vascular density but also with areas of loss of endothelial cell viability.[152] These observations suggest an interaction between choroid function and drusen formation. The presence of drusen in early AMD is associated with minute detachments of the RPE from the BrM, the severity of which is often related to the size and number of confluent drusen present.[153] Finally the presence of drusen causes pigmentary changes, with large soft drusen often associated with hyperpigmentation of the RPE.[153] Macular function is significantly altered in patients with early AMD, although this does not translate into large visual deficits. Accordingly, contrast and central visual field sensitivity is mildly impaired[154] but visual acuity is typically 20/20 (maximal score) or 20/32 (mild impairment) and colour vision is not altered at all.[154]

It is unclear which factors initiate AMD, with most authors suggesting an age-related loss of function of the RPE as the triggering event.[155, 156] Loss of function of the RPE would thus lead to inappropriate function of the visual cycle and recycling of photoreceptor discs, eventually leading to accumulation of debris (possibly contributing to the formation of drusen) and photoreceptor cytotoxicity. In addition, the RPE secretes several growth factors which are necessary for retinal homeostasis but also for endothelial cell viability (e.g. PEDF and VEGF) and hence, choroid function.[37] The "RPE-centric" view supports the idea that death of the RPE would subsequently lead to photoreceptor loss (due to loss of trophic support as well as inappropriate recycling of the photoreceptor discs) and to loss of choroid function (due to reduced trophic support to endothelial cells). Presumably, the loss of endothelial cells in the choroid would be a consequence of reduced VEGF secretion by the RPE. This arises as an obstacle for this theory as VEGF has been reported to be increased in AMD eyes.[157, 158] It seems that drusen formation is influenced by choroid function. It is thus possible that loss of

function of the choroid is the triggering event for early AMD pathology. Supporting this is the fact that the highest environmental risk factors for AMD (i.e. smoking and high lipid diet) as well as age, have been associated with blood vessel damage.[134, 137, 138] Impaired function of the choroid, due to age-related changes such as decreased choriocapillary density and lumen area or inflammatory damage, could lead to oxygen deprivation to the RPE. This in turn, would likely lead to impairment of RPE function, which could lead to drusen formation and photoreceptor loss as discussed above.

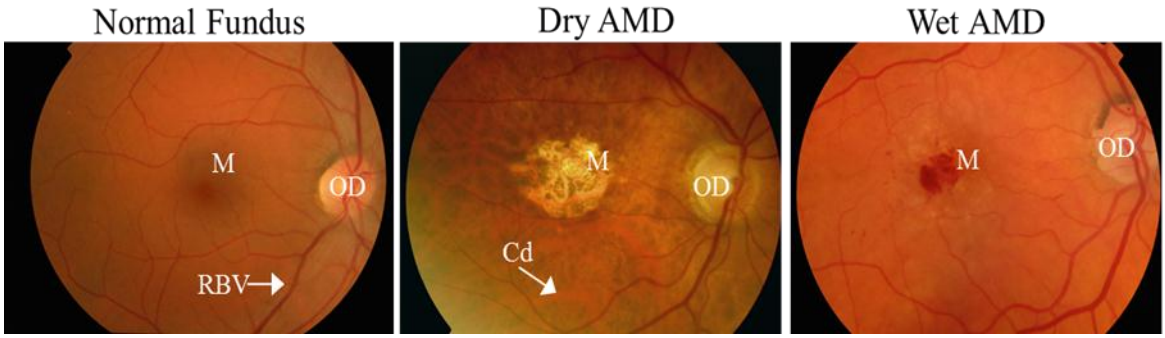

Figure 1.12. Fundoscopy pictures showing the fundus from a normal individual and from individuals suffering from dry or wet AMD.
In the normal fundus the optic disc (OD) can be seen as a brighter circle from where the retinal blood vessels (RBV) radiate. Due to its high concentration of the pigment lutein, the macula is seen as a darker area in the centre of the fundus. In dry AMD the macula is seen as a brighter yellow area due to loss of the underlying RPE. Also due to loss of the RPE, the choroidal blood vessels (CD) can be seen. In wet AMD an area of exudation due to choroidal neovascularisation can be seen as a red circle in the centre of the macula. *Courtesy of Sam Khandhadia*

1.4.3 Dry AMD

Dry AMD is characterised by the presence of drusen and degeneration of discrete areas of the RPE called geographic atrophy (GA).[3, 127, 159] In fundoscopy analysis GA is seen as sharply demarcated areas with a change in colour relative to the surrounding retina, with increased visualisation of the choroidal vessels and decreased retinal thickness (Figure 1.12).[159] These areas of GA are usually surrounded by areas of pigmented alteration,[159] both hypopigmentation (reflecting RPE loss) and hyperpigmented areas (possibly as result of compensatory RPE proliferation).[127] Although not strictly in association with GA lesions, soft drusen is often seen in the eyes of patients suffering from dry AMD. Histologically, areas of GA present with severe loss of cells of the

RPEand underlying photoreceptors. Rarely, in very severe cases damage can spread to the inner layers.[127]

GA develops from early AMD mostly in association with drusen and pigmentary changes. With time drusen can shrink (i.e. drusen regression) and develop foci of calcification before disappearing to leave a local patch of RPE atrophy. It has thus been hypothesised that drusen regression precedes and is associated with focal areas of RPE degeneration,[160] which can then enlarge and evolve into GA.[161] The process of macular atrophy develops over years with formation of single or multiple focal areas of RPE atrophy that can fuse together over time to form a larger atrophic area.[162] This seems to occur in areas of greater pigmentary alteration.[112] In 20% of cases, GA can develop from RPE detachment, without association with drusen.[163] Due to the slow development of atrophic areas, visual loss in "dry" AMD is often gradual and subtle.[162]

The mechanisms involved in the progression of early AMD to dry AMD are poorly understood. As drusen forms between the RPE and the BrM, it could affect exchange of debris from the RPE to the choroid, potentially increasing the size of drusen, but also the delivery of nutrients and oxygen from the choroid to the RPE.[37] Over time, this could become harmful to RPE, leading to cell degeneration and, consequently, the formation of GA. Macrophages/microglia have been reported to be associated with drusen and GA lesions.[164, 165] Drusen regression often precedes focal areas of RPE degeneration.[160] It is possible that monocytes from the blood or local microglia are recruited to aid clearance of drusen. Drusen contains inflammatory molecules such as IgG, complement proteins, oxidised lipoproteins and amyloid-β[13, 149] which can lead to activation of macrophages. This could lead to secretion of pro-inflammatory cytokines (e.g. TNF-α, IL-8, IL-1β) and formation of reactive oxygen species, allowing for clearance of drusen but also damage to the RPE and photoreceptors. The possible involvement of macrophages/microglia in the pathogenesis of AMD is further discussed in 1.5.3.

1.4.4 Wet AMD

Wet AMD is characterized by the abnormal growth of newly formed blood vessels from the choroid into the subretinal space through breaks in the BrM, this is known as

choroidal neovascularisation (CNV; Figure 1.13).[3] CNV can develop both from early and dry AMD.[41, 158, 166] The most common pattern of neovascularisation is that whereby newly formed blood vessels sprout from the choroidal vessels, penetrate through the BrM and grow into the subretinal space. However, less commonly, retinal angiomatous proliferations (RAP) can occur. RAP is the process whereby newly formed vessels derive from the retinal circulation and grow into the subretinal space, sometimes anastomosing with the choroid-derived vessels. [127]

The pathogenesis of wet AMD is better understood than that of early and dry AMD. The growth factor VEGF is constitutively secreted by the RPE and it is essential to maintain viability of the choroid.[37] However, abnormally increased concentrations of VEGF protein can be detected in eyes of patients with CNV.[157, 158, 166] Thus, it has been proposed that elevated concentrations of VEGF lead to abnormal neovascularisation.[167] In fact, therapy for this type of AMD employs monoclonal antibodies that block this growth factor, preventing it from binding to its receptor, VEGFR.[4] Following immunotherapy, CNV lesions regress and vision loss associated with this lesions (but not atrophic lesions) is recovered, [4] further supporting the role of this growth factor in the pathogenesis of wet AMD. However, it is still unclear what is the trigger for increased VEGF secretion and whether microglia/macrophage or RPE are the main producers of pathological VEGF.[168] Recently it has been shown that chronic anti-VEGF therapy can result in development of geographic atrophy.[169] It has been suggested anti-VEGF therapies, in addition to blocking pathological VEGF, lead to removal of trophic action of VEGF. In support of this, studies where VEGF was conditionally knocked-out in mouse RPE led to development of dry AMD-like pathology, including RPE atrophy.[170] These observations alert us to the need for understanding the mechanisms resulting in increased VEGF, so that more targeted therapies can be developed. Evidence from animal models of CNV suggests macrophages recruited from the periphery may play a role in CNV, as macrophage depletion has a protective effect.[171-173] CNV lesions are often associated with microglia/macrophages in humans,[174, 175] it is possible that these cells secrete factors, such as VEGF, contributing to the development of new blood vessels. In addition *in vitro* studies where microglia were co-cultured with RPE monolayers suggest the presence of microglia in the RPE apical side (i.e. subretinal space) could also induce VEGF secretion by the RPE.[168]

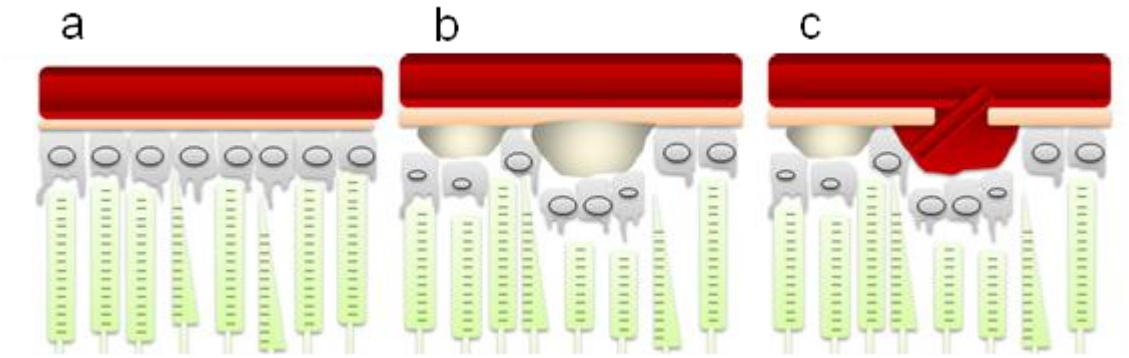

Figure 1.13. Schematic of the changes occurring in the AMD retina.
(a) In the normal eye the choroid is separated from the retina by the Bruch's membrane and the RPE. **(b)** In dry AMD, drusen accumulated between the RPE and the Bruch's membrane, eventually leading to RPE and photoreceptor degeneration. **(c)** In wet AMD newly formed choroidal blood vessels break through the Bruch's membrane into the retina. These blood vessels are weak and can break, leading to haemorrhage and consequent damage to the retina.

Presence and size of areas of hyperpigmentation or hypopigmentation, macular area covered by drusen, number and confluence of drusen have all been associated with higher risk of progression to late stages of AMD. However, it is not clear which factors determine disease progression and development of dry vs wet late AMD.[113]
Inflammation is increasingly recognized as playing a major role in the pathogenesis of AMD.

1.4.5 Treatment for AMD

Although dry AMD represents 90% of all cases of this disease there is currently no effective treatment available.[4] Anti-inflammatory agents such as corticosteroids are currently being tested in clinical trials in combination with anti-VEGF monoclonal antibody (mAb) therapy.[176] Although the use of several other anti-inflammatory agents for AMD therapy is being evaluated, including NSAIDs and immunosuppressant drugs (reviewed in Y. Wang et al 2011)[176] at present there are no reports of anti-inflammatory agents being successfully used for the treatment of dry AMD.[176] Anti-oxidant therapy has been shown to delay disease progression and to mildly improve visual function in some cases, however, it is still not sufficient to treat dry AMD.[62] Treatment for wet AMD is achieved by intravitreous injection of anti-VEGF blocking monoclonal antibodies.[177] Two antibodies are available for clinical use, ranizumab (Lucentis®, a

Fab fragment of the anti-VEGF antibody) and bevacizumab (Avastin®, the whole anti-VEGF IgG1 molecule).[177] Only ranizumab is Food and Drug Administration (FDA)-approved for the use in AMD, however, its short half-life (100 times shorter than that of bevacizumab) makes it necessary to administer it monthly. Bevacizumab is FDA-approved for the use in breast and colon cancer, but not for the use in AMD.[177] However, bevacizumab is cheaper than ranizumab and hence it has been used "off-label".[178] A further advantage of using bevacizumab in the treatment of AMD is that due to its longer half-life repeated injections are not required as frequently as with ranizumab. Contradicting reports on the safety of the two drugs exist. Accordingly, some studies indicate that bevacizumab leads to increased incidence of side-effects[179, 180] such as uveitis, retinal tear, vitreous haemorrhage, hypertension, stroke, vascular death and hospitalisation,[181] while others suggest the two antibodies are equally safe.[177, 182, 183]

1.5 Inflammation and AMD

Strong support for the view of inflammation having a role in AMD came from the identification of immune-related molecules such as vitronectin, amyloid P, apolipoprotein E, Factor X , IgG, molecules of the complement cascade as drusen components. [184] In addition, drusen, geographic atrophy[164, 165] and choroidal neovascularisation[174, 175, 185, 186] lesions are often associated with microglia and macrophages. Further supporting the role of inflammation, genetic studies have shown strong positive correlation between polymorphisms in genes coding for inflammatory regulators (e.g. complement proteins, TLR2/4, HLA-I/II and CX3CR1) and AMD.[184] Following these observations several animal models have been developed which further support the close relationship between inflammation and the development of AMD-like pathology such as RPE and photoreceptor cells damage. Most importantly, an important role for microglia and oxidative damage has been identified.[48] Here evidence supporting inflammation in AMD is discussed.

1.5.1 The complement system

The complement cascade (described in detail in section 1.2.4.5) has been identified as an important factor in the pathogenesis of AMD due to the higher incidence of genetic polymorphisms coding for complement proteins in patients suffering from AMD when

compared to controls.[74, 76] The most significant polymorphism associated with increased risk for AMD was shown to be in the gene coding complement factor H (CFH). CFH is an inhibitor of the alternative complement cascade. Two polymorphisms in CFH have been found, one with a protective effect, that binds C3b more efficiently and one that increases the risk of developing AMD, as it binds to C3b less efficiently, resulting in increased activation of the complement system.[127] Other polymorphisms in complement cascade components have been associated with AMD, albeit less consistently.[187] These include C3[142] and SERPING1.[90] Further supporting the role of complement in AMD is the presence of components of the complement cascade in drusen and in close proximity to sites of RPE damage in AMD patients.[74]

The polymorphism in SERPING1 is of particular interest for the purpose of this thesis, as it is a regulator of the classical complement cascade, initiated by immune complex deposition. Although the mechanisms by which SERPING1 could contribute to AMD are not clear,[188] high levels of circulating C1NH, the protein it codes for, have been shown in AMD patients.[189] Further, increased deposition of complement components was detected in eyes of AMD donors with the SERPING 1 polymorphism.[188]

1.5.2 Oxidative stress

Oxidative damage to the blood vessels of the retina has been described in normal ageing but also in retinal pathologies such as diabetic retinopathy.[190] Indirect evidence for the involvement of oxidative stress in the pathogenesis of AMD came from the fact that cigarette smoking (known to induce oxidative stress) significantly increases the risk of developing this disease.[61] A few experimental models have now supported the role of oxidative stress in the pathogenesis of AMD, including SOD1 and Nrf2 knock-out mice.[191] Of particular relevance for this thesis are the studies performed by Hollyfield. Carboxyethylpyrrole (CEP) is a protein modification derived from the oxidation of docosahexaenoic acid (DHA)-containing lipids and a biomarker of oxidative stress. CEP-modified proteins are elevated in eyes[192] and serum[193] of patients with AMD when compared to age-matched controls. In addition anti-CEP antibody titers are also more elevated in the serum of AMD patients.[193] Immunisation of mice with mouse serum albumin (MSA)-CEP adducts results in several early AMD-like lesions, including changes to the RPE, complement deposition and monocyte accumulation in the subretinal space.[194-196] Interestingly, circulating antibody titer strongly correlated

with severity of pathology, suggesting a role for antibody-mediated responses in this experimental model of AMD. Antibodies against oxidised proteins could thus provide a link between increasing oxidative stress occurring in the ageing eye and pathological inflammation involved in pathogenesis of AMD through the interaction with Fcγ receptors.[194-196]

In the studies by Hollyfield et al the occurrence of CNV following CEP immunisation was not detected. However, the angiogenic properties of CEP-dipeptides and human serum albumin (HSA)-CEP adducts, have been demonstrated in chick chorioallantonic membrane and rat corneal micropocket assays.[197] In these two assays picomole amounts of CEP-dipeptide and HSA-CEP induced neovascularisation that was blocked with neutralising anti-CEP antibodies, but not anti-VEGF antibodies. Additionally *in vitro* treatment of human retinal pigmented epithelial cells with CEP-HSA or CEP-dipeptide did not induce VEGF secretion by the RPE, suggesting that CEP triggers a pathway for neovascularisation that is independent of VEGF.[197] In fact, it has been shown that CEP-protein adducts can cause neovascularisation by activation of TLR2 receptors on vasoendothelial cells, in a MyD88 dependent fashion.[198] It is unclear whether a TLR2-dependent pathway for neovascularisation could be relevant for AMD. Nevertheless, these studies show how oxidative stress, an accepted risk factor for the development of AMD, can induce dry AMD-like pathology through initiation of an immune response marked by the presence of auto-antibodies and deposition of complement.

1.5.3 Microglia and Macrophages in AMD

Evidence for the involvement of microglia and macrophages in the pathogenesis of AMD first came from clinical observations. As described in section 1.2.4.6. upon stimulation by several stimuli microglia can become activated, much like macrophages. For example, when stimulated with LPS, microglia and macrophages both increase expression of markers such as iNOS. This makes distinguishing between microglia and macrophages in the CNS challenging.[35, 36] Electron microscopy and histological studies on human donor eyes have consistently shown the presence of cells expressing macrophage/microglia markers (e.g. CD45, CD11b and iNOS) beneath the BrM.[164, 165, 174, 199] These cells are normally associated with drusen and areas of GA[164, 165] or with BrM breaks and areas of CNV.[174, 175, 185] Microglia are quickly recruited to sites of injury.[35, 36] It is likely that microglia are initially attracted to areas of early AMD

pathology where they may become activated.[174] The phenotype acquired by these cells upon activation could contribute to the progression of early AMD to dry or wet AMD. At later stages, when more severe damage to the RPE and BrM may have ensued, macrophages are likely to also be recruited to the sites of AMD damage.[174] There has been debate on whether M1 or M2 phenotypes predominate in AMD.[200] To our knowledge only one study has addressed this question using human tissue. In normal ageing eyes transcript levels of CCL22 (used as a marker of M2 macrophages) predominated over CXCL11 (used as a marker of M1 macrophages), while CXCL11 predominated in late-stage (wet and dry) AMD. Based on these findings, the authors suggested a pathological shift from M2 to M1 phenotypes as an initiator of AMD pathology.[201] Although this is possible, the late stage of the disease in the eyes examined could have biased these results. In late stage-AMD there is overt damage to the photoreceptors and RPE,[112] which in itself could alter macrophage and microglia phenotype. In late AMD macrophage/microglia phenotype could thus be a consequence of the pathology rather than an initiating factor. In addition, M1 and M2 phenotypes were defined by immunohistochemical and qPCR detection of the chemokines CXCL11 and CCL22, respectively.[201] Macrophage polarisation leads to changes in expression of several cell-surface markers and secretion of different chemokines and cytokines, [95] as detailed in section 1.2.4.6. Moreover, M2 macrophages can be divided into at least three well characterised subtypes with different functions.[95] In particular immune complex activated (M2b) macrophages display characteristics of both the M1 and M2a phenotypes .[96] Investigating expression of more markers in the human tissue would thus be necessary for accurately defining macrophage phenotype. Nevertheless, these observations are still of interest. If a macrophage phenotype switch occurs as a consequence of the disease, the use of pharmacological modulators, such as anti-inflammatories could be beneficial.

1.5.3.1 Microglia and drusen

The observations that microglia are often present in association with drusen in eyes of patients with AMD[164, 165] have led some authors to suggest a role for abnormal microglia dynamics in pathogenic drusen formation.[86] Although this may be possible, it is still unclear which stimuli could be responsible for the initial migration of microglia

into the subretinal space and/or RPE/BrM interface, where drusen forms. It is known that with age RPE function declines.[202] As a result, photoreceptor recycling is less efficient and it is believed that an increased accumulation of debris in the subretinal space and between the RPE and BrM can occur,[120, 202] potentially causing microglia to migrate towards the RPE to aid in clearance of debris. It has been hypothesized that impaired microglia migration from the subretinal space would allow them to act as crystallisation foci for drusen formation.[86] Drusen develops in between the RPE and the BrM, hence it seems unlikely that microglia in the subretinal space could act as the "crystalisation" spots for drusen formation. Nevertheless, these microglia could form clusters of inflammation and contribute to drusen formation by changing the microenvironment, making it permissive for drusen formation.

A few animal models where myeloid cell function is altered lead to accumulation of bloated microglia in the subretinal space which resemble drusen deposits (Table 1.4). Results from mouse models of AMD must be interpreted carefully as a recent study has shown commercial C57BL/6 strains have a spontaneous recessive mutation, rd8, which leads to RPE pigmentary changes and retinal degeneration.[203] Several groups working on the $CCL2^{-/-}$ and $CCL2/CX3CR1^{-/-}$ models have reported the presence of the rd8 mutation on their mice, but this was not present on the $CX3CR1^{-/-}$ mouse strain used by Combadiere et al[143] (personal communication by Dr. Florian Senlaub). Despite the presence of rd8, the presence of microglia in the subretinal space in these models supports a role for microglia and inflammation in neurodegeneration in the retina. Finally, a significant genetic association between two polymorphisms for the gene CX3CR1 (CX3CR1 1249 and M280) and enhanced risk of AMD development has been reported.[143, 204] In 2007, Combadiere et al showed that AMD patients bearing the M280 allele for the CX3CR1 gene, display microglia accumulation in the subretinal space in sites associated with retinal degeneration and/or CNV.[143] In addition $CX3CR1^{-/-}$ mice develop AMD-like pathology (Table 1.4) with microglia accumulation in the subretinal space. These observations provide a possible mechanism by which the human allele M280 may contribute to the development of AMD.

Table 1.4 Age-related macular degeneration-like pathological hallmarks of transgenic models in comparison to age-matched, wild-type control mice.

	$CCL2^{-/-}$	$CX3CR1^{-/-}$	$CCL2^{-/-}/CX3CR1^{-/-}$
Bruch's Membrane Changes	No	N/A	Thickening from 240-350 nm to 500-1000 nm
Increased RPE hypo- or hyperpigmentation, degeneration	No	N/A	Yes, 6 months
Drusen, onset	Yes , 9 months*	Yes, 12 months	Yes, 6 weeks
CNV, onset	Yes, 18 months ↘Laser-induced CNV	No ↗Laser-induced CNV	Yes , 2 weeks
Accelerated Retinal Degeneration, onset	Yes, 16 months No	Yes, 2 months (after light exposure)	Yes, 9 months
Subretinal accumulation of Microglia/MØ,onset	Yes, 20-24 months	Yes, 18 months	Yes, 6 weeks
IgG deposition -localisation	Yes: -Subretinal - Surrounding blood vessels	N/A	Yes: -Subretinal space -Drusen -RPE -Bruch's Membrane
Complement Cascade components deposition	C3c, C5, vitronectin, CD46	N/A	C3d, CD46
Serum autoantibodies against retinal antigens	N/A	N/A	Yes
Other	Impaired MØ recruitment Reduced expression of IFN-γ, IL-4 and IL-5	Increased accumulation of CD11b+ cells around blood vessels	Reduced levels of TLR4 and ERp29 expression

Pathological changes can be inherent to the transgenic mouse (spontaneous) or evident following experimental conditions, such as light exposure or laser damage to the retina.
Features not analysed for a particular mouse model are represented with 'N/A'.
*Luhman et al 2009 only detected drusen at 24 months

References:

CCL2- Ambati J et al 2003,[171] Lu X et al 2009,[205] Luhmann UF et al 2009[203]

CX3CR1- Combadiere C et al 2007[143] , Prinz M et al 2010[206]

CCL2/CX3CR1 – Tuo J et al 2007,[207] Ross RJ et al 2008[208]

1.5.3.2 Microglia, macrophages and dry AMD

The lack of understanding of the mechanisms leading to dry AMD has made it challenging to model it. Hollyfield's MSA-CEP immunisation model (discussed in 1.5.2.) has been one of the few rodent models where features of dry AMD, such as RPE atrophy, have been reproduced. Nevertheless, these features are reported to only occur 12 to 24 months after immunisation, making it challenging to work with this model. In a recent study MSA-CEP immunisation led to recruitment of cells expressing macrophage/microglia markers to the subretinal space. Based on their immunoreactivity for TNF-α and IL-12 and lack of it for IL-10, these cells were classified as having an M1 phenotype. Further, when immunising CCR2 knock-out mice both migration of these TNF-α+IL-12+ cells to the subretinal space and RPE pathology were abolished. The authors have thus suggested M1 macrophages and microglia could contribute to the pathogenesis of dry AMD.[209] There are, however, issues with this study. Firstly, the images of microglia/macrophage and cytokine stains are shown in different magnifications and different areas of the retina, making them rather unconvincing. Secondly, although the authors report that there are no cells in the subretinal space after CCR2 depletion they do not show any images or quantification of this.

Accumulation of debris, drusen formation and initial RPE damage could all act as stimuli for microglia migration. It is thus plausible that these could be recruited to the subretinal space. As the RPE plays an important role in maintaining the retina's immunosuppressive environment, progressive RPE damage/cell death in early AMD could lead to loss of this immunosuppressant environment. The removal of this anti-inflammatory stimulus in conjunction with the presence of drusen and increasing oxidative stress would lead to microglia activation and consequent RPE and photoreceptor bystander damage. Supporting this, in humans, macrophages associated with GA show increased levels of iNOS expression.[174]

1.5.3.3 Microglia, macrophages and wet AMD

It is accepted that increased VEGF concentration is important in mediating CNV in AMD.[167] In the outer normal retina, both RPE and endothelial cells of the choroid secrete homeostatic amounts of VEGF.[170] It is unclear what causes the pathological secretion of VEGF and which cells are responsible for it. Activated macrophages can secrete VEGF.[96] Moreover, microglia have been shown to be key in guiding blood

vessel growth during development of the retina.[89] As these cells are often associated with CNV lesions,[174, 201] it is possible macrophage or microglia-derived VEGF could contribute to formation of CNV. In addition, interaction of these cells with the RPE or/and choroid could contribute to CNV via other pathways. Both CCL2 and CCL2/CX3CR1 knock-out mice, showing microglia and/or macrophage accumulation in the subretinal space, develop CNV,[143, 171] suggesting these cells could have a role in neovascularisation. However, only 10% of the CCL2/CX3CR1 developed CNV and a separate study on CCL2 knock-out mice failed to show any spontaneous CNV.[203] The studies in which these mice showed CNV were done prior to knowledge of the rd8 mutation. Both groups have since then reported the presence of this mutation in their mice;[210, 211] this could have confounded their results. It is thus unclear from these studies whether subretinal microglia and/or macrophages could induce CNV in AMD.

The strongest evidence that macrophages could impact on CNV comes from studies using a laser-induced model of CNV. In this model, the BrM is injured by a laser, allowing blood vessels to grow into the subretinal space. Several studies manipulating macrophage function and recruitment have been performed and are summarised in Table 1.5.

Table 1.5. Table summarising effect of macrophages on lesions size in the laser models of CNV

Model	MΦ Infiltration	CNV lesion	Other	Ref.
$CX3CR1^{-/-}$	↑	↑	-	143
$CCL2^{-/-}$	↓	↓	-	203
Clodronate liposomes	↓	↓	↓ VEGF	172, 173
$IL10^{-/-}$	↑	↓	Intraocular injection of IL-10 reverses phenotype	212
$SRA^{-/-}$	↓	↓	Reduced expression of chemokines and their receptors	213
$MACRO^{-/-}$	↓	↓		
$CD200R^{-/-}$	-	↓	Reduced expression of pro-angiogenic genes by MΦ	214

Most of these studies show a positive correlation between macrophage accumulation and more severe CNV lesions, suggesting macrophages may indeed contribute to pathogenesis of wet AMD. Further studies have tried to address the phenotype of these macrophages and they appear to be IL-10 secreting macrophages. Based on expression

of IL-10 alone many authors call these macrophages "M2 macrophages"[214, 215] and therefore it has been suggested a shift from M1 to M2 macrophages can lead to choroidal neovascularisation and hence, wet AMD. As previously mentioned, macrophage activation phenotypes, although simplified, are very complex and cannot be assertively defined by investigating one or two markers. In addition, most studies failed to address which stimuli could be driving the macrophage polarisation. Immune-complex "M2b" activated macrophages have characteristics of both M1 and M2a ("M2") macrophages. As immune complexes may be present in AMD, these macrophages could also contribute to CNV.

1.6 Immune complex-mediated inflammation and AMD

The presence of circulating retina-specific autoantibodies[15, 16, 216] and the deposition of IgG in drusen and the RPE of AMD patients, [96, 113, 143] suggest immune complex (IC)-mediated inflammation may contribute to AMD pathology. IC can mediate and regulate a variety of immune functions, which is largely dependent on the cell type they interact with. IC interact with cells of the innate immune system (e.g. mast cells, neutrophils and macrophages) and of the adaptive immune system (B cells), bridging these two branches of the immune response.[217] In order to activate effector function, ICs need to interact with antibody receptors, Fc receptors (FcRs), expressed by cells of the immune system.[17]

1.6.1 Fcγ receptors

FcγRs are transmembrane receptors for IgG belonging to the immunoglobulin family.[17] These receptors bind to the Fc fragment of IgG (Figure 1.14.) mediating important functions such as clearance of immune complexes, uptake of the complexed antigens for presentation and regulation of immune cell responses (e.g. B lymphocyte proliferation, phagocytosis by macrophages and mast cell degranulation).[17, 217] To date, four different FcγRs have been identified in mice (mFcγRs I, II, III and IV) and six in humans (hFcγRs I, IIa, IIb, IIc, IIIa, IIIb). Only hFcγRIIb and mFcγRII are inhibitory, signalling through an immunoreceptor tyrosine-based inhibition motif (ITIM). With the exception of hFcγRIIIb, all other FcγRs are activating, signalling through an immunoreceptor tyrosine-based activation motif (ITAM).[17, 217] There is homology between the mouse and human FcγRI,[218] and mFcγRII and hFcγRIIb.[17] In addition, it has been suggested

that in terms of affinity for IgG and function, mFcγRIV and mFcγRIII correspond to hFcγRIIIa and hFcγRIIa, respectively.[17, 219] However there are several differences between mouse and human FcγRs. Particularly, activating mFcγRs are composed of a α-chain, containing the extracellular portion of the receptors, associated with two γ-chains, required for signalling. In human, not all activating FcγRs need to associate to a γ-chain, as some contain ITAM motifs on the intracellular portion of their α-chain[17] (Figure 1.14.). Further adding to these differences is the existence of allelic variants in the human system.[17, 220]

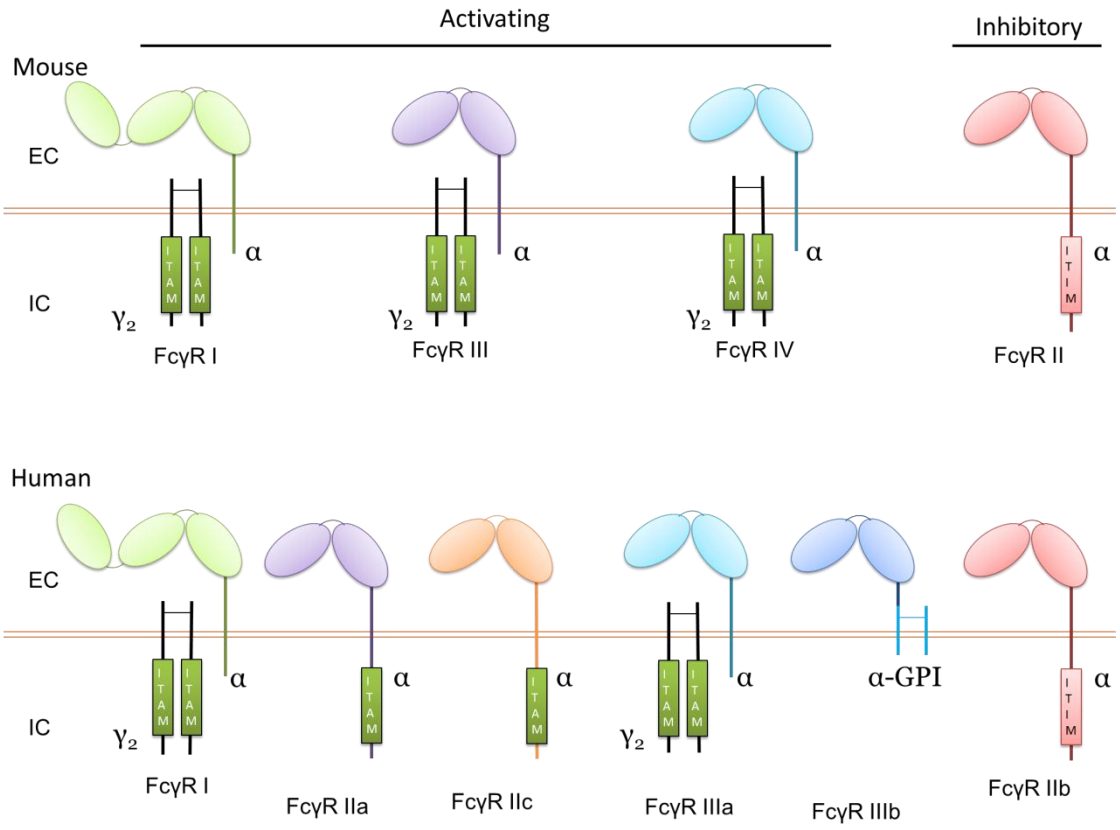

Figure 1.14. Schematic showing human and mouse Fcγ receptors.

The mouse activating FcγRs are composed of a α-chain and a γ-chain containing ITAM motifs required for signalling. The extracellular portion of the αchain contains immunoglobulin-like motifs. Low-affinity receptors contain two of such motifs (D1 and D2), whilst the high affinity FcγRI contains an extra motif (D3).[221, 222] The human FcγRI and IIIa are also associated with a γ-chain, whilst FcγRIIa and IIc both contain ITAM motifs intrinsic to their α-chain. FcγRIIIb is attached to the cell membrane by a glycophosphatidylinositol (GPI) anchor. Both the mouse FcγRII and human FcγRIIb contain an ITIM motif on their α-chain.[17, 220]

1.6.1.1 Fcγ receptors and IgG

In addition to different FcγRs, different IgG subclasses add to the complexity of this system. Four IgG subclasses have been described in in human (hIgG1, hIgG2, hIgG3 and hIgG4) and five in mouse (mIgG1, mIgG2a, mIgG2b, mIgG2c and mIgG3).[217] While all strains of mice produce mIgG1, mIgG2b and mIgG3, mIgG2a or mIgG2c are preferentially produced by different mouse strains. For example, the BALB/c strain produces IgG2a but not IgG2c, whilst the C57BL/6 strain produces IgG2c but not IgG2a.[223] IgG subclasses differ in their ability to interact with the complement system and in their affinity for specific FcγRs, in this way shaping effector function.[224] For example, mIgG2a, which can bind to all four mFcγRs, binds with higher affinity to the activating mFcγRI and mFcγRIV than to the inhibitory mFcγRII, having a high activating/inhibitory (A/I) ratio. This means mIgG2a will preferentially bind to activating mFcγRs, inducing cell activation. In contrast, mIgG1 binds to mFcγRII and only to a single activatory mFcγR, FcγRIII, producing a lower A/I ration and hence, favouring cell inactivation.[224] Accordingly, IgG2a and IgG2b in mice and IgG1 and IgG3 in humans, are the most pro-inflammatory classes of IgG.[224]

FcγRs can be classified according to their affinity for IgG (Table 1.6.). Both in mice and humans the only high affinity receptor is FcγRI. It is the only receptor capable of binding to monomeric IgG. mFcγRI binds to monomeric mIgG2a with an affinity of 10^8-$10^9 M^{-1}$. mFcγRIV has moderate affinity, binding to IgG with a 10-fold lower affinity.[219] The other mFcγRs bind to IgG with a 100-1000 fold lower affinity.[17] Monomeric IgG is not sufficient to activate the lower affinity receptors, instead, IC need to crosslink these FcγRs.[17] This allows for specificity of antibody responses, preventing the initiation of inflammatory responses by unspecific IgG that could potentially damage the host. The high affinity receptor is normally saturated by monomeric IgG, presumably preventing this receptor from binding to immune complexes.[17] However, several studies have shown that this receptor may still contribute to immune complex clearance.[225, 226] It is believed that *in vivo* IgG interactions with FcγRs may not correspond to what would be expected from the affinities of each FcγR and IgG subclasses *in vitro*. For example, although both mFcγRI and III can bind mIgG2a and mIgG2b *in vitro* it appears that *in vivo* both IgG subclasses mediate their function mostly through mFcγRIV,[227] whilst IgG1 seems to selectively bind to mFcγRIII.[228]

Table 1.6. Mouse and Human Fcγ Receptors, their structure and IgG subclass specificity

Mouse

Name	Structure	Affinity (K_a)	IgG Subclass Specificity	Cellular expression
FcγRI	$\alpha\gamma_2$	High (10^8 to 10^9 M^{-1})	2a>2b >> 1,3	Mo, Mϕ
FcγRII	α	Low (10^6 M^{-1})	2b, 2a,1>>3	Mo, Mϕ, Ne, Ba, Eo, BC
FcγRIII	$\alpha\gamma_2$	Low (10^6 M^{-1})	2b> 2a> 1>> 3	Mo, Mϕ, Ne, Ba, Eo, NK
FcγRIV	$\alpha\gamma_2$	Medium (10^7 M^{-1})	2a=2b >> 1, 3	Mo, Mϕ, Ne, Ba, Eo

Human

Name	Structure	Affinity (K_a)	IgG Subclass Specificity	Cellular expression
FcγRI	$\alpha\gamma_2$	High (10^8 to 10^9 M^{-1})	3=1>4>> 2	Mo, Mϕ, Ne
FcγRIIa	α	Low (<10^7 M^{-1})	3=1>>2,4	Mo, Mϕ, Ne, platelets
FcγRIIb	α	Low (<10^7 M^{-1})	3=1>4 >>2	Mo, Mϕ, Ne, BC, EC
FcγRIIc	α	Low (<10^7 M^{-1})	3=1>>>2,4	NK
FcγRIIIa	$\alpha\gamma_2$	Medium ($3x10^7$ M-1)	3=1>>>2,4	Mo, Mϕ, NK
FcγRIIIb	α (GPI)	Low <10^7 M^{-1})	3>>1>>>2,4	Ne, Ba

Mo – Monocytes, Mφ- Macrophages, Ne- Neutrophils, Ba- Basophils, Eo- Eosinophils, NK- Natural Killer cells, BC- B cells, EC – endothelial cells

Adapted from *Niederer, H.A. et al 2010,*[229] *Ravetch, J.V. and Bolland, S. 2005,*[220] *Nimmerjah and Ravetch 2008,*[17] *Dijstelbloem, H.M. et al 2001*[230]

1.6.1.2 Fcγ receptor function

The effector function elicited by FcγRs is also largely dependent on the type of immune cells expressing them (Table 1.7.). In addition, immune cells can further regulate this by changing expression levels of FcγRs, setting the threshold for activation activation.[17, 220] Crosslinking of activating FcγRs leads to ITAM-dependent signalling (Figure 1.15.), which culminate in activation of effector functions, such as phagocytosis of IgG coated pathogens and/or particles, cytokine release, oxidative burst and antibody-dependent cell cytotoxicity (ADCC).[17, 220] Conversely, crosslinking of hFcγRIIb (or mFcγRII) leads to inhibition of the signalling cascade via ITIM signalling. The hFcγRIIb is the only FcγR expressed by B cells; it can interact with the B cell receptor (BCR), also inhibiting signalling.[17, 220] Expression of FcγRs is controlled by a variety of inflammatory stimuli; TNF-α, IFN-γ, LPS and C5a all have been shown to increase FcγR expression. Further, cytokine stimulation can differentially regulate specific FcγRs. For example, IL-4, IL-10 and TGF-β stimulation results in increased expression

of FcγRII,[231, 232] whilst IFN-γ stimulation results in upregulation of the activating FcγRs.[231] The fact that expression of these receptors can be modulated by various inflammatory stimuli illustrates the important role of these receptors in mediating immune responses. Both inhibitory and activating receptors are necessary for appropriate mounting of immune responses. Depletion of mFcγRII results in exacerbated immune responses and susceptibility to autoimmunity[233, 234] Expression of the γ-chain is required for expression of activating mFcγRs. Depletion of the γ-chain results in abolished expression of activating mFcγRs and leads to an immunocompromised phenotype due to impaired antibody responses.[235]

Table 1.7. The effect of activating Fcγ receptors on immune cell effector function

Cell Type	Effector function
Monocytes/MΦ	Phagocytosis Secretion of pro-inflammatory cytokines Oxidative burst Antibody dependent cytotoxicity (ADCC)
Mast Cells	Degranulation Secretion of chemoattractants Secretion of vasoactive molecules
Neutrophils	Phagocytosis Oxidative burst Secretion of chemoattractants Secretion of cytotoxic substance
Dendritic cells	Antigen presentation Regulation of tolerance

Adapted from *Nimmerjhan and Ravetch 2008*[17]

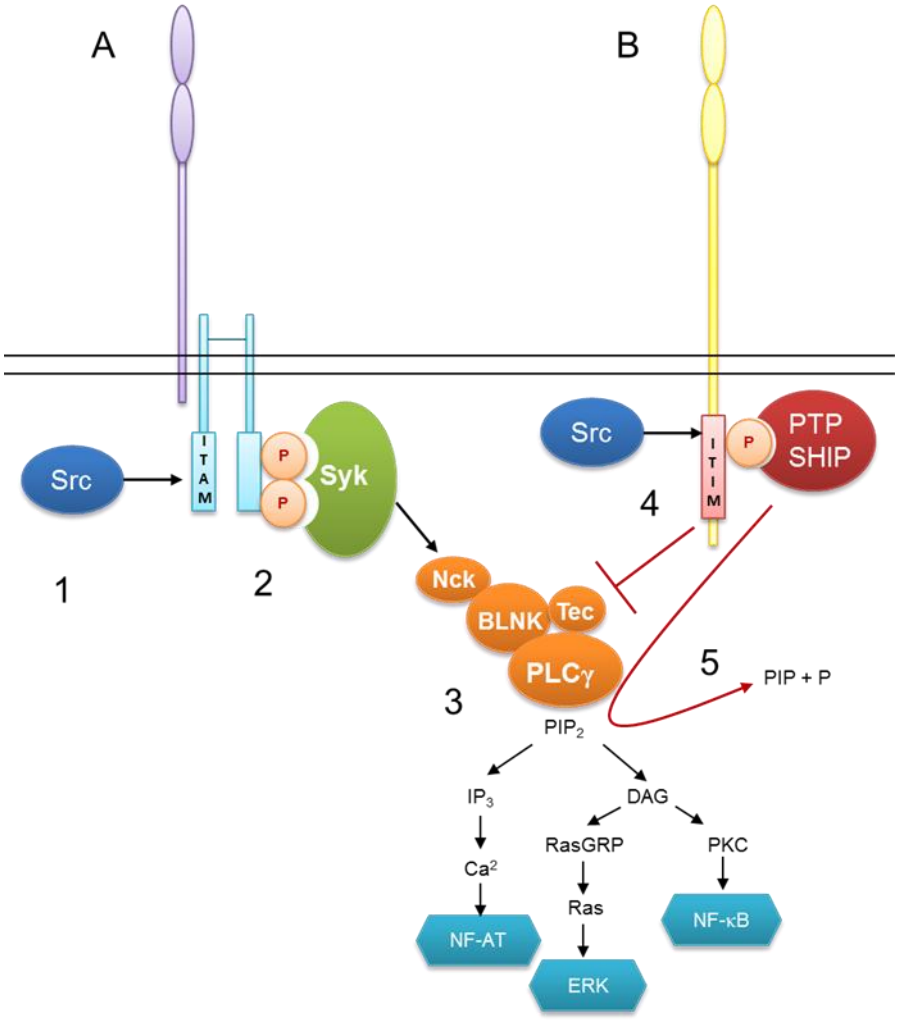

Figure 1.15. Diagram representing the signalling cascades of Fc receptors using ITAMs and ITIMS. (A) ITAMs of consensus YxxI/Lx(6–12)YxxI/L are encoded in the cytoplasmic tail of receptors. **(1)** Upon ligand recognition and receptor clustering, tyrosine (Y) residues are phosphorylated by Src family protein kinases. **(2)** The dual phosphorylated ITAM serves as a docking site for the SH2 domains of the Syk family of protein kinases (eg ZAP-70 or Syk). **(3)** The Syk family of protein kinases phosphorylate a series of substrates leading to the formation of membrane-proximal scaffolds which in turn recruit important effector molecules such as phospholipase Cγ (PLCγ) activating calcium signalling pathways and PKC with consequent activation of the transcription factor NF-kB,[236] a mediator of physiological immune and pathological inflammatory responses,[237] as well as Ras activation resulting in stimulation of the ERK pathway and cellular activation. **(B)** The negative regulating receptors contain one or more ITIMs of consensus S/I/V/LxYxxI/V/L. Ligand engagement results in ITIM phosphorylation by Src and recruitment of **(4)** phosphotyrosine phosphatases (PTP), such as SHP-1 and SHP-2, or **(5)** the inositolphosphatase, SHIP. PTP recruitment can result in decreased tyrosine phosphorylation of activation pathway effectors such as Syk, PLCγ and transmembrane-associated adaptor proteins, such as the FcR common gamma chain, ultimately resulting in inhibition of activating pathways. SHIP phosphorylates PIP2, preventing calcium signalling and PKC activation. [236-238]

1.6.2 The neonatal Fc receptor

The neonatal Fc receptor (FcRn) is a receptor for IgG.[239, 240] Both mFcRn and hFcRn bind with high affinity to all mIgG and hIgG subclasses, respectively, at a pH lower than 6.5.[241] Structurally FcRn resembles MHC I with three extracellular α domains, a transmembrane domain and a short cytoplasmic tail. FcRn expression is mostly intracellular with a small fraction of FcRn being expressed extracellularly. This receptor can be expressed by a variety of cells such as macrophages, dendritic cells, endothelial cells and some types of epithelium (e.g. intestinal epithelium).[240, 241] Similar to FcγRs, FcRn performs a variety of functions, the nature of which is highly dependent on the cell type expressing this receptor. For example, in dendritic cells, FcRn sorts multimeric IgG-containing immune complexes to intracellular compartments associated with antigen processing, thus contributing to antigen processing and presentation. In haematopoietic cells, such as macrophages, FcRn expressed in endosomal compartments binds to IgG, protecting it from degradation. Finally, FcRn expressed by epithelial and endothelial cells mediates transport of IgG across cells by transcytosis.[239, 240] Of particular interest, FcRn expressed by endothelial cells in the brain is proposed to play a role in transport of IgG from the brain across the endothelium to the blood stream.[240] Endothelial cells of the retinal blood vessels and choroid express FcRn,[242, 243] where similar roles in transporting IgG from the retina could be performed.[240]

1.6.3 Immune complexes and AMD

One of the hallmarks of macular degeneration, both dry and wet types, is the formation of drusen in the macula region, accompanied by RPE pathology.[14, 148, 149] All types of drusen seem to have a similar lipid and carbohydrate composition,[148, 149] thought to derive from degraded RPE[40], and the protein vitronectin.[40, 244, 245] However, protein components can vary in different types of drusen.[13, 40, 245] Several studies have tried to identify proteins that are common in drusen from eyes of AMD patients. Interestingly, protein components involved in immune complex mediated responses seem to be common in drusen derived from AMD eyes. These include acute phase proteins such as vitronectin and C-reactive protein (CRP),[14, 149] complement factors and regulators such as CD46,[40] C1q,[246] C3c, C3d,[40, 246] C4,[246] C5-C9[13] and of most interest to us, IgG.[13, 40, 149, 245, 246] Furthermore, IgG deposition in the RPE in eyes from AMD donors has also been shown.[156] In concordance with these findings, complement and IgG deposition

have also been reported in drusen of aged Macaca fascicularis monkeys[247] and mouse models of AMD.[171, 208]

It is unclear whether immune complexes could play a role in the pathogenesis of AMD. However, the observation that key components of immune complex-mediated inflammation are present in drusen suggests that they may be involved. In addition, the presence of drusen has been described in the eyes of patients suffering from immune complex-mediated diseases, such systemic lupus erythematosus (SLE)[248] and membranoproliferative glomerulonephritis (MPGN).[13, 14, 249] Evidence for the formation of drusen in patients suffering from lupus is limited but one study in a group of 70 SLE patients has shown a 10% incidence of drusen.[248, 250] In contrast, there have been consistent reports of patients suffering from MPGN, an autoimmune disease characterised by immune complex-mediated damage to the kidney's glomerular basement membrane, developing drusen.[13, 14, 249] These drusen are indistinguishable from AMD-associated drusen histologically and in their immunoreactivity and ultrastructural characteristics.[251] The observations that patients suffering from immune complex-mediated diseases may develop drusen suggest there may be mechanistic parallels between these diseases and AMD.

Accumulation of debris between the RPE and BrM due to age-related and/or environmental damage to the RPE or retina could provide an initial stimulus for the development of a local immune response allowing for inflammation to occur.[74] This could potentially lead to infiltration of macrophages that could phagocytose cellular debris and subsequently act as antigen presenting cells (APCs) in peripheral lymph organs, leading to the development of a humoral response with the production of auto-antibodies against retinal antigens.[74] The formation of immune complexes could occur, eventually leading to the formation of soft, AMD-related drusen and retinal damage.[74] Finally, immune complex deposition could lead to macrophage activation via interaction with FcγRs, potentially contributing to AMD pathology.

1.6.4 Fcγ receptors and immune complex-mediated activation of macrophages

The effect of IC on macrophage function has been mostly studied by polarising macrophages into an M2b phenotype, which has characteristics of both pro- and anti-

inflammatory macrophages. This type of polarisation requires co-stimulation of macrophages with soluble IC and TLR4 agonists such as LPS.[252, 253] M2b macrophages show a prostaglandin E2 (PGE_2) dependent increase in secretion of the anti-inflammatory cytokine IL-10 and decrease in secretion of the pro-inflammatory cytokine IL-12.[254] In addition, M2b macrophages also secrete high levels of the pro-inflammatory cytokines TNF-α, IL-1β, IL-8 and IL-6.[255-258] IC stimulation of macrophages leads to enhanced phagocytosis of soluble IC and IgG-opsonised pathogens[259-261] and production of reactive oxygen species and NO.[238, 262] M2b macrophages were suggested to have a role in inhibiting inflammation while promoting T_H2 responses, scavenging of debris, angiogenesis and tissue remodelling, having been named "regulatory macrophages".[96] The notion that IC activation of macrophages would lead to an anti-inflammatory phenotype was, however, inconsistent with the reports showing increased levels of several pro-inflammatory cytokines, but also with the findings that macrophages isolated from patients suffering from autoimmune diseases such as rheumatoid arthritis had a more pro-inflammatory phenotype.[256, 258]

C.A. Ambarus et al have provided a very comprehensive study which helps the understanding of this complex phenotype.[263] Firstly, the authors compared the effects of stimulation with soluble IC or soluble IC and TLR4 ligands on polarised macrophages. The findings from this study show that, whilst stimulation with IC alone has little effect on the already polarised macrophages, co-stimulation of polarised macrophages with TLR agonists leads to a shift in phenotype towards increased IL-10 secretion, as previously reported. It thus appears that this shift towards M2 alternative activation requires co-stimulation of TLRs and that IC alone is not sufficient to induce it. Secondly, the authors compared the responses of polarised macrophages to stimulation with soluble or immobilised IC. Interestingly, stimulation with immobilised IC (such as may be found in blood vessel walls or drusen) led to robust secretion of pro-inflammatory cytokines, without skewing towards IL-10 secretion.[263] These results illustrate the complexity of IC-mediated inflammation, where the size and solubility of IC, the previous state of activation of macrophages and co-stimulation with other factors all impact on effector function. Previous stimulation of macrophages, tissue microenvironment and interaction with other cells may change expression of different FcγRs, which could account for differences in IC-mediated effector function.

The scavenging and tissue remodelling functions of IC activated macrophages as well as their ability to secrete pro- and anti-inflammatory cytokines (potentially leading to tissue damage or angiogenesis) makes them attractive to study in AMD.

1.6.5 Fcγ Receptors and AMD

1.6.5.1 Autoimmunity

Evidence from animal models as well as clinical studies supports a role for FcγR and susceptibility for autoimmunity. For example deletion of the inhibitory mFcγRII in predisposed mice leads to accelerated SLE-like pathology.[233, 264] In contrast deletion of the activating mFcγRIII protects mice from kidney pathology associated with SLE.[265] These results highlight the importance of appropriate function and expression of inhibitory and activating Fcγ receptors for the control of immune responses. In addition, polymorphisms on this family of receptors are associated with development and progression of autoimmune disease in humans.[266] As FcγRs mediate IgG immune responses, if there is an autoimmune component of AMD pathology then this family of receptors is likely to play a role.

Autoimmunity has been implicated in AMD as 94% of patients with early-AMD and 83% of patients with late-stage AMD display high levels of serum autoantibodies against retinal proteins (as opposed to 9% on healthy age-matched controls).[11, 12, 15] Several studies have identified retinal antigens against which these autoantibodies are raised. These include proteins such as: glial fibrillary acidic protein (GFAP),[16, 267] carboxyethylpyrrole (CEP) protein adducts,[193] vitronectin,[244] α-crystalline, α-enolase,[267] and annexin II (a protein expressed in the RPE).[247] As most of these are intracellular antigens, it is likely that they are generated post cell damage/degeneration. It is unclear whether these autoantibodies have a causative role or are merely a consequence of the disease progression; nevertheless they have the potential to exacerbate pathology if they are allowed to reach the retina, bind to their target to form immune complexes and interact with FcγRs.

Under normal conditions, FcγR expression in the CNS is low.[268] However, it has been shown expression of these receptors is upregulated in the CNS in response to pathologic stimuli such as viral infections.[18] Furthermore, a recent microarray study has shown increased expression of FcγRs in the ageing brain.[269] It is possible that a similar

upregulation occurs in the retina. This would allow FcγR crosslinking by IgG, activation of effector function and possibly contribute to pathology progression via secretion of reactive oxygen species and pro-inflammatory cytokines.

1.6.5.2 Immunotherapy

Current therapy for wet AMD consists of monoclonal antibodies directed against VEGF.[177] Although generally successful not all patients respond well to treatment with Avastin. Efficacy of antibody therapy is often dependent on FcγR-antibody interaction.[270] Accordingly, polymorphisms in hFcγRs affecting their affinity for IgG have been associated with differential patient response to immunetherapy.[271] In particular, polymorphisms resulting in increased affinity for hIgG1 in hFcγRIIa (H131) and hFcγRIIIa (V158) have been associated with significantly better outcome in cancer patients treated with the monoclonal antibodies trastuzumab, rituximab and cetuximab.[272] The contribution of each genotype to outcome of monoclonal antibody therapy seems to vary not only with the monoclonal antibody used but also with the type of cancer being treated.[272] To date, no studies on the association of these polymorphisms with outcome of anti-VEGF immunotherapy in wet AMD have been reported. A single study failed to identify an association between hFcγRIIIa (V158) and outcome of metastic colorectal cancer therapy with Avastin, the same anti-VEGF drug used to treat wet-AMD.[273] The improved outcome of cancer therapy with trastuzumab, rituximab and cetuximab in patients with the H131 and V158 polymorphisms is presumably due to stronger effector function as a result of higher affinity for these therapeutic antibodies.[271] Antibodies used in "wet" AMD immunotherapy, such as Avastin, are intended to neutralise VEGF, preventing it to bind to its receptors, in this way preventing new blood vessels formation. This effect is independent of FcγR-antibody interaction.[274] However, as a whole hIgG1 molecule, Avastin has the potential to interact with FcγRs, which could mediate undesirable side effects. In fact, the use of Avastin vs Lucentis for the treatment of AMD is associated with a significant higher risk of developing intraocular inflammation,[275, 276] retinal bleed or detachment[277] and increased incidence of systemic complications such as thromboembolic events.[276, 278] Hence, polymorphisms of activating FcγR that potentiate FcγR-IgG interactions, as well as effector function, could be detrimental following anti-VEGF mAb treatment in AMD and possibly explain differences in individual response to therapy.

Antibodies can be engineered so that their interactions with FcγR are modified in order to improve therapeutical outcome without undesired side effects.[270] Understanding the role of FcγR and immune complex mediated inflammation in the retina is thus essential to allow improved monoclonal antibody therapy.

1.7 Summary

AMD is a multifactorial disease with no single factor causing it. Several lines of evidence now support a role for inflammation in the pathogenesis of AMD. Environmental factors contributing to development of the disease, such as smoking and high dietary intake of lipid are known to cause oxidative stress, which in turn can contribute to inflammation. Similarly, gene polymorphisms associated with higher risk of disease incidence are closely linked with inflammation. Further supporting a role of inflammation are clinical and experimental observations showing abnormal accumulations of macrophages near injury sites. The presence of high titers of anti-retinal autoantibodies and the deposition of IgG and drusen and RPE in AMD eyes suggest a possible role for immune complex-mediated inflammation in the development of AMD. Fcγ receptors have been shown to be key mediators of immune complex-mediated responses, thus, they may be important in pathogenesis of AMD. In addition, FcγR activation may also provide a possible mechanism by which therapeutic antibodies can induce inflammation and thus cause unwanted side-effects. This thesis aims to investigate whether immune complex-mediated inflammation may be one of the factors contributing to pathology of AMD.

1.8 Aims

The main aims of this project are:

1. To investigate the biological effect of immune complex formation in the retina, including the induction of inflammation and the kinetics of the response.
2. To investigate the role of activating Fcγ receptors in immune complex-mediated responses in the retina.
3. To investigate the presence of immune complex and Fcγ receptors in human AMD.
4. To investigate the effect of pro-inflammatory mediators secreted from polarised macrophages on human RPE barrier function.

Chapter 2:

Materials and Methods

2.1 In vivo methods

2.1.1 Animals

All mice were housed in groups of 4-10 in plastic cages under standard light (12h:12h light-dark cycle with light on at 07.00h) and temperature (19-23^{o}C) regimes with wood chip bedding and a red plastic shelter as environmental enrichment. Mice were fed standard Chow diet (RM1, SDS, UK) and water *ad libitum*. All procedures were performed in accordance with the United Kingdom Home Office Licensing Inspectorate and after obtaining ethical approval by the University of Southampton.

Mice used for the experiments in this thesis were bred at the Biomedical Research Facility (BRF), Southampton, UK. Six- to eight-week old female C57BL/6, BALB/c, C1q deficient (C1q$^{-/-}$), Fcγ chain deficient ($\gamma^{-/-}$), FcγRI deficient (CD64$^{-/-}$), FcγRIII deficient (CD16$^{-/-}$) and FcγRIV deficient (FcγRIV$^{-/-}$) on a BALB/c background were used. γ-chain$^{-/-}$ mice on a C57BL/6 background were obtained from The Jackson Laboratory, CD64$^{-/-}$ mice on a C57BL/6 background were obtained from Jan G. J. van der Winkel (Utrecht, The Netherlands), CD16$^{-/-}$ mice on a C57BL/6 background were obtained from Sjef Veerbek (Leiden, The Netherlands) and FcγRIV$^{-/-}$ mice on a C57BL/6 background were generated by H.T. Claude Chan (Southampton, UK). $\gamma^{-/-}$, CD64$^{-/-}$, CD16$^{-/-}$ and FcγRIV$^{-/-}$ mice were back crossed for 10 generations onto a BALB/c background in house. C1q$^{-/-}$ mice on a BALB/c background were obtained from Aras Kadioglu (Leicester, UK) with permission from Marina Botto (London, UK).

2.1.2 Induction of Immune Complexes in the Retina

Mice were immunised against ovalbumin (OVA) by intraperitoneal (i.p.) injection of 50µg of OVA (Sigma-Aldrich, UK) in a 1:1 mixture of physiological sterile saline (0.9% NaCl, Fannin, UK) and Imject Alum Adjuvant (Alum; Thermo Scientific, UK). Two and four weeks after the initial immunisation, mice received an additional dose of OVA without adjuvant i.p. (100µg of OVA in saline). Six weeks after the initial immunisation, 10µg of endotoxin- free EndoGrade OVA (Hyglos, Germany) in 1µl saline was injected intravitreously under anaesthesia with a 10% Ketaset (Fort Dodge Pharma, UK)/5% Xylazine (Bayer, UK) mixture in saline. Anaesthetics were administered i.p. at a dose of 10µl/g of body weight. Intravitreal injections were

performed using a fine-glass micropipette with a diameter of less than 50µm (Sigma-Aldrich, UK). After intravitreous injection, Lacri-lube eye ointment (Allergan, UK) was directly applied to both eyes and mice were left to recover in a regulated temperature chamber at 38^{o}C. Animals sensitised to OVA and injected intravitreously with 1µl physiological sterile saline, or naive animals receiving 10µg of EndoGrade OVA intravitreously in 1µl in saline, were used as controls. Tissue was collected at several time points after intravitreous injection, up to 14 days (Figure 2.1.).

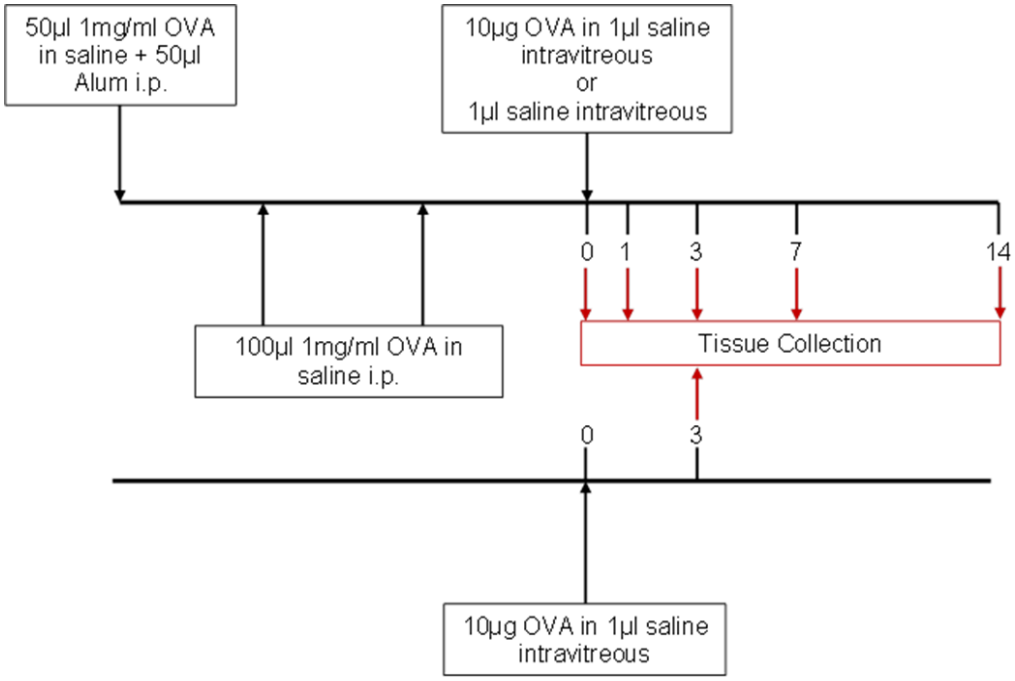

Figure 2.1. Timeline of immunisation protocol, intravitreous injection and tissue collection. Mice were immunised against OVA by i.p. injection with 50µg of OVA in 100µl of a 1:1 Alum and saline mixture and boosted at 2 and 4 weeks after with 100µg OVA in 100µl saline. Mice were then challenged intravitreously with 10µg of OVA in 1µl saline on day 0. Animals sensitised to OVA and injected intravitreously with 1 µl physiological sterile saline, or naive animals receiving 10µg of OVA intravitreously in 1 µl in saline, were used as controls. Tissue was collected at several time points after intravitreous injection, up to 14 days.

2.1.3 Macrophage depletion

Macrophage depletion was performed with liposomes containing clodronate (Cl_2MBP; Dichloromethylenediphosphonic acid; Sigma, UK). Liposomes containing phosphate buffered saline (PBS) were used as a control. Liposomes containing clodronate or PBS

were kindly prepared by Stephen Beers (Southampton, UK). Mice were sensitised to OVA (Sigma-Aldrich, UK) as in section 2.1.2. Two and one day before intravitreous injection of OVA, 100µl of liposomes containing 0.6M of clodronate in dH_2O or PBS were injected intravenously. Mice were then injected intravitreously with 10µg of endotoxin-free OVA (Hyglos, Germany) in saline. Tissue was collected at 3 and 7 days after injection (Figure 2.2.).

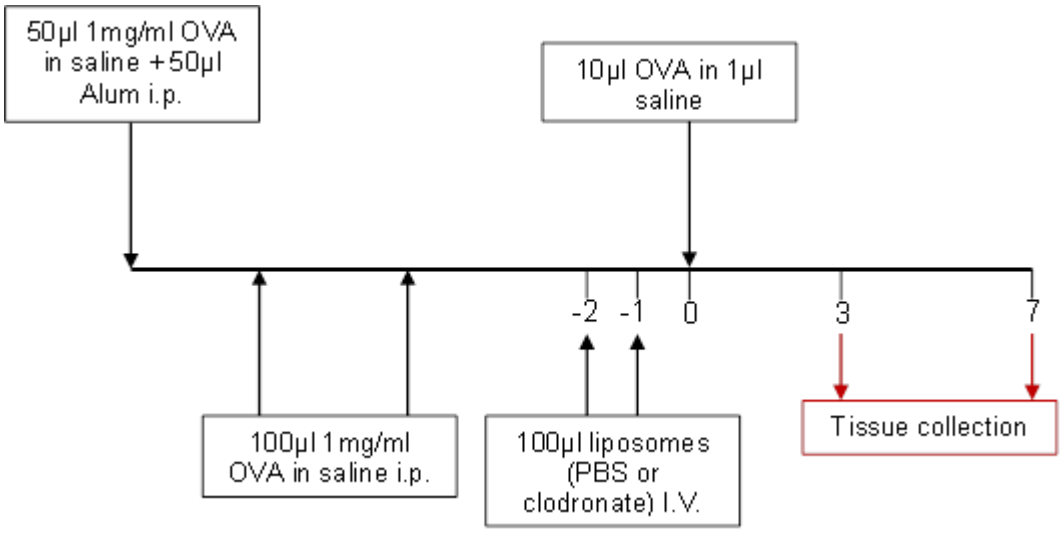

Figure 2.2. Macrophage depletion with liposomes containing clodronate.
Mice were immunised against OVA by i.p. injection with 50µg of OVA in 100µl of a 1:1 Alum and saline mixture and boosted at 2 and 4 weeks after with 100µg OVA in 100µl saline. 100µl of liposomes containing clodronate or PBS were injected intravenously on two consecutive days. Mice were then challenged intravitreously with 10µg of OVA and tissue was collected 3 and 7 days after intravitreous challenge.

2.1.4 Study of retinal physiology

2.1.4.1 Fundoscopy

In vivo imaging of mouse retinae was carried out using a Micron III camera (Phoenix Research Laboratories, USA). Mice were anaesthetised as in section 2.1.2. Immediately after injection of anaesthetic, a drop of 1% tropicamide (Centaur Services, UK) was administered on the surface of each eye for pupil dilation. Five minutes after tropicamide administration Viscotear Liquid Gel (Centaur Services, UK) was generously applied on to each eye, to avoid corneal drying. Mice were laid down on a freely rotating support, and their eyes aligned with the Micron III camera imaging probe

(Figure 2.3.). A bright field light filter was used and images were acquired once for both eyes on each mouse using the Phoenix Micron IV Retinal Imaging Microscope Software (Phoenix Research Laboratories, USA). Mice were left to recover as before (section 2.1.2.).

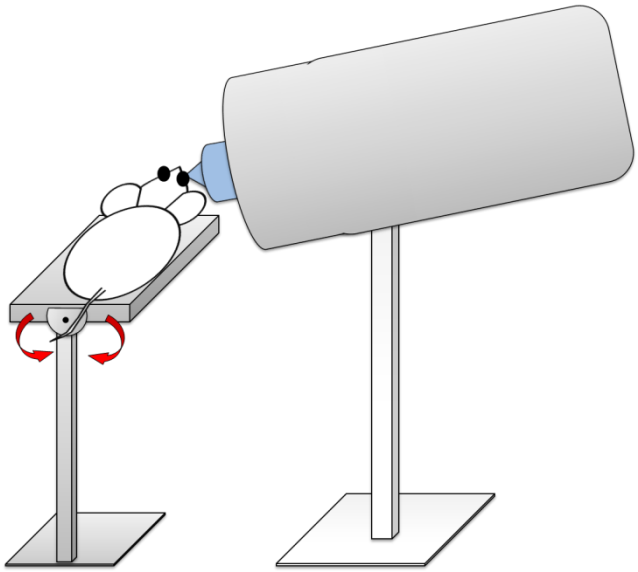

Figure 2.3. Schematic of *in vivo* imaging set-up
Mice are put on a freely rotating support (red arrows) and their eyes aligned with the imaging probe (blue cone).

2.1.4.2 Fluorescein Angiography

Fluorescein angiography was performed using a Micron III camera (Phoenix Research Laboratories, USA). Mice were anaesthetised and their pupils dilated as described in section 2.1.4.1 and then injected i.p. with 100µl of 2.5% w/v fluorescein (Sigma-Aldrich, UK) in physiological saline. Immediately after fluorescein injection mice were prepared for imaging as described in section 2.1.4.1. Mice were laid down on a freely rotating support and their eyes aligned with the Micron III camera imaging probe (Figure 2.3.). The light filter was switched to 490nm and pictures were acquired every 30 seconds for 5 minutes and then at 10 and 15 minutes using the Phoenix Micron IV Retinal Imaging Microscope Software (Phoenix Research Laboratories, USA).

2.1.4.3 Electroretinogram

Electroretinograms (ERGs) were recorded using a Phoenix Image-Guided Focal ERG System (Phoenix Research Laboratories, USA). As the predominant type of photoreceptor in the mouse retina are the rods, scotopic ERGs were recorded. For dark

adaptation, mice were left in their cages with food and water and under regulated temperatures (19-23^{o}C) in a dark room for 4 hours, after which mice were anaesthetised, their pupils dilated as before (sections 2.1.2. and 2.1.4.1.) and prepared for ERG analysis. Mice were placed on a freely rotating support and two electrodes were attached to each mouse: a ground electrode at the base of the tail and a reference electrode subcutaneously between the ears. ERGs were recorded from dark adapted mice by placing a gold-tipped ring corneal electrode attached to the Micron III camera (Phoenix Research Laboratories, USA) in contact with the cornea (Figure 2.4.). Responses to a 2490cd/m^2 white light flash stimulus delivered in the dark by the LED light component of the Phoenix Image-Guided Focal ERG System (Phoenix Research Laboratories, USA) were recorded, stored and analysed using LabScribe Data Recording Software (iWorx, USA). Baseline recordings were taken at least 7 days before treatment. All procedures were performed under dim red light.

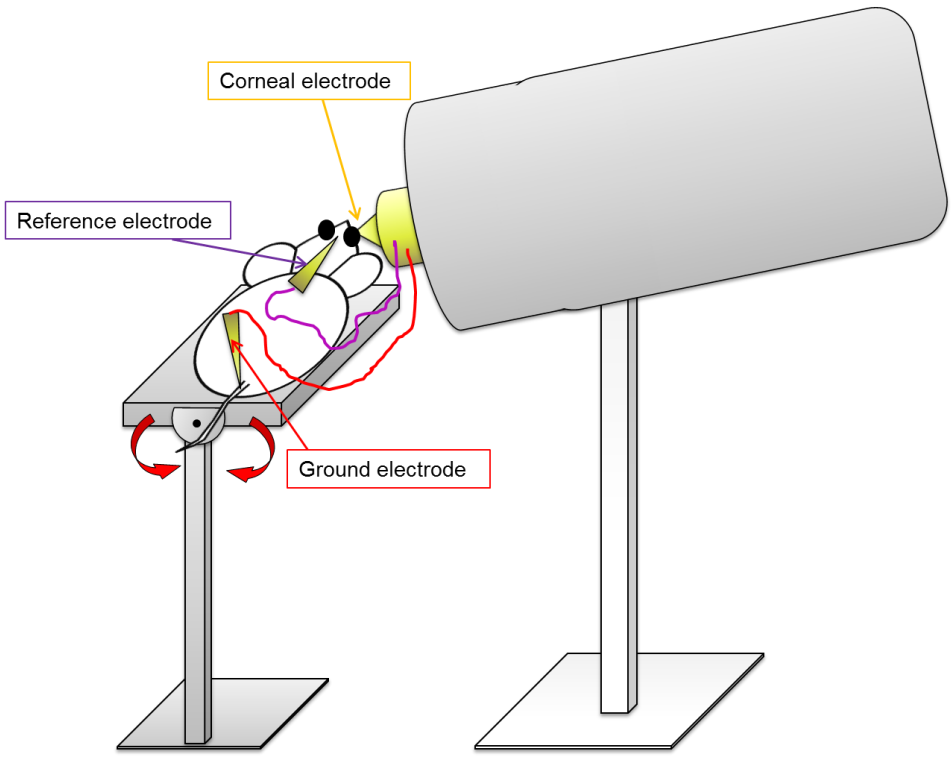

Figure 2.4. Schematic of ERG set-up.

Mice are placed in a freely rotating support (red arrows). A ground electrode (red line) is inserted at the base of the tail and a reference electrode subcutaneously between the ears (purple line). A corneal electrode (golden cone) is placed on the cornea.

2.1.5 Tissue harvesting

2.1.5.1 Tissue harvesting for immunohistochemistry

Mice were terminally anaesthetized with 2,2,2, tribromoethanol in tertiary amyl alcohol (rat Avertin) and transcardially perfused with 0.9% saline with heparin (5000units/ml; CP Pharmaceuticals, UK). Eyes and spleen were collected, embedded in optimal cutting temperature medium (OCT; Sakura Finetek, UK), quickly frozen in isopenthane (Fisher Scientific, UK) above dry ice and stored at -20 ºC until used. 20µm eye sections or 10µm spleen sections were cut on a cryostat, transferred onto 3'Aminopropyltriethoxysilane (APES)-coated slides and kept at -20 ºC until used for immunohistochemistry.

For retinal whole-mounts mice were terminally anaesthetized with rat Avertin and transcardially perfused with heparinised saline and perfused-fixed with 4% paraformaldehyde (PFA). Eyes were collected and post-fixed for 4h at RT in 4% PFA and stored in PBS at 4^{o}C until used.

2.1.5.2 Tissue harvesting for qPCR analysis

Mice were terminally anaesthetised with rat Avertin and transcardially perfused with heparinised saline (section 2.1.5.1). The eyes were collected and the retina was immediately separated from the rest of the eye cup. After dissection, the retinae were snap frozen in liquid nitrogen and kept at -80^{o}C until further use.

2.1.5.3 Serum collection for analysis of anti-OVA antibody titers

Upon terminal anaesthesia mice were exsanguinated by puncture to the right atrium and a blood sample was collected. Samples were centrifuged at 956xg at 4^{o}C for 10 minutes to separate erythrocytes and white blood cells from serum. The serum was collected and kept at -20^{o}C until further use.

2.2 Histology

2.2.1 Haematoxylin and Eosin stain

20µm eye sections were retrieved from -20^{o}C, dried at 37ºC for 40 minutes, fixed in 100% ethanol at 4ºC for 15 minutes and then left in tap water for 2 minutes. The slides

containing the eye sections were then immersed in Harris Haematoxylin (BDH Laboratory Supplies, UK) for 10 minutes followed by three washes in tap water and 1 minute in Acid Alcohol (70% Ethanol 1% HCl) for nuclear staining. For cytoplasmic staining, the slides were immersed in 0.5% Eosin for 1 minute. Finally the sections were dehydrated and coverslipped with Depex (Fisher Scientific, UK) mounting medium. The sections were analysed with a Leica DM5000 microscope (Leica Microsystems Inc., USA).

2.2.2 Immunofluorescence

Immunofluorescence was performed to assess microglial phenotype changes (CD11b, CD45 and MHC II), Fcγ Receptor expression (CD64, CD16, CD32/CD16 and FcγRIV), immune-complex formation (OVA, IgG, IgG1, IgG2a, IgG2b) and leukocyte infiltration (CD3, CD4, CD8, Neutrophil Elastase). Antibody details are shown in Table 2.1.

20μm sections were dried at 37ºC for 40 minutes and fixed in 100% ethanol (Fisher Scientific, UK) at 4ºC for 15 minutes followed by 3 x 5 minutes washing steps in PBS. The sections were blocked in 5% w/v Bovine Serum Albumin (BSA; Fisher Scientific, UK) and appropriate 10% animal serum (Table 2.2., Vector Laboratories, UK) with 0.01% Triton X100 (Sigma-Aldrich, UK) in PBS for 30 minutes and consequently incubated with primary antibodies (Table 2.1.) for 30-48 hours at 4^{o}C. The sections were washed 3 x 5 minutes in PBS and incubated with secondary antibodies (Table 2.2.) in PBS+0.01% Triton X100 for 1 hour at room temperature. Following another 3 x 5 minutes washing steps in PBS the slides were coverslipped with DAPI (4',6-diamidine2-phenylindole) containing ProLong Gold Antifade Reagent mounting medium (Invitrogen, UK).

Table 2.1. Primary antibodies used for immunohistochemistry with mouse tissue

Primary antibody	Antibody Details	Catalogue Number	Distributor	Optimal concentration
CD11b (5C6)	Rat mAb	MCA711G	AbD Serotec, UK	2 μg/ml (1:500)
CD45 (YW62.3)	Rat mAb	MCA1388	AbD Serotec, UK	1 μg/ml (1:1000)
CD32/CD16 (FCR4G8)	Rat mAb, FITC	MCA2305F	AbD Serotec, UK	2 μg/ml (1:500)
CD64 (AT152-9)	Rat mAb	*	Cancer Sciences, FoM, Southampton, UK*	2 μg/ml (1:500)
CD16 (AT154-2)	Rat mAb	*	Cancer Sciences, FoM, Southampton, UK*	4 μg/ml (1:250)
FcγIV (AT137)	Rat mAb	*	Cancer Sciences, FoM, Southampton, UK*	2 μg/ml (1:500)
MHC II (M5/114.15.2)	Rat mAb	ab64528	Abcam, UK	2 μg/ml (1:500)
OVA	Rabbit pAb	W59413R	Biodesign International, UK	1 μg/ml (1:1000)
Mouse IgG	Sheep F(ab')2, FITC	F2266	Sigma-Aldrich, UK	2 μg/ml (1:500)
Mouse IgG	AF546	115-586-062	Jackson ImmunoResearch, US	750 ng/ml (1:2000)
Mouse IgG1	Goat pAb, AF488	115-545-205	Jackson ImmunoResearch, US	1.5 μg/ml (1:1000)
Mouse IgG2a	Goat pAb, AF488	115-545-206	Jackson ImmunoResearch, US	1.5 μg/ml (1:500)
Mouse IgG2b	Goat pAb, AF488	115-545-207	Jackson ImmunoResearch, US	1.5 μg/ml (1:500)
CD3 (KT3)	Rat mAb	ab33429	Abcam, UK	200 ng/ml (1:5000)
CD8 (53-6.7)	Rat mAb	14-0081-81	eBioscience	2 μg/ml (1:500)
CD4 (GK1.5)	Rat mAb	MCA4635GA	AbD Serotec	2 μg/ml (1:500)
Neutrophil Elastase	Rabbit pAb	ab21595	Abcam, UK	1μg/ml (1:1000)

* Antibodies were a kind gift from Professor Mark Cragg.

Table 2.2. Secondary antibodies used for immunohistochemistry with mouse tissue

Primary antibody	Antibody Details	Catalogue Number	Distributor	Optimal concentration	Serum used for blocking
Rat IgG	Donkey pAb, AF488	A21208	Invitrogen, UK	2 μg/ml (1:500)	Donkey
Rabbit IgG	Goat pAb, AF488	A11008	Invitrogen, UK	2 μg/ml (1:500)	Goat
Rabbit IgG	Donkey pAb, AF568	A21206	Invitrogen, UK	2 μg/ml (1:500)	Donkey

2.2.3 Quantification of cell staining

Sections were analysed with a Leica DM5000 microscope (Leica Microsystems Inc., USA). Nonoverlapping photomicrographs spanning the retinal sections (over a mean

length of 3.75mm per mouse retina) were collected using the 20x objective and blinded. After acquiring the images each image was given a random code. The codes were only unmasked after quantification.CD11b, CD45, MHC II, CD16, CD64, CD16/CD32, CD3, CD4 and neutrophil elastase positive cells were counted in the subretinal space, plexiform layers and ganglion cell layer only when DAPI-positive nuclei were visible. The number of cells was quantified using the Photoshop CS5 count tool (adobe Systems Inc., UK) and normalised per millimetre of retina using the formula:

$$N° \; of \; cells \; in \; 1000\mu m = \frac{N° \; of \; cells \; per \; section \; x \; 1000}{Length \; of \; section \; (\mu m)}$$

2.3 Quantitative PCR analysis

2.3.1 RNA isolation

Total RNA was extracted using RNeasy Mini Kit (Qiagen, UK) according to the manufacturer's instructions. Briefly, eye tissue (isolated retinae) or cells were homogenised in 350µl of lysis buffer (RLT) containing 1% β-mercaptoethanol. The homogenate was transferred to a gDNA Eliminator spin column and spun at 8000xg for 30 seconds to remove genomic DNA. The flow through was thoroughly mixed 1:1 in 70% ethanol, transferred to an RNeasy spin column and spun for 15 seconds at 8000xg. The column was washed by adding 350µl RW1 Buffer and centrifugation for 15 seconds at 8000xg, followed by two washing steps with 500µl of Buffer RPE and centrifugation for 15 seconds and two minutes at 8000xg. To dry the RNeasy column membrane, the column was transferred to a new collection tube and centrifuged at 8000xg for 1 minute. RNA was eluted by addition of 30µl of RNAse-free dH_2O, which was centrifuged through the column at 8000xg for 1 minute. The eluent was collected and stored at -80^{o}C until further use.

2.3.2 Analysis of RNA quantity and purity

Quantity and purity of the RNA was assessed with a Nanodrop ND-100 Spectophotometer (Fisher Scientific, UK). Nucleic acids absorb at 260nm. Purity of RNA is measured by analysis of the absorbance ratios 260nm/280nm and 260nm/230nm. The 260nm/280 ratio should be close to 2.0 for pure RNA. Values above/below may suggest protein or phenol contamination, which absorb highly at

280nm. The 260nm/230nm ratio should be range between 2.0-2.2. Values bellow or above may suggest contamination with carbohydrates, alcohol, phenol or other substances that absorb at 230nm.

2.3.3 cDNA synthesis

cDNA was synthesised using reagents from Applied Biosystems (UK), unless otherwise stated. 400ng of RNA were added to RNAse free molecular grade water (Sigma-Aldrich, UK) to make up a volume of 7.7µl. This was added to 2µl of RT Buffer, 4.4µl of 25mM $MgCl_2$, 4µl 10mM dNTPs, 1µl 50µM random hexamers, 0.4µl of 20U/µl RNase inhibitor and 0.5µl of 50U/µl Multiscribe RT. The mixtures were incubated at 25^{o}C for 10 minutes, 40^{o}C for 30 minutes and cooled to 4^{o}C for 5 minutes in a PTC240 tetrad 2 peltier thermal cycler (MJ Research, Canada). The resulting DNA was diluted 1:5 and stored at -20^{o}C until further use.

2.3.4 Primer design

Primer sequences were obtained from the Primer Bank (http://pga.mgh.harvard.edu/primerbank/). The sequences were blasted for specificity using NCBI Primer Blast. If possible, primers that crossed exon-exon boundary were chosen. Primers were synthesised and ordered from Sigma-Aldrich Custom DNA Oligos (Sigma-Aldrich, UK). Specificity of primers was assessed through analysis of melting curves of a quantitative PCR (qPCR) run and by loading qPCR products on a 1.5% w/v agarose gel (Fisher Scientific, UK) with 0.003% v/v ethidium bromide (Fisher Scientific, UK) run at 90mV for approximately 20minutes depending on the expected size of the product.

2.3.5 Quantitative PCR

5µl of the diluted cDNA was used for the qPCR reaction. A master mix was made by adding 0.6µl of 10µM primers to 10µl of SYBR Green Supermix (SYBG, Bio-Rad laboratories, UK) and 3.8µl of molecular grade water (Sigma-Aldrich, UK). The master mix and sample were pipetted onto 96 well non-skirted low profile plates (Starlab, UK). The plates were then covered with optical caps (Starlab, UK), centrifuged for 2min at 1721xg and placed into a PTC-200 peltier thermal cycler (MJ Research, Canada) for the qPCR reaction. After incubating at 95^{o}C for 5 minutes 44 qPCR cycles were performed

and consisted of denaturing at 95^{o}C for 30 seconds, annealing at 60^{o}C for 1 minute, plate read and extension at 72^{o}C for 1 minute. After the qPCR cycles a melting curve from 55^{o}C to 90^{o}C at intervals of 0.2^{o}C was constructed, and then the samples were incubated at 4^{o}C until the cycle was terminated.

All samples were pipetted onto the plates in duplicate. A negative control (master mix + 5µl molecular grade water) and a positive control (master mix + 5µl cDNA sample with expected robust expression of target gene) were also loaded in duplicate onto each plate. Change in fluorescence in each well was measured and recorded using MJ Opticon Monitor 3.1.32 software (BioRad, UK). Glyceraldehyde-3-phosphate dehydrogenase (GAPDH) was measured in each sample as a reference gene (RG). The primer sequences for the reference gene and genes of interest (GoI) used for mouse tissue are listed on Table 2.3. Primers used for qPCR analysis of ARPE19 cells are listed in Table 2.4. Analysis of C(t) values was carried out using the $2^{\wedge\Delta\Delta C(t)}$ method, where relative gene expression of a gene of interest is compared to expression of the house-keeping gene using the formula:

$$Relative\ expression = 2\wedge(C(t)RG - C(t)GoI)$$

Table 2.3. qPCR primer sequences for murine genes

Gene	Oligonucleotide	Sequence
GAPDH	Forward	5’ TCCACCACCCTGTTGCTGTA-3’
GAPDH	Reverse	5’TGAACGGGAAGCTCACTGG-3’
TNF-α	Forward	5’CTCCAGGCGGTGCCTATG-3’
TNF-α	Reverse	5’GGGCCATAGAACTGATGAGAGG-3’
IL-10	Forward	5’ GCTCTTACTGACTGGCATGAG-3’
IL-10	Reverse	5’CGCAGCTCTAGGAGCATGTG-3’
IL-6	Forward	5’CCAGAGATACAAAGAAATGATGG-3’
IL-6	Reverse	5’ACTCCAGAAGACCAGAGGAAAT-3’
iNOS	Forward	5’CCAAGCCCTCACCTACTTCC-3’
iNOS	Reverse	5’CTCTGAGGGCTGACACAAGG-3’
Arg1	Forward	5’CTCCAAGCCAAAGTCCTTAGAG-3’
Arg1	Reverse	5’AGGAGCTGTCATTAGGGACATC-3’
CCL2	Forward	5’AGCATCCACGTGTTGGCTC-3’
CCL2	Reverse	5’CCAGCCTACTCATTGGGATCAT-3’
CCL5	Forward	5’CATATGGCTCGGACACCA-3’
CCL5	Reverse	5’ACACACTTGGCGGTTCCT-3’
C5	Forward	5’GCATTTCTGACACCAGGCTTC-3’
C5	Reverse	5’ AGCGCACAGRCAGCRRCCA -3’
C5R1	Forward	5’GCCATCCGCAGGTATGTTAG-3’
C5R1	Reverse	5’TTACCACAGAACCCAGGAGG-3’
VEGF	Forward	5’GATCCGCAGACGTGTAAATGTT-3’
VEGF	Reverse	5’TCACCGCCTCGGCTTGTCACAT-3’

Table 2.4. Primers used for qPCR analysis of ARPE19 cells

Gene	Oligonucleotide	Sequence
β- Tubulin	Forward	5'AATCCCCACCTTTTCTTACTCC-3'
β- Tubulin	Reverse	5'AAAGATGGAGGAGGGTTCCC-3'
ZO-1	Forward	5'GACCAATAGCTGATGTTGCCAGA-3'
ZO-1	Reverse	5'TGCAGGCGAATAATGCCAGA-3'
Occludin	Forward	5'AAGAAGTTGACAGTCCCATGGCAT-3'
Occludin	Reverse	5'ATCCACAGGCGAAGTTAATGGAA-3'
CFH	Forward	5'GTGAAGTGTTTACCAGTGACAGC-3'
CFH	Reverse	5'AACCGTACTGCTTGTCCAAAA-3'
CD64	Forward	5'ATGTGGTTCTTGACAACTCTG-3'
CD64	Reverse	5'GTAGCTGGGGGTCGAGGT-3'
CD32b	Forward	5'CTCTCCCAGGATACCCTGAGT-3'
CD32b	Reverse	5'GGTGCATGAGAAGTGAATAGGTG-3'

2.4 ELISA detection of anti-OVA IgG

96 MicroWell Solid plates (Nunc Brand Products, UK) were coated with OVA (Sigma-Aldrich, UK) by placing 100µl of 10µg/ml of OVA in 0.05M $NaHCO_3$ (Fisher Scientific, UK)/Na_2CO_3 (AnalaR, UK) buffer (pH 9.6) and left overnight at room temperature. The following day the plate was washed 4 times with washing buffer (PBS + 0.05% Tween; ICN Biomedicals, UK). Blocking was performed by incubating with 150µl of 1% BSA in PBS per well at room temperature for 30 minutes. The block was aspirated and 100µl of 1% BSA in PBS were added per well. 10µl of serum samples were added to each well of the first row, diluted across the plate 1 in 10, and left to

incubate for 1 hour at room temperature on a shaker, after which the plate was washed 4 times with washing buffer. 100µl of anti-mouse IgG antibody (Table 2.4.) at appropriate dilution in 1% BSA in PBS were added to each well and left to incubate for 1 hour on a shaker at room temperature. After 4 washes with washing buffer 100µl of Streptavidin-polyHRP (1:10000; Sanquin, Netherlands) in 1% BSA were added to each well and incubated at room temperature for 30 minutes. Substrate solution (1x1mg tablet of 3,3',5,5'–Tetramethylbenzidine (TMB; Sigma-Aldrich, UK) in 1ml Dimethyl sulfoxide (DMSO; Fisher-Scientific, UK) + 9ml 0.05M Citrate buffer (Sigma-Aldrich, UK)) was prepared and 100µl added per well for approximately 30 seconds. To stop the reaction 100µl of H_2SO_4 were added. Optical density was measured using a microtiter recorder set to 450/570 nm.

Table 2.5. Antibodies used for ELISA

Primary antibody	Antibody Details	Catalogue Number	Distributor	Optimal concentration
Mouse IgG	Horse pAb, biotinylated	BA-2001	Vector Labs, UK	500 ng/ml (1:1000)
Mouse IgG1	Rat mAb, biotinylated	MCA336B	AbD Serotec, UK	500 ng/ml (1:2000)
Mouse IgG2a	Rat mAb, biotinylated	MCA1588B	AbD Serotec, UK	250 ng/ml (1:1000)
Mouse IgG2b	Rat mAb, biotinylated	MCA424B	AbD Serotec, UK	500 ng/ml (1:2000)

2.5 Human tissue

2.5.1 Tissue Harvesting

Experiments using human tissue were performed in collaboration with Robert Mullins (University of Iowa, USA). Human donor eyes were obtained from the Iowa Lions Eye Bank (Iowa City, IA) following informed consent from the donors' families. The study was approved by Southampton & South West Hampshire Research Ethics Committee (A; REC No. 09/H0504/67). Tissue was collected and processed by Robert Mullins, Aditi Khanna and Miles Flamme-Wiese (Iowa, USA). Briefly donor eyes were placed in 4% PFA and using a razorblade the anterior and posterior portions of the eye were separated. Four incisions were cut on the posterior part of the eye creating a "cloverleaf" (Figure 2.5.). Using an 8mm trephine punch the macula was collected. The tissue was then rinsed in PBS + 5% sucrose 3x5 minutes on a rocker. For cryoprotection

tissue was sequentially incubated for 30 minutes on a rocker in three mixtures of 5% and 20% sucrose, initially at a 2:1 (5% : 20%) ratio, then 1:1 and finally 1:2, before leaving the tissue to incubate in 20% sucrose in PBS at 4°C overnight. Finally tissue was incubated in a mix of 20% sucrose and OCT (2:1 ratio) for 30 minutes before transfer to an embedding mould and freezing in OCT by submerging the face of the mould on liquid nitrogen. 8µm sections were cut on a cryostat and stored at -20°C until use.

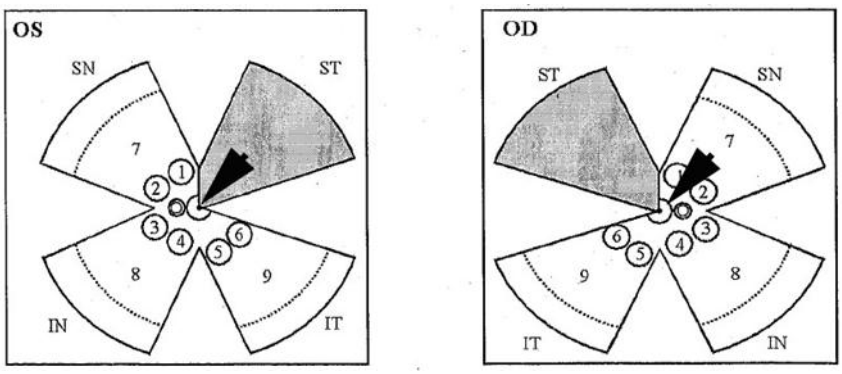

Figure 2.5. Schematic of human donor eyes.
Tissue was collected from the superior-temporal quadrant (ST), macula (arrows), 6mm punches from 1-6 and quadrant "left-overs" 7-9 for immunohistochemistry. ST-superior temporal quadrant, SN – superior nasal quadrant, IT-inferior temporal quadrant, SN- superior nasal quadrant, OS – Oculus Sinistrus (left eye), OD – Oculus Dextrus (right eye). *Courtesy of R. Mullins*

2.5.2 Immunofluorescence

Staining for IgG and UEA1, IgG and MAC, CD45 and CD32b, CD45 and CD64 and CD45 and CD16 was performed at the University of Iowa, whilst staining for IgG and C1q, CD45 and CD32a, CD3, mast cell tryptase and neutrophil elastase was performed at the University of Southampton.

After drying at room temperature for 10 minutes, the sections were blocked in 10% w/v BSA (Fisher Scientific) in PBS containing 1mM $CaCl_2$ (Fisher Scientific) and 1mM $MgCl_2$ (Fisher Scientific) for 15 minutes after which the primary antibodies (Table 2.5.) in PBS were added and incubated for 1 h. After 3x5 minutes washing steps in PBS, secondary antibody (Table 2.6.) dilutions in PBS (University of Southampton) or in PBS containing 1:2000 DAPI (Sigma, USA; University of Iowa) were incubated for 30 minutes at room temperature. Following another 3x5 minutes washing steps in PBS the slides were coverslipped. Sections stained at the University of Iowa were coverslipped

with Aquamount (Sigma-Aldrich, USA) mounting medium, sections stained at the University of Southampton were coverslipped with DAPI containing ProLong Gold Antifade Reagent mounting medium (Invitrogen, UK).

Table 2.6. Primary antibodies used for immunofluorescence with human tissue

Primary antibody	Antibody Details	Catalogue Number	Distributor	Optimal concentration
Human IgG	Donkey Fab2	706-096	Jackson Labs, UK	1 µg/ml (1:1000)
C1q	Rabbit pAb	A0136	Dako, UK	2 µg/ml (1:500)
MAC (aE11)	Mouse mAb	M0777	Dako, US	2 µg/ml (1:500)
CD45 (HI30)	Mouse mAb	555480	BD Biosciences, US	2 µg/ml (1:500)
UEA1*	*Lectin – Biotinylated	B-1065	Vector Laboratories, US	1 µg/ml (1:1000)
CD32b (EP888Y)	Rabbit mAb	Ab45143	Abcam, UK	2 µg/ml (1:500)
CD32a (EPR6658)	Rabbit mAb	ab125013	Abcam, UK	2 µg/ml (1:500)
CD64	Goat pAb	AF1257	R&D Systems	2 µg/ml (1:500)
CD16 (2H7)	Mouse mAb	MCA1816	AbD Serotec, UK	-
CD3 (7.2.38)	Mouse mAb	Ab699	Abcam, UK	10 µg/ml (1:100)
Neutrophil Elastase	Rabbit pAb	Ab21595	Abcam, UK	-
Mast Cell Tryptase (AA1)	Mouse mAb	Ab2378	Abcam, UK	5 µg/ml (1:200)

Table 2.7. Secondary antibodies used for immunofluorescence with human tissue

Primary antibody	Antibody Details	Catalogue Number	Distributor	Optimal concentration
mouse IgG	Donkey pAb, AF488	A21208	Invitrogen	2 µg/ml (1:500)
mouse IgG	Donkey pAb, AF546	A21208	Invitrogen	2 µg/ml (1:500)
Rabbit IgG	Donkey pAb, AF488	A21206	Invitrogen	2 µg/ml (1:500)
Streptavidin	Streptavidin 546	S11225	Invitrogen	2 µg/ml (1:500)

2.5.2.1 Quantification of cell staining

Sections were photographed using the x20 objective of a fluorescence microscope. Sections labelled at the University of Iowa were photographed using a BX41 microscope (Olympus Corporation Inc, USA) and sections labelled at the University of Southampton were photographed using a Leica DM5000 microscope (Leica

Microsystems Inc., USA). Human samples were given random codes based on date of tissue collection by the staff in Rob Mullins lab. The codes were only unmasked after quantification. Nonoverlapping photomicrographs spanning the sections (over a mean length of 511µm per donor) were collected. Stained cells were counted only when DAPI-positive nuclei were visible. In the retina cells were counted across all of the layers, in the choroid/RPE complex only cells outside vascular lumens and within 25µm from the BrM were counted (ensuring only cells in close proximity to choriocapillaris, BrM and RPE are accounted for). The length of the Bruch's membrane was measured and the numbers of cells were then estimated to Burch membrane lengths of 100µm using the formula:

$$N° \; of \; cells \; in \; 100\mu m = \frac{\text{N° of cells per section x } 100}{\text{Length of BrM } (\mu m)}$$

2.6 Cell Culture

2.6.1 ARPE19 cells

ARPE-19 cells were obtained from the American Tissue Culture Collection (ATCC, USA). Cells were maintained at 37^{o}C under humidified atmosphere with 5% CO_2 in culture medium comprising 1:1 (vol/vol) mixture of Dulbecco's modified Eagle's medium (DMEM):F12 (Life Technologies, UK) supplemented with 1% antibiotic-antimycotic solution (10000 units/ml penicillin G, 10mg/ml streptomycin sulphate, 25 mg/ml amphotericin B; Sigma-Aldrich) and 10% foetal bovine serum (FBS; ATCC, USA). The cells were used at passages 22 to 28 and were maintained in tissue culture flasks (Corning, UK). Media was changed twice a week. When confluent, cells were passaged by trypsinisation.

2.6.1.1 Trypsinisation of ARPE19 cells

Cells were washed twice with 8ml of Hank's Balanced Salt Solution (HBSS; Life Technologies, UK) and then incubated at 37^{o}C for 5 minutes with 3 ml of 0.5% trypsin (ATCC, USA). 5ml of fresh media were added to stop the reaction. The cell suspension was then centrifuged at 120xg for 5 minutes. Cells were resuspended in 2ml of fresh media, 25µl of cell suspension was stained with 25µl of tryphan blue (Sigma-Aldrich, UK) and cell counts were performed using a hemocytometer.

2.6.1.2 ARPE19 cell seeding

For measurement of transepithelial electrical resistance (TEER) ARPE-19 cells were seeded onto Transwell Permeable Supports with a 0.4μm pore polyester membrane on 24-well plates (transwell filter; Corning, UK). Transwell membranes were coated with 10μg/cm^2 of laminin (Sigma-Aldrich, UK) in sterile PBS (Life Technologies, UK) overnight and washed 3 times with sterile PBS before seeding. To allow formation of confluent cell layers and measurement of TEER, ARPE-19 cells were seeded at a density of $3x10^5$cells/cm^2. Confluent monolayers were cultured in 300μl of culture medium (DMEM/F12 + 1% antibiotic-antimycotic solution + 10% FBS) in the apical chamber and 600μl in the basal chamber (Figure 2.6.). Culture medium was changed every 48 hours.

For qPCR experiments, ARPE19 cells were seeded onto 24 well plates (Corning, UK) at a density of $3x10^5$ cells/cm^2. To allow formation of functional tight junctions, cells were grown for at least a week after confluence in 600μl of culture medium (DMEM/F12 + 1% antibiotic-antimycotic solution + 10% FBS) before stimulation. Culture medium was changed every 48 hours.

For immunocytochemistry cells were seeded onto 5mm diameter glass coverslips (VWR international, UK) on 48 well plates at a density of $3x10^5$ cells/cm^2. Glass coverslips were washed by placing in 2% Micro90 (Sigma-Aldrich, UK) in distilled water in a beaker at 60^{o}C on a water bath for 30 min, followed by 4 rinses in distilled water. The beaker containing the coverslips in distilled water was placed again at 60^{o}C on the water bath for 15 min. After rinsing a further 4 times coverslips were placed in 100% ethanol and sterilised by flaming before seeding. To allow formation of functional tight junctions, cells were grown for at least a week after confluence in 300μl of culture medium (DMEM/F12 + 1% antibiotic-antimycotic solution + 10% FBS). Culture medium was changed every 48 hours.

2.6.2 Human Macrophages isolation and polarisation

Supernatants from polarised macrophages derived from human blood were a kind gift from Stephen Beers (Southampton, UK) and human macrophage isolation and polarisation experiments were performed by Lekh Dahal (Southampton, UK). Briefly macrophages and monocytes were isolated from whole-human-blood using

Lymphoprep gradient separation (STEMCELL technologies, UK). The isolated cells were cultured with 100ng/ml M-CSF (Peprotech, UK) in macrophage cell culture medium (DMEM + Penicillin/Streptomycin + L-glutamine + sodium pyruvate + 10% FCS) for 2 days, after which the medium was changed to macrophage cell culture medium with 50ng/ml M-CSF (Peprotech, UK). To induce macrophage polarisation towards a pro-inflammatory M1, alternatively activated M2a or M2c, or immune complex-activated phenotype, macrophages were stimulated 6 days after isolation. Macrophages were stimulated with 50 ng/ml LPS (Sigma-Aldrich, UK) and 2 ng/ml IFN-γ (M1; Peprotech, UK) ,10 ng/ml IL-4 and 10 ng/ml IL-13 (M2a; Peprotech, UK), 10 ng/ml IL-10 (M2c; Prepotech, UK) or 10 μg/ml of large heat-aggregated human IgG (MIC) in macrophage culture medium for 48 hours. The concentrations of cytokines were chosen based on experiments performed by Lekh Dahal. To analyse the effect of Avastin and Lucentis on macrophage activation, isolated macrophages were seed onto 96-well plates coated with 5μg/ml of Avastin or Lucentis at a density of $4x10^5$ cells/ml ($4x10^4$ cells/well) and incubated for 48 hours. The concentration of Avastin and Lucentis and cell density were chosen based on previous experiments performed in our lab by James Fuller. Supernatants were collected and stored at -20^oC until use.

2.6.3 ARPE19 cell stimulation

For assay optimisation, ARPE19 cells were stimulated with the following stimuli in serum free DMEM/F12 + 1% antibiotic-antimycotic solution: 50 ng/ml LPS (Sigma-Aldrich, UK) and 2 ng/ml IFN-γ, 10 ng/ml IL-4 and 10 ng/ml IL-13 and 10 ng/ml IL-10. To determine the effect of direct stimulation on ARPE19 cell function, the same stimuli as above in macrophage culture medium (section 2.6.2.) were added. To determine the additional effect of macrophage activation, conditioned media of M1, M2a, M2c or MIC polarised macrophages as described in section 2.6.2. were added to ARPE19 cells. Macrophage culture medium or conditioned medium from non-stimulated macrophages were added as controls. (All recombinant cytokines used in these experiments were acquired from Prepotech, UK).

For TEER experiments ARPE19 cells were grown on transwell filters until stable TEER were obtained (typically 7 to 15 days for TEER values of 35-50 Ω/cm2). Cells were stimulated by adding 300μl of stimuli (as above) in the apical chamber. For qPCR and

immunocytochemistry ARPE19 cells were stimulated by adding 600µl or 300µl, respectively, of medium containing different stimuli (as above) to the wells.

2.6.4 Transepithelial electrical resistance (TEER)

TEER was measured using an epithelial voltohmmeter (EVOM2; World Precision Instruments, UK) with a STX2 electrode (World Precision Instruments, UK). The STX2 electrode was introduced in the apical and basal chambers simultaneously (Figure 2.6.) and TEER measurements were taken at several time points after stimulation (section 2.6.3), up to 24 hours. All TEER measurements were taken immediately after removal of the transwells on 24 well plates from the incubator. Measurements were taken at least 3 times for each transwell and averaged. Each experiment was performed in duplicate or triplicate and independently at least three times.

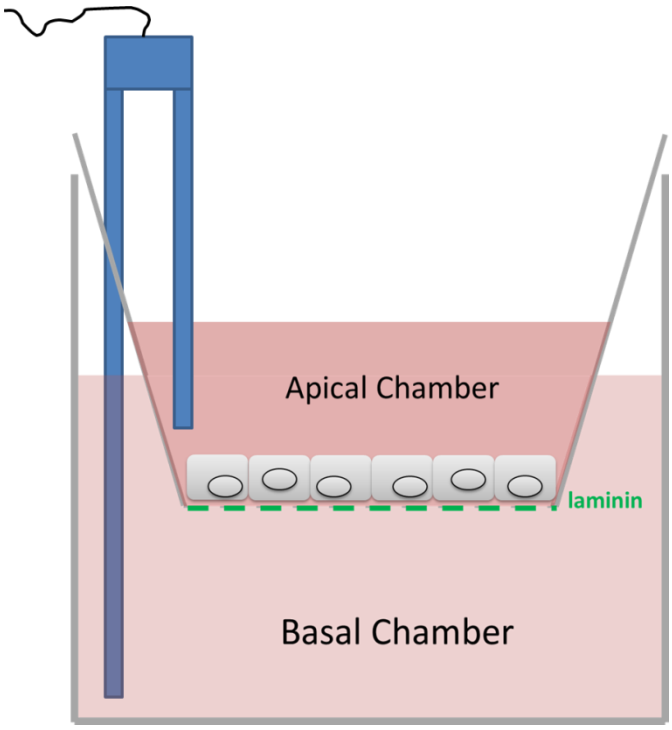

Figure 2.6. Transwell filter schematic.

Transwell Permeable Supports with 0.4µm pore polyester membranes subdivide the culture dish into two medium chambers, with the ARPE19 cells (grey blocks) forming a confluent monolayer on the laminin-coated filter. To measure TEER a STX2 electrode (blue) is inserted in the apical and basal chamber simultaneously.

2.6.5 Lactate dehydrogenase (LDH) cytotoxicity Assay

Cell cytotoxicity was assessed by measuring LDH activity using a cell cytotoxicity kit (Roche). Unless specified, all reagents used were from Roche. A positive control corresponding to 100% cytotoxicity was obtained by adding 300µl of a 2% triton-X100 solution (Sigma-Aldrich, UK) to the apical chamber of a transwell filter containing a confluent monolayer of ARPE19 cells for 30 minutes. Culture medium was used as a negative control and supernatant from non-stimulated ARPE19 cells was used as a "low" control for baseline LDH release.

For 100 reactions 250µl of a catalyst solution are added to 11.25ml of a chromogenic solution (tetrazolium salt). 50µl of the mixture is then added to 50µl of cell supernatant and incubated for 30 minutes, after which absorbance is read at 490nm.

Cytotoxicity was determined using the formula:

$$Cytotoxicity\ (\%) = \frac{experimental\ value - low\ control}{high\ control - low\ control} x100$$

2.6.6 Immunocytochemistry

Tight junction integrity and FcγR expression on ARPE19 cells grown on glass cover slips were used for immunocytochemistry. Antibodies used are listed in Table 2.7.

24 hours after stimulation the cells on coverslips were washed 1x with HBSS (Life technologies, UK) and fixed with ice-cold 4% P.F.A. (Sigma-Aldrich, UK) for 15 minutes. All subsequent steps were performed at room temperature. Cells were permeabilised with 0.2% Triton X-100 (Sigma-Aldrich, UK) for 3 minutes, followed by 3 washes in PBS. Cells were then blocked with 1% BSA (Fisher, UK) + 5% normal serum (Sigma-Aldrich, UK) for 15 minutes and incubated with primary antibodies for 1 hour at room temperature. After 3 washes in PBS cells were incubated with secondary antibodies for 30 minutes. The coverslips were then washed 3x in PBS and mounted onto a glass slide with DAPI containing ProLong Gold Antifade Reagent mounting medium (Invitrogen, UK).

Table 2.8. Details of primary antibodies used for immunocytochemistry

Primary antibody	Antibody Details	Catalogue Number	Distributor	Optimal concentration
Phalloidin	Phalloidin AF488	A12379	Invitrogen, UK	0.3U/ml (1:1000)
ZO1 (1A12)	Mouse mAb	33-9100	Invitrogen, UK	10 µg/ml (1:100)
Occludin (OC-3F10)	Mouse mAb, AF594	331594	Invitrogen, UK	4 µg/ml (1:100)
CD32b (EP888Y)	Rabbit mAb	Ab45143	Abcam, UK	2 µg/ml (1:500)
CD32a (EPR6658)	Rabbit mAb	ab125013	Abcam, UK	2 µg/ml (1:500)
CD64	Goat pAb	AF1257	R&D Systems	2 µg/ml (1:500)
CD16 (2H7)	Mouse mAb	MCA1816	AbD Serotec, UK	-

2.6.7 Griess Assay

The formation of nitric oxide (NO) was investigated by detection of nitrate (NO_2-), a stable breakdown product of NO. 50µl of sulphonamide (Sigma-Aldrich, UK) are added to 50µl of ARPE19 supernatants for 10 minutes, after which 50µl of N-1-naphthyl-ethylenediamine dihrdochloride (NED) (Sigma-Aldrich, UK) were added to the mixture and incubated for 10 minutes. A 12 point 1:2 serial dilution of 100nM of NO_2- (Sigma-Aldrich, UK) was used as a standard curve. Absorbance was then read at 520 nm.

2.6.8 Cytokine and Growth-Factor measurement

2.6.8.1 VEGF and MCP-1 (CCL2) ELISA

VEGF and MCP-1 (CCL2) duo-set ELISA kits were obtained from R&D systems. 96 MicroWell Solid plates (Nunc Brand Products, UK) were coated with 1µg/ml of capture antibody for both assays in 0.05M $NaHCO_3$ (Fisher Scientific, UK)/Na_2CO_3 (AnalaR, UK) buffer (pH 9.6) and left overnight at room temperature. Plates were washed 3 times with washing buffer (PBS + 0.05% Tween; ICN Biomedicals, UK). Blocking was performed by incubating with 150µl of 1% BSA in PBS per well at room temperature for 1 hour. After aspirating the block 100µl of sample or standard were added to the wells. An 8 point standard starting at 2ng/ml was used for both assays. For the VEGF ELISA samples were diluted 1:2 and for the CCL2 ELISA samples were diluted 1:10 for 2 hours at room temperature on a shaker at 400 rpm, after which the plates were

washed 3 times with washing buffer. 100µl of 100ng/ml detecting antibody in 1% BSA in PBS were added to each well and left to incubate for 2 hour at room temperature with shaking. After 3 washes with washing buffer 100µl of Streptavidin-polyHRP (1:10000; Sanquin, Netherlands) in 1% BSA was added to each well and incubated at room temperature for 30 minutes. Substrate solution (1x1mg tablet of 3,3',5,5'–Tetramethylbenzidine (TMB; Sigma-Aldrich, UK) in 1ml Dimethyl sulfoxide (DMSO; Fisher-Scientific, UK) + 9ml 0.05M Citrate buffer (Sigma-Aldrich, UK)) was prepared and 100µl added per well for approximately 5 minutes for both assays. To stop the reaction 100µl of H_2SO_4 were added. Optical density was measured using a microtiter recorder set to 450/570 nm.

2.6.8.2 Mesoscale multiplex cytokine assay

Cytokines secreted by polarised macrophages and ARPE19 were measured using a Human-Proinflammatory II 4-plex Ultra-sensitive kit (IL-1β, IL-6, IL-8, TNF-α; MesoScale Discovery, USA) and a Human-Proinflammatory 7-Plex Ultrasensitive kit (IFN-γ, IL-1β, IL-10, IL-12 (p70), IL-6, IL-8, TNF-α; MesoScale Discovery, USA). Plates were blocked with 150µl of 1% w/v solution of Blocker B (MesoScale Discovery, USA) for 1 hour at room temperature with shaking at 400 rpm and then washed 3x in PBS + 0.05% Tween X20 (Fisher Scientific). 25µl of sample or calibrator (MesoScale Discovery, USA) were then added to the plate and incubated for 2 hours with shaking. 25µl of detection antibody mix (MesoScale Discovery, USA) were added to the plate and incubated for 2 hours with shaking. After washing with 3x with PBS + 0.05% Tween X20 150µl of reading buffer were added to each well and the plates read using a Sector Imager 2400 (MesoScale Discovery, USA). Data was analysed using MSD Discovery Workbench software (MesoScale Discovery, USA).

2.7 Statistical Analysis

All data was analysed using GraphPad Prism Software (La Jolla, CA, USA). All data was initially tested for normal distribution using a D'Agostino and Pearson omnibus normality test. Normally distributed data was analysed using parametric statistical tests, including the Student's t-test, One-way ANOVA and Two-way ANOVA. When not normally distributed, data was transformed using the equation log (y=1+data) and tested for normality. If normally distributed data was analysed as above, if not, a non-

parametric test was then used. When data were analysed with ANOVA an F-ratio was calculated to test the hypotheses that the means of the effects (e.g. time or treatment) are significantly different. If the effects were significantly different post-hoc analysis was performed to analyse the statistical significance of differences between groups (e.g. saline vs OVA). Bonferroni correction for multiple-comparisons was performed. The tests used for each set of data are specified in the results section of each chapter.

Chapter 3:

Characterisation of immune complex-mediated inflammation in the mouse retina

3.1 Introduction

IC diseases (e.g. SLE, GMNP, and rheumatoid arthritis) are intricate diseases involving the deposition of antibody-antigen ICs and subsequent inflammation and tissue damage. The deposition of soluble ICs and their interaction with FcγRs expressed on immune cells and complement proteins (C1q/r/s) are common pathogenic mechanisms.[220] However, the clinical presentation of IC diseases is largely dependent on antibody specificity and the site of IC deposition.[279]

AMD is a multifactorial disease. Whilst no single causing factor has been identified, several studies suggest inflammation is a prominent factor in AMD pathogenesis.[10] In particular, the Y402H (H/H) polymorphism in CFH has been associated with an increased risk of developing AMD.[140, 280] However, factors other than dysregulation of the alternative complement pathway may contribute to the pathogenesis of AMD. The presence of high titers of circulating retinal-specific antibodies,[11, 12, 15, 16] the deposition of IgG in the drusen of AMD patients,[14] and the increased risk of developing AMD associated with polymorphisms in SERPING 1,[281] suggest that antibody-mediated immune responses may also contribute to the pathology of the disease.

Typically, deposition of ICs results in a rapid inflammatory response (type III hypersensitivity response), peaking at 4 to 8 hours after IC formation, and characterised by oedema, haemorrhage, robust neutrophil infiltration and tissue injury.[220, 279] In the brain, type III hypersensitivity responses are delayed, peaking at 3 to 7 days after IC formation, and do not lead to neutrophil infiltration. Despite these differences, IC deposition in the brain still induces a strong inflammatory response, with accompanying transient changes to neuronal function.[282] Despite the evidence supporting IC-mediated responses in the pathology of AMD, to our knowledge this type of antibody-mediated inflammation has not been investigated in detail in the retina.

In this chapter a model of IC deposition in the retina was developed to investigate how IC deposition may lead to inflammation and altered retinal physiology and how this may relate to changes observed in AMD. Changes in activation of microglia, recruitment of immune cells to the retina and mRNA transcript levels

of cytokines and complement components were used as measures of inflammation. Retinal physiology was assessed by fundoscopy to analyse deposition of proteins (reminiscent of drusen) and fluorescein angiography to assess vascular function and permeability.

3.2 Methods

To induce IC deposition in the retina, the reverse Arthus reaction model of type III hypersensitivity was used in the retina as described in section 2.1.2. Briefly, mice were sensitised to OVA and subsequently challenged intravitreously with 10µg of OVA or saline as a control. Serum was collected to confirm high OVA antibody titers. Eyes were collected for immunohistochemical analysis 1, 3, 7 and 14 days after intravitreal OVA injection, and for qPCR analysis 1, 3 and 7 days after injection as detailed in section 2.1.5. Quantification of immunohistochemistry was performed by counting the number of stained cells per mm of retina, only when DAPI+ nuclei were visible (as detailed in 2.2.3). For statistical analysis of immunohistochemistry, n= 4-6 mice per treatment group were analysed for each time point. For statistical analysis of qPCR n=3-4 mice per treatment group were analysed for each time point. Three days after intravitreous challenge fundus photographs and fluorescein angiography readings were obtained as detailed in section 2.1.4. to assess retinal physiology *in vivo*. For *in vivo* assessment of the retina n=3-6 per treatment group were analysed.

3.3 Results

3.3.1 Co-immunolocalisation of OVA and IgG in the mouse retina suggest immune complex deposition and clearance within 14 days.

To investigate antibody-mediated inflammation in the retina the reverse Arthus reaction was applied to the eyes of wild-type BALB/c mice (Figure 3.1.). OVA immunised mice had high circulating levels of anti-OVA antibodies with IC50 values of $>1:10^8$ dilution (Figure 3.1.a). Co-immunolocalisation of IgG (green) and OVA (red) indicated IC formation in the retina following intravitreous injection with OVA. Intravitreal injection of saline did not result in accumulation of IgG in OVA sensitised mice. At 24 hours and 3 days after intravitreous OVA injection, co-localization of IgG and OVA was found in the inner plexiform layer (IPL), ganglion cell layer (GCL), the inner and outer

photoreceptor segment layers (PR) and subretinal space (SR), here defined as the space directly adjacent to the RPE. At 7 days after injection the extent of IgG and OVA co-localisation in the GCL, PR and SR was reduced and at 14 days IgG and OVA co-localisation was no longer detectable in the retina (Figure 3.1.b), suggesting clearance of IC.

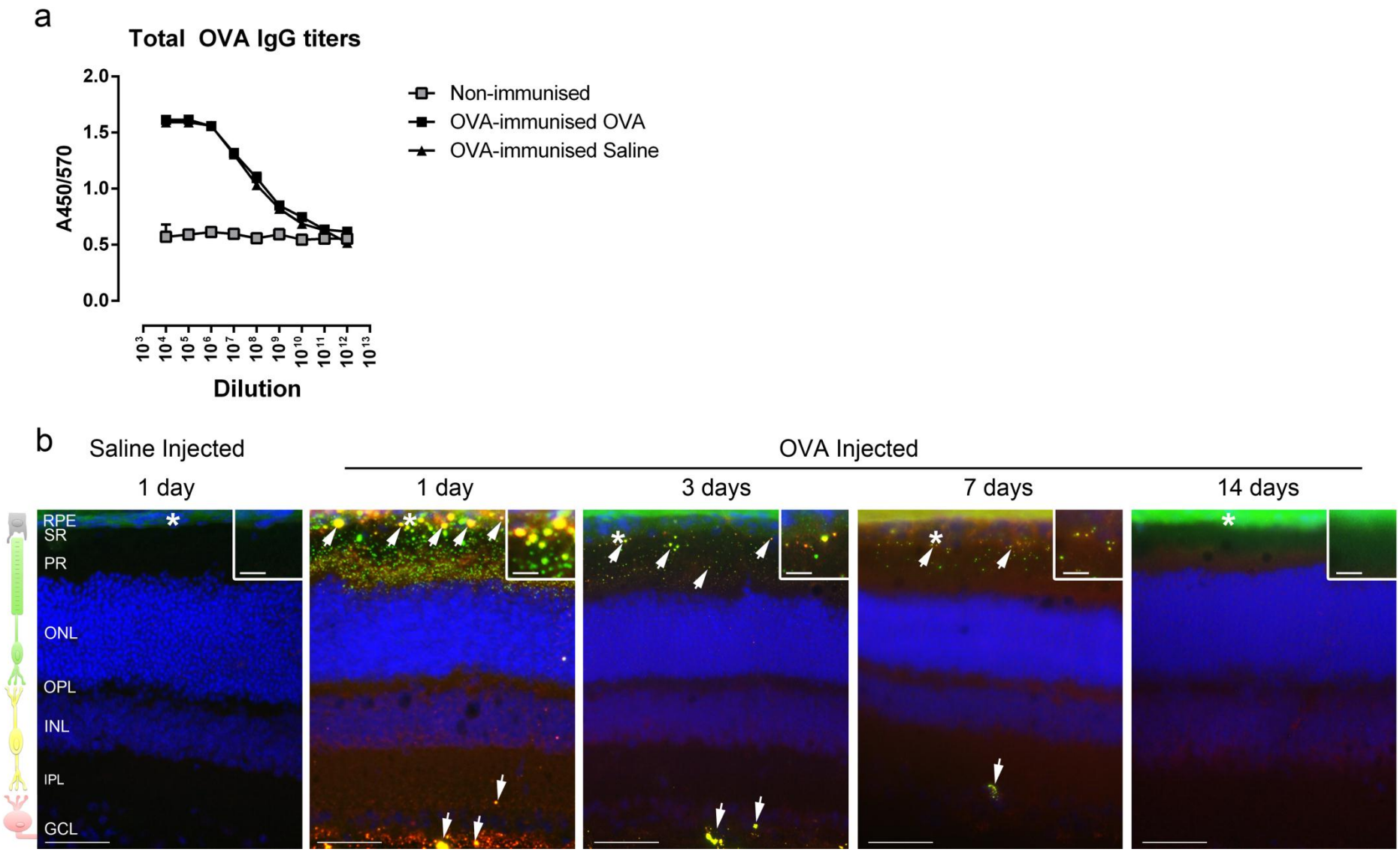
a
Total OVA IgG titers
A450/570
2.0
1.5
1.0
0.5
0.0
10^3 10^4 10^5 10^6 10^7 10^8 10^9 10^{10} 10^{11} 10^{12} 10^{13}
Dilution
Non-immunised
OVA-immunised OVA
OVA-immunised Saline
b
Saline Injected
OVA Injected
1 day
1 day
3 days
7 days
14 days
RPE
SR
PR
ONL
OPL
INL
IPL
GCL

Figure 3.3.1. Immune complexes form throughout the retina of sensitised mice following intravitreous injection of OVA.

(a) Immunisation of mice with OVA resulted in high titers of anti-OVA circulating antibodies (total IgG) in mice injected intravitreously with OVA (n=8) or saline (n=3) as detected by ELISA. Serum from non-immunised mice was used as a control (n=4). **(b)** Immunohistochemical detection of OVA (red) and IgG (green) 24 hours (1 day) after saline injection and 1, 3, 7 and 14 days after OVA injection (n=4-6 mice per group). Cell nuclei were stained with DAPI (blue). Immune complexes (co-localisation, arrows) formed transiently in the inner plexiform, ganglion cell layers, photoreceptor inner and outer segments layers and subretinal space and were detected from 1 day after OVA challenge. * indicates origin of inset. RPE, retinal pigmented epithelium; SR, subretinal space; PR, photoreceptors; ONL, outer nuclear layer; OPL, outer plexiform layer; INL, inner nuclear layer; IPL, inner plexiform layer; GCL, ganglion cell layer. Scale bars - 50μm; inset scale bars - 10μm.

3.3.2 Immune complex formation leads to neuroinflammation

Microglia are the tissue resident macrophages of the retina and they rapidly respond to disturbances of homeostasis and tissue injury.[35] In order to investigate whether the presence of immune complexes induced changes in microglial phenotype and/or led to the recruitment of leukocytes from the circulation, immunohistochemistry for the myeloid and general leukocyte markers CD11b and CD45, respectively, was performed (Figure 3.2.). Microglia cells were identified based on their expression of CD11b and ramified morphology. In the saline treated control mice, microglia expressed low levels of CD11b and positive cells were present in the inner and outer plexiform layers (Figure 3.2.b). Typical resting resident microglia have a ramified morphology, characterised by a small cell body and the presence of long thin processes radiating from it[35] (Figure 3.2. a). In the saline treated control mice, microglia appeared to have a resting phenotype, as some processes were observed (Figure 2b, inset). Following activation, microglia retract their processes and adopt a larger cell body and shorter or no processes, acquiring an "amoeboid" morphology[35] (Figure 3.2. a). From 24 hours up to 7 days after intravitreal challenge with OVA, $CD11b^+$ microglia in the IPL and GCL appeared to have an amoeboid morphology, with less visible processes. $CD11b^+$ cells with a round morphology, characteristic of recruited leukocytes, were found in the GCL. In addition, amoeboid $CD11b^+$ cells were present in the subretinal space 24 hours and 3 days after injection of OVA (Figure 3.2.b). Two-way ANOVA analysis revealed that OVA treatment resulted in a significant effect on the total number of $CD11b^+$ cells/mm of retina ($F(1,6)=107.3$, $p<0.0001$), number of CD11b+ cells/mm in the

subretinal space ($F(1,6)=29.95$, $p=0.0016$), number of CD11b+ cells/mm in the IPL and GCL ($F(1,6)=34.95$, $p=0.001$) and number of CD11b+ cells/mm with round morphology ($F(1,6)=221.8$, $p<0.0001$). The total number of CD11b+ cells peaked 3 days after OVA injection at 63.6±8.9 cells/mm of retina (mean±SEM), a 2.71-fold increase when compared to saline injected controls ($p<0.0001$, Figure 3.3.a). The number of $CD11b^+$ cells with round morphology also peaked 3 days after injection at 27.52±11.06 cells/mm of retina (mean±SEM, $p<0.0002$; Figure 3.3.a). At 14 days after injection microglia were only seen in the plexiform layers with similar morphology to the saline treated control mice (Figure 3.2.b, insets). No $CD45^+$ cells were detectable in the retinae of saline injected mice (Figure 3.2.c). 24 hours following intravitreal injection of OVA, $CD45^+$ cells with a round morphology were observed exclusively in the GCL. From 3 through 7 days both $CD45^+$ cells with a microglia-like and round morphology were observed in the IPL and GCL (Figure 3.2.c). Two-way ANOVA analysis revealed that OVA treatment had a significant effect on the total number of $CD45^+$ cells/mm of retina ($F(1,6)=125.9$, $p<0.0001$),$CD45^+$ cells/mm of retina in the subretinal space ($F(1,6)=17.87$, $p=0.0055$) and IPL and GCL ($F(1,6)=84.10$, $p<0.0001$) and in the number of $CD45^+$ cells with a round morphology ($F(1,6)=81.58$, $p=0.001$). The total number of CD45 cells/mm of retina peaked 7 days after intravitreous injection at 60.15±5.36 cells/mm of retina (mean±SEM, $p=<0.0001$). The number of CD45+ cells/mm of retina with a round morphology peaked at the same time point at 27.74±7.39 (mean±SEM, $p<0.0001$; Figure 3.3.b). 14 days following OVA challenge no $CD45^+$ cells were detectable in the retina (Figure 3.2.c). Eyes from naive mice injected intravitreously with OVA were analysed 3 days after injection. Immunoreactivity of CD11b or CD45 was similar in non-immunised mice after intravitreous injection of OVA and immunised mice injected with saline intravitreously (Appendix I, A2).

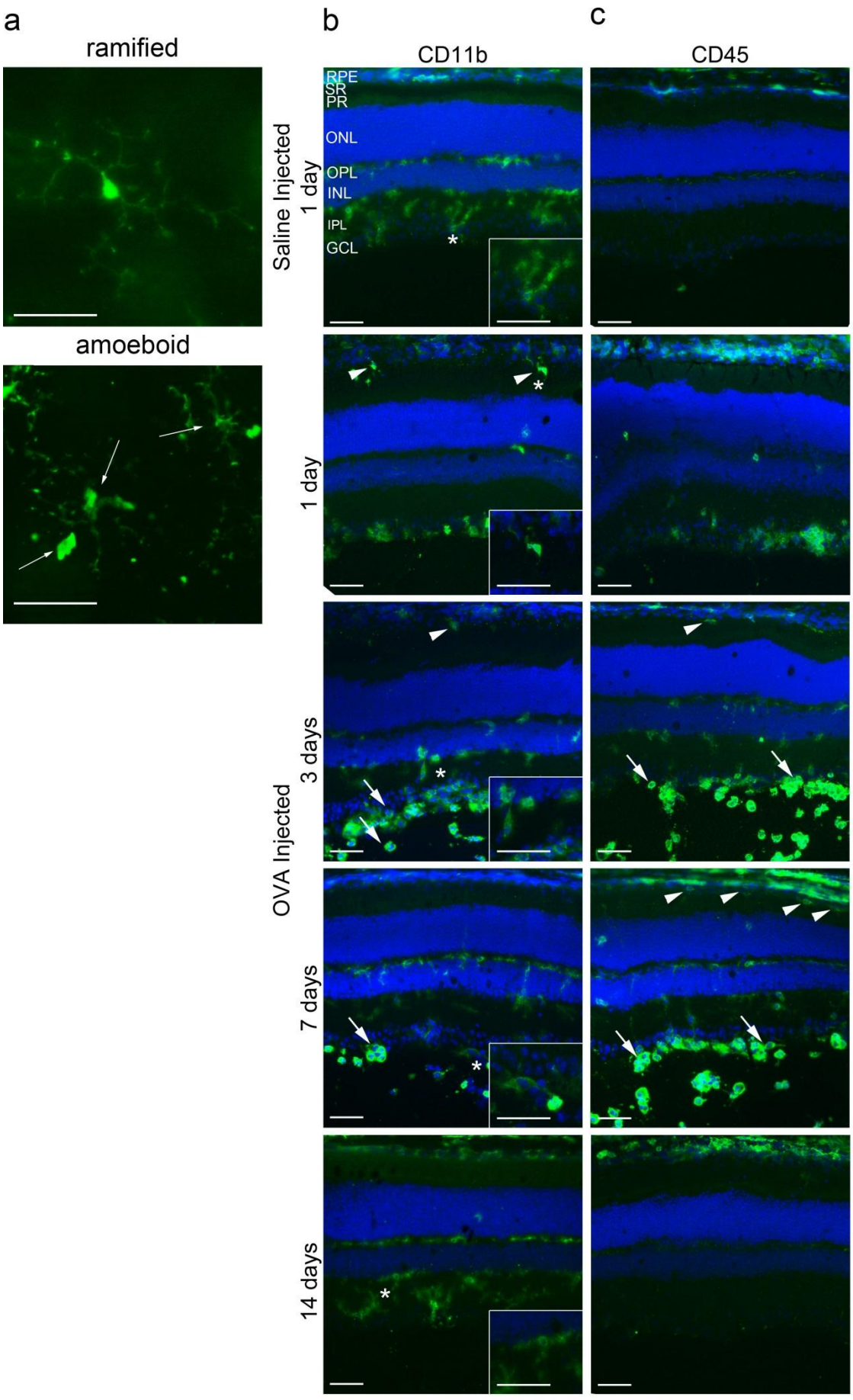
a
ramified
amoeboid
b
CD11b
c
CD45
RPE
SR
PR
ONL
OPL
INL
IPL
GCL
Saline Injected
1 day
1 day
OVA Injected
3 days
7 days
14 days

Figure 3.2. Immune complex formation in the retina leads to activation of microglia and recruitment of leukocytes.

(a) Retina whole-mount showing CD11b+ microglia (green). Ramified microglia have long thin processes and a small round cell body. Amoeboid microglia retract their processes and become rounder. **(b)** CD11b immunoreactivity (green) 24 hours (1 day) after intravitreous saline injection and 1, 3, 7 and 14 days after OVA injection. Cell nuclei were stained with DAPI (blue). In saline injected control mice $CD11b^+$ microglia with processes were present in the OPL and IPL. 1, 3 and 7 days after intravitreous OVA challenge microglia with amoeboid-like morphology (insets) were seen in the IPL and ganglion cell layer and $CD11b^+$ round cells (arrows) were seen in the ganglion cell layer and vitreous. Subretinal $CD11b^+$ amoeboid-like cells were observed at 1 and 3 days after OVA challenge. At 14 days after injection, $CD11b^+$ microglia returned to the plexiform layers, had more processes (inset) and no $CD11b^+$ cells with round morphology were detected. **(b)** CD45 staining (green) 24 hours (1 day) after saline injection and 1, 3, 7 and 14 days after OVA injection. Cell nuclei were stained with DAPI (blue). No $CD45^+$ cells are detected in control retinae. 1, 3 and 7 days after intravitreous OVA challenge $CD45^+$ cells with round morphology (arrows) or with processes were observed, up until 14 days, where almost no $CD45^+$ cells were detectable. * indicates origin of inset. n=4-6 mice per group. RPE, retinal pigmented epithelium; SR, subretinal space; PR, photoreceptors; ONL, outer nuclear layer; OPL, outer plexiform layer; INL, inner nuclear layer; IPL, inner plexiform layer; GCL, ganglion cell layer. Scale bars - 50μm.

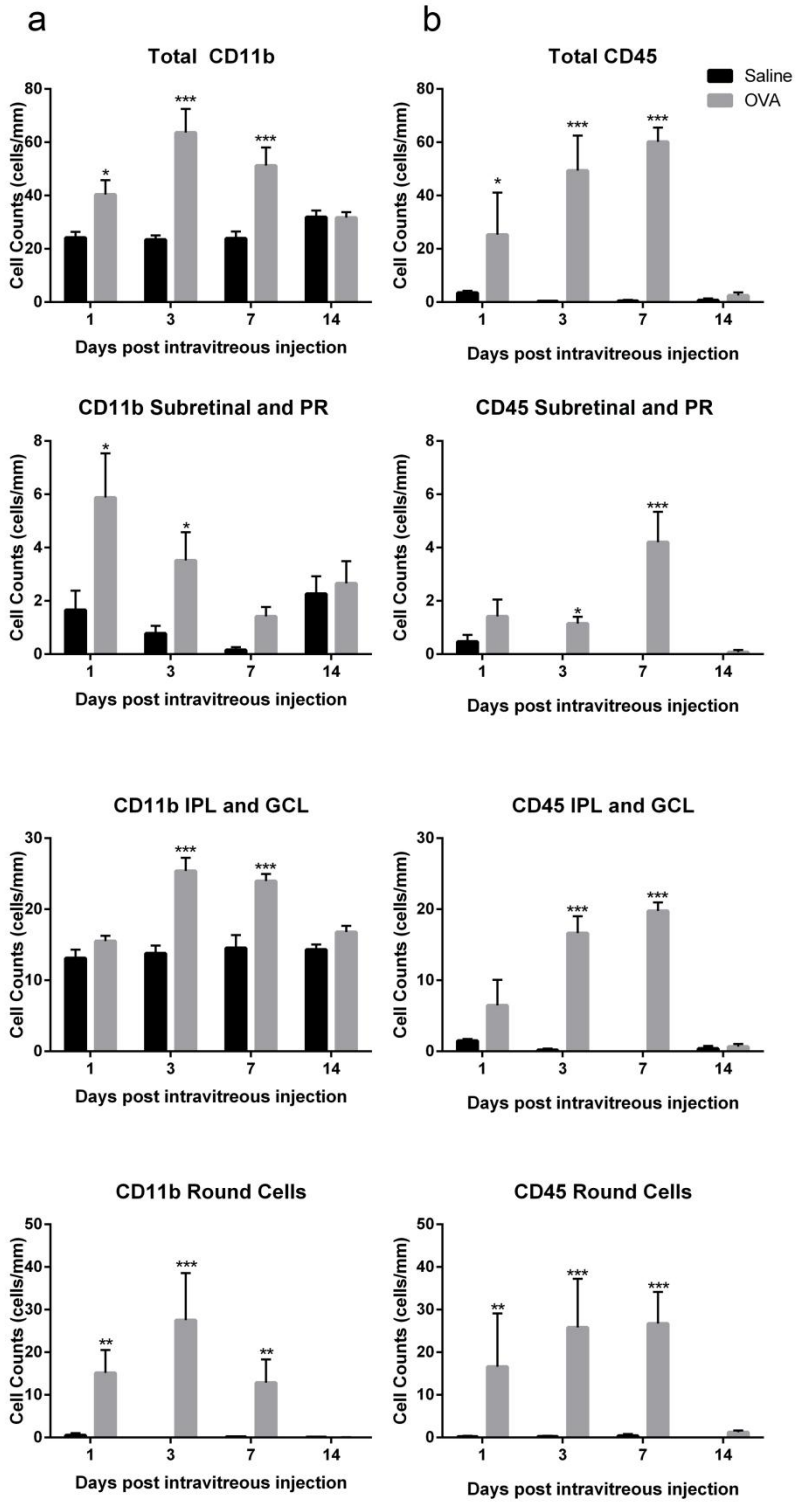

Figure 3.3. Quantification of CD11b$^+$ and CD45$^+$ cells following immune complex formation in the retina.

Quantification of **(a)** CD11b$^+$ or **(b)** CD45$^+$ cell number/mm of retina (n=4-6 per group). Data are expressed as number of cells/mm of retina +SEM and were analysed using two-way ANOVA followed

by Bonferroni correction. *p<0.05, **p<0.01, ***p<0.001 when compared to saline control at corresponding time point.

3.3.3 Immune-complex formation leads to increased expression of FcγRs and MHC II

Resting microglia express low levels of the IgG receptors FcγRs[283] and do not express detectable levels of MHC II.[284] Microglia have been shown to upregulate FcγRs and MHC II in response to immune complex formation in the brain,[282] therefore we next investigated expression of these markers after intravitreal challenge with OVA or saline. Cells expressing FcγRI were detected in saline control mice but their number was increased 3 and 7 days after intravitreal challenge with OVA (Figure 3.4.a). Very few cells expressing FcγRII/III (Figure 3.4.b) or FcγRIII (Figure 3.4.c) were detected in saline controls or 24 hours after OVA injection. However, the number of cells expressing FcγRII/III or FcγRIII was increased at 3 and 7 days after intravitreal injection of OVA and low levels of expression were still detectable after 14 days. Both FcγRIV (Figure 3.4. d) and MHC II (Figure 3.4.e) were undetectable in saline controls and 24 hours after OVA injection, but increased 3 and 7 days following intravitreal injection of OVA. 14 days after injection no cells expressing these markers were detectable. Quantification of cell numbers (Figure 3.5.) revealed increased numbers of cells expressing these markers following OVA challenge (FcγRI: $F(1,6)=60.59$, $p=0.0002$; FcγRII/III: $F(1,6)=47.35$, $p=0.0005$; FcγRIII: $F(1,6)=6.28$, $p=0.0461$; FcγRIV: $F(1,6)=151.3$, $p<0.0001$; MHC II $F(1,6)=303.7$, $p<0.0001$). Immunoreactivity for FcγRs and MHC II was low or undetectable in non-immunised mice injected intravitreally with OVA (Appendix I, A2). These results suggest that immune complex formation leads to microglial activation with upregulated expression of FcγRs and MHC II and to recruitment of leukocytes expressing these markers.

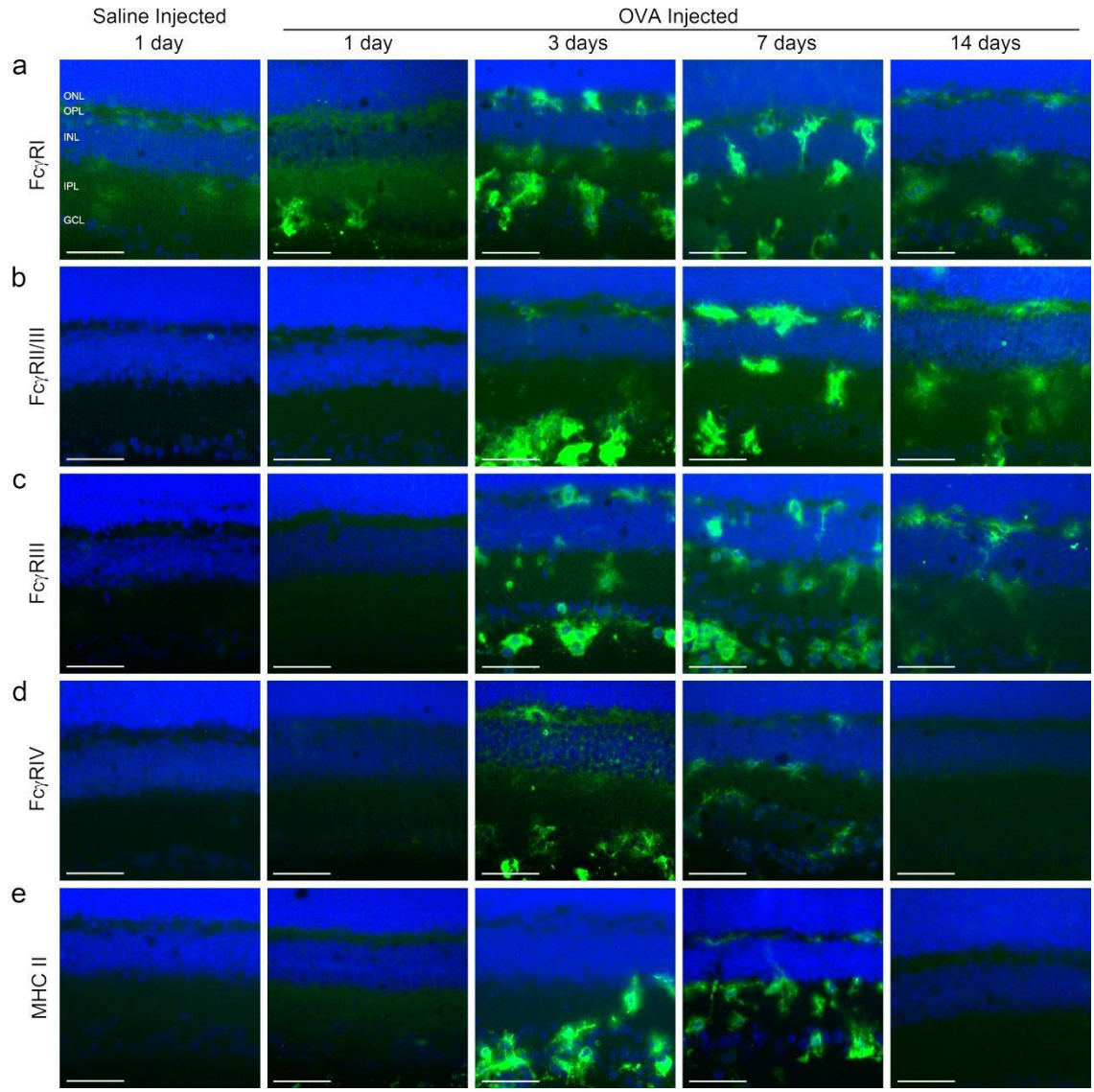

Figure 3.4. Immune complex formation in the retina results in increased expression of FcγRs and MHC II.

(a-e) Immunohistochemistry for FcγR I **(a)**, FcγR II/III **(b)**, FcγR III **(c)**, FcγR IV **(d)** and MHC II **(e)** 24 hours (1 day) after saline injection and 1, 3, 7 and 14 days after OVA injection (green). Cell nuclei were stained with DAPI (blue).Intravitreous challenge with OVA led to upregulation of all FcγRs and MHC II from 3 through to 7 days post OVA challenge (n=4-6 mice per group). ONL, outer nuclear layer; OPL, outer plexiform layer; INL, inner nuclear layer; IPL, inner plexiform layer; GCL, ganglion cell layer. Scale bars - 50μm.

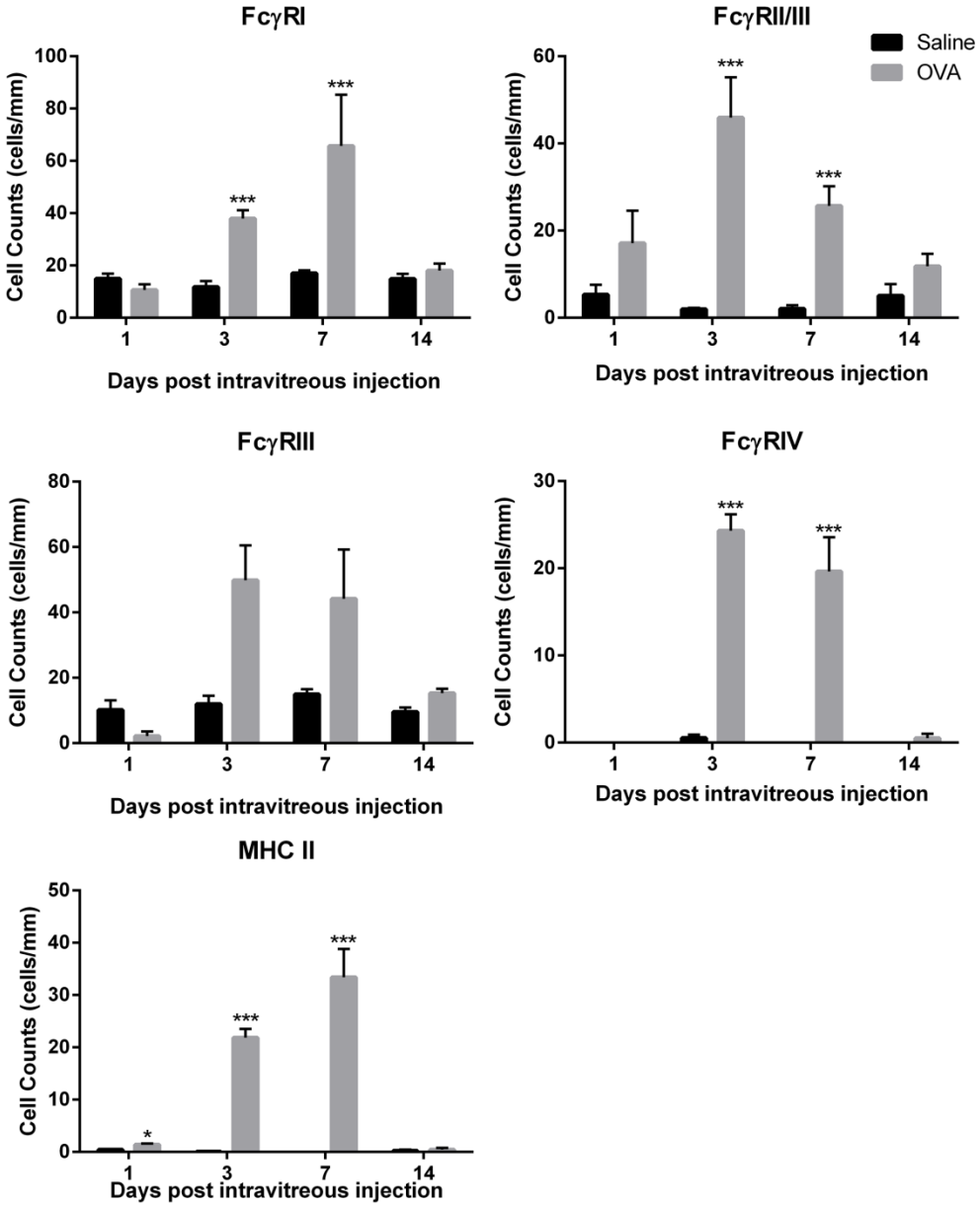

Figure 3.5. Quantification of number of cells expressing FcγRs and MHC II.
Quantification of cell number/mm of retina expressing each marker showed an increase in cell numbers expressing FcγRII/III, FcγRIII and FcγRIV peaking at 3 days and FcγRI and MHC II peaking at 7 days (n=4-6 mice per group). Data are expressed as number of cells/mm of retina +SEM and were analysed using two-way ANOVA followed by Bonferroni correction. Error bars represent SEM; *p<0.05, ***p<0.001 when compared to saline control at corresponding time point.

3.3.4 Immune complex formation leads to recruitment of T lymphocytes

Immune complex formation in peripheral organs, such as the lung or skin, results in leukocyte recruitment, with neutrophils mediating most of the tissue damage.[285, 286] T

lymphocytes are recruited during IC-mediated inflammation and could also mediate tissue damage.[287] The presence of these cell types was investigated by immunohistochemical staining for the T lymphocyte markers CD3 and CD4, and the neutrophil marker, neutrophil elastase (NE). No cells expressing CD3 (Figure 3.6.a) or CD4 (Figure 3.6.b) were detectable in saline injected eyes. Both $CD3^+$ and $CD4^+$ cells were observed in the subretinal space from 1 day after intravitreous OVA challenge (Figure 3.6., arrows). 3 days after intravitreous injection of OVA $CD3^+$ and $CD4^+$ cells were present in the subretinal space and GCL (Figure 3.6., arrows). 7 days after OVA injection $CD3^+$ and $CD4^+$ cells were present throughout all retinal layers, suggesting infiltration of these cells into the retina (Figure 3.6., arrows). Quantification revealed a significant increase in total number of $CD3^+$ and $CD4^+$ cells/mm of retina after OVA challenge (CD3: $F(3,27)=4.7$, $p<0.0001$; CD4: $F(1,27)=28.45$, $p<0.0001$; Figure 3.7). OVA challenge resulted in a non-significant increase in number of $CD3^+$ or $CD4^+$ cells at 1 day (CD3: $p=0.42$, CD4: $p>0.99$), a small but significant increase at 3 days (CD3: $p=0.02$, CD4: $p=0.01$) and an increase from no cells in saline injected controls to an average of 18.74 $CD3^+$ and 16.93 $CD4^+$ cells/mm of retina (CD3:$p<0.0001$; CD4: $p=0.0003$; Figure 3.7) at 7 days after challenge. Immunohistochemistry for $CD8^+$ cells was also performed but strong non-specific binding to retinal neurons was detected (Appendix I, A3), therefore these data were not further analysed. However, similar numbers of CD3+ and CD4+ cells indicate that most infiltrating T lymphocytes are CD4+ and not CD8+ cells. Staining for NE to detect neutrophils revealed NE^+ cells at the choroid (Figure 3.6., arrowheads) of OVA challenged mice but no NE^+ cells were detected in the retinal layers at any time point after intravitreous injection of OVA (Figure 3.6).

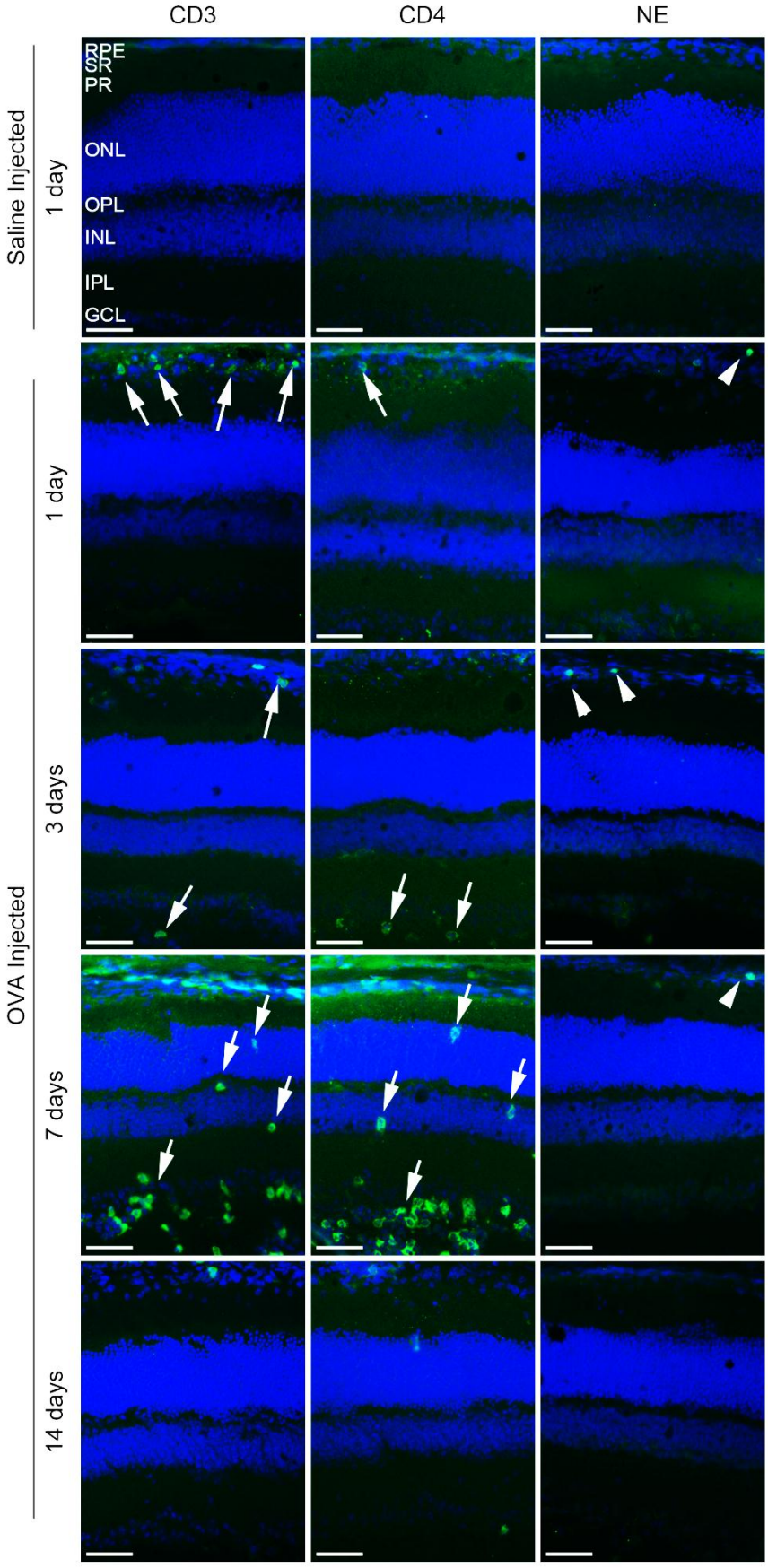
CD3
CD4
NE
RPE
SR
PR
ONL
OPL
INL
IPL
GCL
Saline Injected
1 day
OVA Injected
1 day
3 days
7 days
14 days

Figure 3.6. Immune complex formation in the retina results in recruitment of $CD3^+$ and $CD4^+$ cells but not neutrophils.

Immunohistochemistry for CD3 (green), CD4 (green) and neutrophil elastase (NE; green) 24 hours (1 day) after saline injection and 1, 3, 7 and 14 days after OVA injection. Cell nuclei were stained with DAPI (blue). Intravitreous challenge with OVA led to recruitment of $CD3^+$ and $CD4^+$ from 1 through to 7 days post OVA challenge (arrows). Neutrophils were detected at the choroid (arrowheads) but not in the retinae of controls or OVA challenged mice (n=4-6 mice per group). RPE, retinal pigmented epithelium; SR, subretinal space; PR, photoreceptors; ONL, outer nuclear layer; OPL, outer plexiform layer; INL, inner nuclear layer; IPL, inner plexiform layer; GCL, ganglion cell layer. Scale bars - 50μm.

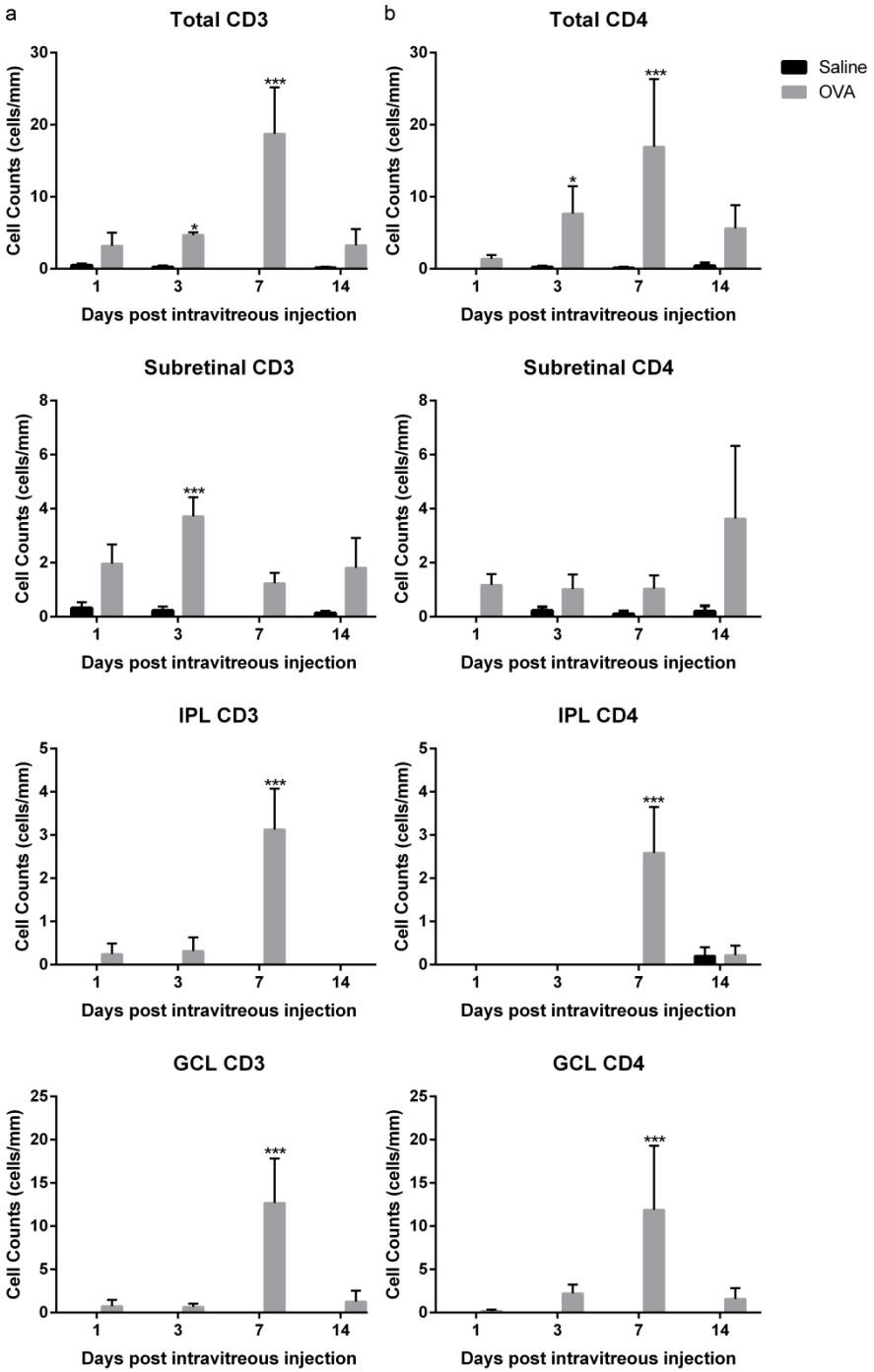

Figure 3.7. Quantification of number of cells expressing CD3 and CD4.

Quantification of cell number/mm of retina expressing each marker showed a significant increase in cell numbers expressing CD3 and CD4 from 3 to 7 days, peaking at 7 days (n=4-6 mice per group). Data are expressed as cells/mm of retina + SEM and were analysed using two-way ANOVA followed by Bonferroni correction. Error bars represent SEM; *$p<0.05$, ***$p<0.001$ when compared to saline control at corresponding time point.

3.3.5 Immune complex leads to increased expression of MCP-1 but not other inflammatory genes

C5a and MCP-1 are two molecules with well-known chemotaxic properties. C5a is produced following immune complex deposition, mediating myeloid cell recruitment, including neutrophils and macrophages, whilst MCP-1 (i.e. CCL2) is known to be important in recruitment of monocytes/macrophages to sites of injury,[288] therefore transcript levels of these two chemokines and C5R1, the receptor for C5a, were investigated. To further characterise the IC-mediated inflammatory response, transcriptional changes for the macrophage activation markers iNOS and arginase 1 (Arg1) and inflammatory mediators thought to be involved in IC-mediated inflammation (IL-6, TNF-α, IL-10, CCL5) were also assessed (Figure 3.8.). Only Arg1 and MCP-1 transcript levels were detected in the retinae of BALB/c mice. No difference was found in expression levels of the M2 marker, Arg1, between saline controls and OVA-challenged mice ($F(2,17)=2.809$, $p=0.11$). In contrast, OVA challenge resulted in a significant increase in transcript levels of the chemokine MCP-1 ($F(1,17)=6.043$, $p=0.025$). 24 hours (1 day) after intravitreous injection of OVA the transcript levels of MCP-1 were increased by 18-fold when compared to saline injected mice at 24 hours ($p=0.006$). At 3 and 7 days after OVA challenge there were no differences in the transcript levels of MCP-1 between OVA injected or saline injected control eyes ($p>0.09$; Figure 3.8.a).

To ensure that only specific products are being detected, melting curves were obtained as described in section 2.3.5 (Figure 3.8.b). The melting curves revealed that only qPCR reactions with GAPDH, Arg1 and MCP-1 specific primers produced a single peak, indicating that a single PCR product was amplified. Melting curves for all other qPCR reactions revealed multiple peaks, indicating amplification of multiple unspecific products, including in positive control tissue (retina with intravitreous injection of LPS). The melting curves for iNOS, CCL5 and IL-10 specific primers are shown. (Figure 3.8.b.).

3.3.6 Immune complex formation does not induce detectable functional changes to the retina

In vivo imaging of the retina was performed 3 days after saline or OVA injection, using naive C57BL/6 mice as a positive control for imaging technique. Fundoscopy has been

used to detect accumulations of subretinal macrophages or debris in mouse models of AMD,[143, 207] therefore the fundus of mice following OVA challenge was examined. In the fundus of C57BL/6 mice the retinal blood vessels can be clearly seen (Figure 3.9. a, arrows) radiating from the optic disc (OD), visible as a pale circle, while the retina appears with a "greyish-yellow" colour with some contrast differences in discrete areas. The fundus of BALB/c mice clearly showed the retinal blood vessels (arrows). However, the retina appeared much brighter, showing a pink colour, with almost no contrast differences, so that the OD is no longer visible as a paler circle. (Figure 3.9.a). There were no apparent differences between the fundus of saline controls and OVA challenged mice. To assess changes in blood vessel permeability fluorescein angiography was performed as detailed in section 2.1.4.2. Fluorescein angiography in C57BL/6 mice revealed clearly defined blood vessel borders from 1 up to 15 minutes after fluorescein injection. In BALB/c mice no clear blood vessel borders were seen. From 1 up to 15 minutes after fluorescein injection, the whole retina appeared green, possibly due to fluorescein circulating in the choroid (Figure 3.9.b). No differences were detected by fluorescein angiography between saline controls or OVA challenged mice. To further investigate the effect of immune complex formation in the retina electroretinograms (ERGs) were performed, but high background noise prevented reliable results to be obtained (Appendix I, A4).

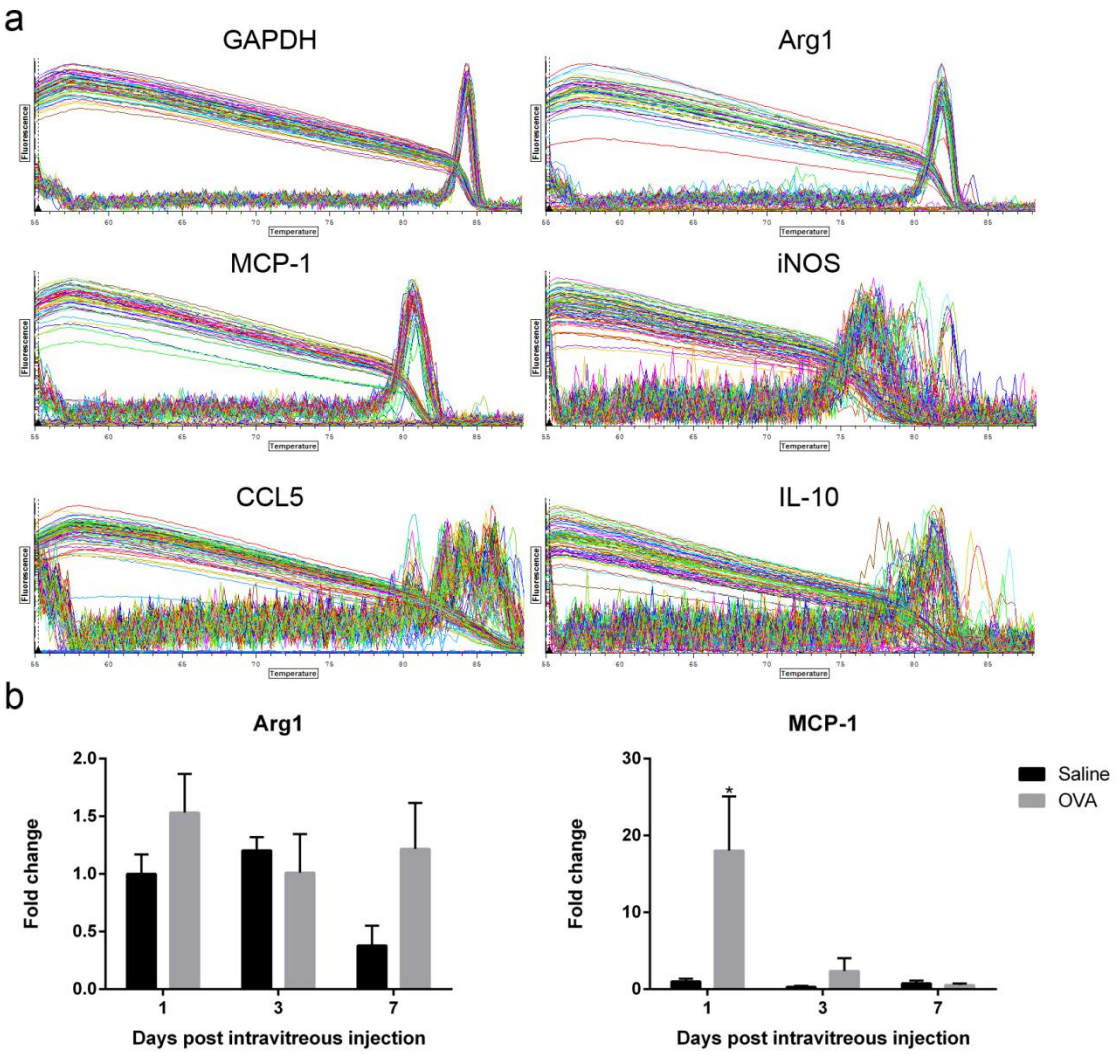

Figure 3.3.8. Immune complex induced transcriptional changes in inflammatory genes.
(a) Melting curves of qPCR reactions. A single peak in qPCR reactions with GAPDH, Arg1 and MCP-1 primers indicate specific amplification of PCR products. Multiple peaks in qPCR reaction with iNOS, CCL5 and IL-10 indicate unspecific amplification of PCR products. **(b)** Changes in transcription levels of Arg1 and MCP-1. Data are represented as fold change from saline injected controls at 24 hours (1 day) +SEM and analysed using two-way ANOVA followed by Bonferroni correction (n=3-4 mice per group). Error bars represent SEM; *p<0.05, ***p<0.001 when compared to saline control at corresponding time point.

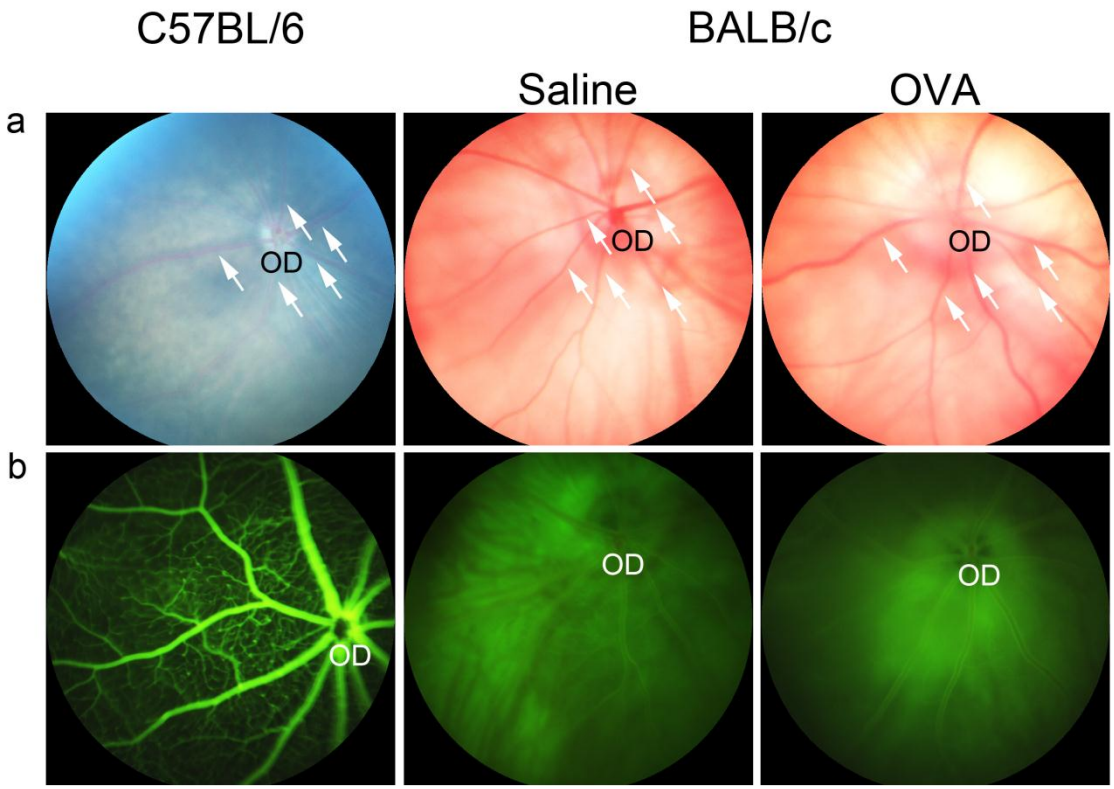

Figure 3.9. *In vivo* imaging of the retina following immune complex formation.
C57BL/6 mice were used as a positive control for *in vivo* imaging of the retina. **(a)** Images of the fundus of naive C57BL/6 and BALB/c mice following saline or OVA injection. Arrows show the retinal blood vessels radiating from the optic disc (OD) **(b)** Images of fluorescein angiography of naive C57BL/6 and BALB/c mice following saline or OVA injection. Images are representative of n=3-6.

3.4 Discussion

Inflammation is an important component in the pathogenesis of AMD.[10] Both clinical and experimental data support the concept that immune complex-mediated inflammation may play a role in disease progression. In the present study a mouse model was developed to investigate the effect of immune complex formation in the retina. To optimise the model the reverse Arthus reaction was induced in the retina of C57BL/6 and BALB/c mice (section 2.1.2). Immunisation of C57BL/6 mice resulted in 10x lower levels of circulating anti-OVA IgG and reduced immune complex formation following intravitreous challenge with OVA when compared to BALB/c mice (Appendix I, A1). Therefore, for further studies BALB/c mice were used. In this chapter the biological effect of immune complex deposition in the retina was studied. Immune complexes formed throughout all retinal layers resulting in a robust local inflammatory response, characterised by activation of microglia, upregulation of FcγRs and MHC II,

increased transcript levels of the chemokine MCP-1, and recruitment of leukocytes, including T lymphocytes but not neutrophils. With the techniques used in the present chapter no changes in morphology of the retina or permeability of retinal blood vessels were detected. Immune complex deposition in AMD eyes could contribute to pathology by inducing inflammation and recruitment of leukocytes.

3.4.1 Immune complex formation in the retina

Patients suffering from early stage AMD have elevated levels of circulating IgG reactive to retinal antigens.[11, 12, 15] The BRB restricts passage of large molecules, such as IgG, from the blood stream to the retina[50] and thus it is unclear whether these autoantibodies could enter the eye and contribute to pathogenesis of AMD. Preliminary data suggests that the presence of circulating autoantibodies with retinal specificity alone is not sufficient to induce retinal degeneration (Appendix I, A5). The data presented in this chapter shows that upon introduction of OVA in the vitreous, IgG-OVA immune complexes can form throughout the retina of immunised mice. Intravitreous injection allows for delivery of substances (e.g. OVA) without mechanical disruption of the BRB. Therefore, the IgG-OVA immune complexes in the present mouse model appear to form despite an intact BRB.

Approximately 0.1% of total IgG can gain access to the brain parenchyma through passive transport.[289] Due to the similarities between the BBB and the BRB it is possible that the same phenomenon occurs in the eye. If so, following antigenic challenge, the small amount of antibodies that can cross the blood barrier may be enough to initiate immune complex deposition as they encounter their antigen in the retina. In support of this, in the present model, immune complexes form in close proximity to the retinal and choroidal blood vessels. This is a mechanism by which auto-antibodies could cross into the retina in early AMD and form immune complexes.

3.4.2 Immune complex-mediated inflammation in the retina

The presence of specific autoantibody signatures in dry and wet AMD in humans[15] and cynomolgus monkeys with AMD-like pathology[247] suggest a relationship between these antibodies and the pathogenic mechanisms of AMD. The biological effects of immune complex deposition have been well characterised in non-neuronal tissue, resulting in an inflammatory response characterised by oedema, haemorrhage, neutrophil infiltration

and tissue injury.[279, 285, 286, 290] A number of studies have shown that immune complex formation in the anterior ocular chamber leads to increased permeability of the blood-aqueous-barrier but responses in the retina were not studied.[291, 292] In the brain parenchyma antibody-mediated inflammation is delayed when compared to peripheral organs and no neutrophil infiltration is observed.[282] Similarly, immune complex formation in the retina leads to a delayed inflammatory response that peaks at 3 days after antigen challenge and is characterised by activation and migration of microglia and CD11b+ leukocytes to the sites of immune complex formation. Although no neutrophil infiltration was observed, some neutrophils were found in the choroid where they could mediate damage of choroidal blood vessels.

While in non-neuronal tissue the main effector cells associated with immune complex inflammation are neutrophils and mast cells,[279, 285, 290] in the brain and retina it appears that microglia and macrophages recruited from the circulation are the main effector cells. Microglia seem to rapidly migrate towards sites of immune complex formation. At the earliest time point studied, 24 hours after OVA challenge, almost no microglia are seen in the plexiform layers, where they normally reside. Instead $CD11b^{+}$ microglia seem to concentrate in the sites of immune complex deposition (subretinal space and GCL). From 3 days after OVA challenge, microglia can still be found in the sites of immune complex deposition, but also in the plexiform layers. Altogether these results suggest that upon immune complex formation there is a first rapid microglial response, involving migration of microglia towards immune complexes, and a second slower response, involving recruitment of cells from the circulation and/or microglia proliferation. Supporting the former is the presence of $CD11b^{high}CD45^{high}$ cells with a round morphology characteristic of monocytes/macrophages in the GCL from 3 days after OVA challenge. In addition, macrophage depletion with clodronate-filled liposomes resulted in reduced number of $CD11b^{+}$, $CD45^{+}$ and MHC II^{+} cells 7 days after intravitreous injection challenge with OVA (Appendix I, A6).

C5a, a product of C5 cleavage, has been shown to be important for initial immune cell migration following immune complex deposition[293, 294] and could provide the initial signal for microglia migration. No C5 expression was detected by qPCR, which was likely due to low levels of cDNA. The most likely source of C5 in the retina are the microglia, which make up only 0.5-1.5% [86] of all retinal cells. It is plausible that not enough mRNA for C5 is present in a single retina to be detected by this assay.

Supporting this, for most inflammatory markers investigated by PCR in this chapter, including C5, product was only obtained at late $C_{(t)}$cycles (35-40) and the melting curves revealed several peaks, indicating amplification of unspecific products. A better way of detecting transcriptional changes in inflammatory genes may be to isolate microglia prior to cDNA extraction, as described by W. Ma et al 2013.[8] In contrast to C5, MCP-1 was shown to be increased by 18-fold 24 hours after OVA challenge. It is possible that MCP-1 is secreted by the RPE after immune complex deposition and serves as an initial signal for microglia migration. Another possibility is that once recruited to the sites of immune complex formation, microglia secrete MCP-1 which can then further mediate recruitment of microglia and macrophages.[295]

In resting conditions microglia have a $CD11b^{low}/CD45^{low}$ phenotype and a ramified morphology, and can be distinguished from peripheral myeloid cells based on their expression of CD45.[296] Following immune complex formation microglia acquired a $CD11b^{high}/CD45^{high}$ phenotype and an amoeboid-like morphology, indicating microglia activation. In addition, there was an increase in the number of microglia and cells with round morphology (possibly macrophages) expressing FcγRI, II/III, III and IV and MHC II. FcγRs are important receptors for macrophage effector function and increased expression of these receptors and MHC II by macrophages has been demonstrated following immune complex stimulation in the brain.[282] These results indicate microglia activation by immune complexes. To further characterise the phenotype acquired my microglia after immune complex deposition, expression of the activation markers iNOS and Arg, IL-10, IL-6, TNF-α, CCL5, C5 and MCP-1 was studied by qPCR. With the exception of Arg1 and MCP-1 no detectable levels of any of these markers was found, likely due to technical reasons, as discussed above. Immune complex activation of macrophages induces an M2-like phenotype without expression of Arg1, but with increased expression of IL-10.[95] Consistent with this, there were no detectable changes in Arg1 expression following immune complex formation. Microglia activation and macrophage recruitment from the circulation has been associated with human AMD[174, 201] as well as with several mouse models of AMD, including the $CX3CR1^{-/-}$ mouse[143] and a laser-induced CNV model.[210] The results in this chapter clearly show activation of microglia following immune complex formation and an increase in numbers of $CD45^{high}$ cells with a round morphology characteristic of monocytes/macrophages.

3.4.3 Recruitment of lymphocytes

Immune complex-mediated inflammation is often associated with T cell infiltration,[287] therefore the presence of these cells was investigated. T cell recruitment was observed from as early as 1 day after intravitreous injection of OVA. The number of T cells peaked at 7 days after challenge, when $CD3^+$ were seen throughout all retinal layers. Two studies have reported increased levels of T lymphocytes in the circulation ($CD56^+CD28^-$ T lymphocytes)[297] or choroid ($CD8^+$ T lymphocytes)[298] of AMD patients; however, there has not been a strong association of these cells with AMD pathology.[10] In contrast, the presence of $CD8^+$ T cells in the retina is a known component of other autoimmune inflammatory diseases of the eye (e.g. uveitis).[10] To further assess the possible role of T cells in immune complex-mediated inflammation in the retina, staining for CD4 (T helper; T_H cells) or CD8 (cytotoxic T cells) was performed. CD8 immunohistochemistry showed strong neuronal non-specific staining and therefore was not analysed (Appendix I, A3). However, staining with CD4 revealed the number of $CD4^+$ cells was similar to that of $CD3^+$, indicating that most T cells detected were $CD4^+$. Curiously, expression of MHC II by microglia peaked at 7 days, when the highest number of T cells is observed. MHC II expressing microglia could lead to the activation of $CD4^+$ T cells and promote their differentiation into a specific T_H cell phenotype. Immune complex activation of macrophages has been associated with induction of both T_H2[96] and T_{reg}[98] cells *in vitro*. It is tempting to speculate that the T cells observed in these results could be differentiating into T_{reg} cells, which have a role in resolving inflammation. Consistent with this is the fact that T cells infiltration peaks after the peak of microglia responses, when immune complex deposition is less pronounced, and that by 2 weeks after OVA challenge the inflammatory response is resolved. However, antigen specificity studies and detection of T_H phenotype specific markers (e.g. TH2: GATA3, Treg: Foxp3)[299] will have to be performed to confirm T cell phenotype and to better understand what their role in immune complex-mediated inflammation may be.

3.4.4 *In vivo* assessment of the retina

To study if immune complex deposition could induce AMD-like morphological changes in the retina, fundoscopy analysis was performed. Spots in the fundus of mice corresponding to sites of subretinal macrophage accumulation have been described for

several mouse models of AMD.[143, 203] Despite migration of microglia to the subretinal space as seen by immunohistochemistry, no differences in the fundus of control or OVA challenged mice were detected. Most AMD models used are on a C57BL/6 background. Due to the more robust deposition of immune complex, BALB/c mice were used in these experiments. The lack of pigmentation in these mice results in reduced contrast and therefore it may be more technically challenging to detect small changes such as macrophage accumulation. A similar problem was found when performing fluorescein angiography on the BALB/c mice. While the same protocol performed on C57BL/6 mice allowed for visualisation of the retinal blood vessels, in BALB/c mice it led to an overall green appearance of the whole fundus for both control and OVA challenged mice. It thus appears that it is technically challenging to investigate the retinae of BALB/c mice by fundoscopy or fluorescein angiography.

3.4.5 Conclusion

The results from this chapter clearly show that immune complex deposition in the retina induces a transient but robust inflammatory response. Of particular interest is the fact that the retina, similar to the brain, appears to deal with immune complexes in manner different to that that has been described in peripheral organs. The main effector cells appear to be microglia and macrophages recruited from the circulation and the inflammatory response is delayed relative to peripheral sites, peaking at 3 days, when the highest number of $CD11b^{+}$ and FcγR II/III, III and IV expressing cells are observed. Further, no neutrophil infiltration was observed. These results highlight the importance of understanding immune complex-mediated responses in the retina, as it may elucidate how immune complexes could contribute to AMD pathology.

FcγRs have been shown to be essential for the initiation of immune complex-mediated inflammation in the periphery. The next clear step was to investigate the role of these receptors in the immune complex-mediated responses observed in the retina.

Chapter 4:

The role of Fcγ receptor subtype in immune complex-mediated inflammation in the retina

4.1 Introduction

Histological studies have shown the presence of macrophages and IgG in AMD lesions.[14, 174] Macrophage recruitment and/or activation in AMD may be partly induced by deposition of IgG and IC formation. These could bind FcγRs on retinal macrophages and microglia, contributing to early stages of AMD pathogenesis and/or progression of disease.

Immune complexes can mediate pathogenicity by initiating the classical complement cascade, via binding of C1q, or by cross-linking of FcγRs on effector cells, such as macrophages and microglia.[17] Cross-linking of activating FcγRs activates cell effector functions such as phagocytosis, oxidative burst and cytokine production, which are inhibited by ligation of the inhibitory FcγRII.[17] The indispensable role of activating FcγRs in mediating immune complex induced pathology is well documented. FcR gamma chain knock-out mice ($\gamma^{-/-}$) lack cell surface expression of the activating FcγRs and are protected against immune complex-mediated inflammation, including type III hypersensitivity responses.[282, 300, 301] Activation of the complement cascade also has an important role, in particular in tissue damage. Deficiency of specific complement components such as C5 or its receptor, C5R1, results in attenuated inflammation in response to immune complex formation in several models.[302-304]

Interestingly, due to their differential ability to fix complement[305] and affinity for each FcγR,[224] specific IgG subclasses (in mouse IgG1, IgG2a, IgG2b and IgG3) activate different effector responses. In mouse three activating FcγRs (FcγRI, FcγRIII and FcγRIV) have been described. FcγRI, the high affinity receptor, is generally saturated with endogenous IgG2a[17] and it is thought to have a limited contribution to immune complex-mediated responses.[224, 306, 307] More recent studies suggest FcγRI has a more important role in IgG2a-mediated responses than previously thought.[225, 308, 309] FcγRIII is the only receptor capable of binding all complexed IgG isotypes *in vivo*.[224] In view of that, it has been shown to be important in several IgG1, IgG2a and IgG2b-mediated models of immune complex pathology.[224, 225, 228, 304, 307, 309, 310] Finally, the most recently discovered FcγR, FcγRIV[219] has been shown to bind IgG2a and IgG2b with moderate affinity *in vivo* and key in mediating immune complex pathology mediated by these IgG subclasses.[225, 227, 306, 307, 311] Further adding to the remarkable complexity of immune

complex responses is the apparent tissue-specific requirement for certain complement components or FcγRs.[312]

The newly developed model of antibody mediated retinal inflammation described in Chapter 3 demonstrated that immune complex deposition in the retina leads to a transient, yet robust inflammatory response. Due to the potential involvement of immune complexes in AMD pathology it is important to understand the mechanisms regulating immune complex-mediated inflammation in the retina. In this study the contribution of the classical complement cascade and activating Fcγ receptors to immune complex-mediated inflammation in the retina is examined using $\gamma^{-/-}$ and $C1q^{-/-}$ mice. To further dissect the differential role of individual activating FcγRs mice lacking FcγRI, FcγRIII or FcγRIV were used.

4.2 Methods

To investigate the role of Fcγ receptors and classical complement cascade in initiating immune complex-mediated inflammation in the retina, the reverse Arthus reaction was applied to the eyes of $\gamma^{-/-}$ and $C1q^{-/-}$ mice on a BALB/c background as described in section 2.1.2. To study the role of individual activating FcγRs, the same protocol was performed on $FcγRI^{-/-}$, $FcγRIII^{-/-}$ and $FcγRIV^{-/-}$ mice on a BALB/c background. Wild-type (WT) BALB/c mice immunised with OVA and challenged with OVA intravitreously were used as a positive control and WT BALB/c mice immunised with OVA and injected intravitreously with saline were used as a negative control. For simplicity, OVA-immunised wild-type mice injected with saline are referred to as "WT saline control" from here onwards.

The results in Chapter 3 show the inflammatory response to immune complex deposition in the retina peaks at 3 days. Therefore, eyes and serum were collected 3 days after intravitreous challenge with OVA (section 2.1.5.). The serum was used to detect the titers of circulating OVA specific IgG1 and IgG2a (section 2.4.). The eyes were analysed for the presence of immune complexes, IgG subclass, microglial activation and leukocyte recruitment by immunohistochemistry as described in section 2.2.2. Quantification of immunohistochemistry was performed by counting the number of stained cells per mm of retina, only when DAPI+ nuclei were visible (as detailed in

2.2.3). For statistical analysis of immunohistochemistry, n= 4-6 mice per treatment group were analysed.

4.3 Results

4.3.1 Differential role of complement and Fcγ Receptors in immune complex responses in the retina.

The contribution of FcγRs and the complement system to immune complex-mediated inflammation in the retina was examined by forming OVA-anti-OVA immune complexes in the retina of $\gamma^{-/-}$ and $C1q^{-/-}$ mice. Immunisation with OVA resulted in comparable levels of anti-OVA IgG1 in all genotypes but in reduced levels of IgG2a in $\gamma^{-/-}$ and $C1q^{-/-}$ mice when compared to WT. (Figure 4.1. a). Following OVA challenge, co-immunolocalisation of OVA and IgG was observed in the subretinal space (SR), the outer photoreceptor segment layer (PR) and ganglion cell layer (GCL) of OVA sensitised WT, $\gamma^{-/-}$ and $C1q^{-/-}$ mice (Figure 4.1. b, arrows), indicating IC formation. Immune complexes formed abundantly in all mice immunised with OVA.

Due to the differences in their affinity for FcγRs and ability to fix complement, IgG subclass composition of the immune complexes likely impacts on the extent of the inflammatory response. To determine the prevalence of each IgG subclass in the immune complexes, immunohistochemical labelling of IgG1, IgG2a and IgG2b was performed (Figure 4.2.). IgG3 is the least common and least pathogenic mouse IgG subclass[217, 313] and therefore was not investigated. Co-immunolocalisation of total IgG revealed that IgG1 was the most abundant IgG subclass. IgG1 was detected in most of the IgG deposits forming across the retina, whilst IgG2a and IgG2b were only detected in a few deposits (Figure 4.2. a, arrows). Particularly, IgG1 was detected in both large and small deposits (forming predominantly in the PR), whereas IgG2a and IgG2b were only detected in larger immune complexes (forming predominantly in the inner retinal layers; Figure 4.2. b).

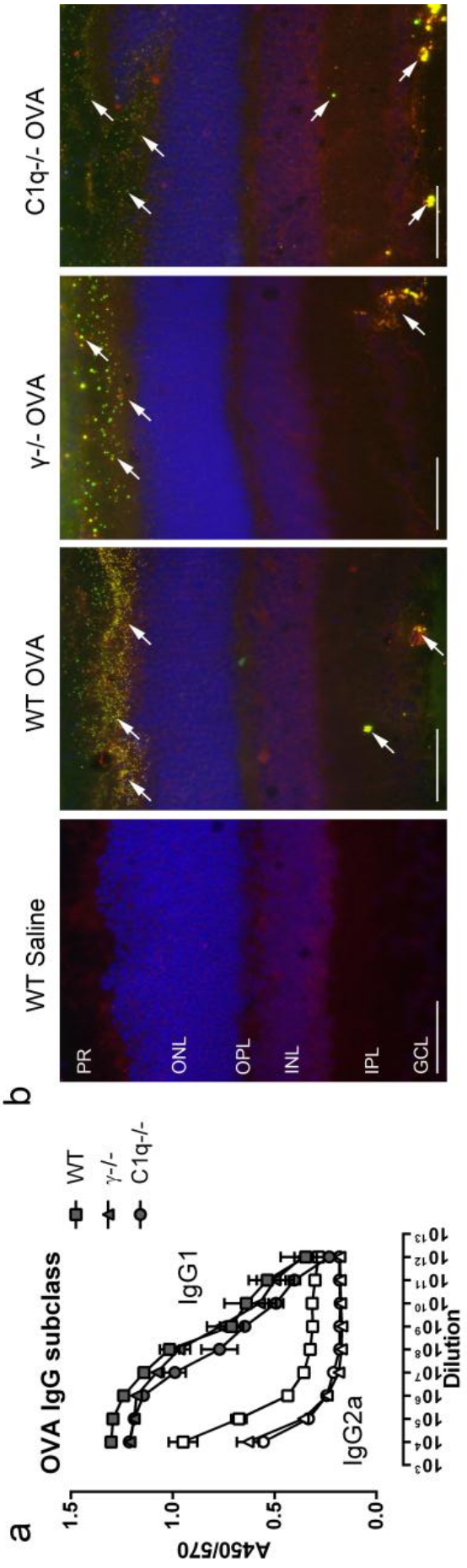
a
OVA IgG subclass
WT
γ-/-
C1q-/-
IgG1
IgG2a
A450/570
1.5
1.0
0.5
0.0
Dilution
10³
10⁴
10⁵
10⁶
10⁷
10⁸
10⁹
10¹⁰
10¹¹
10¹²
10¹³
b
WT Saline
WT OVA
γ-/- OVA
C1q-/- OVA
PR
ONL
OPL
INL
IPL
GCL

Figure 4.1. Immune complexes form in wild-type BALB/c, FcγR gamma chain KO and C1q KO sensitised mice following intravitreous challenge with OVA.

(a) Detection of anti-OVA circulating IgG1 and IgG2a antibodies by ELISA showed WT (n=8), *γ-/-* (n=4) and *C1q-/-* (n=4) sensitised mice had comparable titers of anti-OVA IgG1 and IgG2a antibodies. **(b)** Immunohistochemical detection of OVA (red) and IgG (green) 3 days after intravitreous OVA or saline challenge in WT, $\gamma^{-/-}$ and $C1q^{-/-}$ immunised mice (n=5-6). Cell nuclei were stained with DAPI (blue). Co-localisation of OVA and IgG (yellow) confirmed immune complex formation throughout the retina in WT, *γ-/-* and *C1q-/-* BALB/c mice after OVA challenge (arrows). PR, photoreceptors; ONL, outer nuclear layer; OPL, outer plexiform layer; INL, inner nuclear layer; IPL, inner plexiform layer; GCL, ganglion cell layer. Scale bars - 50μm.

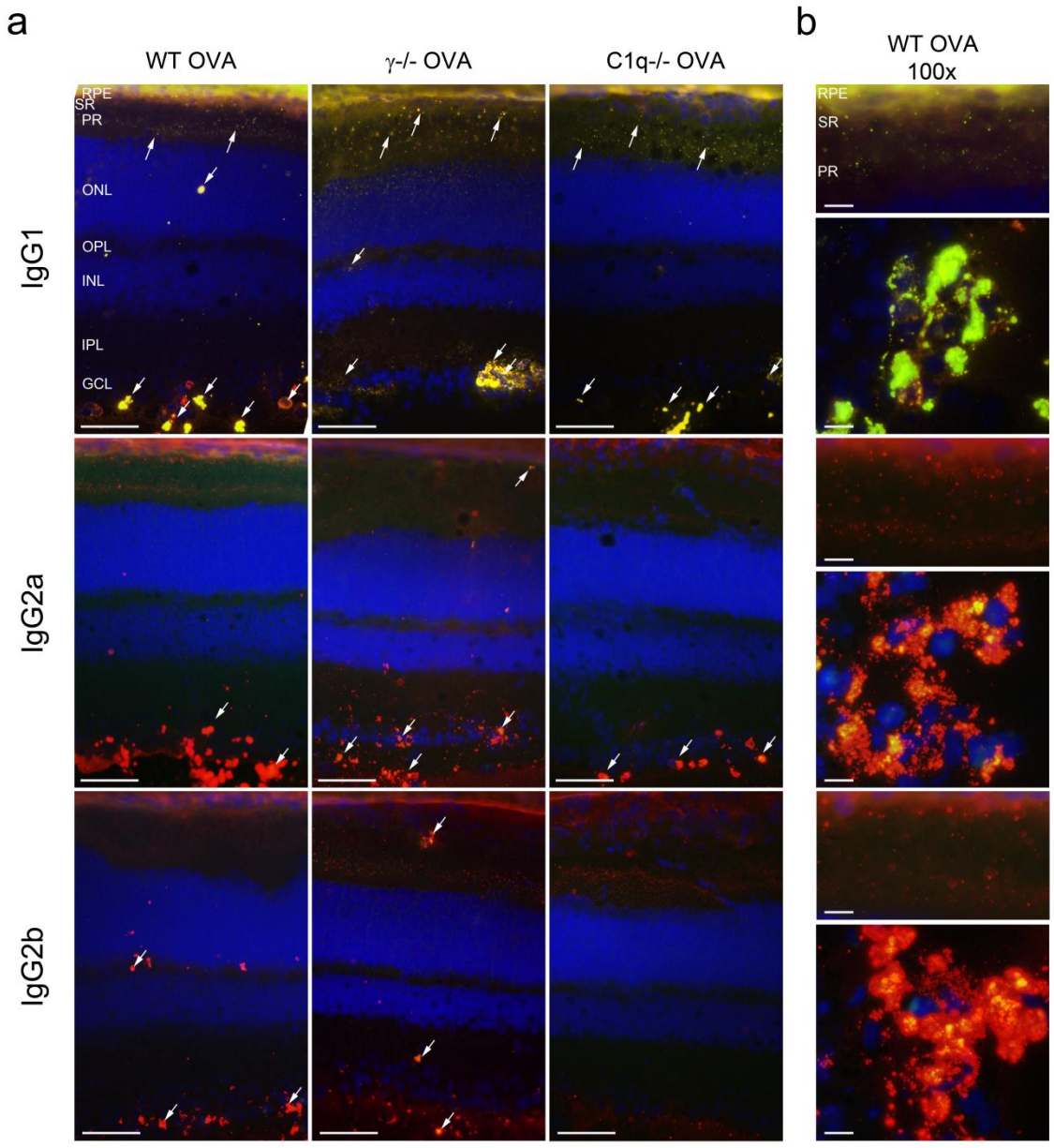

Figure 4.2. IgG deposits in wild-type BALB/c, FcγR gamma chain KO and C1q KO sensitised mice contain IgG1, IgG2a and IgG2b.

(a) Immunohistochemical detection of total IgG (red) and IgG1 (green), IgG2a (green) or IgG2b (green) 3 days after intravitreous challenge with OVA in WT, *γ-/-* and *C1q-/-* sensitised mice (n=5-6). IgG1 was abundant in both small and large IgG deposits (arrows) in all immunised mice (arrows). IgG2a and IgG2b were detected in larger deposits but not in smaller ones (arrows). Scale bars - 50μm. **(b)** Images of small and large IgG deposits in wild-type BALB/c mice taken at 100x magnification. Cell nuclei were stained with DAPI (blue). Scale bars -10 μm. RPE, retinal pigmented epithelium; SR, subretinal space; PR, photoreceptors; ONL, outer nuclear layer; OPL, outer plexiform layer; INL, inner nuclear layer; IPL, inner plexiform layer; GCL, ganglion cell layer.

The results in Chapter 3 showed that immune complex deposition in the retina results in a robust inflammatory response, characterised by microglia activation and recruitment of leukocytes. 3 days after OVA challenge in WT mice, $CD11b^+$ microglia migrated towards sites of immune complex formation (mostly PR and GCL) and adopted an amoeboid-like morphology characteristic of activated microglia. $CD11b^+$ cells with a round morphology characteristic of monocytes/macrophages were present in the GCL and vitreous. 3 days after OVA challenge in $C1q^{-/-}$ mice, similar changes in CD11b were observed (Figure 4.3. a). In contrast, following OVA challenge in $\gamma^{-/-}$ mice, $CD11b^+$ microglia were only present in the plexiform layers and displayed a ramified-like morphology similar to that of saline injected controls, and no round $CD11b^+$ cells were observed (Figure 4.3. a). In WT saline controls no $CD45^+$ cells are observed. Immune complex deposition in WT mice resulted in expression of CD45 by microglia and recruitment of $CD45^+$ cells with a round morphology. Similar changes were observed in $C1q^{-/-}$ mice following OVA challenge. In $\gamma^{-/-}$ mice, intravitreous OVA challenge resulted in expression of CD45 by cells with a microglia-like morphology, however, no $CD45^+$ round cells were detected (Figure 4.3. b). Quantification revealed that intravitreous injection of OVA resulted in an increase in number of cells/mm expressing CD11b and CD45 in WT mice (CD11b: $p=0.0019$, CD45: $p=0.0011$) and $C1q^{-/-}$ (CD11b: $p=0.0087$, CD45: $p=0.0030$) when compared with WT saline control. These responses were not observed in $\gamma^{-/-}$ mice (Figure 4.4.). CD11b and CD45 staining looked similar in contralateral non-injected eyes of $\gamma^{-/-}$, $C1q^{-/-}$ mice and in WT saline controls (not shown).

OVA challenge in WT mice led to increased number of cells expressing FcγRI (Figure 4.3. c), FcγRII/III (Figure 4.3. d), FcγRIII (Figure 4.3. e), FcγRIV (Figure 4.3. f) and MHC II (Figure 4.3. g), indicating activation of microglia and recruitment of leukocytes

following immune complex formation. Similar changes were observed in *C1q*$^{-/-}$ mice (Figure 4.3 c-g). Although the number of MHC II^{+} cells in *C1q*$^{-/-}$ mice was increased when comparing with WT saline control mice, deficiency of C1q resulted in a small but statistically significant decrease in the number MHC II^{+} cells when compared to WT mice challenged with OVA (Figure 4.4). As expected, $\gamma^{-/-}$ mice did not show any expression of FcγRI, FcγRIII, and FcγRIV. FcγRII/III positive cells were detected in $\gamma^{-/-}$ mice, likely due to expression of the inhibitory FcγRII. In addition, there were no detectable MHC II^{+} cells in $\gamma^{-/-}$ mice following immune complex formation (Figure 4.3. c-g). FcγRI, FcγRII/III, FcγRIII, FcγRIV and MHC II staining looked similar in contralateral non-injected eyes of $\gamma^{-/-}$, *C1q*$^{-/-}$ and in WT saline controls (not shown).

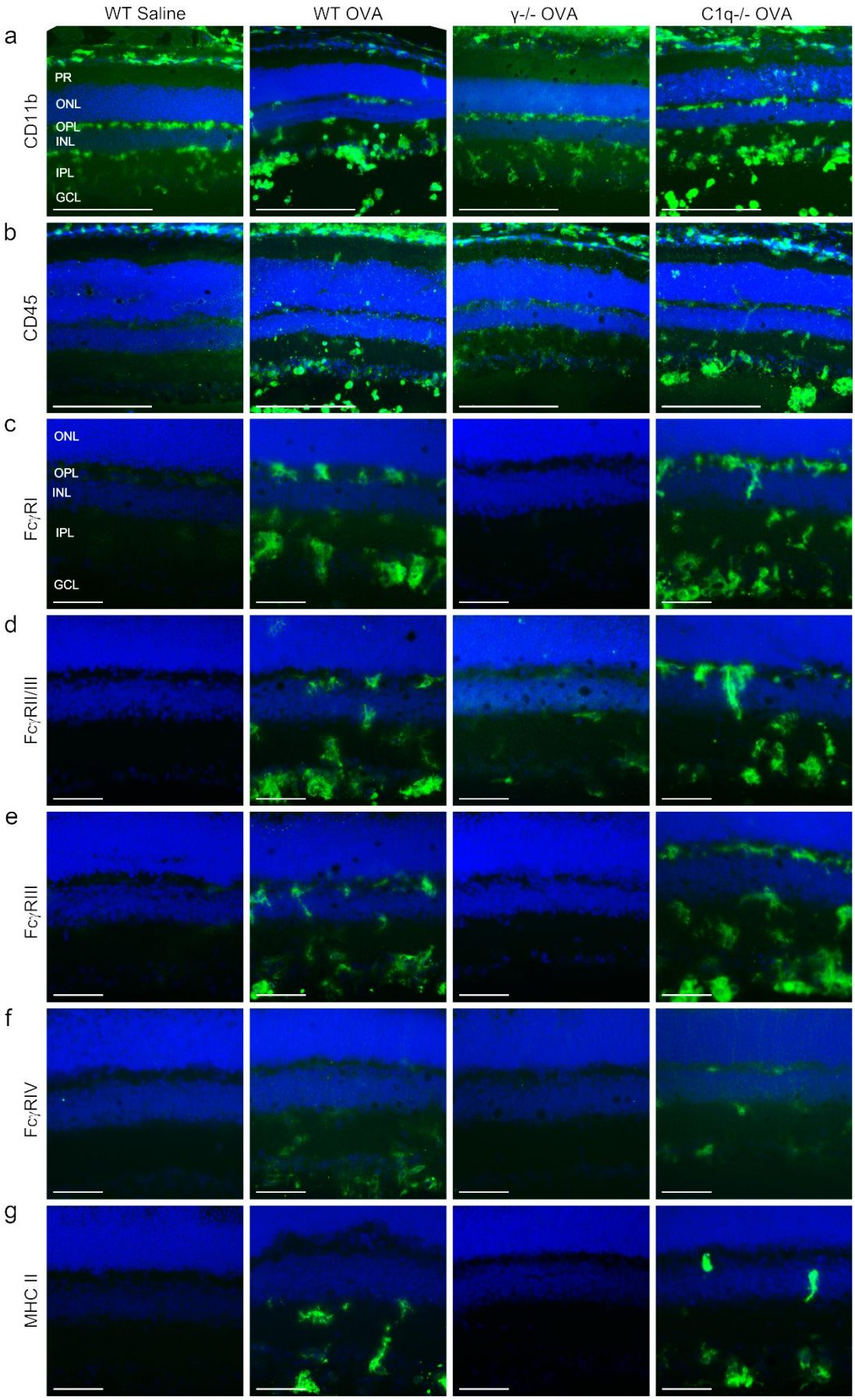
WT Saline
WT OVA
γ-/- OVA
C1q-/- OVA
a
CD11b
PR
ONL
OPL
INL
IPL
GCL
b
CD45
c
FcγRI
ONL
OPL
INL
IPL
GCL
d
FcγRII/III
e
FcγRIII
f
FcγRIV
g
MHC II

Figure 4.3. Immune complex mediated inflammation is dependent on the presence of activating FcγRs.

(a-g) Immunohistochemistry for CD11b **(a)**, CD45 **(b)**, FcγRI **(c)**, FcγRII/III **(d)**, FcγRIII **(e)**, FcγRIV **(f)** and MHC II **(g)** 3 days after intravitreous injection of saline in WT and of OVA in in WT, $\gamma^{-/-}$ and $C1q^{-/-}$ immunised mice (green). Cell nuclei were stained with DAPI (blue). OVA-immunized mice injected with saline intravitreously showed $CD11b^{+}$ microglia **(a)** with a ramified morphology with low expression of FcγRs **(c-f)**, MHC II and CD45 **(g, b)**. Following intravitreous challenge with OVA an inflammatory response was induced as evidenced by changes in morphology and numbers of $CD11b^{+}$ microglia **(a)** and increased expression of FcγRs, MHC II and CD45 **(b-g)**. These changes were not observed in $\gamma^{-/-}$ mice but occurred in $C1q^{-/-}$. PR, photoreceptors; ONL, outer nuclear layer; OPL, outer plexiform layer; INL, inner nuclear layer; IPL, inner plexiform layer; GCL, ganglion cell layer. Scale bars - 50μm.

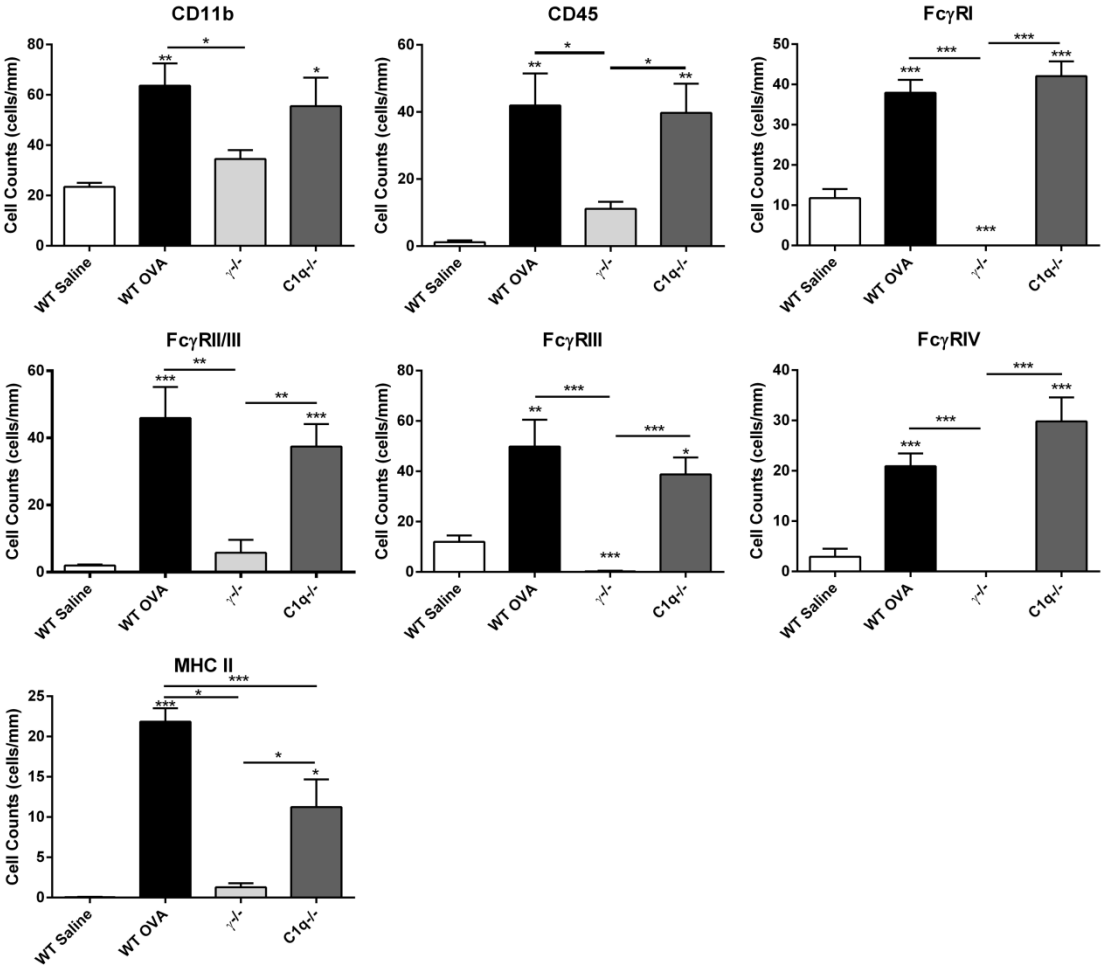

Figure 4.4. The number of cells expressing inflammatory markers following OVA challenge is decreased in FcγR gamma chain KO but not C1q KO mice.

Quantification of cell number/mm of retina expressing CD11b, CD45, FcγRI-IV and MHC II in wild type, $\gamma^{-/-}$ and $C1q^{-/-}$ immunised mice. Data are expressed as cells/mm of retina +SEM and were analysed using one-way ANOVA followed by Bonferroni correction, n=5-6 mice per group. *p<0.05, **<0.01, ***p<0.001 when compared to WT saline unless otherwise specified with line bars.

Finally the effect of the absence of activating FcγRs and C1q on recruitment of CD3 and CD4 positive cells was examined. Both $\gamma^{-/-}$ and $C1q^{-/-}$ mice showed a significant decrease in the number of infiltrating $CD3^+$ and $CD4^+$ cells when compared to WT mice challenged with OVA (Figure 4.5). However, $C1q^{-/-}$ mice showed a significantly higher number of $CD3^+$ and $CD4^+$ cells when compared to WT saline control mice.

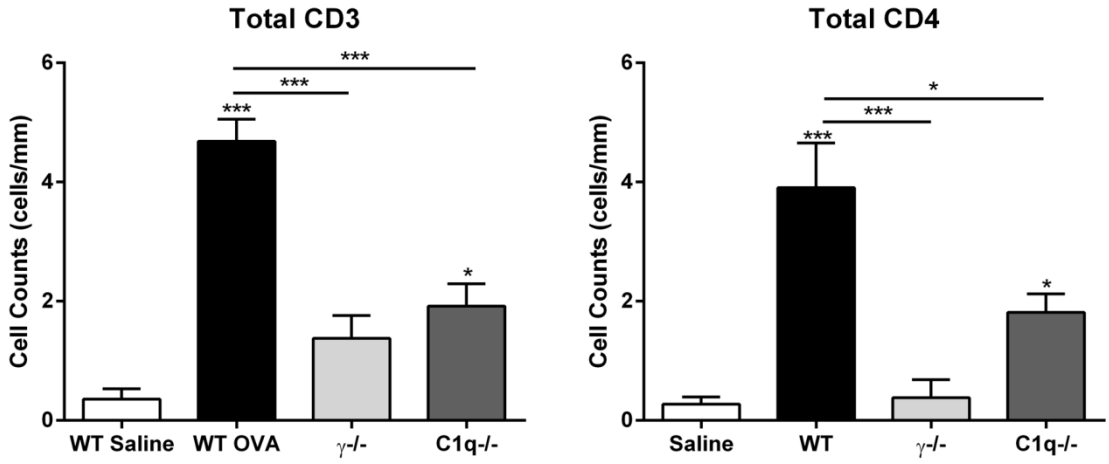

Figure 4.5. The number of infiltrating T cells following OVA challenge is decreased in both FcγR gamma chain KO and C1q KO mice.

Quantification of the number of cells/mm of retina expressing CD3 or CD4 in wild type, $\gamma^{-/-}$ and $C1q^{-/-}$ immunised mice. Data are expressed as cells/mm of retina +SEM and were analysed using one-way ANOVA followed by Bonferroni correction, n=5-6 mice per group. *p<0.05, **<0.01, ***p<0.001 when compared to WT saline unless otherwise specified with line bars.

4.3.2 Contribution of individual activating Fcγ receptors to immune complex-mediated inflammation

Individual FcγRs have been shown to have differential contribution to immune complex-mediated inflammation. To dissect the role of individual activating FcγRs, the reverse Arthus reaction was induced in the retina of mice deficient in FcγRI ($FcγRI^{-/-}$), FcγRIII ($FcγRIII^{-/-}$) and FcγRIV ($FcγRIV^{-/-}$). Immunisation with OVA led to a similar immune response in $FcγRI^{-/-}$, $FcγRIII^{-/-}$ and $FcγRIV^{-/-}$ mice, with comparable titers of circulating anti-OVA IgG1 or IgG2a. These were higher than the levels of IgG1 and IgG2a in WT mice (Figure 4.6. a). Immune complex formation was assessed 3 days after OVA challenge (Figure 4.6. b). Co-localisation of OVA and IgG revealed that although immune complexes formed in all strains of mice (Figure 4.6. b) there was some notable differences. In $FcγRI^{-/-}$ mice, immune complexes were observed mainly in

the SR and PR, with only scarce deposition of immune complexes in the inner layers in all mice. OVA challenge in both *FcγRIII*$^{-/-}$ and *FcγRIV*$^{-/-}$ resulted in abundant immune complex deposition in the SR, PR and GCL, similar to WT mice. However, at the 3 day time point, immune complexes appeared to be more abundant, in both size and number, in *FcγRIV*$^{-/-}$ than in *FcγRIII*$^{-/-}$ (Figures 4.6 and 4.7). The prevalence of IgG1, IgG2a and IgG2b was also investigated. Similar to the previous results, IgG1 was the predominant IgG subtype in all mice, and was abundantly present in small as well as large immune complexes. IgG2a and IgG2b were only detected in a few large immune complexes. The prevalence of each IgG subtype was similar in all genotypes (Figure 4.7).

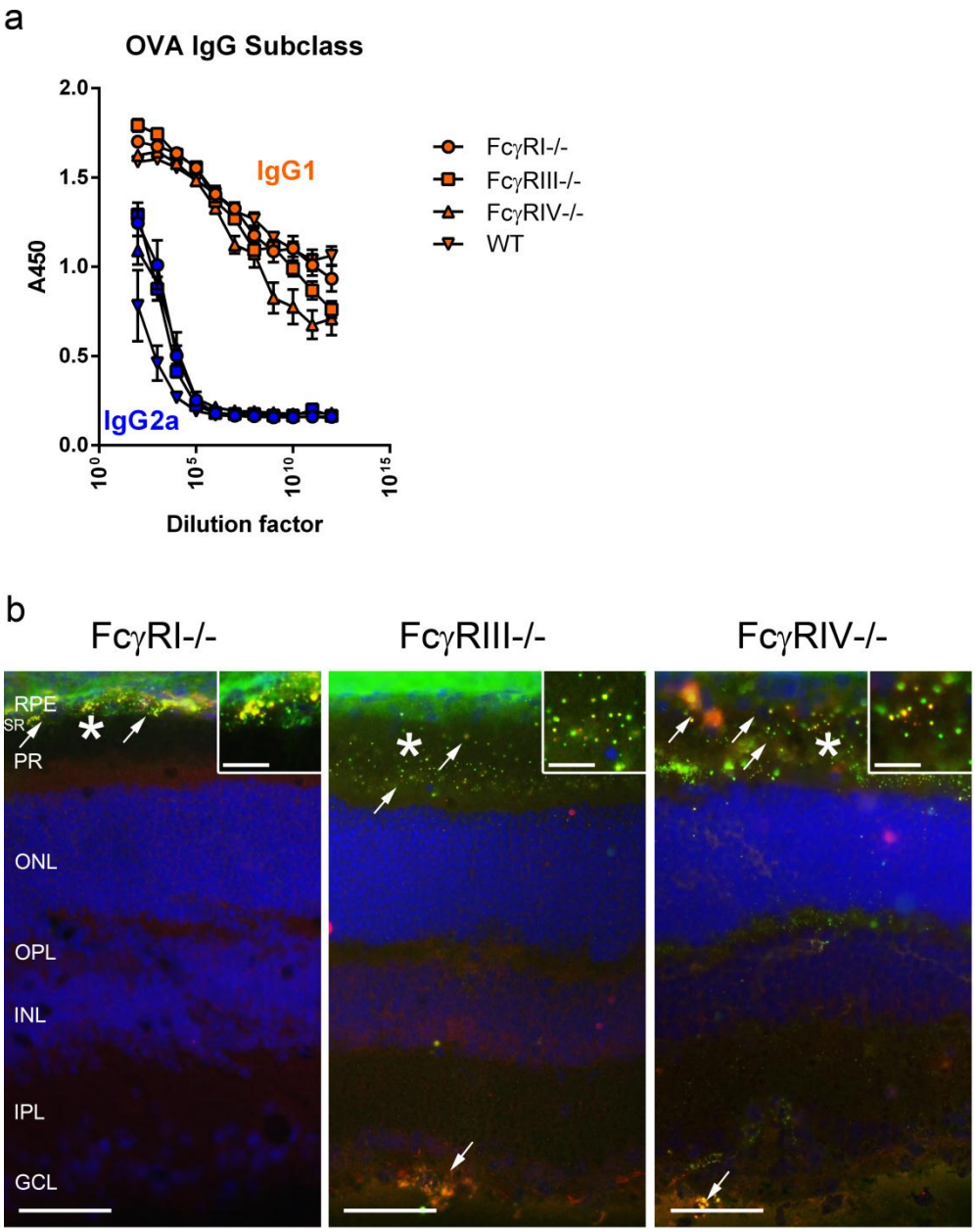

Figure 4.6. Immune complexes form in FcγRI-, FcγRIII- and FcγRIV-deficient mice sensitised to OVA following intravitreous challenge with OVA.

(a) Detection of anti-OVA circulating IgG1 and IgG2a antibodies by ELISA showed WT (n=4), *FcγRI*$^{-/-}$ (n=4), *FcγRIII*$^{-/-}$ (n=4) and *FcγRIV*$^{-/-}$ (n=4) immunised mice had similar titers of anti-OVA IgG1 and IgG2a antibodies. **(b)** Immunohistochemical detection of OVA (red) and IgG (green) 3 days after intravitreous challenge with saline in *FcγRI*$^{-/-}$, *FcγRIII*$^{-/-}$ and *FcγRIV*$^{-/-}$ immunised mice (n=4-6). Cell nuclei were stained with DAPI (blue). Co-localisation of OVA (red) and IgG (green) showed immune complex formation after OVA challenge (arrows). * indicates origin of inset. RPE, retinal pigmented epithelium; SR, subretinal space; PR, photoreceptors; ONL, outer nuclear layer; OPL, outer plexiform layer; INL, inner nuclear layer; IPL, inner plexiform layer; GCL, ganglion cell layer. Scale bars - 50μm; inset scale bars - 50 μm.

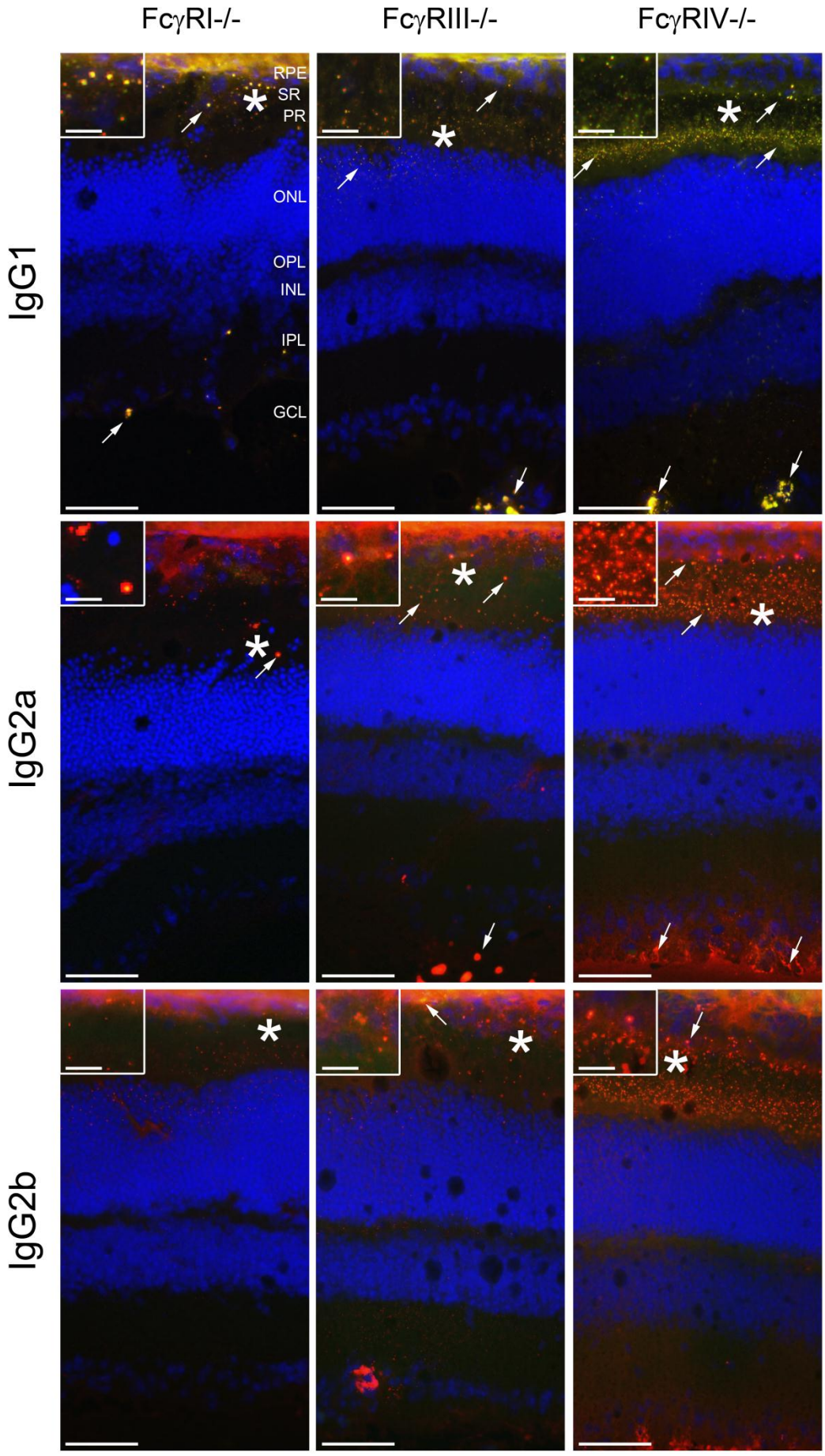
FcγRI-/-
FcγRIII-/-
FcγRIV-/-
IgG1
IgG2a
IgG2b
RPE
SR
PR
ONL
OPL
INL
IPL
GCL

Figure 4.7. IgG deposits in FcγRI-, FcγRIII- and FcγRIV-deficient mice sensitised to OVA contain IgG1, IgG2a and IgG2b.

(a) Immunohistochemical detection of total IgG (red) and IgG1, IgG2a or IgG2b (green) 3 days after intravitreous challenge with OVA in *FcγRI*$^{-/-}$, *FcγRIII*$^{-/-}$ and *FcγRIV*$^{-/-}$ immunised mice (n=4-6). Cell nuclei were stained with DAPI (blue). IgG1 was abundant in both small and large IgG deposits (arrows). IgG2a and IgG2b were detected in larger deposits but not in smaller ones (arrows). * indicates origin of inset. RPE, retinal pigmented epithelium; SR, subretinal space; PR, photoreceptors; ONL, outer nuclear layer; OPL, outer plexiform layer; INL, inner nuclear layer; IPL, inner plexiform layer; GCL, ganglion cell layer. Scale bars - 50μm; inset scale bars - 50 μm.

4.3.3 The response to immune complex formation in the retina of Fcγ receptor I deficient mice

Deficiency of FcγRI was confirmed by immunohistochemistry (Figure 4.8. a); no cells expressing FcγRI were detected in the retinae of *FcγRI*$^{-/-}$ following OVA challenge. Next, the inflammatory response to immune complex formation was investigated. Staining for CD11b revealed CD11b^{+} microglia were predominantly present in the plexiform layers, similar to saline WT controls and $\gamma^{-/-}$ mice. These microglia had short processes and an amoeboid-like morphology, similar to WT mice after OVA challenge (Figure 4.8. b, inset). Only scarce CD11b^{+} cells with round morphology were observed. Cells with microglia-like morphology expressing CD45, FcγRII/III, FcγRIV and MHC II could be observed, but no round cells expressing these markers were detected (Figure 4.8. b,c). In addition, recruitment of CD3^{+} and CD4^{+} cells following OVA challenge was reduced in *FcγRI*$^{-/-}$ mice relative to WT (Figure 4.14.).

Quantification revealed that 3 days after OVA challenge, *FcγRI*$^{-/-}$ mice exhibited an attenuated inflammatory response to immune complex, similar to $\gamma^{-/-}$ mice. Reduced number of cells expressing all markers investigated, except FcγRIII, were counted when compared to WT mice challenged with OVA (CD11b, p=0.0001; CD45, p=0.031; FcγRII/III, p=0.032; FcγRIII, p=0.32; FcγRIV, p=0.0004; MHC II, p<0.0001). The number of cells expressing CD11b in *FcγRI*$^{-/-}$ and $\gamma^{-/-}$ or WT saline controls was indistinguishable. In contrast, there were more cells expressing CD45 and MHC II in *FcγRI*$^{-/-}$ than WT saline controls (CD45, p=0.031; MHC II, p=0.01), but not $\gamma^{-/-}$ mice. There was an increase in FcγRII/III^{+} and FcγRIII^{+} cells in *FcγRI*$^{-/-}$ when compared to $\gamma^{-/-}$ mice (FcγRII/III, p=0.001; FcγRIII, p<0.0001), whilst a higher number of FcγRII/III^{+} but not FcγRIII^{+} cells was seen when compared to WT saline controls (p=0.001).

Finally the number of FcγRIV^{+} and MHC II^{+} cells was higher, but not significantly increased in *FcγRI*$^{-/-}$ when compared to $\gamma^{-/-}$ mice (FcγRIV, p=0.34; MHC II, p=0.46; Figure 4.9.).

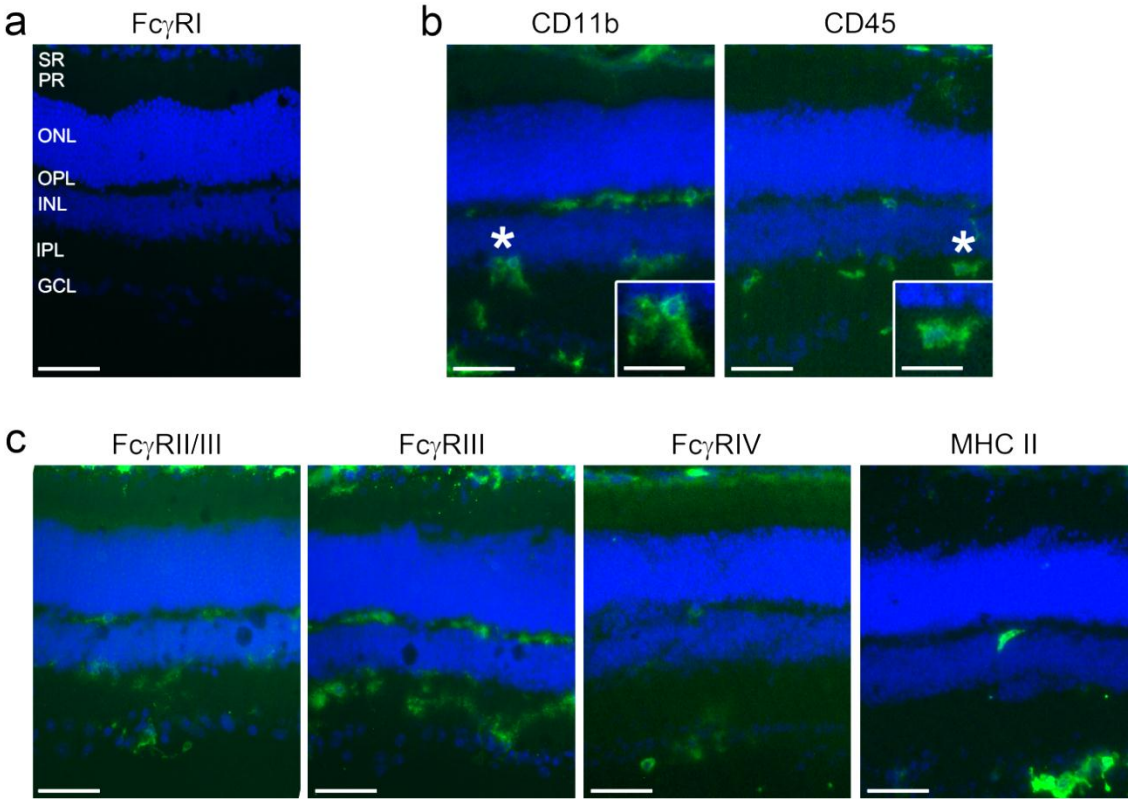

Figure 4.8. FcγRI depletion results in reduced immune complex-mediated inflammation following intravitreous challenge with OVA.

(a) No FcγRI expression (green) was detected by immunohistochemistry in *FcγRI*$^{-/-}$ mice. **(b)** Following OVA challenge in sensitised *FcγRI*$^{-/-}$ mice, CD11b^{+} and CD45^{+} cells (green) with microglia-like morphology were present in the plexiform layers but only few round CD11b^{+} and no round CD45^{+} cells were observed. **(c)** Following OVA challenge in immunised *FcγRI*$^{-/-}$ mice, FcγRII/III, FcγRIII, FcγRIV and MHC II expressing cells (green) with microglia-morphology were present in the plexiform layers. Cell nuclei were stained with DAPI (blue). (n=5 mice). * indicates origin of inset. SR, subretinal space; PR, photoreceptors; ONL, outer nuclear layer; OPL, outer plexiform layer; INL, inner nuclear layer; IPL, inner plexiform layer; GCL, ganglion cell layer. Scale bars - 50µm, inset - 25µm

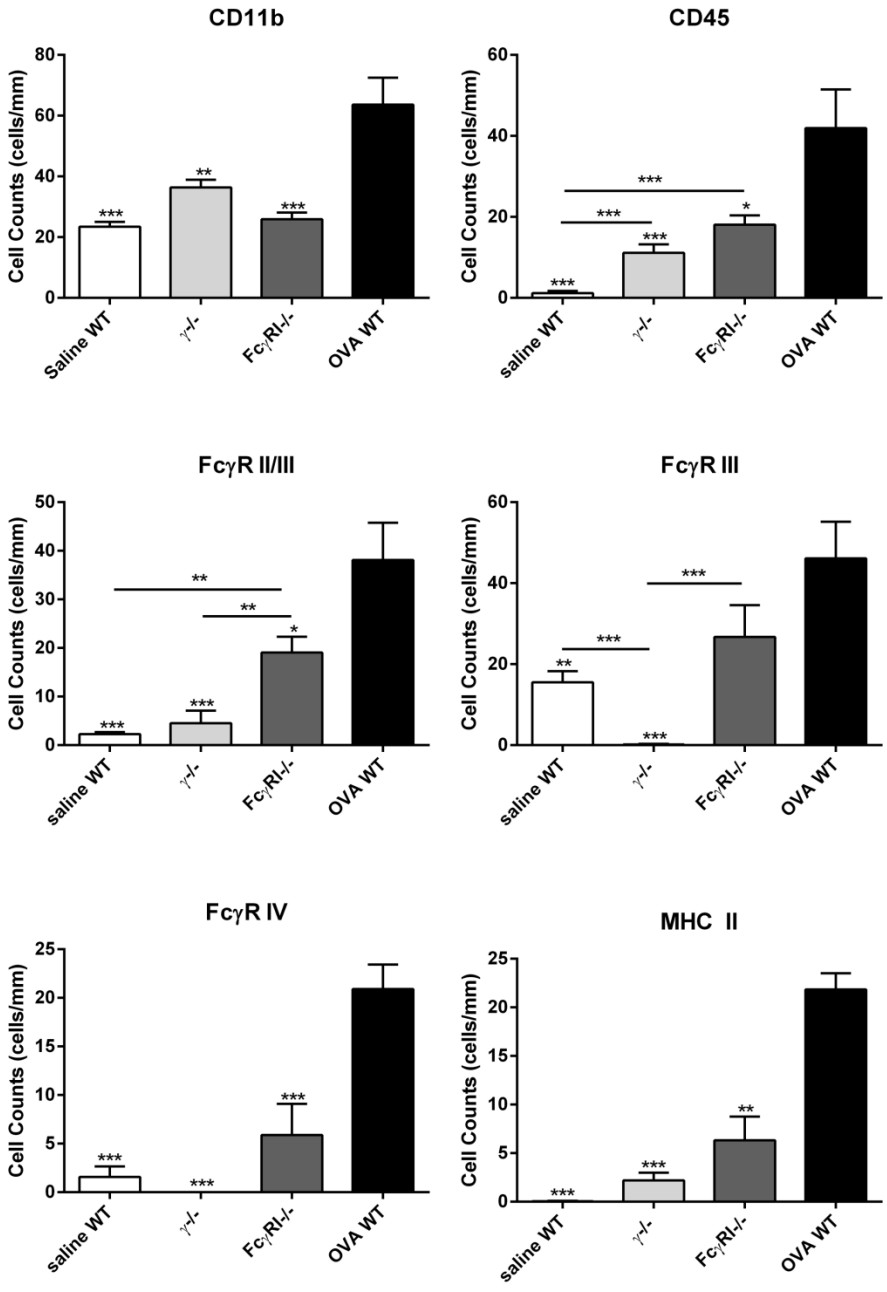

Figure 4.9. Quantification of cell number/mm of retina expressing CD11b, CD45, FcγRI-IV and MHC II in WT, $\gamma^{-/-}$ and $FcγRI^{-/-}$ mice.

Data are expressed as cells/mm of retina +SEM and were analysed using one-way ANOVA followed by Bonferroni correction, n=5-6 mice per group. *p<0.05, **<0.01, ***p<0.001 when compared to WT OVA unless otherwise specified with line bars.

4.3.4 The response to immune complex formation in the retina of Fcγ receptor III deficient mice

$FcγRIII^{-/-}$ mice also showed a reduced inflammatory response to immune complex formation in the retina. Immunohistochemistry confirmed the lack of detectable

expression of FcγRIII in these mice (Figure 4.10. a). CD11b immunoreactivity revealed microglia were present in the plexiform layers, similar to WT saline controls, and had a morphology that appeared to be intermediate to those observed in WT saline control and WT mice challenged with OVA (Figure 4.3. a, inset), with a round cell body and short processes (Figure 4.10. b). No $CD11b^+$ cells with round morphology were observed. Microglia expressing CD45, FcγRI, FcγRII/III and FcγRIV were observed in the plexiform layers and no round cells expressing any of these markers were detected (Figure 4.10. a, b). Few MHC II^+ cells were seen in the retina of *FcγRIII*$^{-/-}$ following OVA challenge (Figure 4.10. c). In addition, recruitment of $CD3^+$ and $CD4^+$ cells following OVA challenge was reduced in *FcγRIII*$^{-/-}$ mice (Figure 4.14.).

3 days after OVA challenge, *FcγRIII*$^{-/-}$ mice exhibited reduced number of cells expressing all markers investigated when compared to WT mice challenged with OVA (CD11b, p=0.0002; CD45, p=0.019; FcγRI, p=0.009; FcγRII/III, p=0.008; FcγRIV, p=0.002; MHC II, p<0.0001). The number of cells expressing CD11b in *FcγRIII*$^{-/-}$ and $\gamma^{-/-}$ or WT saline controls was indistinguishable, whilst the number of $CD45^+$ cells was increased in *FcγRIII*$^{-/-}$ when compared to WT saline controls (CD45, p<0.0001) but not $\gamma^{-/-}$ mice. The number of FcγRII/III^+ and $FcγRI^+$ cells was increased in *FcγRIII*$^{-/-}$ when compared to WT saline controls (FcγRII/III, p=0.009; FcγRI, p=0.009) and $\gamma^{-/-}$ mice (FcγRII/III, p<0.0001; FcγRI, p<0.0001). The number of $FcγRIV^+$ was significantly increased when comparing with $\gamma^{-/-}$ mice (p=0.015), but not WT saline controls, whilst the number of MHC II^+ cells was increased when compared to WT saline controls but not $\gamma^{-/-}$ mice (p=0.042; Figure 4.11.).

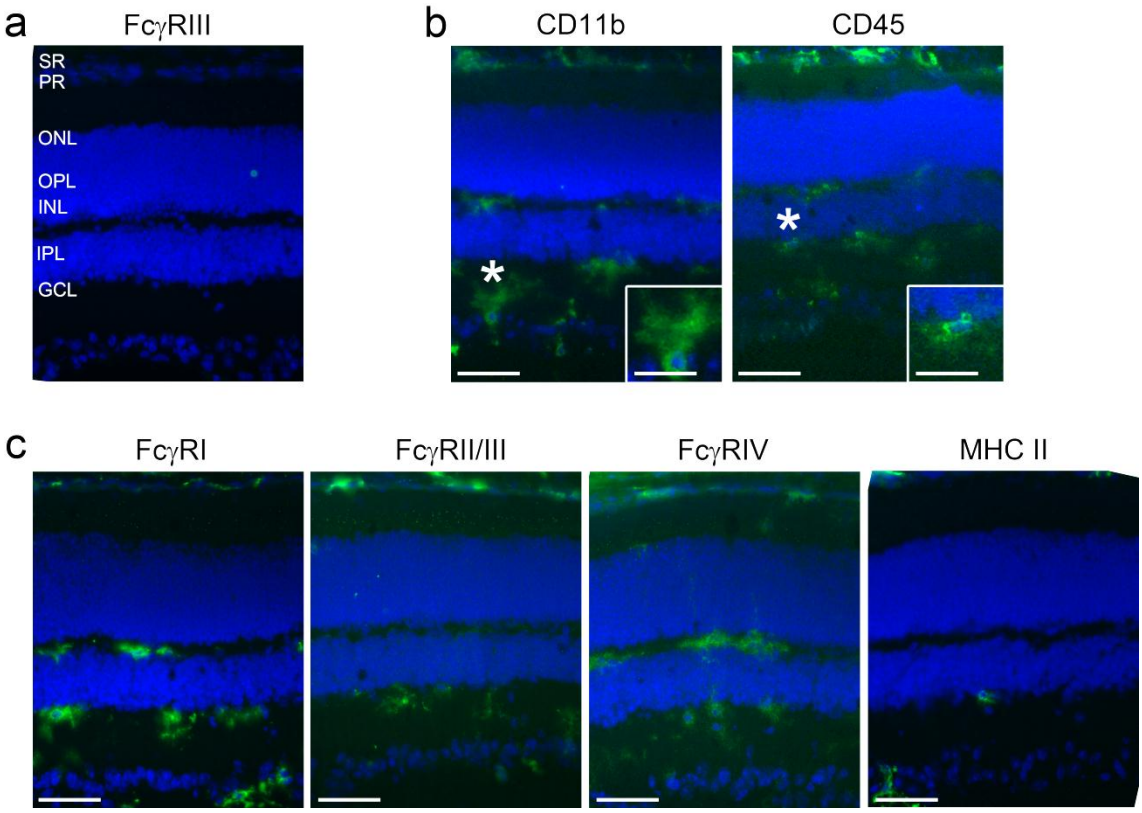

Figure 4.10. FcγRIII depletion results in reduced immune complex-mediated responses following intravitreous challenge with OVA.

(a) No FcγRIII expression (green) was detected by immunohistochemistry in *FcγRIII*$^{-/-}$ mice. **(b)** Following OVA challenge in immunised *FcγRIII*$^{-/-}$ mice, CD11b^{+} and CD45^{+} cells (green) with microglia-like morphology were present in the plexiform layers but no round CD11b^{+} or CD45^{+} cells were observed. **(c)** Following OVA challenge in immunised *FcγRIII*$^{-/-}$ mice, FcγRI, FcγRII/III, FcγRIV expressing cells (green) with microglia-morphology were present in the plexiform layers. Cell nuclei were stained with DAPI (blue). Only few MHC II^{+} cells were detected. (n=6 mice) * indicates origin of inset. SR, subretinal space; PR, photoreceptors; ONL, outer nuclear layer; OPL, outer plexiform layer; INL, inner nuclear layer; IPL, inner plexiform layer; GCL, ganglion cell layer. Scale bars - 50μm, inset - 25μm.

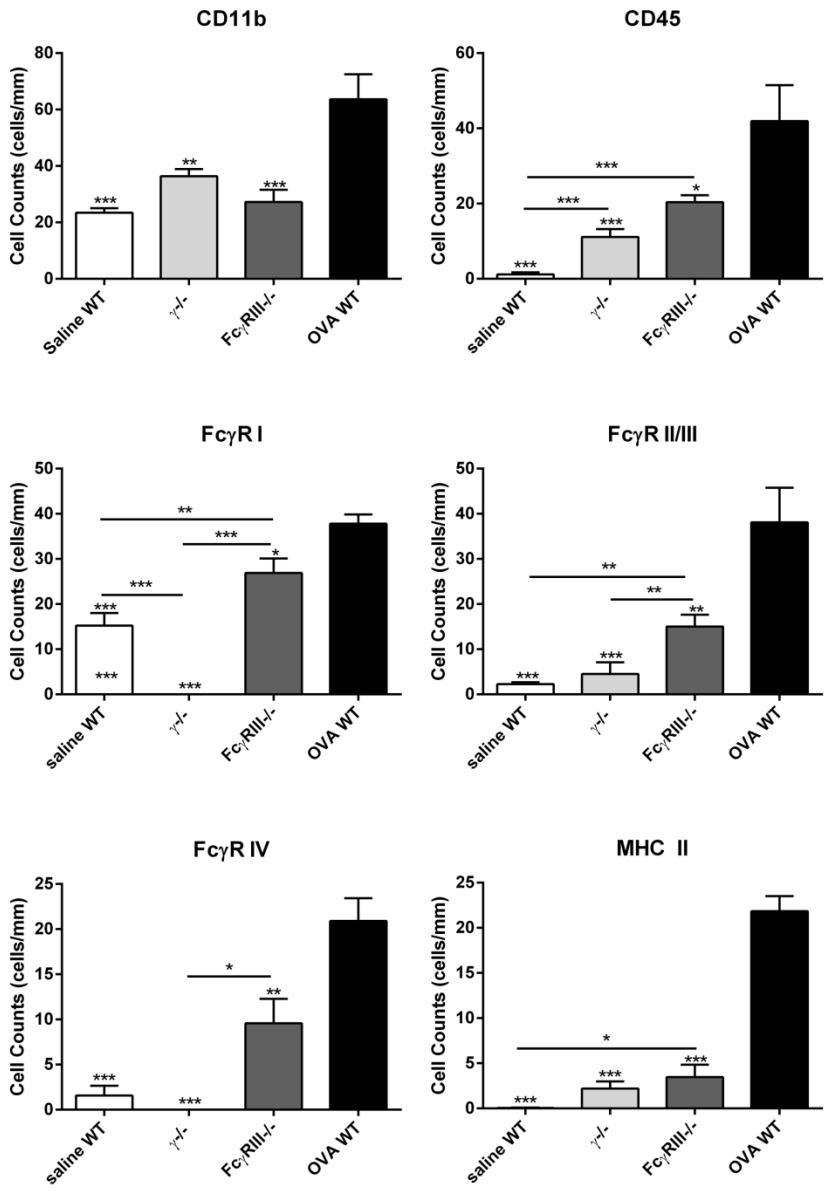

Figure 4.11. Quantification of cell number/mm of retina expressing CD11b, CD45, FcγRI-IV and MHC II in WT, *γ*$^{-/-}$ and *FcγRIII*$^{-/-}$ mice.

Data are expressed as cells/mm of retina +SEM and were analysed using one-way ANOVA followed by Bonferroni correction, n=5-6 mice per group. *p<0.05, **<0.01, ***p<0.001 when compared to WT OVA unless otherwise specified with line bars.

4.3.5 The response to immune complex formation in the retina of Fcγ receptor IV deficient mice

Finally immune complex formation was induced in *FcγRIV*$^{-/-}$ mice (n=6). It is worth mentioning that during tissue collection, two of the OVA challenged mice showed extensive bleeding in the OVA-injected eyes and these collapsed after removal from the

orbital space, suggesting severe inflammation in the tissue. No cells expressing FcγRIV in the retina of these mice were detected (Figure 4.12. a). Surprisingly, there was a strong inflammatory response to immune complex deposition in these mice. Staining for CD11b revealed microglia were present in nuclear, plexiform and ganglion cell layers, indicating microglia migration and, thus, activation. $CD11b^+$ microglia had an amoeboid-like morphology, with round cell body and no processes radiating from it. In addition, cells with a round morphology resembling that of monocytes/macrophages, were observed in the GCL and vitreous. Some cells with amoeboid-like morphology expressed CD45, but more notably cells with a round morphology in the GCL and vitreous were detected, likely indicating recruitment of cells (Figure 4.12. b). In addition, both cells with amoeboid-like and round morphologies expressing FcγRI, FcγRII/III, FcγRIII and MHC II were observed in the retina of *FcγRIV*$^{-/-}$ mice following OVA challenge (Figure 4.12. c). Recruitment of $CD3^+$ and $CD4^+$ cells following immune complex deposition was similar in *FcγRIV*$^{-/-}$ and WT mice.

Quantification showed the number of cells in *FcγRIV*$^{-/-}$ mice expressing all inflammatory markers investigated was increased when compared to WT saline controls (CD11b, $p=0.005$; CD45, $p<0.0001$; FcγRI, $p<0.0001$; FcγRII/III, $p=0.0002$; FcγRIII, $p<0.0001$; MHC II, $p<0.0001$) and $\gamma^{-/-}$ mice (CD11b, $p=0.005$; CD45, $p<0.0001$; FcγRI, $p<0.0001$; FcγRII/III, $p=0.0002$; FcγRIII, $p<0.0001$; MHC II, $p<0.0001$) and similar or increased when compared to WT mice challenged with OVA. The number of cells expressing CD11b, FcγRII/III and MHC II was similar in *FcγRIV*$^{-/-}$ when compared to WT mice challenge with OVA, whilst the number of CD45, FcγRI and FcγRIII was significantly increased when compared to WT mice challenged with OVA (CD45, $p=0.009$; FcγRI, $p=0.0002$; FcγRIII, $p=0.0002$; MHC II, $p<0.0001$; Figure 4.13.).

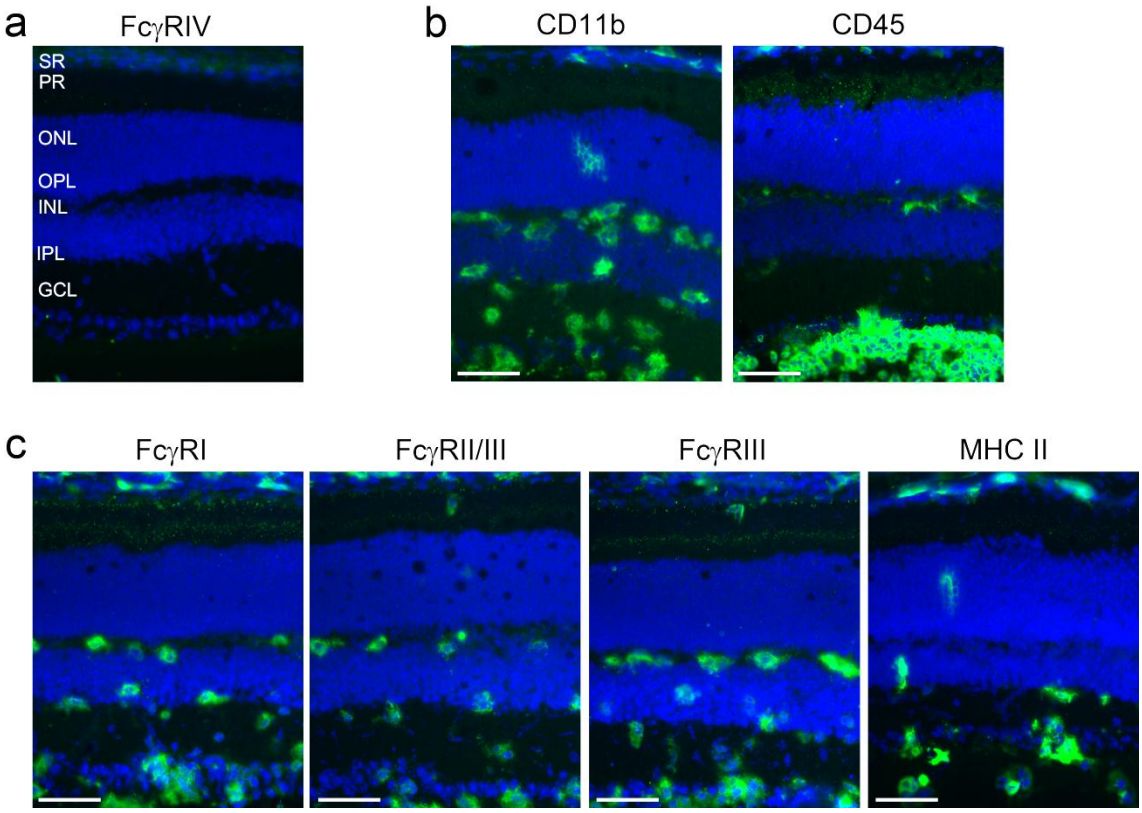

Figure 4.12. FcγRIV depletion results in robust immune complex-mediated inflammation following challenge with OVA.

(a) No FcγRIV expression (green) was detected by immunohistochemistry in *FcγRIV*$^{-/-}$ mice. **(b)** Following OVA challenge in sensitised *FcγRIV*$^{-/-}$ mice, CD11b^{+} cells (green) with amoeboid-like morphology were present in the plexiform and nuclear layers and in the GCL. Large numbers of CD45^{+} cells (green) with round morphology were seen in the GCL and CD45^{+} cells with microglia-like morphology in the plexiform layers. **(c)** Following OVA challenge in sensitised *FcγRIV*$^{-/-}$ mice, FcγRI, FcγRII/III, FcγRIII and MHC II expressing cells (green) were present throughout the retina. Cell nuclei were stained with DAPI (blue). (n=4 mice). SR, subretinal space; PR, photoreceptors; ONL, outer nuclear layer; OPL, outer plexiform layer; INL, inner nuclear layer; IPL, inner plexiform layer; GCL, ganglion cell layer. Scale bars - 50μm.

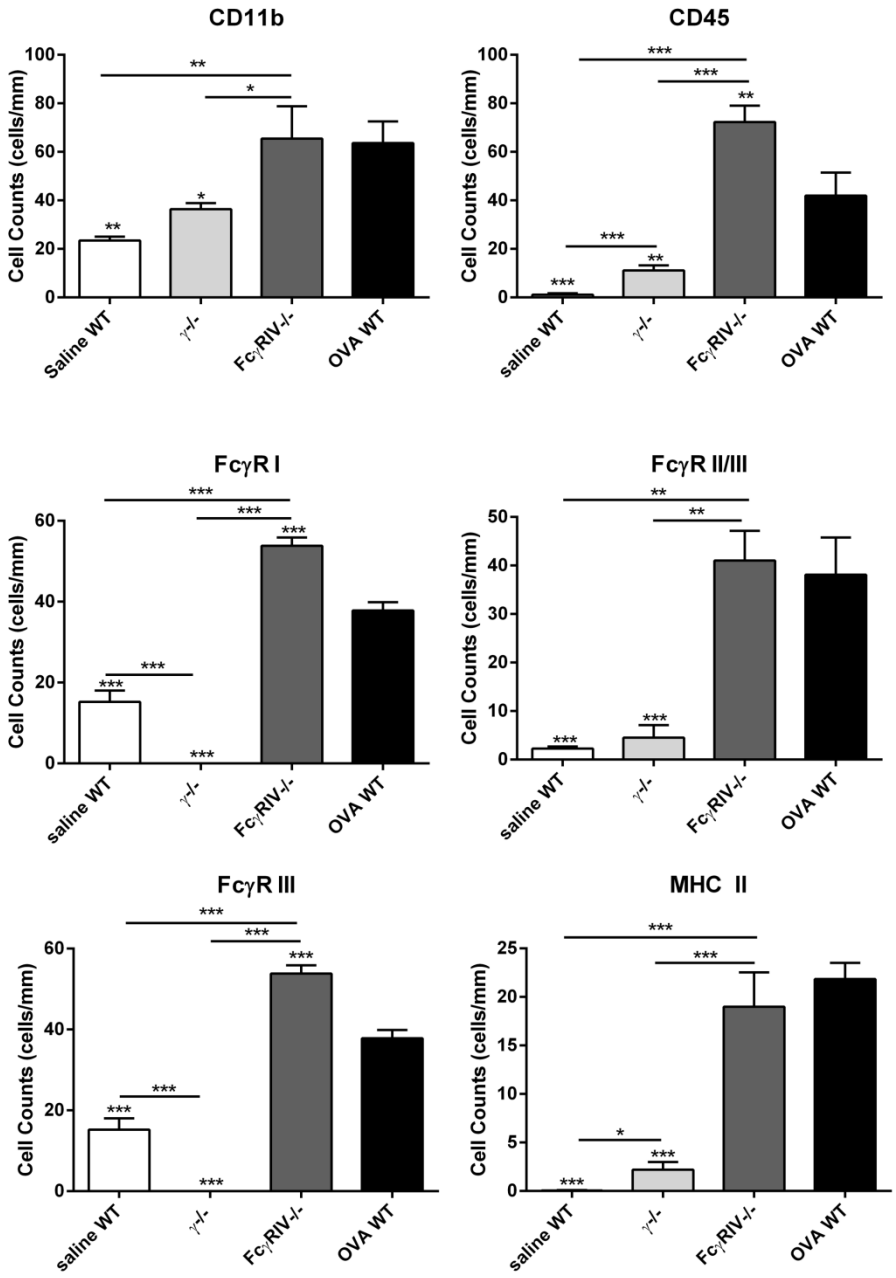

Figure 4.13. Quantification of cell number/mm of retina expressing CD11b, CD45, FcγRI-IV and MHC II in WT, $\gamma^{-/-}$ and *FcγRIV*$^{-/-}$ mice.

Data are expressed as cells/mm of retina +SEM and were analysed using one-way ANOVA followed by Bonferroni correction, n=4-6 mice per group. *p<0.05, **<0.01, ***p<0.001 when compared to WT OVA unless otherwise specified with line bars.

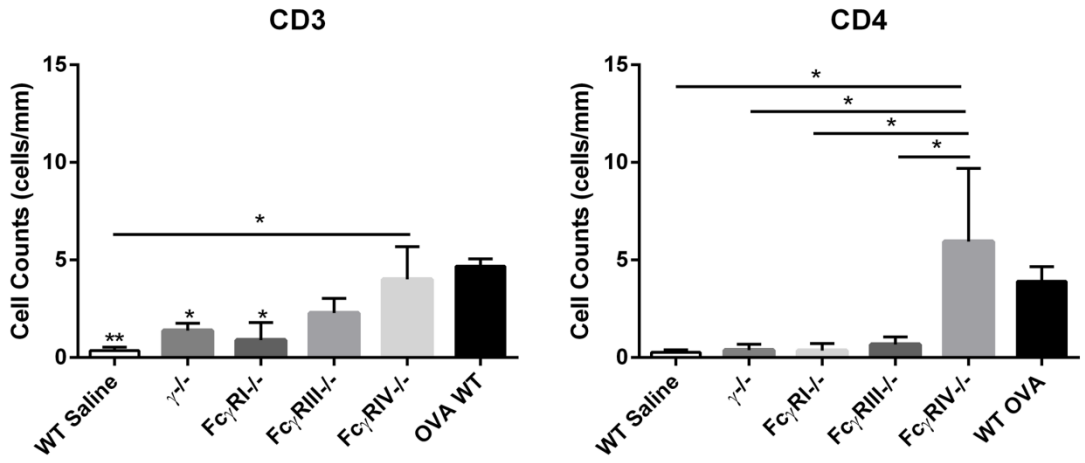

Figure 4.14. Quantification of the number of cells/mm of retina expressing CD3 or CD4 in wild type, $\gamma^{-/-}$ FcγRI-, FcγRIII- and FcγRIV-deficient mice sensitised to OVA following intravitreous challenge.

Data are expressed as cells/mm of retina +SEM and were analysed using one-way ANOVA followed by Bonferroni correction, n=4-6 mice per group. *p<0.05, **<0.01, ***p<0.001 when compared to WT saline unless otherwise specified with line bars.

4.4 Discussion

Immune complex formation in the retina results in a robust local inflammatory response characterised by activation of microglia, upregulation of FcγRs and MHC II and recruitment of leukocytes, including T cells. The results demonstrate that this inflammatory response is dependent on the presence of activating FcγRs, but not C1q, highlighting the importance of the FcγR system for the initiation of immune complex-mediated inflammation. Additionally, a differential role for the three activating FcγRs was demonstrated as deficiency of FcγRI or FcγRIII resulted in an attenuation of immune complex-mediated responses, whereas absence of FcγRIV resulted in an exaggerated inflammatory response.

4.4.1 Differential role of Fcγ Receptors and complement in immune complex-mediated inflammation

Immune complexes can induce inflammation via interaction with FcγRs expressed on immune cells and by activation of the classical complement cascade, following C1q/r/s deposition.[17] The crucial role of FcγRs in mediating immune complex pathology has

been demonstrated in several animal models, including the Arthus reaction.[301] Deposition of immune complexes in the skin,[301] kidney[314] and brain[282] of $\gamma^{-/-}$ mice, results in complete inhibition of the inflammatory response. In the present study $\gamma^{-/-}$ mice were protected from microglia activation and leukocyte recruitment in response to immune complex formation in the retina, indicating activating FcγRs are required for initiation of immune complex inflammation in the retina.

There is a tissue-specific requirement for proteins of the complement cascade in immune complex-mediated responses. Whilst depletion of early complement components of the classical pathway such as C3 and C4 has no effect on the development of the Arthus reaction in the skin,[300] C3 is required for neutrophil infiltration in the Arthus reaction in the lung.[312] Depletion of C5 or C5R results in either attenuation, or full inhibition of immune complex-mediated responses in several models, including the reverse Arthus reaction in the skin,[304, 312] lung[302, 303, 312] and kidney.[315] In this study, depletion of C1q did not affect the inflammatory response to immune complex deposition in the retina, suggesting activation of the classical complement cascade by C1q is not required for initiation of immune complex-mediated inflammation, and microglial activation. Cross-linking of FcγRs in mice can lead to secretion of C5a by effector cells, which is essential for development of full-blown autoimmune haemolytic anemia.[316] Secretion of C5a by microglia and/or macrophages following engagement of FcγRs could thus bypass the need for C1q to activate the complement cascade in the *C1q*$^{-/-}$ mouse. To fully assess the contribution of complement to immune complex-mediated inflammation in the retina, C3, C5 or C5R knock-out mice may need to be used. In conclusion, these studies do not rule out the involvement of complement in immune complex mediated inflammation in the retina, but rather show a non-redundant role of activating FcγRs in initiating immune complex-mediated inflammation, and in particular microglial activation and leukocyte recruitment.

4.4.2 The role of FcγRI in immune complex-mediated inflammation in the retina

FcγRI is the only FcγR with high affinity for IgG and is capable of binding to monomeric IgG2a, possibly reducing its accessibility to immune complexes. FcγRI is also capable of binding to IgG2a, IgG2b and IgG3 in immune complexes, but not to

IgG1.[226] FcγRI has been shown to be redundant to IgG1-, IgG2a- and IgG2b-mediated tumour and platelet depletion,[227] IgG2b-mediated autoimmune haemolytic anaemia (AHA)[225, 227] and IgG1-mediated hyperacute rejection (HAR).[317] Moreover, FcγRI appears to be redundant in the rabbit IgG-mediated reverse Arthus reaction in the skin[306] and the lung.[307] Here, immune complex formation in the retina of *FcγRI*$^{-/-}$ mice resulted in a much attenuated inflammatory response, much like what is observed in $\gamma^{-/-}$ mice, with reduced activation of microglia and almost no recruitment of CD11b^{+} or CD45^{+} leukocytes. This suggests FcγRI may have a role in immune complex-induced inflammation in the retina.

Depletion of FcγRI does not seem to impact on IgG1-mediated responses, likely due to the low affinity of IgG1 for this FcγR.[311] Competition for binding from endogenous monomeric IgG2a has been proposed as the reason for the lack of FcγRI involvement in immune complex-mediated responses. Recent studies showing reduced IgG2a-mediated tumour depletion[309] and AHA[225] suggest FcγRI may have a more important role in IgG2a-mediated responses than previously thought. In this chapter's experiments the predominant IgG subclass present in the retina was IgG1. It is possible that FcγRI contributes to immune complex-mediated inflammation through interaction with IgG2a and/or IgG2b which, albeit at lower levels, were still detected in the retina. This could explain why FcγRI depletion results in reduced immune complex-mediated inflammation in the retina.

With the exception of FcγRII/III^{+} and FcγRIII^{+} cell number, the response to immune complex formation in the retina of *FcγRI*$^{-/-}$ and $\gamma^{-/-}$ mice was very similar, despite the presence of FcγRIII in the former. FcγRIII can interact with IgG1, IgG2a and IgG2b immune complexes,[224] and thus could still induce inflammation in *FcγRI*$^{-/-}$ mice. The inhibitory FcγRII, which was expressed in the retinae of *FcγRI*$^{-/-}$ mice following immune complex formation, has a higher affinity for IgG1 than for IgG2b.[224] Interaction of IgG1 with FcγRII could be, at least in part, mediating inhibition of immune complex-induced inflammation in these experiments. Characterising the response to immune complex formation in mice lacking both FcγRI and FcγRII would be an interesting future direction. The reduced response to immune complex in *FcγRI*$^{-/-}$ could potentially be further explained by the fact that immune complexes seem to form less abundantly in the retina of *FcγRI*$^{-/-}$ mice than in WT, $\gamma^{-/-}$, *FcγRIII*$^{-/-}$ and *FcγRIV*$^{-/-}$ mice. It would be interesting to study the eyes of these mice 24 hours after immune

complex formation to investigate whether immune complexes form at similar levels, and at 7 and 14 days, in order to investigate whether immune complexes are cleared more efficiently in *FcγRI*$^{-/-}$ mice. Finally, the observation that FcγRI, in contrast to what has been reported in the literature, appears to contribute to the Arthus reaction in the present experiments, could potentially be explained by a tissue-specific involvement of FcγRI. In a normal retina there are low levels of IgG.[242] It is thus possible that, in contrast to the skin, kidney and lung, FcγRI expressed by resting retinal microglia is not saturated and hence available to bind to monomeric IgG and immune complexes, once they form. This is worth further studying as it may have strong implications, e.g. for immunotherapy. The human and mouse FcγRI are homologous and are both high affinity receptors,[17] thus, if in the retina FcγRI are not saturated, they could possibly bind to immune complexes or monomeric therapeutic antibodies, such as Avastin, and activate effector functions. This may affect safety and efficacy of monoclonal antibody therapy for retinal diseases.

4.4.3 The role of FcγRIII in immune complex-mediated inflammation in the retina

FcγRIII is the activating FcγR whose contribution for immune complex mediated responses is less debatable. FcγRIII has low affinity for monomeric IgG1, IgG2a and IgG2b and preferentially binds to immune complexes. Importantly, FcγRIII binds to all these IgG subclasses *in vivo* [228, 318] and it has been consistently shown to be essential for promoting immune complex-mediated inflammation in the Arthus reaction in the skin[310] and lung,[307, 319] IgG1-mediated cutaneous anaphylaxis,[228] IgG2a- and IgG2b-mediated nephrotoxic nephritis[318] and AHA[225, 320] . Moreover, it is thought that IgG1 triggers immune effector function mostly through interaction with FcγRIII.[228] Not surprisingly, immune complex deposition in *FcγRIII*$^{-/-}$ mice resulted in strong attenuation of the inflammatory response, similar to $\gamma^{-/-}$ mice.

FcγRIII can mediate inflammation by interacting with IgG1, IgG2a and IgG2b. Following immune complex formation in the retina of *FcγRIII*$^{-/-}$ mice there was an increase in the number of cells expressing FcγRI, FcγRII/III and FcγRIV, when compare to saline WT controls and $\gamma^{-/-}$ mice. In particular FcγRI and FcγRIV may still interact with IgG2a and IgG2b to induce inflammation. As discussed previously, binding of IgG1 to the inhibitory FcγRII, may explain in part the reduced inflammation

seen in these mice. Performing these experiments in mice lacking both FcγRIII and FcγRII would allow testing this hypothesis. Nonetheless, these results suggest FcγRIII is an important receptor in mediating immune complex responses in the retina, similar to other non-neuronal organs.

4.4.4 The role of FcγRIV in immune complex-mediated inflammation in the retina

FcγRIV was first described in 2005, being the most recently discovered mouse FcγR.[219] Several studies have now demonstrated FcγRIV is a potent mediator of immune complex inflammation and it has been proposed that this is due to its affinity for IgG2a and IgG2b.[227] Blocking of FcγRIV leads to inhibition of IgG2a- and IgG2b-mediated arthritis,[227, 311] nephrotoxic nephritis,[227, 318] tumour clearance[227] and AHA.[225, 227, 307] In addition, the rabbit IgG-induced lung and skin Arthus reactions can also be inhibited in *FcγRIV*$^{-/-}$ mice.[306, 307] Unexpectedly, depletion of the activating FcγRIV led to an exaggerated inflammatory response to immune complex deposition in the retina, characterised by activation of microglia and increased recruitment of leukocytes when compared to WT mice.

In a single study, depleting FcγRIV had no effect on either the classical or reverse Arthus reaction on the skin, as measured by volume of oedema (i.e. area of Evans blue influx).[227] Although not statistically different when quantified, the representative pictures in this previous work appeared to show increased area of Evans blue influx in *FcγRIV*$^{-/-}$ mice when compared to WT. The authors proposed that their results could be explained by the fact that the main effector cells in the Arthus reaction, mast cells, do not express FcγRIV. However, neutrophils and macrophages, which are also important effector cells in the Arthus reaction, do express FcγRIV.[321] Although the presence of mast cells was not investigated, in Chapter 3 we show that the main effector cells in the response to immune complex formation in the retina are the microglia and/or infiltrating myeloid cells and that there is no neutrophil infiltration. In spite of this, depletion of FcγRIV resulted in an exaggerated response to immune complex. Therefore, there must be another explanation for the lack of effect of FcγRIV in the Arthus reaction in the retina.

Despite the immunisation protocol resulting in similar OVA specific IgG titers and subclasses in all mice, *FcγRIV*$^{-/-}$ appeared to have more abundant immune complex deposition in the retina, which could account for increased inflammation. Interestingly, immune complex formation in the retina resulted in increased FcγRI^{+} and FcγRIII^{+} cell number in *FcγRIV*$^{-/-}$ mice when compared to WT mice challenged with OVA. The results in this chapter clearly show these two FcγRs are important for mediating immune complex-induced inflammation, therefore, increased numbers of FcγRI^{+} and FcγRIII^{+} cells could also explain the more severe inflammatory response. Inducing immune complexes in the retina of *FcγRI/FcγRII/FcγRIII*$^{-/-}$ mice, expressing only FcγRIV of the four FcγRs may help to test this hypothesis.

An interesting aspect of these results is the apparent divergent role of FcγRI and FcγRIV in mediating immune complex responses in the retina or the periphery. If these differences are due to tissue-specific requirements for each of the receptors, this may change our understanding of how the retina deals with immune complexes. Although many studies on immune complex mediated inflammation have been described in WT, FcγRI and FcγRIV deficient mice no direct comparison has been reported. It would therefore be important to test our protocol to induce immune complex responses in a non-neuronal organ that has been well characterised, such as the lung and directly compare the effect in the retina of FcγRI and FcγRIV deficient mice under the same conditions. This would allow confirming whether the differences are tissue-specific and not inherent to the genotype of the mice used in these experiments or due to differences in IgG subclass resulting from the immunisation protocol used for these studies.

4.5 Conclusion

These results clearly show a requirement for activating FcγRs, but not activation of the classical complement cascade, in immune complex-mediated inflammation in the retina. In particular, FcγRI and FcγRIII, but not FcγRIV, were shown to be important for the development of the inflammatory response to immune complex formation. Depletion of either FcγRI or FcγRIII resulted in greatly reduced immune complex-mediated inflammation, similar to what is observed in γ$^{-/-}$ mice, lacking expression of all activating FcγRs. In contrast, deletion of FcγRIV resulted in a more severe inflammatory response to immune complex deposition, unlike what has been previously reported in the literature. These differences may be explained by differences in IgG

subclass or, more interestingly, tissue-specific responses. These studies highlight the importance of FcγRs in mediating antibody responses in the retina and the need to better understand the workings of this complex system. Understanding the mechanism of immune complex-mediated inflammation in the retina may help understanding of AMD pathology.

Chapter 5:

Immune complex deposition and FcγR expression in human AMD

5.1 Introduction

AMD is a multifactorial disease with several risk factors contributing to its pathogenesis. Inflammation is well accepted as an important contributor to the pathology of the disease.[10] Evidence for the role of inflammation in AMD comes from genetic studies which have identified an association between polymorphisms in innate immune genes (e.g. CFH,[127] C3,[142] SERPING1,[141] HLA-I/II[145]) and higher risk of developing AMD. Increased numbers of circulating leukocytes have been associated with higher incidence of AMD[322] and cells expressing microglia/macrophage markers have been associated with drusen, geographic atrophy and exudative lesions.[174, 185, 201, 298] Despite these observations, it is still not clear whether inflammation has a causative role or if it is merely a consequence of on-going AMD pathology.

In some animal models of AMD, inflammation is a key initiator of retinal pathology.[91, 143, 203] In the CEP-immunisation model of dry AMD (see section 1.5.2.), where mice are immunised against oxidised lipoproteins such as those found in drusen, an increase in the number of macrophages infiltrating the retina can be observed and it has been suggested these are key in initiating RPE pathology in this model.[209] In the laser-induced model of CNV, macrophage infiltration and function can greatly affect the area of the neovascular lesion. In particular, Arg1 and/or IL-10 expressing macrophages (often termed M2 macrophages) have been shown to increase the size of these lesions[212-214] and depletion of peripheral macrophages to decrease the size of the lesion.[173] In spite of the experimental evidence from animal models, there is limited histopathological data that phenotypically describes and compares the population of immune cells, including macrophages, in normal aged matched and AMD eyes. This represents an obstacle for translation of findings from animal models into the human disease.

As discussed previously (section 1.6.4.), there is evidence that immune complexes could form in the RPE and subretinal space of AMD eyes. In this study, human donor eyes from patients suffering from early AMD and healthy age-matched controls were used to investigate whether immune complex inflammation may be present at early stages of the disease. Accordingly, immunohistochemistry was used to detect IgG, complement components, immune cells and FcγR expression. Microglia/macrophage function appears to impact on neovascular lesions in animal models. Moreover, FcγR could

interact with monoclonal antibodies used for therapy of wet AMD and, therefore, eyes from donors suffering from wet AMD were also investigated for the presence of immune complexes and FcγR.

5.2 Methods

These experiments were done in collaboration with Robert Mullins (Iowa, USA) and tissue was collected and processed for immunohistochemistry by Aditi Khanna and Miles Flamme-Wiese (Iowa, USA) as described in section 2.5.1. Human donor eyes were obtained from the Iowa Lions Eye Bank (Iowa City, IA) following informed consent from the donors' families. This study was approved by Southampton & South West Hampshire Research Ethics Committee (A; REC No. 09/H0504/67). Briefly, eyes were fixed in 4% P.F.A. and frozen in OCT before cutting. 8μm sections were used for immunohistochemistry (section 2.5.2). Details of donors are shown in table 5.1. Quantification of immunohistochemistry was performed by counting the number of stained cells per mm of BrM, only when DAPI+ nuclei were visible (as detailed in 2.5.2.1). In the retina, stained cells were counted across all layers. In the choroid stained cells were only counted within 25μm from the BrM. For statistical analysis of immunohistochemistry, n=5-11 donor eyes per group were analysed.

5.3 Results

5.3.1 Characteristics of donor groups

A total of 11 healthy, 9 early AMD and 5 wet AMD eyes were obtained. The cause of death was obtained for only half of the donors, therefore it was not taken into consideration for any of the analyses performed in this study. The percentage of female and male donors was similar in healthy and early AMD groups with 65% females in healthy control and 67% females in early AMD groups. The age (mean±SD) between these two groups was also similar: 82.63±5.44 years of age for healthy control and 85.44±8.15 years of age for early AMD groups. Only male donors suffering from wet AMD were obtained, with age averaging 88.83±2.27 years of age.

Table 5.1. Details of eye donors

Sample	Age	Sex	AMD	Notes
07005 OSMAC	69	F	Early AMD	COD: COPD
10006 OSMAC	82	F	Early AMD	-
07044 OSMAC	86	F	Early AMD	-
07034 OSMAC	88	F	Early AMD	COD: CVA
07043 ODMAC	90	F	Early AMD	COD: CVA
10011 OSMAC	99	F	Early AMD	COD: acute pancreatitis
07011 OSMAC	79	M	Early AMD	COD: lymphoma
08003 OSMAC	83	M	Early AMD	-
08020 OSMAC	93	M	Early AMD	-
08014 ODMAC	79	F	No	-
07048 ODMAC	81	F	No	-
08019 OSMAC	82	F	No	-
07038 ODMAC	85	F	No	-
07012 OSMAC	86	F	No	COD: heart disease
07037 ODMAC	90	F	No	COD: CVA
08024 ODMAC	73	M	No	COD: throat cancer
08024 OSMAC	73	M	No	COD: throat cancer
08017 OSMAC	85	M	No	-
08030 ODMAC	87	M	No	-
08010 ODMAC	88	M	No	-
07033 OSMAC	86	M	Wet AMD	Treated with Kenalog (Triamicinolone)
11042 ODMAC	87	M	Wet AMD	-
11042 OSMAC	87	M	Wet AMD	Received Lucentis
11064 OSMAC	91	M	Wet AMD	-
09013 OSMAC	92	M	Wet AMD	-

COD, cause of death; COPD, chronic obstructive pulmonary disease; CVA, cardiovascular accident.

5.3.2 Immune complex inflammation in the retina of early AMD eyes

To evaluate the possible role of immune complexes in the pathogenesis of AMD, the presence of IgG, C1q and membrane attack complex (MAC, C5b-9) in eyes from healthy donors and patients suffering from early AMD was analysed. Double labelling for IgG and the endothelial cell marker Ulex europaeus Agglutinin I (UEA1) showed IgG was present within the retinal blood vessels in healthy and early AMD eyes alike (Figure 5.1. a). Activation of the complement cascade terminates with formation of MAC, which can lead to cell damage. To investigate the occurrence of complement-mediated cell damage in early AMD, immunohistochemistry for MAC was performed. No MAC was detected in the retinae of early AMD or healthy controls (Figure 5.1. b) Additionally no C1q deposition in these retinae was observed (not shown).

Retinal inflammation has been associated with the pathogenesis of AMD,[91] thus early AMD-related changes to the retinal microglia were investigated. Microglia were identified based on their expression of CD45, morphology and distribution across the retina. There were no apparent differences in $CD45^+$ microglia between early AMD and age-matched control retinae (Figure 5.2. a). Additionally, there were no differences in the number of $CD45^+$ cells in the retinae of the two groups (Figure 5.2. b).

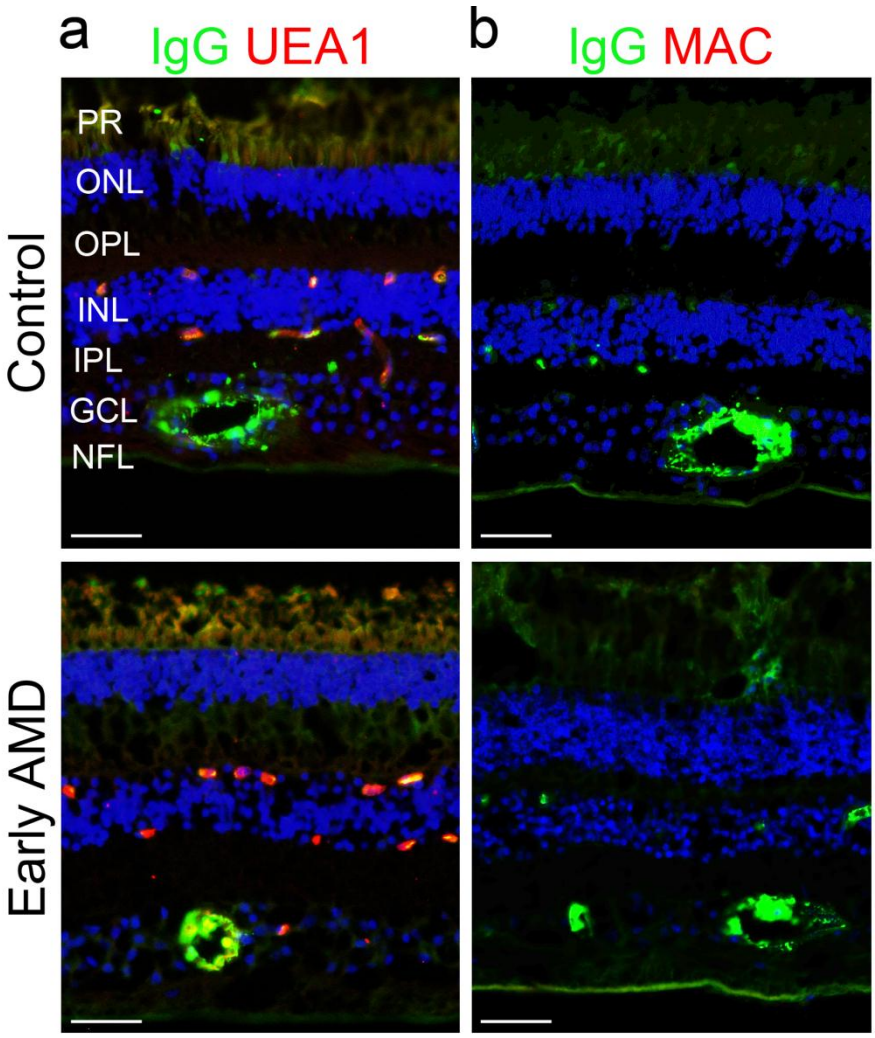

Figure 5.1. IgG immunoreactivity and complement activation in the retina of healthy and early AMD donors.

(a) Immunohistochemical detection of IgG (green) and *Ulex europaeus* Lectin I (UEA1, red) (n=9-10 per group) revealed presence of IgG in close proximity to retinal blood vessels in both control and early AMD eyes. **(b)** Immunohistochemical detection of IgG (green) and MAC (C5b-9, red) in aged matched control and early AMD patients (n=9 per group) revealed no MAC deposition in the retina. Cell nuclei were stained with DAPI (blue). PR, photoreceptor outer segments; ONL, outer nuclear layer; OPL, outer plexiform layer; INL, inner nuclear layer; IPL, inner plexiform layer; GCL, ganglion cell layer; NFL, nerve fibre layer . Scale bar - 50µm.

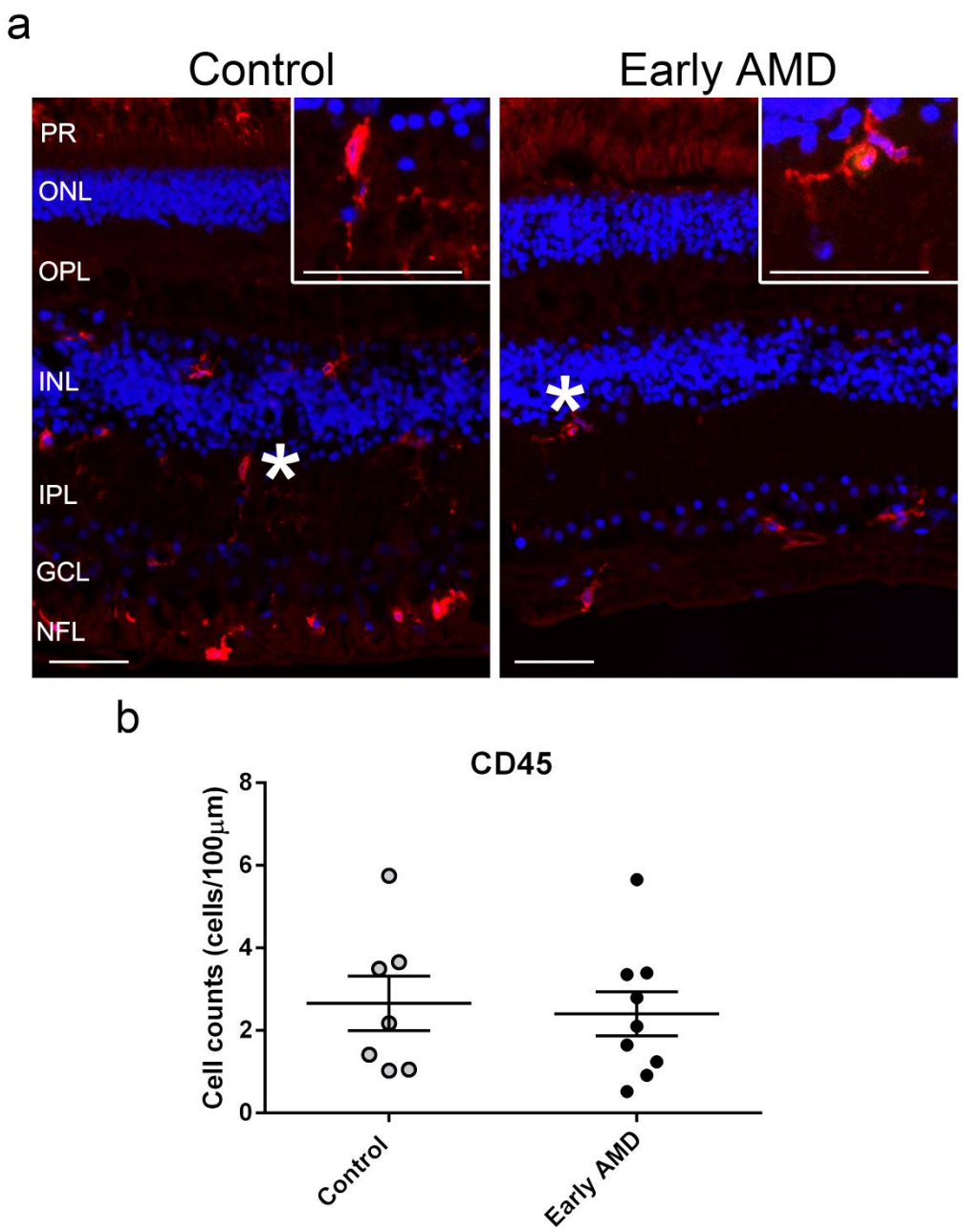

Figure 5.2. CD45$^+$ microglia in the retina of control and early AMD donors.
(a) Immunohistochemical detection of CD45 (red) revealed no differences between control and early AMD eyes. Cell nuclei were stained with DAPI (blue). **(b)** Quantification of CD45$^+$ cell number/100μm of Bruch's membrane (n=7-9 per group). Error bars represent SEM. PR, photoreceptor outer segments; ONL, outer nuclear layer; OPL, outer plexiform layer; INL, inner nuclear layer; IPL, inner plexiform layer; GCL, ganglion cell layer; NFL, nerve fibre layer . * indicates origin of inset. Scale bars - 50μm.

Expression of FcγRs was investigated next. No staining was obtained for FcγRIII (not shown) possibly due to masking of the epitope by fixation of the tissue, as this antibody has been successfully used to detect FcγRIII in other tissues (Alison Tutt, University of

Southampton). Co-immunolocalisation of FcγRI and CD45 revealed expression of FcγRI by microglia (Figure 5.3. a, inset). However, immunoreactivity for FcγRI was also detected in the lumen of retinal blood vessels (Figure 5.3. a, arrows), suggesting non-specific binding of the antibody. For this reason, no further analysis was done for FcγRI. $CD45^+$ microglia expressing FcγRIIa or FcγRIIb were detected in the retina of both healthy and early-AMD donor eyes (Figure 5.3. b, c; insets). Quantification revealed no differences in the total number of $FcγRIIa^+$ or $FcγRIIb^+$ cells between the two groups. To correct for differential number of microglia, the number of $CD45^+/FcγRIIb^+$ or $CD45^+/FcγRIIa^+$ cells as a fraction of the total $CD45^+$ cells per section were analysed. There were no differences in the percentage of $CD45^+$ cells expressing either FcγR between healthy and early AMD retinae (Figure 5.3. d).

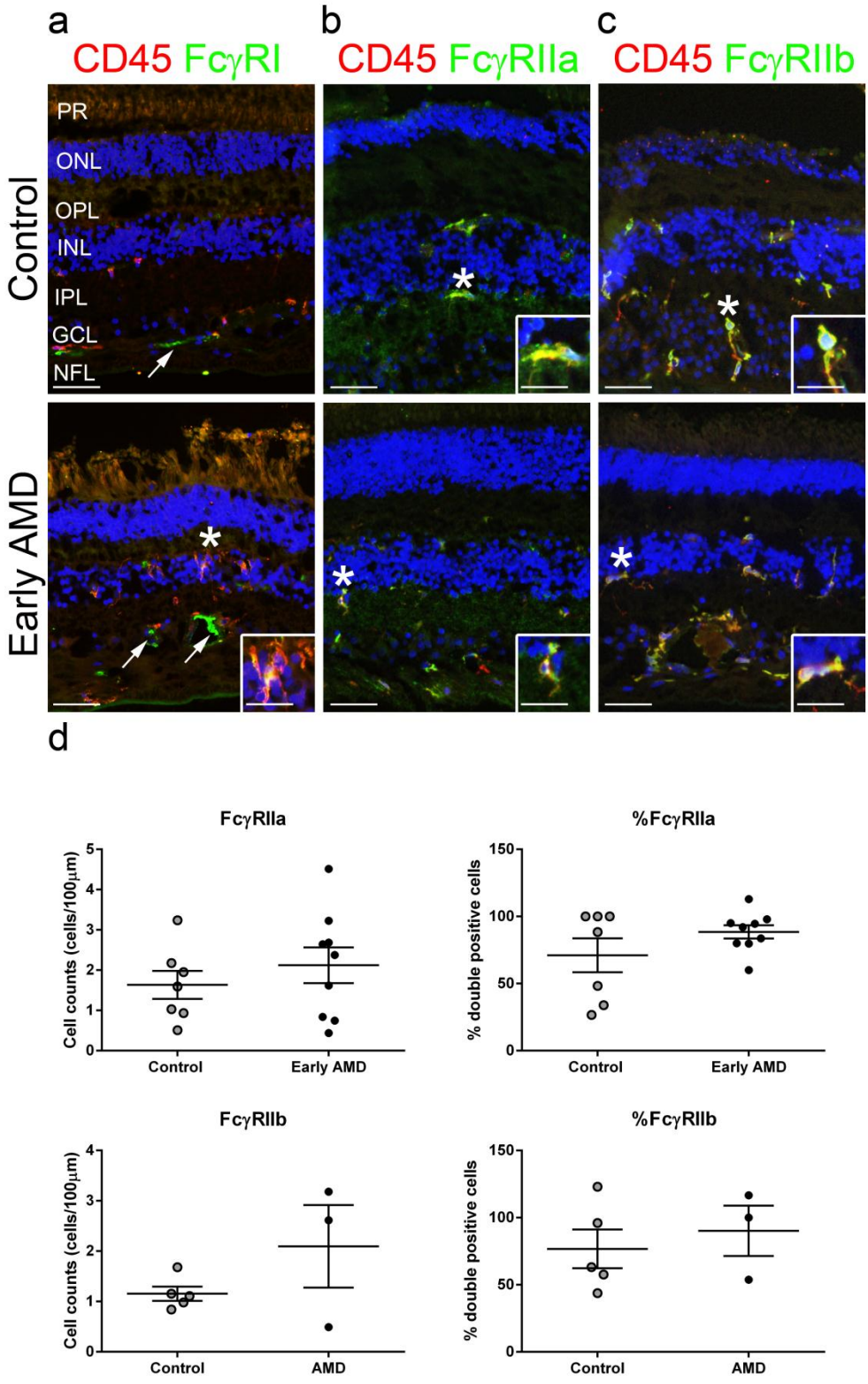

Figure 5.3. Expression of FcγRI, FcγRIIb, FcγRIIa in the retinae of healthy and early AMD donor eyes.

(a-c) Immunohistochemical detection of CD45 (red) and **(a)** FcγRI, **(b)** FcγRIIa and **(c)** FcγRIIb (green). Cell nuclei were stained with DAPI (blue). $CD45^{+}$ microglia expressed FcγRI, FcγRIIa and FcγRIIb (insets). **(a)** Immunoreactivity for FcγRI was detected in the lumens of blood vessels, where no

CD45 was detected (arrows). **(d)** Quantification of FcγRIIb$^+$ or FcγRIIa$^+$ cell number/100µm of Bruch's membrane and percentage of CD45 and FcγRIIb or FcγRIIa double positive cells (n=3-9 per group). Error bars represent SEM. PR, photoreceptor outer segments; ONL, outer nuclear layer; OPL, outer plexiform layer; INL, inner nuclear layer; IPL, inner plexiform layer; GCL, ganglion cell layer; NFL, nerve fibre layer . * indicates origin of inset. Scale bar - 50µm, scale bar inset - 25µm

5.3.3 Immune complex inflammation in the choroid of early AMD eyes

No evidence for immune complex deposition or immune complex-induced inflammation was found in the retina of early AMD eyes. Some studies suggest changes to the choroid may lead to AMD pathology.[105, 152] Thus, we investigated the presence of immune complexes in the choroid. Double labelling for IgG and the endothelial cell marker UEA1 showed IgG was present within the capillaries of the choroid (choriocapillaris) in both healthy and early AMD eyes (Figure 5.4. a). C1q was detected within the choriocapillaris in early AMD eyes but not in age-matched controls (Figure 5.4. b). No C1q deposition was observed in drusen (Figure 5.4. b, inset). To investigate whether IgG and C1q deposition could lead to activation of the complement cascade double labelling for IgG and MAC was performed. MAC deposition was observed in the space surrounding the choriocapillaris in healthy donor eyes, but in early-AMD this was increased and co-localised with IgG staining (Figure 5.4. c).

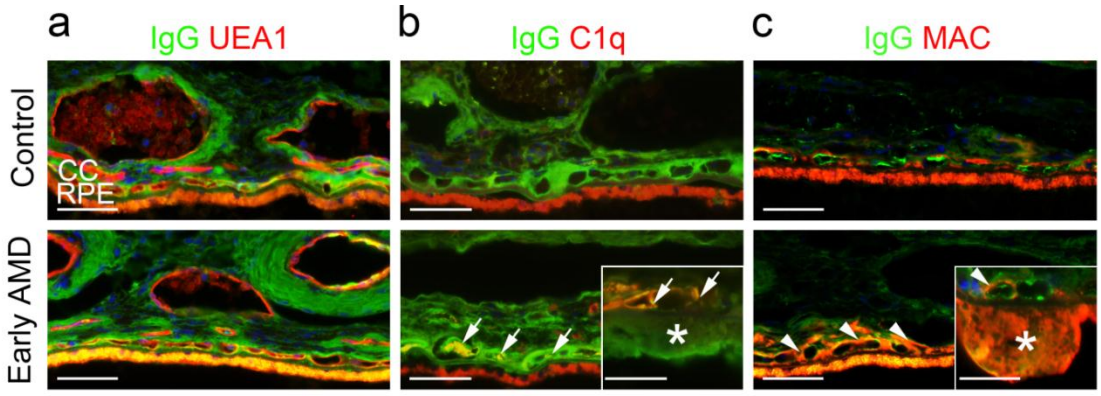

Figure 5.4. IgG and C1q deposition and complement activation in the choriocapillaris of early AMD patients.

(a) Immunohistochemical detection of IgG (green) and *Ulex europaeus* Lectin I (UEA1, red) (n=9-10 per group) revealed IgG deposition in close proximity to choriocapillaris in both control and early AMD eyes. **(b)** Immunohistochemical detection of IgG (green) and C1q (red) (n=9 per group) in aged matched control and early AMD patients showed co-localization of IgG and C1q (arrows) in the lumen of blood vessels, indicating formation of immune complexes, but not in drusen (star) **(c)** Immunohistochemical detection of IgG (green) and MAC (C5b-9, red) in aged matched control and early AMD patients (n=9

per group) revealed MAC and IgG co-localization around the choriocapillaris (arrowheads) and in drusen (star) in early AMD (inset). Cell nuclei were stained with DAPI (blue). Note the intense autofluorescence of the RPE due to lipofuscin autofluorescence. CC, choriocapillaris; RPE, retinal pigmented epithelium. Scale bars - 50μm, inset scale bars- 25μm.

To investigate whether the IgG and C1q deposits in the choroid of early AMD eyes were associated with an inflammatory response, the presence of leukocytes in the choroid was investigated by immunohistochemical detection of CD45. $CD45^+$ cells with varied morphology (Figure 5.5. a) and varied $CD45^+$ expression levels were detected in the choroid of healthy and early AMD eyes (Figure 5.5. b). No significant differences in the number of total $CD45^+$ cells were detected between the choroids of the two groups, which was likely due to three AMD patients showing minimal CD45 immunoreactivity. (Figure 5.5. c). To investigate whether the $CD45^+$ leukocytes in early AMD could be associated with immune complex-mediated inflammation, the presence of mast cells (mast cell tryptase), neutrophils (neutrophil elastase) and T cells (CD3) was investigated. No immunoreactivity for neutrophil elastase or CD3 was detected (not shown). Mast cells were detected in both healthy and early AMD eyes and quantification showed no differences in the number of these cells between the two groups (Figure 5.5.). No macrophage specific markers were available at the time of these experiments, therefore macrophages were identified based on their elongated morphology, as previously described [298] (Figure 5.5. a).

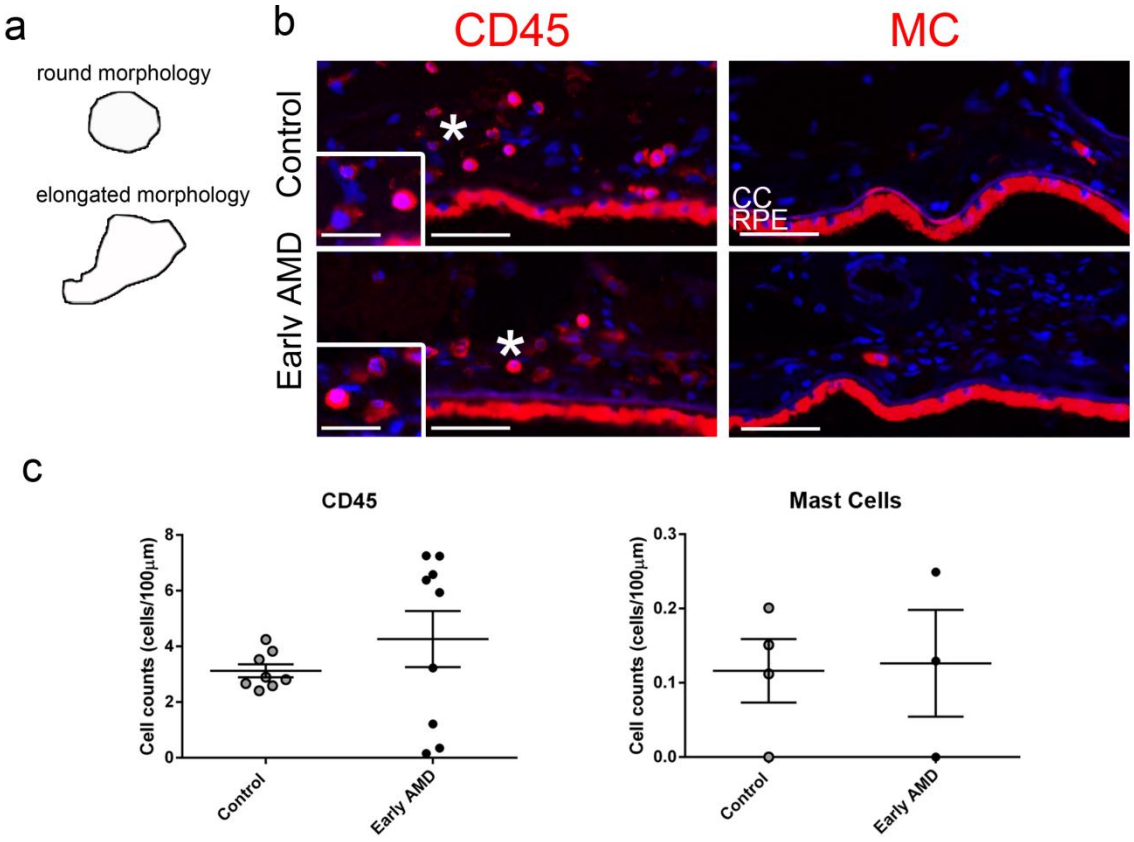

Figure 5.5. CD45$^+$ leukocytes and mast cells in the choroid of control and early AMD donors. **(a)** Schematic of cells with round or elongated morphology, characteristic of lymphocytes or macrophages, respectively. **(b)**Immunohistochemical detection of CD45 (red) and mast cell tryptase (red). Cell nuclei were stained with DAPI (blue). CD45 cells with round and elongated morphology and varied intensity of CD45 immunoreactivity can be detected (inset). **(c)** Quantification of CD45$^+$ (n=8-9 per group) and mast cell number/100µm of Bruch's membrane (n=3-4 per group). Error bars represent SEM. Scale bars - 50µm; inset - 25µm.

Due to their important role in mediating immune complex-induced inflammation expression of FcγRs was next investigated. No FcγRI$^+$ cells were detected in the choroid in any of the samples analysed, possibly due to saturation of the FcγRI with monomeric IgG. In contrast, staining for FcγRIIb (Figure 5.6. a) or FcγRIIa (Figure 5.6. b) revealed expression of both these FcγRs in the choroid of early AMD patients and age-matched controls. FcγRs appeared to be expressed mostly by cells with elongated morphology, characteristic of macrophages. There was a non-significant increase in the total number of FcγRIIb or FcγRIIa in early AMD choroid, when compared to age-matched controls. When corrected for the total number of CD45$^+$ leukocytes, an increase in the percentage

of CD45$^+$/FcγRIIb$^+$ cells (from 39% to 62%, p=0.0381) and CD45$^+$/FcγRIIa$^+$ cells (from 41% to 71%, p=0.0037) was observed in the choroid of early-AMD donors.

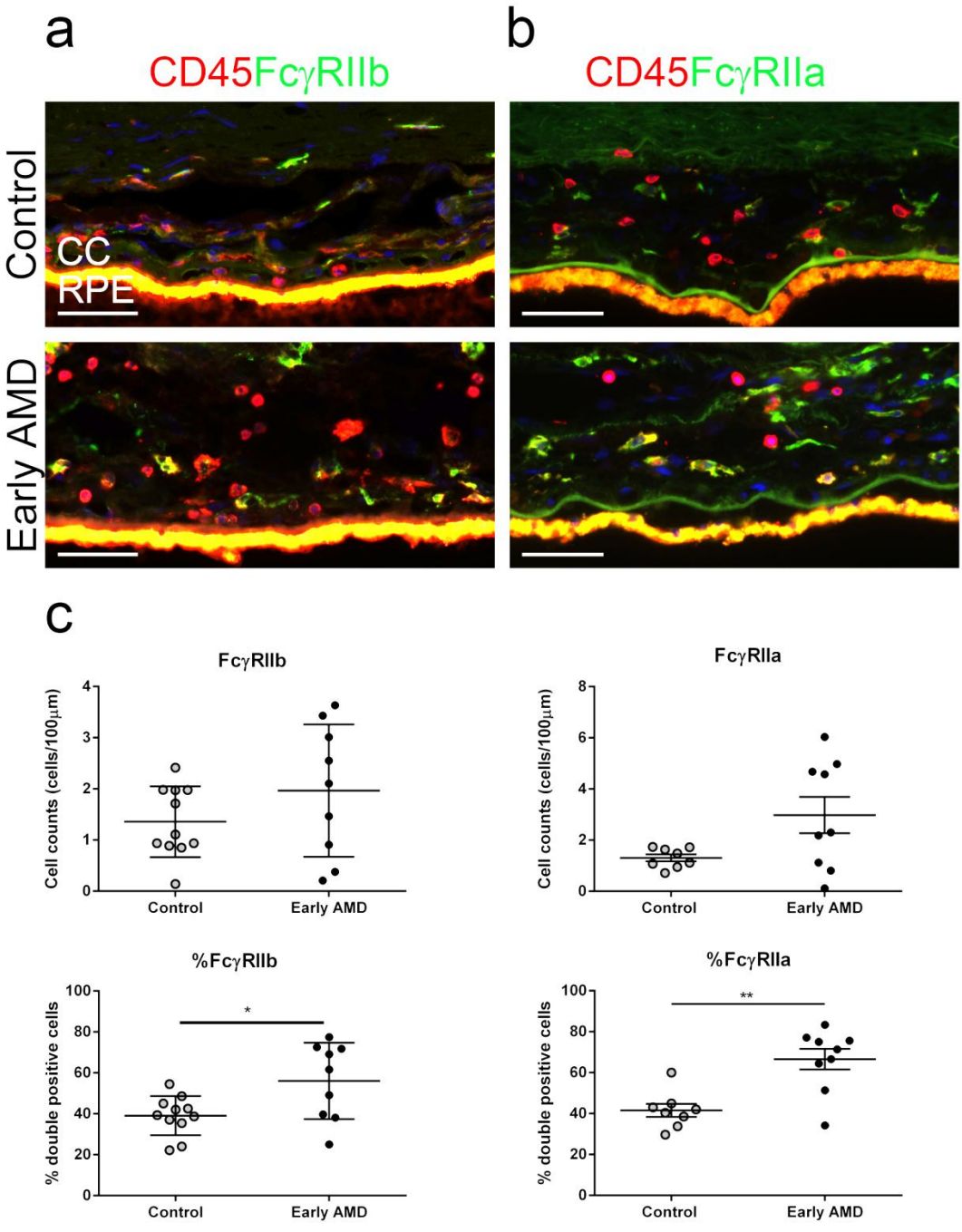

Figure 5.6. Increased number of FcγRIIb$^+$ and FcγRIIa$^+$ leukocytes in the choroid is associated with early AMD.

(a,b) Immunohistochemical detection of CD45 (red) and FcγRIIb **(**green, **a)** and FcγRIIa **(**green, **b)**. Increased numbers of both FcγRIIb and FcγRIIa was observed in the choroids of early-AMD patients, when compared to healthy age-matched controls. Cell nuclei were stained with DAPI (blue). **(c)**

Quantification of FcγRIIb or FcγRIIa cell numbers/100μm of Bruch's membrane and percentage of CD45 and FcγRIIb or FcγRIIa double positive cells (n=9-11 per group). Cells were counted only within 25μm of the Bruch's membrane. Error bars represent SEM; *p=0.0381, **p=0.0037. CC, choriocapillaris; RPE, retinal pigmented epithelium. Scale bar - 50μm

5.3.4 Immune complex inflammation in wet AMD

Finally, evidence for immune complex inflammation in wet AMD was investigated. The extent of pathology in wet AMD eyes varied greatly from donor to donor. Moreover, in most eyes the extent of the neovascular lesions was such that the BrM could no longer be identified. Hence, quantitative analysis of $CD45^+$, $FcγRIIa^+$ and $FcγRIIb^+$ cell number was not performed in these eyes. Double immunohistochemical labelling for IgG and UEA1 revealed IgG was present in the lumens of intact choriocapillaris in late AMD and in some areas of choroidal neovascular membranes (CNVM) (Figure 5.7.). Immunoreactivity for MAC was detected around the choriocapillaris but not in the retina of wet AMD donor eyes. Some MAC may have been present in parts of CNVM, but it was challenging to discern it from fragmented RPE in these (Figure 5.7., arrows). Next the expression of CD45, FcγRI, FcγRIIb and FcγRIIa in eyes from patients suffering from wet AMD was investigated (Figure 5.8.). CD45, FcγRIIb (Figure 5.8. a), FcγRIIa (Figure 5.8. b) and FcγRI (Figure 5.8. c) expression was widespread throughout the choroid and retina in the late stage of AMD.

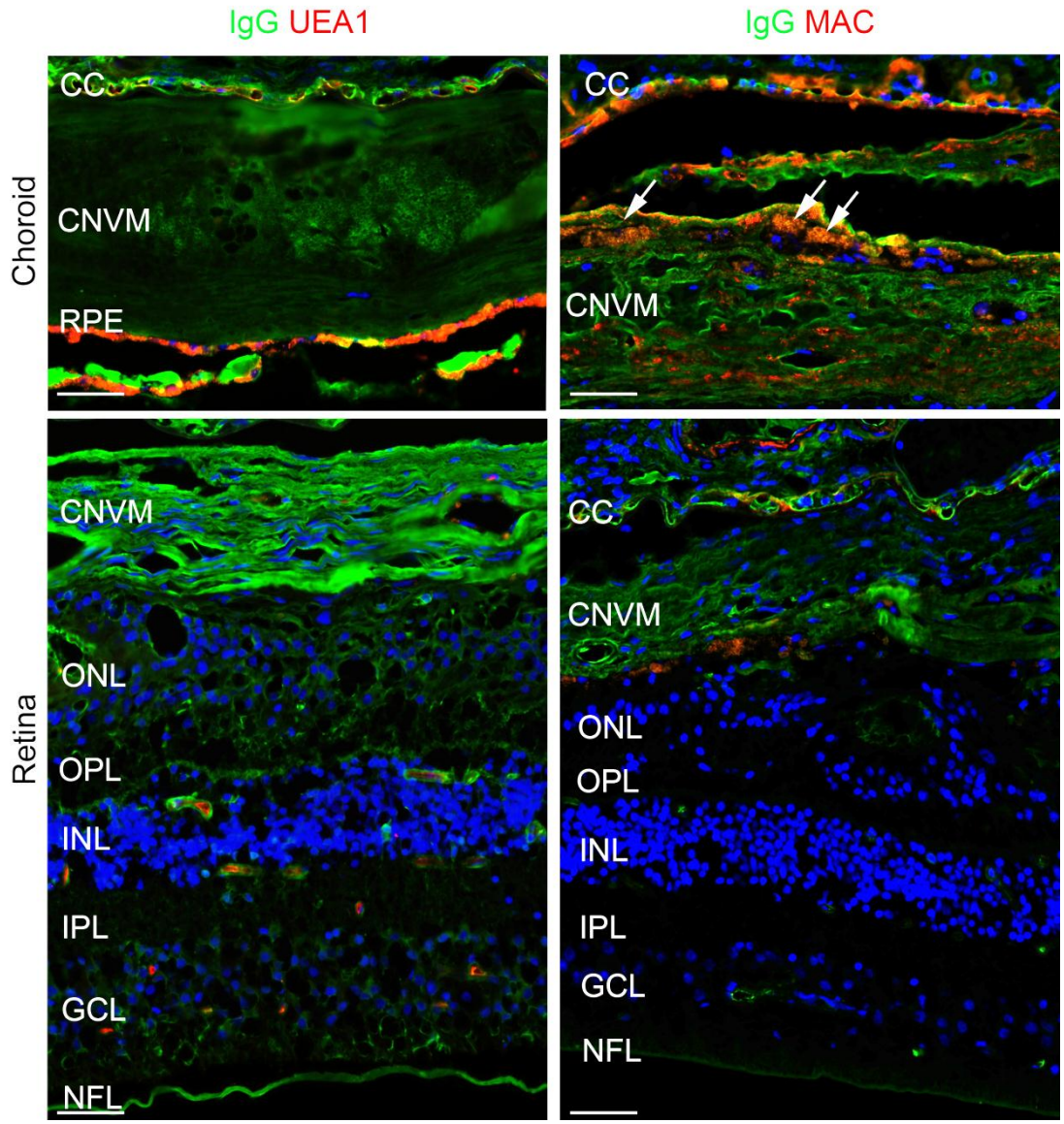

Figure 5.7. IgG immunoreactivity and complement activation in the wet AMD eyes.
Immunohistochemical detection of IgG (green) and *Ulex europaeus* Lectin I (UEA1, red) and IgG (green) and MAC (C5b-9, red) in in the choroid and retina of wet AMD (n=5). Cell nuclei were stained with DAPI (blue). IgG was present in the lumen of the choriocapillaris and CNVM. Fragmented RPE could be seen in the CNVM (arrows), making it difficult to discern between RPE and MAC. CC, choriocapillaris; CNVM, choroidal neovascular membrane; RPE, retinal pigmented epithelium; PR, photoreceptor outer segments; ONL, outer nuclear layer; OPL, outer plexiform layer; INL, inner nuclear layer; IPL, inner plexiform layer; GCL, ganglion cell layer; NFL, nerve fibre layer . Scale bar - 50μm.

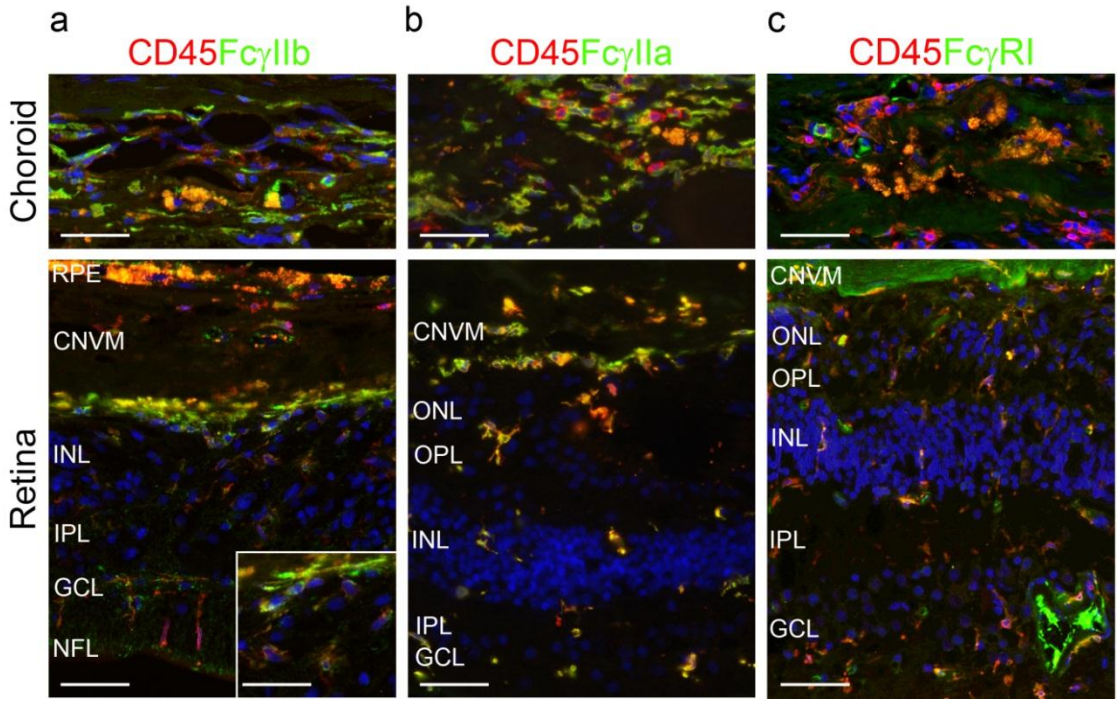

Figure 5.8. FcγRIIb, FcγRIIa and FcγRI expression by CD45$^+$ cells in the choroid and retina of wet AMD.

(a,b,c) Immunohistochemical detection of CD45 (red) and FcγRIIb (green, **a**), FcγRIIa (green, **b**) or FcγRI (green, **c**) in the choroid and retina of eyes from donors with wet AMD (n=5). Cell nuclei were stained with DAPI (blue). RPE, retinal pigmented epithelium; CNVM, choroidal neovascular membrane; ONL, outer nuclear layer; OPL, outer plexiform layer; INL, inner nuclear layer; IPL, inner plexiform layer; GCL, ganglion cell layer; NFL, nerve fibre layer . Scale bar - 50μm, inset scale bar-25 μm.

5.4 Discussion

Although inflammation is a well-known risk factor for AMD, the precise mechanisms by which it could contribute to pathogenesis of this disease are not well understood. In several mouse models showing features of AMD such as drusen-like deposits, RPE atrophy and CNV, retinal inflammation is an early feature.[91] However, only a handful of studies have investigated inflammatory changes in the eyes of patients suffering from early AMD. This study's results show evidence for the deposition of IgG and C1q in the choroid, but not retina, suggesting deposition of immune complexes. The immune complexes in early AMD eyes are accompanied by an increase in number of immune cells expressing FcγRIIa and FcγRIIb. Further, FcγRI, FcγRIIa and FcγRIIb were expressed by the microglia in the retina of wet AMD eyes.

5.4.1 Limitations of using human donor tissue

One issue that arises with the use of human donor tissue is the great number of variables, such as age, sex, lifestyle and co-morbidities, all of which could impact on AMD pathology.[127] In this study co-morbidities and cause of death, which could potentially lead to changes in the retina (e.g. diabetes) were not controlled for. However, the percentage of male and female samples and age in the groups used for statistical analysis were all similar. Changes in the retina, such as tissue damage or degeneration, can induce activation of microglia and inflammation.[91] Studying human tissue from patients suffering from early AMD, rather than late stage AMD where tissue damage has already occurred, may give a better representation of the inflammatory factors contributing to initiation of AMD. Diagnosis of early AMD in the samples used in this study relied mostly on the presence of drusen.[41] This may lead to incorrect premature diagnosis of AMD, as patients with drusen may end up not developing late stage AMD.[41] Similar, AMD pathology may have started in donors deemed "healthy", despite the lack of drusen.[41] It is important to keep these factors in mind, as they may bias the results. The sex and age distribution of the samples were very similar across groups and in this study a moderate number of 8-10 donors per group was obtained. *A priori* power analysis (Appendix III) using the immunohistochemistry quantification data led to the prediction that in the choroid a minimum sample size of n=6 is sufficient to detect significant differences in CD45+FcγRIIa+ cell number, while an n=14 is required to detect significant differences in CD45+FcγRIIb+ cell number. Additionally, a sample size of n=36 is predicted to be needed to detected potentially significant differences in CD45+FcγRIIa+ cell number in the retina. Based on this analysis it can be assumed that a minimum sample size of n=36 is required to detect small differences in FcγR expression by CD45+ cells in the retina. Hence, while enough donor eyes were obtained to study the choroid, future studies focusing on changes in the retina should consider using bigger sample sizes.

5.4.2 The retina in early AMD

Retinal pigmented epithelial cells are believed to be the main affected cells in early AMD, with dysfunction of these cells leading to accumulation of cell debris and subsequent photoreceptor degeneration.[74] However, in several mouse models, including the *CCL2*$^{-/-}$ and CEP-immunisation models, displaying AMD-like pathology such as

drusen formation and RPE atrophy, subretinal inflammation is an early feature.[143, 171, 203, 209] It has thus been suggested that inflammatory changes to the retina could contribute to initiation of the disease.[86, 91] In the results presented in this chapter no differences between the retinae of early AMD and healthy donors were observed with respect to IgG and complement deposition, microglia activation and FcγR expression, suggesting inflammation in the retina itself may not be an initiating factor of this disease.

FcγRIII expression has been previously described in healthy human retinal microglia,[18] but FcγRIII^{+} cells were not detected in the retina or choroid of any of the samples studied here. This was possibly due to masking of the epitope by fixation of the eye tissue used in these experiments. Unfortunately positive control tissue to test this was not available. A possible positive control could have been kidney or spleen fixed and frozen in the same way as the tissue used in these experiments. Finally, although CD45^{+} cells expressing FcγRI were detected, immunoreactivity for FcγRI was also detected in association with blood vessels. Although this could be due to expression by perivascular macrophages, this is unlikely as these cells also express CD45^{+}.[94] In addition, human endothelial cells do not express FcγRI,[17] hence it is unlikely that the immunoreactivity detected is due to expression of FcγRI by these cells.

It is possible that early changes in the retina not investigated here, may contribute to pathogenesis of AMD. For example, altered photoreceptor function due to ageing and/or oxidative stress could lead to altered retina homeostasis and, consequently, to AMD. Microglia are extremely responsive to disturbances in their environment,[80] thus this hypothesis seems unlikely, as the populations of these cells in control and early AMD eyes were very similar at least with the markers used in this study. Thus, it appears that changes in the retina may not contribute to initiation of AMD pathology.

5.4.3 Immune complex deposition in the choroid of early AMD eyes

Deposition of IgG has been reported in drusen and in the RPE of AMD patients.[14] An apparent increase in IgG deposition in the lumen of the vessels of the choriocapillaris in early AMD was observed and accompanied by deposition of C1q and MAC, indicating immune complex formation and activation of the complement system and possibly cell lysis and death. Thinning of the choroid has been demonstrated in ageing[323] but it

remains controversial whether this is more pronounced in AMD.[105] Evidence for immune complex formation in the choriocapillaris, but not retina of early-AMD donor eyes was found. Immune complex-mediated inflammation could lead to damage to the choriocapillaris in early AMD and consequent impaired drainage of debris from the retina, contributing to the formation of drusen and RPE cell damage. Supporting this hypothesis are reports of patients suffering from vasculitis due to systemic immune-complex disease, such as SLE[248, 250] and GMNP types I[249] and II,[14, 324] developing drusen and RPE atrophy.

Immune complex formation can lead to inflammation through activation of effector cells via activation of the classical complement cascade or through FcγR cross-linking.[17] Genetic studies have put forward over-activation of the alternative complement cascade as an important factor in AMD pathogenesis.[325] In addition, histochemical analysis of AMD donor eyes has shown that deposition of complement proteins such as C3, C5 and MAC is associated with AMD from early through late stages of the disease.[326] An increase in C1q and MAC deposition in early AMD, suggests that the classical complement cascade, via immune complex formation, could also contribute to AMD by amplifying the activation of the complement cascade.

5.4.4 Characterisation of the leukocyte population in the choroid of early AMD eyes

Increased numbers of leukocytes in the choroid have been associated with AMD.[322] In contrast, the results in this study show that the number of leukocytes in the choroid of early AMD and healthy eyes is similar. Using a total of 8 eyes (4 per group) M.K. Ezzat et al have shown that although the total number of $CD45^+$ cells is not different in non-drusen and drusen containing donor eyes, there is a an increase in the ratio of $CD8^+/CD4^+$ cells in AMD.[298] To assess whether cells involved in immune complex responses were present in the choroid of early AMD eyes, immunohistochemical detection of mast cells, neutrophils and T cells was performed. No T cells or neutrophils were detected in any of the eyes examined. Similar to FcγRIII, this could be due to masking of the epitope by fixation, but no positive controls were available. Conflicting reports regarding the presence of mast cells in the choroid of AMD exist, with some authors reporting increased number of mast cells in late AMD,[185] and others reporting their absence.[327] In this study, a similar number of mast cells was detected in the

choroid of both early AMD and healthy eyes, suggesting these cells are not specific to AMD pathology. These experiments were limited by the availability of eye samples, only 3-4 eyes per group were available for this part of the study. Due to the variability between donors, this may be too small a sample number to detect any differences.

5.4.5 Fcγ receptor expression in the choroid of early AMD eyes

Immune complex formation can further contribute to inflammation via cross linking of FcγRs, resulting in generation of pro-inflammatory mediators such as NO, TNF-α, IL-6, MCP-1 and upregulation of MHC II.[17] The balance of activating versus inhibitory FcγR expression determines cellular phenotype following cross-linking with immune complexes, with increasing expression of activating FcγRs favouring cell activation.[17] In early AMD donor tissue increased numbers of $CD45^+$ cells expressing FcγRIIa and FcγRIIb were detected in the choroid. Activation of FcγRIIa at the choroid could lead to immune activation and increased pro-inflammatory cytokine production potentially damaging the blood vessels of the choroid and/or the RPE. This data suggests that immune complexes may contribute to AMD pathogenesis by activating cell effector function via FcγR interaction and by complement-mediated damage of the choroid.

5.4.6 Fcγ receptors and wet AMD

In wet AMD, newly formed blood vessels grow from the choroid to the retina. These blood vessels are not fully functional and are weak and leaky, resulting in haemorrhage in the retina.[328] Patients suffering from AMD, including wet AMD, have high titers of circulating autoantibodies against retinal antigens,[11, 12, 15, 16] these could reach the retina in areas of haemorrhage, where they would have access to their cognate antigen, possibly forming immune complexes. In this study no evidence for the presence of immune complexes in wet AMD eyes was found. This could be due to the stage of the neovascular membrane. Early CNV is characterised by the formation of capillaries, which eventually form a network of blood vessels and fibrous tissue between the RPE and the BrM, and, subsequently, lead to the formation of a fibrovascular scar.[328] It is possible that at the different CNV stages IgG-mediated responses could have different contributions. Supporting this idea, there were differences in the immunoreactivity for IgG in different donor eyes.

Although macrophages/microglia are often present in wet AMD lesions it is unclear whether they have a causative role or are merely a consequence of exudative damage to the retina. In the retinal sections from wet AMD donors analysed in this study, it appears that macrophages/microglia line the neovascular membrane. It is possible that these macrophages could be reacting to the neovascular lesion by promoting the laying down of scar tissue, perhaps preventing the leakage of blood components to the retina, thus restricting bystander damage to the retina. Additionally, several $CD45^+$ cells expressing FcγRIIa were detected throughout the retina and choroid of these donors. These cells could also be mediating inflammation and in this way promoting neovascularisation. However, further studies would need to be done to confirm these hypotheses.

Although the role of microglia and infiltrating macrophages in wet AMD remains unresolved, these cells clearly expressed FcγRs. Monoclonal antibodies against VEGF are currently employed for the treatment of wet AMD and two antibodies are applied in the clinic, a full length human IgG1 (Avastin; Bevacizumab) and a Fab fragment (Lucentis, Ranibizumab).[329, 330] Although efficacy of these two agents appears similar, different side-effect profiles have been reported.[331, 332] These results show that FcγRI and FcγRIIa are widely expressed in the retina of wet-AMD. Crosslinking of these receptors by Avastin, but not Lucentis (lacking the Fc fragment), could trigger inflammation and impact on efficacy and safety of therapy. Understanding the antibody interactions with FcγRs in the retina is increasingly important as new therapies for the treatment of choroidal neovascularisation such as Aflibercept, which containing an Fc portion, emerge.[333]

5.5 Conclusion

In this study, evidence for the formation of immune complexes in the choriocapillaris of early AMD with accompanying increased number of $Fc\gamma R^+$ cells when compared with controls is provided. These results provide a possible molecular mechanism for antibody-mediated inflammation in AMD. Although leukocytes expressing FcγRs in the retinae from patients with wet-AMD were also observed, it remains unresolved what the role of these cells may be. $Fc\gamma R^+$ cells also have the potential to interact with therapeutic antibodies, especially when complexed with their antigen, which could impact on efficacy and safety of AMD therapy.

Chapter 6:

The impact of macrophage mediated inflammation on RPE cell function *in vitro*

6.1 Introduction

The RPE is a monolayer of polarised epithelial cells that are essential for maintaining retinal homeostasis.[37] These cells perform important functions such as maintaining integrity of the BRB, regulation of the microenvironment in the choroid (through basal secretion) and outer retina (through apical secretion), phagocytosis of photoreceptors outer segments and recycling of retinol during the visual cycle.[37] Damage and degeneration of the RPE is thought to be one of the primary events in AMD leading to subsequent degeneration of photoreceptors.[115]

The presence of subretinal macrophages/microglia in proximity with drusen, geographic atrophy and neovascular membranes has been consistently reported,[143, 174, 201] suggesting a role for these cells in the pathogenesis of AMD. A number of studies characterised AMD-associated subretinal macrophages/microglia, with a particular focus on macrophage polarization into classically activated M1 versus the alternatively activated M2a macrophages.[10] Increased neovascularisation associated with the presence of M2 macrophages in the laser induced mouse models of CNV, suggest M2 macrophages have a role in promoting neovascularisation.[215] Based on immunoreactivity for iNOS[174] and the M1 chemokine CCL11[201] in human eyes it has been proposed that a switch from M2 to M1 macrophages may contribute to AMD pathology. One problem with these studies is that a single marker has been used and this is insufficient to reliably characterise a macrophage phenotype. Additionally, these studies have disregarded other well characterised macrophage modes of activation, including the M2b and M2c activated macrophages,[96] as well as emerging ones such as the Mox[100] and M2d[99] macrophages.

It is unclear whether the presence of macrophages in the subretinal space is just a consequence of ongoing pathology or whether they have a causative role.[10] Macrophages have been shown to regulate RPE function both *in vivo* and *in vitro*[71, 334, 335] and complement deposition in the RPE and choroid is associated with AMD pathology.[149, 326, 336] Interestingly, C. Luo and colleagues reported increased expression of several complement components (including C3, CFB and CFH) and pro-inflammatory cytokines (IL-6 and IL1-β) in cultured murine RPE following apical stimulation with supernatant from M1 and M2b polarised macrophages.[335] While these

data suggest a role of macrophages in inducing altered RPE function, the mechanism underlying activation of macrophages *in vivo* remains elusive.

Activated macrophages/microglia can secrete diverse inflammatory mediators including pro-inflammatory cytokines, such as IL1-β, IL-6 and IL-8.[96] These could interact with their cognate receptors expressed by the RPE[337] inducing functional changes (e.g. altered barrier function) [13] and/or degeneration.[72, 337] In this chapter, subretinal inflammation and its effect on human RPE barrier function, cytokine secretion and CFH mRNA transcript levels was modelled by stimulating ARPE19 monolayers either directly with cytokines or immune complexes or indirectly with conditioned media from polarised macrophages. Further, the effect of conditioned media from macrophages exposed to plate-immobilised Avastin or Lucentis on RPE function was investigated.

6.2 Methods

6.2.1 Characterisation of ARPE19 monolayers

To characterise the effect of cytokine stimulation on ARPE19 monolayers an experiment was carried out to determine the most appropriate time point for functional analysis, as detailed in section 2.6.3. Briefly, ARPE19 monolayers grown in transwells were stimulated on their apical surface with 50ng/ml LPS + 2ng/ml IFN-γ, 10ng/ml IL-4 + 10ng/ml IL-13 and 20ng/ml IL-10 (Figure 6.1.). Changes in transepithelial electrical resistance (TEER), apical cytokine secretion and complement factor H (CFH) transcript levels were investigated 4, 8, 12 and 24 hours after stimulation, as detailed in sections 2.6.4, 2.6.9 and 2.6.7. For statistical analysis of TEER and cytokine measurements, n=9 transwells per treatment group were assessed. For statistical analysis of qPCR studies, n=6 well per treatment group for each time point were assessed.

6.2.2 The effect of inflammation on ARPE19 monolayers

Based on the results of the pilot experiment 8 and 24 hour stimulation was chosen to investigate the effect of inflammatory stimuli on RPE function. ARPE19 monolayers were stimulated directly with 50ng/ml LPS + 2ng/ml IFN-γ,10ng/ml IL-4 + 10ng/ml IL-13, 20ng/ml IL-10 or 10μg/ml of large heat-aggregated human IgG (immune complex, IC), or indirectly with conditioned medium of macrophages polarised with the same stimuli for 48 hours; M1 (50ng/ml LPS + 2ng/ml IFN-γ), M2a (10ng/ml IL-4 + 10ng/ml

IL-13), M2c (20ng/ml IL-10) and MIC (10μg/ml of large heat-aggregated human IgG) on the apical surface (Figure 6.1.). Non-stimulated ARPE19 cells or ARPE19 stimulation with conditioned media from non-stimulated macrophages (MNS) were used as controls. TEER (section 2.6.4), lactate dehydrogenase (LDH; section 2.6.5), cytokine measurements (section 2.6.9) and immunocytochemistry (section 2.6.6) were performed at 24 hours and qPCR analysis at 8 hours (section 2.6.7). Cytokine measurements were performed in the apical and basal chambers. Unless stated otherwise, only results from the apical chamber, modelling subretinal inflammation, are shown in this chapter. For results from basal chamber see Appendix II, A7. For statistical analysis of TEER and cytokine measurements, n=9 transwells per treatment group were assessed. For statistical analysis of qPCR studies, n=6 well per treatment group were assessed.

6.2.3 The effect of Avastin and Lucentis on ARPE19 monolayers

The effect of Avastin and Lucentis on ARPE19 monolayers was investigated by adding conditioned medium from macrophages stimulated with Avastin or Lucentis-coated plates (section 2.6.2) as a model of insoluble immune complex to the apical chamber (section 2.6.3, Figure 6.1.). TEER and cytokine measurements were performed 24 hours after stimulation (as detailed in sections 2.6.4 and 2.6.9). Cytokine measurements were performed in the apical and basal chambers. Unless stated otherwise, only results from the apical chamber are shown in this chapter. For results from basal chamber see Appendix II, A7. For statistical analysis of TEER and cytokine measurements, n=6 transwells per treatment group were assessed.

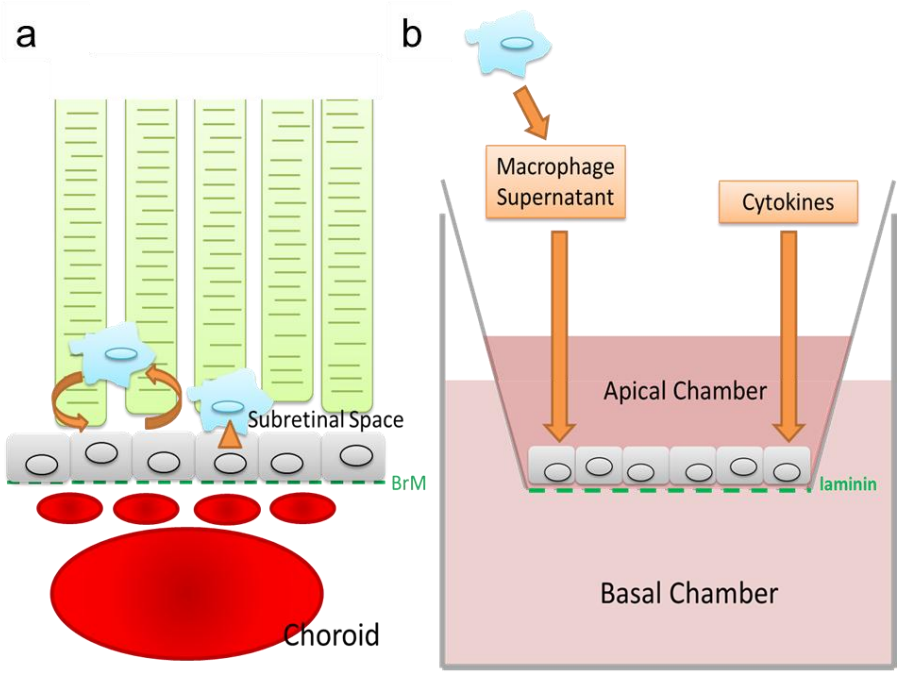

Figure 6.1. Schematic showing (a) subretinal microglia/macrophages and the RPE in the outer retina and (b) the ARPE19 monolayer model of subretinal inflammation used in these experiments.

(a) *In vivo* subretinal microglia/macrophages and the RPE can interact with each other via secretion of cytokines (arrows) or cell-to-cell contacts (triangle)[47, 215] so that the RPE can modulate macrophages/microglia function and vice-versa. **(b)** In the cell culture model used in this chapter, recombinant cytokines or supernatant from activated macrophages are added to the apical chamber as a model of subretinal inflammation.

6.3 Results

6.3.1 Characterisation of the ARPE19 monolayers

To determine optimal time-points to measure changes in RPE function, a time-course experiment was first set up where ARPE19 monolayers stimulated with recombinant cytokines and/or LPS were monitored over time for changes in TEER, cytokine secretion and CFH mRNA transcript levels.

6.3.1.1 The effect of immune stimulation on the TEER of ARPE19 monolayers

Changes in TEER were measured as a percentage of the initial TEER, i.e. "time 0" prior to stimulation, for each individual well at 4, 8, 12 and 24 hours after cytokine stimulation (Figure 6.2). In these experiments ARPE19 monolayers developed TEER

values of approximately 30-50Ω/cm^2, as previously reported in the literature.[338] The TEER of non-stimulated (NS) ARPE19 control monolayers decreased slightly over 24 hours, to 90% of initial TEER. 4 hours after stimulation with IFN-γ+LPS the TEER decreased slightly when compared to NS controls (p=0.045), to 89% of initial TEER. By 8 hours the TEER of ARPE19 monolayers stimulated with IFN-γ+LPS was indistinguishable from that of NS controls. Stimulation with IL-4+IL-13 led to a significant decrease in TEER at 8 (p=0.005), 12 (p=0.0008) and 24 hours (p<0.0001) to 81%, 84% and 66% of initial TEER, respectively. IL-10 stimulation did not have an effect in TEER when compared to NS controls.

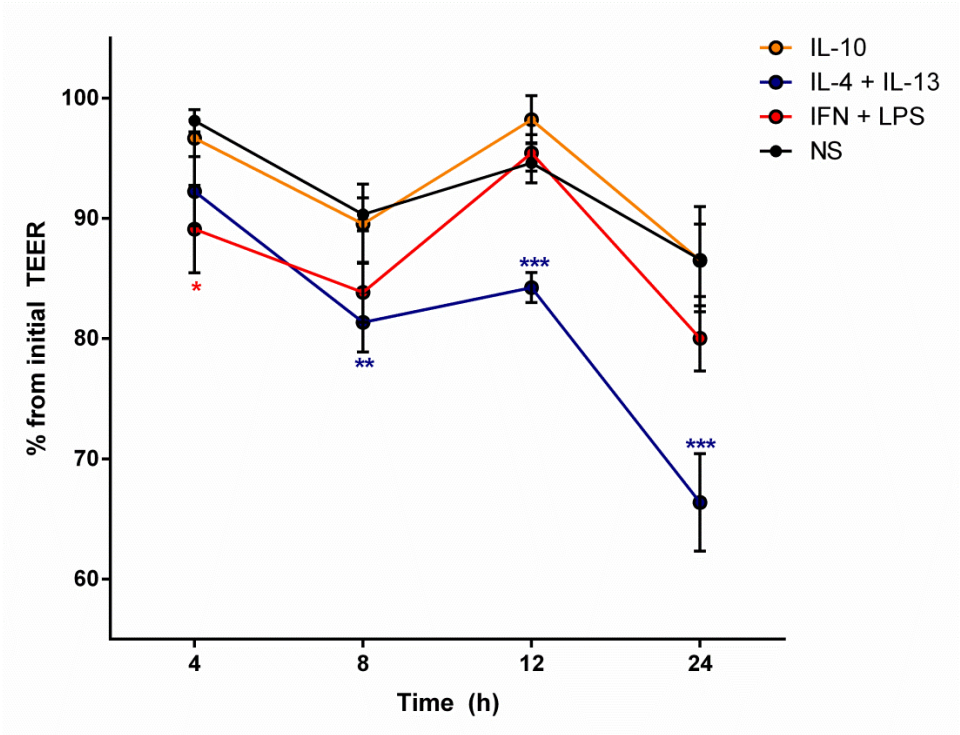

Figure 6.2. The effect of apical immune stimulation on TEER of ARPE19 monolayers.
TEER measurements 4, 8, 12 and 24 hours after stimulation of ARPE19 monolayers with IL-10, IL-4+IL-13 and IFN-γ+LPS (n=9 per group). NS ARPE19 cells were used as a control (n=9). Data shown are pooled from three independent experiments and expressed as percentage from initial TEER±SEM. Data were analysed using repeated measures (RM) two-way ANOVA followed by Bonferroni correction. *p<0.05, **p<0.01, ***p<0.001vs non-stimulated (NS) control.

6.3.1.2 The effect of immune stimulation on inflammatory mediator secretion by ARPE19 monolayers

To determine whether stimulation of ARPE19 monolayers with recombinant cytokines and/or LPS led to inflammatory cytokine production by ARPE19 cells, IL-8, IL-6, IL-

1β, TNF-α, MCP-1 (CCL2) and VEGF (VEGFA) were measured in the apical chamber at 4, 8, 12 and 24 hours after stimulation (Figure 6.3).

Addition of IFN-γ+LPS led to significantly elevated levels of IL-6 at 8 ($p=0.0128$), 12 ($p=0.0006$) and 24 hours ($p<0.0001$) when compared to NS controls. The concentration of IL-6 peaked at 24 hours after addition of IFN-γ+LPS at approximately 377pg/ml, compared to 57pg/ml in NS controls. This was likely due to accumulation of IL-6 over the 24h time period. IFN-γ+LPS addition also led to an increase in MCP-1 concentration at 4 ($p=0.048$), 8 ($p=0.0005$) and 24 hours ($p=0.019$). MCP-1 concentration peaked at 8 hours at 8ng/ml and was maintained elevated at 24 hours, while concentration of MCP-1 in NS controls averaged 4ng/ml at these time points. Stimulation with IL-4+IL-13 resulted in an increase in IL-6 concentration from 4 hours after stimulation ($p=0.002$). The levels of IL-6 continued to be elevated at 8 ($p=0.004$) and 12 hours ($p=0.0001$), where IL-6 concentration peaked at 380pg/ml in IL-4+IL-13 stimulated monolayers. At 24 hours, IL-6 levels were still significantly elevated when compared to NS controls ($p<0.0001$) at a concentration of 219pg/ml. Addition of IL-10 did not lead to any significant changes in the concentration of the cytokines investigated. IL-8, IL-1β, TNF-α and VEGF concentrations did not change after stimulation of the ARPE19 monolayers.

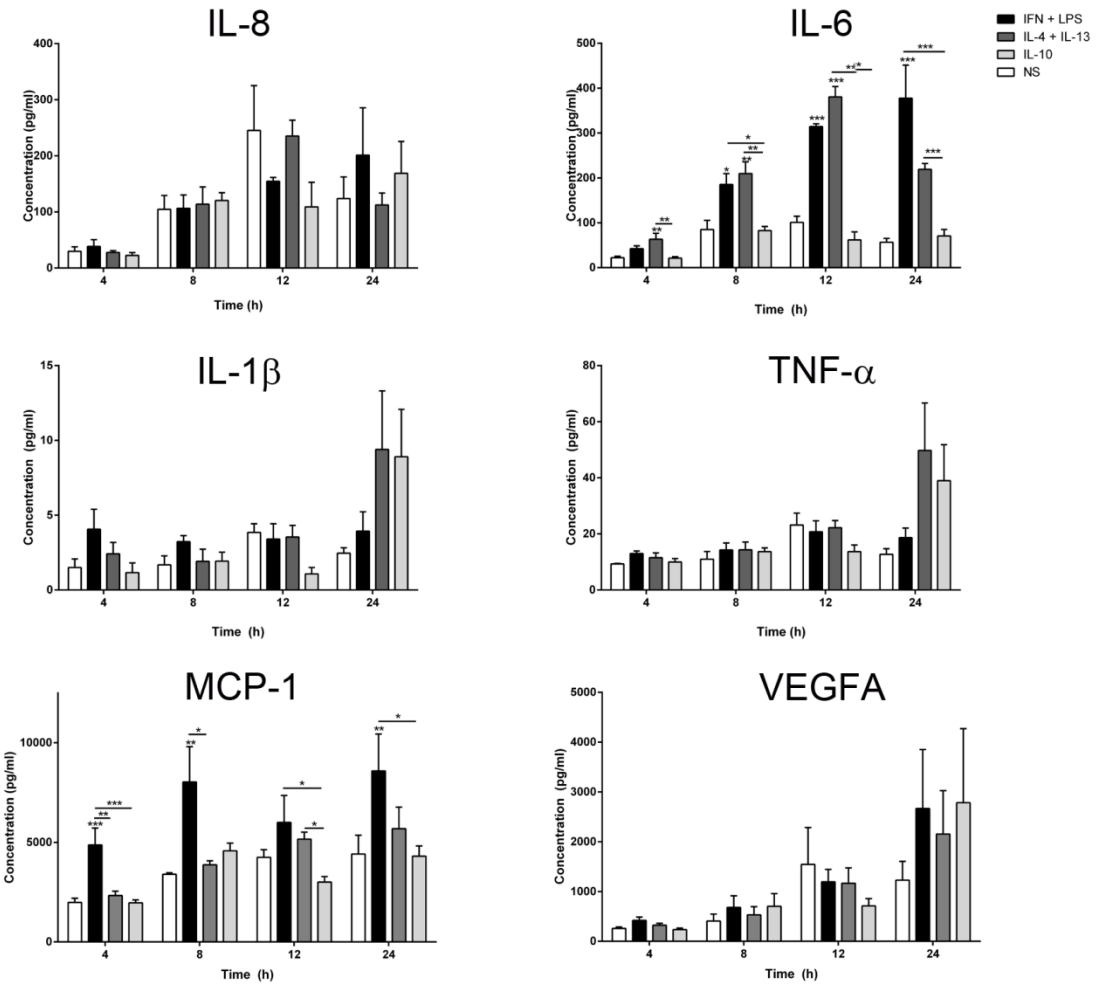

Figure 6.3. Concentration of inflammatory mediators in the apical chamber following immune stimulation of ARPE19 monolayers.

Cytokine measurements 4, 8, 12 and 24 hours after stimulation of ARPE19 monolayers with IL-10, IL-4+IL-13 and IFN-γ+LPS (n=9 per group). NS ARPE19 cells were used as a control (n=9). Data shown are pooled from three independent experiments and expressed as pg/ml+SEM. Data were analysed using RM two-way ANOVA followed by Bonferroni correction. *p<0.05, **p<0.01, ***p<0.001 vs NS control.

6.3.1.3 The effect of immune stimulation on CFH expression

AMD patients have decreased levels of CFH in the RPE when compared to healthy age-matched controls.[336] To investigate if cytokine stimulation of ARPE19 monolayers led to changes in CFH expression, qPCR analysis was performed (Figure 6.4). When compared to NS control, the levels of CFH expression were increased at 8 hours after stimulation ($p<0.0001$) with IFN-γ+LPS, but not any of the other stimuli.

These results suggest that optimal cytokine detection and TEER measurement occur 24 hours after stimulation, whilst changes in expression levels of CFH are best detected at 8 hours, therefore subsequent experiments were performed according to these time points.

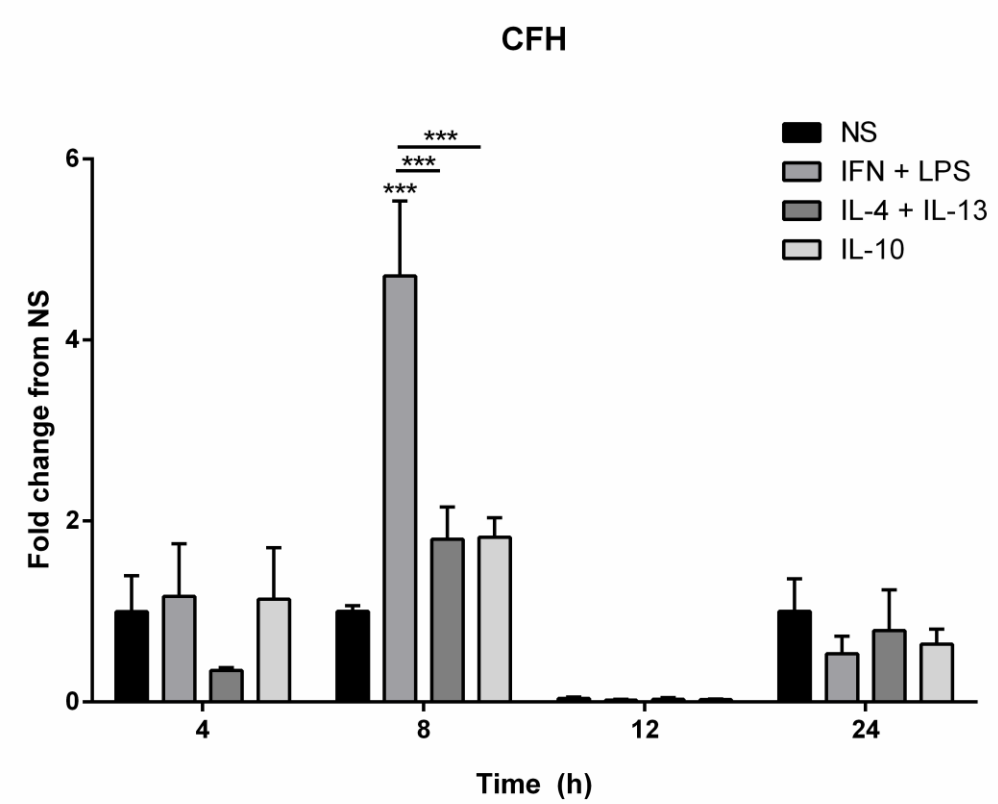

Figure 6.4 The effect of immune stimulation of ARPE19 monolayers on complement factor H mRNA transcript levels.

Change in CFH mRNA transcript levels 4, 8, 12 and 24 hours after stimulation of ARPE19 monolayers with IL-10, IL-4+IL-13 and IFN-γ+LPS (n=6 per group). NS ARPE19 cells were used as a control (n=6). Data shown are pooled from two independent experiments and expressed as fold change from NS controls ±SEM. Data were analysed using RM two-way ANOVA followed by Bonferroni correction. *p<0.05, **p<0.01, ***p<0.001vs NS control unless otherwise indicated.

6.3.2 The effect of inflammatory stimuli on ARPE19 function

To investigate the effect of inflammatory mediators that may be present during subretinal inflammation on RPE physiology, direct stimulation of ARPE19 monolayers with recombinant cytokines, LPS and immune complexes or indirect stimulation with conditioned medium from polarised macrophages was compared.

6.3.2.1 The effect of inflammatory stimuli on ARPE19 viability

Cell damage or death due to stimulation of ARPE19 monolayers may affect TEER measurements. Therefore, release of LDH against a positive control of ARPE19 monolayers lysed with 2% triton X-100 was used as a measure of cytotoxicity. No significant cytotoxicity was detected in response to direct immune stimulation or stimulation with macrophage conditioned media of ARPE19 monolayers using this method (Figure 6.5). LDH activity in cell culture medium has been shown to decrease over time,[339] therefore, it is possible that cytotoxicity may have occurred despite these results.

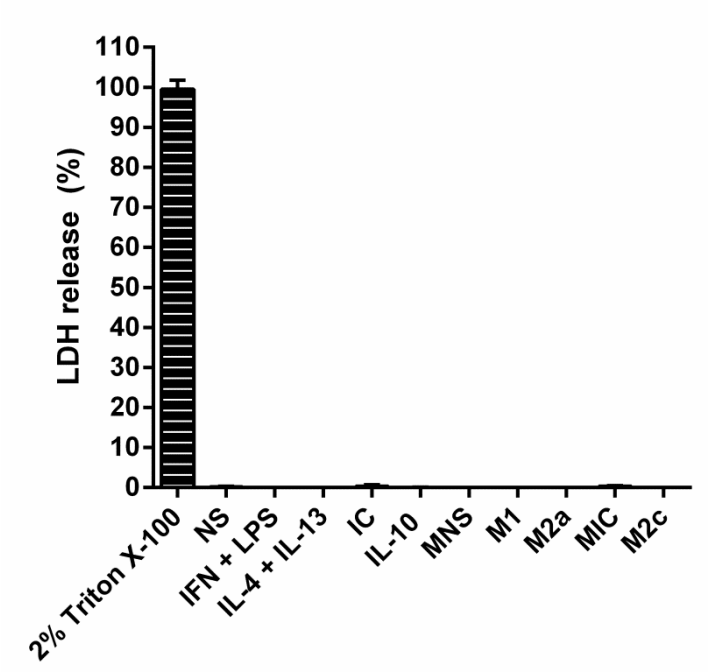

Figure 6.5. Cytotoxicity induced by stimulation of ARPE19 monolayers with inflammatory stimuli. LDH was measured in the apical chamber supernatant 24 hours after stimulation (n=9 per group). Data are pooled from three independent experiments and expressed as percentage from positive control+SEM. Data were analysed using a non-parametric RM Friedman test followed by Dunn's correction. *p<0.05, **p<0.01, ***p<0.001vs NS.

6.3.3 The effect of inflammatory stimuli on ARPE19 monolayer barrier function

Tight junctions between cells of the RPE are essential to permit barrier function of RPE monolayers and thus key in maintaining the BRB.[37] Changes in RPE barrier function could result in a disturbed BRB, allow plasma proteins and immune cells into the retina

and, therefore, contribute to AMD pathology.[340] The barrier function of ARPE19 monolayers was assayed by measuring TEER and analysing transcript and protein levels of the tight junction proteins ZO-1 and occludin.

6.3.3.1 The effect of direct stimulation on ARPE19 barrier function

At 24 hours, the TEER of NS monolayers was approximately 100% of initial TEER, i.e. "time 0" prior to stimulation. Stimulation of ARPE19 monolayers with IL-4+IL-13 led to a significant decrease in TEER ($p=0.0462$) to 86.81% of initial TEER. Addition of IFN-γ+LPS, IC or IL-10 did not induce any changes in TEER (Figure 6.6. a). Transcript levels of occludin and ZO-1 were measured 8 hours after stimulation, at this time point mRNA transcript levels were not altered by any of the treatments (Figure 6.6. b). The distribution pattern of these tight junction proteins was investigated at 24h; immunocytochemistry revealed the distribution of ZO-1 and occludin was continuous and regular around ARPE19 cells in NS monolayers, forming a "cobble-stone" pattern characteristic of ARPE19 cells.[338] Analysis of ZO-1 and occludin in IFN-γ+LPS stimulated monolayers revealed fragmented staining, with some areas showing more intense expression and others loss of expression. This was particularly evident in monolayers stained for occludin. IL-4+IL-13 stimulated monolayers appeared to have irregular staining for ZO-1 and occludin and weaker immunoreactivity for ZO-1 when compared to NS controls. Both IC and IL-10 stimulated monolayers showed continuous and regular staining for ZO-1 and occludin similar to that of NS controls (Figure 6.6. c).

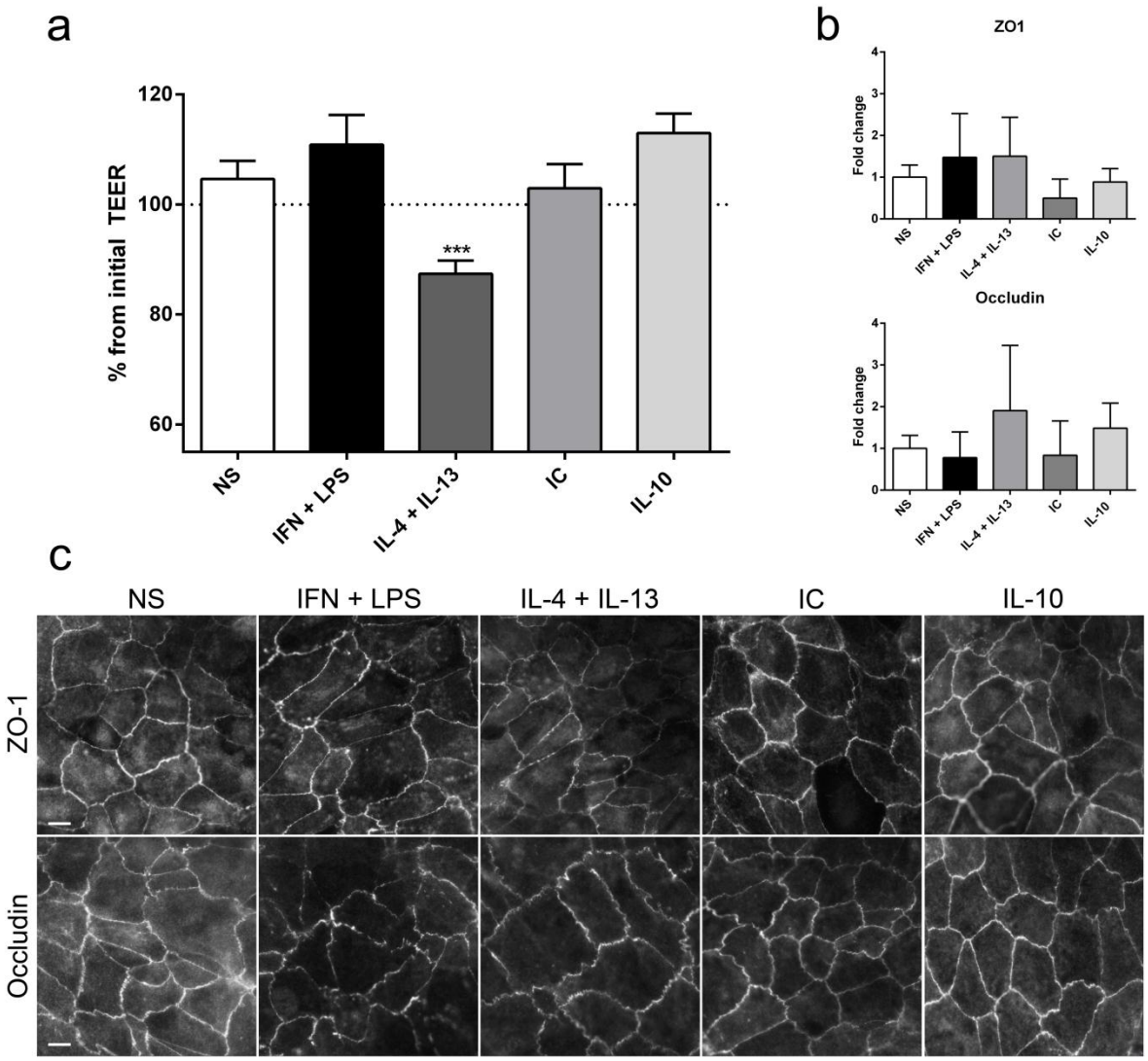

Figure 6.6 The effect of direct immune stimulation on ARPE-19 barrier function.

(a) TEER measurements 24 hours after stimulation of ARPE19 monolayers with IFN-γ+LPS, IL-4+IL-13, IC and IL-10 (n=9 per group). NS ARPE19 cells were used as a control (n=9). Data shown are pooled from three independent experiments and expressed as percentage from initial TEER±SEM. Data were analysed using non-parametric RM Friedman test followed by Dunn's correction. *p<0.05, **p<0.01, ***p<0.001vs NS control. **(b)** Changes in mRNA transcript levels of tight junction proteins were investigated at 8 hours after stimulation of ARPE19 monolayers with IFN-γ+LPS, IL-4+IL-13, IC and IL-10 (n=3-6 per group). NS ARPE19 cells were used as a control (n=6). Data shown are pooled from two independent experiments and expressed as fold change from NS controls +SEM. **(c)** Changes in distribution of tight junctions were investigated by immunocytochemistry for the tight junction proteins ZO-1 and occludin at 24 hours after stimulation of ARPE19 monolayers with IFN-γ+LPS, IL-4+IL-13, IC and IL-10 (n=3 per group). NS ARPE19 cells were used as a control (n=3). Scale bars – 10μm.

6.3.3.2 The effect of polarised macrophage conditioned media on RPE barrier function

Addition of conditioned media (CM) from non-stimulated macrophages (MNS) to the ARPE19 monolayers led to a substantial but non-significant decrease in TEER ($p=0.19$) to 87% of initial values. Stimulation of ARPE19 monolayers with CM from M2a polarised macrophages, but not any other CM, led to a significant decrease in TEER ($p=0.011$) when compared to NS controls, to approximately 78% of initial TEER (Figure 6.7. a). 8 hours after addition of macrophage supernatants, no changes in mRNA levels of ZO-1 or occludin (Figure 6.7. b) were detected. Despite the differences in TEER, immunocytochemistry revealed regular distribution of ZO-1 and occludin in both NS and MNS monolayers. Monolayers stimulated with M1 CM appeared to have weaker and irregular staining for both ZO-1 and occludin when compared to NS controls. Monolayers stimulated with M2a CM had irregular staining for both ZO-1 and occludin, evident as fuzzy borders around individual cells. Finally, monolayers stimulated with CM from both immune complex stimulated (MIC) and M2c macrophages appeared to have regular staining similar to NS and MNS controls and stronger immunoreactivity for both ZO-1 and occludin (Figure 6.7. c).

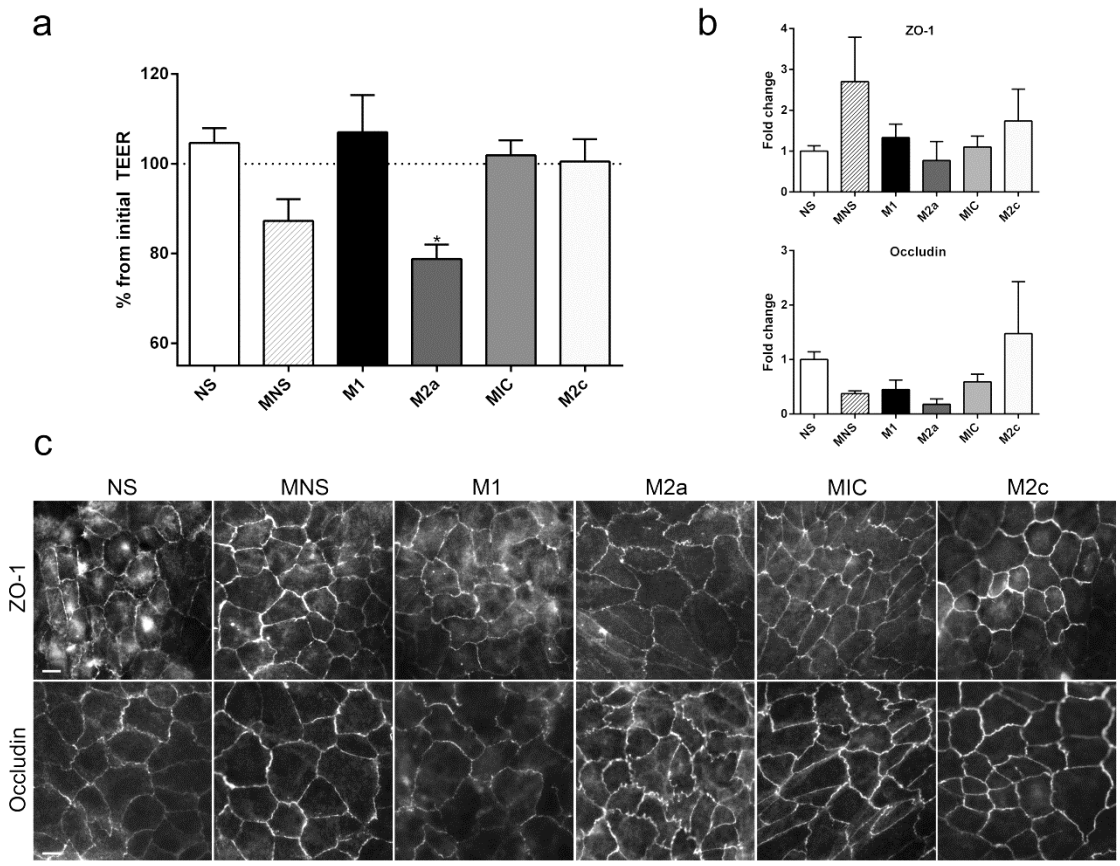

Figure 6.7. The effect of indirect stimulation with macrophage conditioned media on ARPE19 barrier function.

(a) TEER measurements 24 hours after stimulation of ARPE19 monolayers with MNS, M1, M2a, MIC and M2c conditioned media (n=9 per group). NS ARPE19 cells were used as a control (n=9). Data shown are pooled from three independent experiments and expressed as percentage from initial TEER±SEM. Data were analysed using RM one-way ANOVA followed by Bonferroni correction. *p<0.05, **p<0.01, ***p<0.001vs NS control. **(b)** Changes in mRNA transcript levels of tight junction proteins were investigated at 8 hours after stimulation of ARPE19 monolayers with MNS, M1, M2a, MIC and M2c conditioned media (n=3-6 per group). NS ARPE19 cells were used as a control (n=3). Data shown are pooled from two independent experiments and expressed as fold change from NS controls +SEM. **(c)** Changes in distribution of tight junctions were investigated by immunocytochemistry for the tight junction proteins ZO-1 and occludin at 24 hours after stimulation of ARPE19 monolayers with MNS, M1, M2a, MIC and M2c conditioned media (n=3 per group). NS ARPE19 cells were used as a control (n=3). Scale bars – 10μm.

6.3.4 The effect of inflammatory stimuli on the inflammatory milleu in the apical chamber

It has been proposed that the presence of pro-inflammatory cytokines in the subretinal space can lead to activation and/or recruitment of inflammatory cells and consequent

damage to the RPE and photoreceptors in AMD.[341] To investigate whether direct stimulation with cytokines, LPS and immune complex or indirect stimulation with macrophage CM could change the levels of inflammatory mediators a panel of pro-inflammatory cytokines was measured.

6.3.4.1 The effect of direct stimulation on apical secretion of cytokines by ARPE19 monolayers

NS ARPE19 monolayers expressed basal low levels of all cytokines investigated. IFN-γ+LPS stimulation significantly increased the levels of IL-6 (p=0.0001), IFN-γ (p=0.0292) and IL-12 (p70; p=0.019) in the apical chamber, from 33.13pg/ml, 3.7pg/ml and 1.22pg/ml to 302.6pg/ml, 32.76pg/ml and 3.83pg/ml, respectively. IL-4+IL-13 stimulation led to increased levels of IL-6 (p=0.046) to 113.3pg/ml. Addition of IL-10 to ARPE19 monolayers led to increased levels of IL-10 (p=0.019), possibly due to the recombinant IL-10 used for stimulation accumulating in the apical chamber. Stimulation with IC did not induce any significant changes in the cytokines measured (Figure 6.8.).

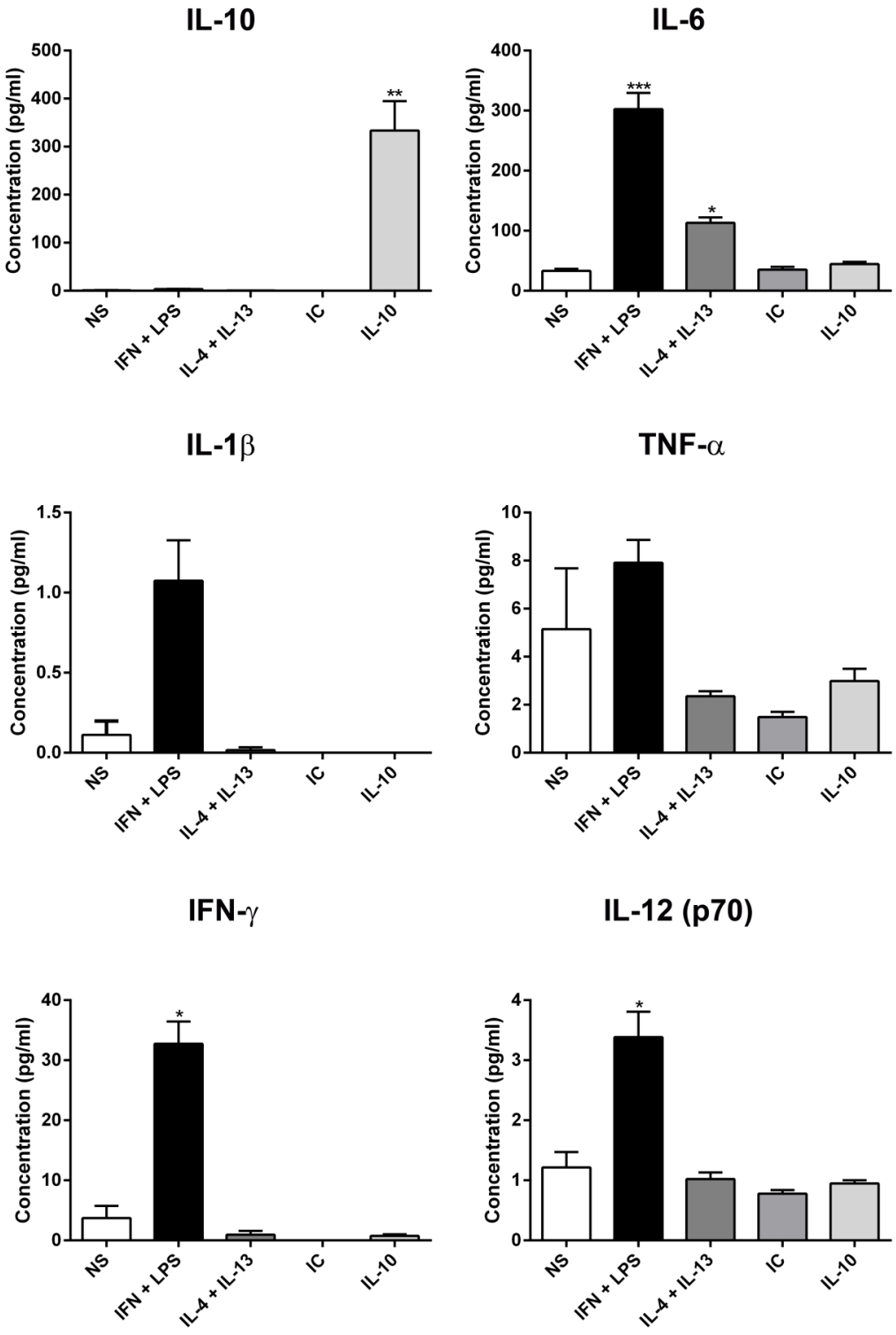

Figure 6.8. Concentration of pro-inflammatory cytokines in the apical chamber following direct stimulation of ARPE19 monolayers.

Cytokine measurements 24 hours after stimulation of ARPE19 monolayers with IFN-γ+LPS, IL-4+IL-13, IC and IL-10 (n=9 per group). NS ARPE19 cells were used as a control (n=9). Data shown are pooled from three independent experiments and expressed as pg/ml+SEM. Data were analysed using a

non-parametric RM Friedman test followed by Dunn's correction. *p<0.05, **p<0.01, ***p<0.001 vs NS control.

6.3.4.2 The effect of polarised macrophage conditioned media on the concentration of cytokines in the apical chamber

The concentration of cytokines in the CM of polarised macrophages is shown in Table 6.1. M1 stimulated macrophages release elevated levels of IFN-γ, IL-10, IL-12, IL-1β, IL-6 and TNF-α when compared to MNS. Both M2a and MIC cells appeared to have increased levels of IL-6 when compared to MNS. High levels of IL-8 were detected in all CM, particularly in MNS CM at approximately 8ng/ml. Only low levels of VEGF (less than 12pg/ml) were detected in the CM of all macrophages.

Table 6.1. Mean concentration of cytokines (pg/ml) in macrophage conditioned medium

	MNS n=3	M1 n=3	M2a n=3	MIC n=3	M2c n=3
IFN-γ	38	158	25	35	51
IL-10	16	365	22	24	2932
IL-12 (p70)	5	19	4	5	7
IL-1β	2	26	2	2	4
IL-6	22	6191	97	50	21
IL-8	8014	4851	1407	6821	6297
TNF-α	21	4727	27	19	23
VEGFA	8	4	4	12	12

At 24 hours basal levels of cytokines in the apical chamber of NS RPE monolayers were 1.8pg/ml IL-10, 33pg/ml IL-6, 0.1pg/ml IL-1β, 5pg/ml TNF-α, 3.7pg/ml IFN-γ and 1.2 pg/ml IL-12 (p70). Stimulation with CM from non-stimulated macrophages (MNS) led to an increase in IL-6 (p=0.019), IL-1β (p=0.0082), IFN-γ (p=0.0005) and IL-12 (p=0.0053) to 98pg/ml, 2pg/ml, 16pg/ml, 31pg/ml and 5pg/ml, respectively. Addition of M1 CM led to an increase in all cytokines investigated: Il-10 (p<0.0001), IL-6 (p<0.0001), IL-1β (p<0.0001), TNF-α (p<0.0001), IFN-γ (p<0.0001) and IL-12 (p=0.001) to 128pg/ml IL-10, 4.2ng/ml IL-6, 11pg/ml IL-1β, 2.2ng/ml TNF-α, 48pg/ml IFN-γ and 5pg/ml IL-12. M2a CM stimulation led to an increase in IL-10 (p=0.04), IL-6 (p<0.0001), IL-1β (p=0.003), TNF-α (p=0.019), IFN-γ (p=0.028) and IL-12 (p70; p=0.0125) to 16pg/ml IL-10, 417pg/ml IL-6, 2.5pg/ml IL-1β, 20pg/ml TNF-α, 19pg/ml IFN-γ and 4pg/ml IL-12. Addition of M2c supernatant to ARPE19 monolayers led to a

significant increase in IL-10 ($p<0.0001$) to 1.3ng/ml. Addition of CM from MIC macrophages did not lead to any significant changes in the pro-inflammatory cytokines investigated (Figure 6.9.).

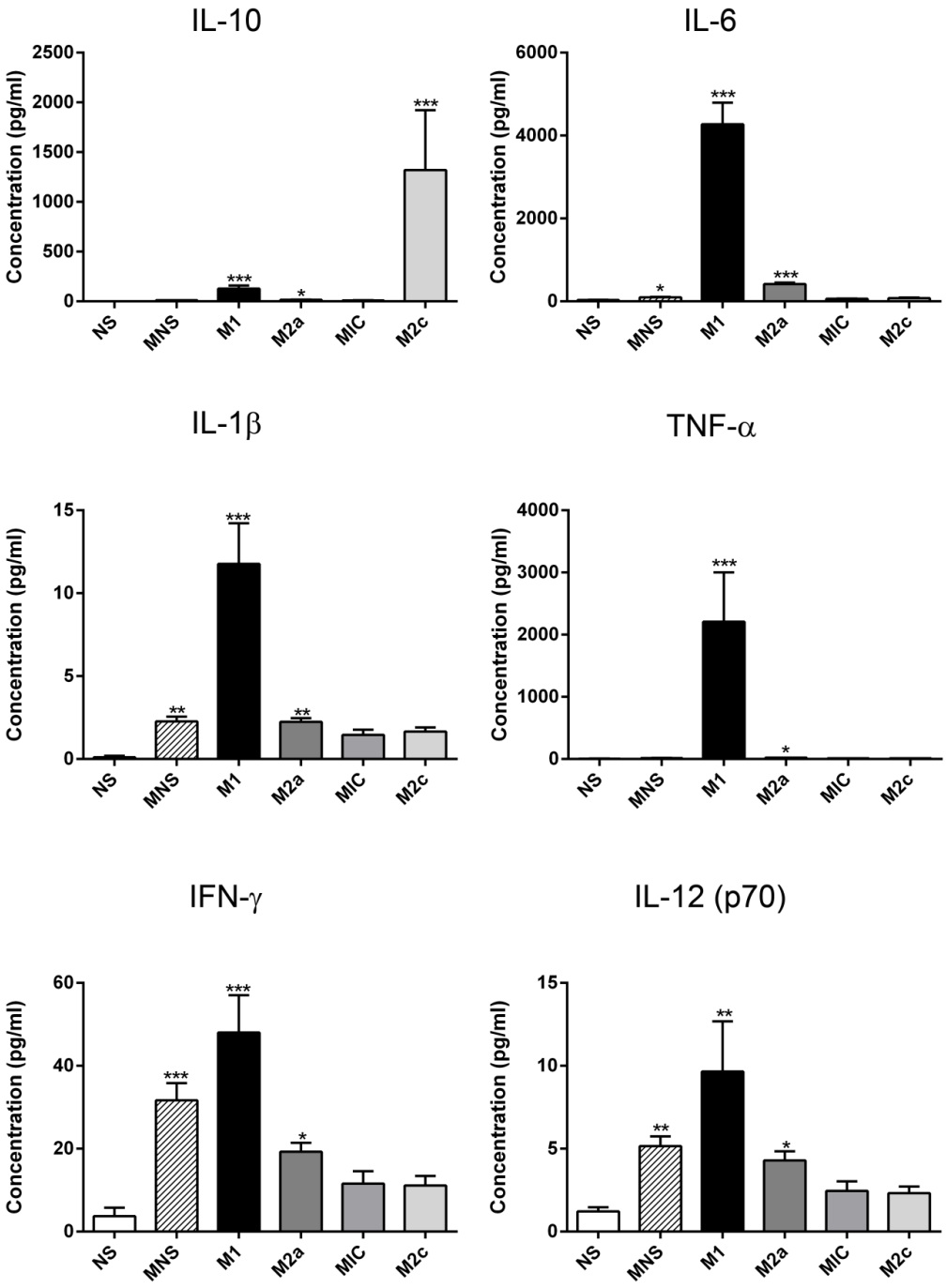

Figure 6.9. Concentration of pro-inflammatory cytokines in the apical chamber following addition of macrophage conditioned media to ARPE19 monolayers.

Cytokine measurements 24 hours after stimulation of ARPE19 monolayers with MNS, M1, M2a, MIC and M2c conditioned media (n=9 per group). NS ARPE19 cells were used as a control (n=9). Data

shown are pooled from three independent experiments and expressed as pg/ml+SEM. Data were analysed using RM one-way ANOVA followed by Bonferroni correction. *p<0.05, **p<0.01, ***p<0.001 vs NS control.

6.3.5 The effect of inflammation on factors associated with AMD

The effect of inflammatory stimuli on the factors associated with AMD IL-8, VEGF and CFH was investigated. Due to degradation of the MCP-1 protein used for the standard curve in the ELISA assay, it was not possible to detect MCP-1 in these experiments.

6.3.5.1 The effect of direct stimulation on factors associated with AMD

At 24 hours the concentrations of IL-8 and VEGF (VEGFA) in NS ARPE19 monolayers were 578.2pg/ml and 800pg/ml, respectively. The concentration of IL-8 in the apical chamber was increased to 2554pg/ml (p=0.0003) after stimulation of monolayers with IFN-γ+LPS. Stimulation with IL-4+IL-13, IC or IL-10 did not induce any changes in the concentration of IL-8. Stimulation of monolayers with IFN-γ+LPS also led to a small but significant increase in VEGF concentration to 1000pg/ml (p=0.05). Stimulation with IL-4+IL-13 and IL-10 led to a similar but non-significant increase in VEGF concentration (Figure 6.10. a). Transcript levels of CFH were measured 8 hours after direct stimulation. Stimulation with IFN-γ+LPS, but not any other stimulus, led to a non-significant 4-fold increase in CFH transcript levels when compared to NS monolayers (Figure 6.10. b).

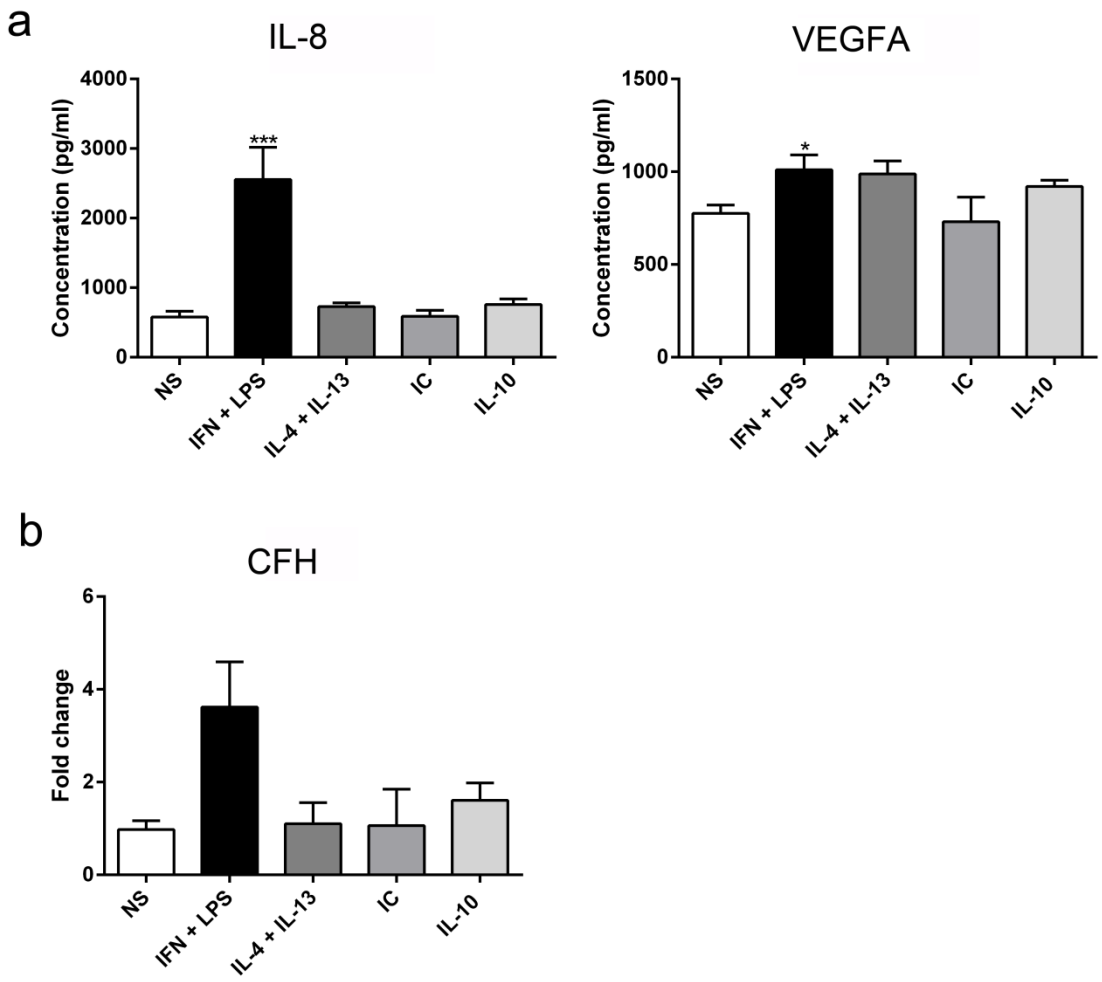

Figure 6.10. The effect of direct stimulation of ARPE19 monolayers on factors linked to AMD. **(a)** Measurement of VEGF and IL-8 24 hours after stimulation of ARPE19 monolayers with IFN-γ+LPS, IL-4+IL-13, IC and IL-10 (n=9 per group). NS ARPE19 cells were used as a control (n=9). Data shown are pooled from three independent experiments and expressed as pg/ml+SEM. Data were analysed using RM one-way ANOVA followed by Bonferroni correction. *p<0.05, **p<0.01, ***p<0.001 vs NS control. **(b)** Changes in mRNA transcript levels of CFH were investigated at 8 hours after stimulation of ARPE19 monolayers with IFN-γ+LPS, IL-4+IL-13, IC and IL-10 (n=5 per group). NS ARPE19 cells were used as a control (n=5). Data shown are pooled from two independent experiments and expressed as fold change from NS controls +SEM. Data were analysed using RM one-way ANOVA followed by Bonferroni correction. *p<0.05, **p<0.01, ***p<0.001 vs NS control

6.3.5.2 The effect of polarised macrophage conditioned media on factors associated with AMD

The concentration of IL-8 in the apical chamber at 24 hours was increased by stimulation with MNS (p=0.0003), M2a (p=0.0021) and MIC (p=0.0008) CM from 13pg/ml in NS controls to 45pg/ml, 41pg/ml and 43pg/ml, respectively. This was likely

due to the high concentration of IL-8 in the CM (Table 6.1.). Surprisingly, stimulation with M1 CM did not lead to increased levels of IL-8 in the apical chamber (p=0.592). VEGF concentration was only affected by stimulation with M1 supernatants, resulting in an increase in VEGF concentration from 735pg/ml to 1712pg/ml (p=0.05; Figure 6.11. a), in spite of the low levels of VEGF in CM (Table 6.1.). Stimulation of monolayers with MIC CM, but none of the other supernatants, led to a non-significant 3-fold increase in the transcript levels of CFH (p>0.05; Figure 6.11. b).

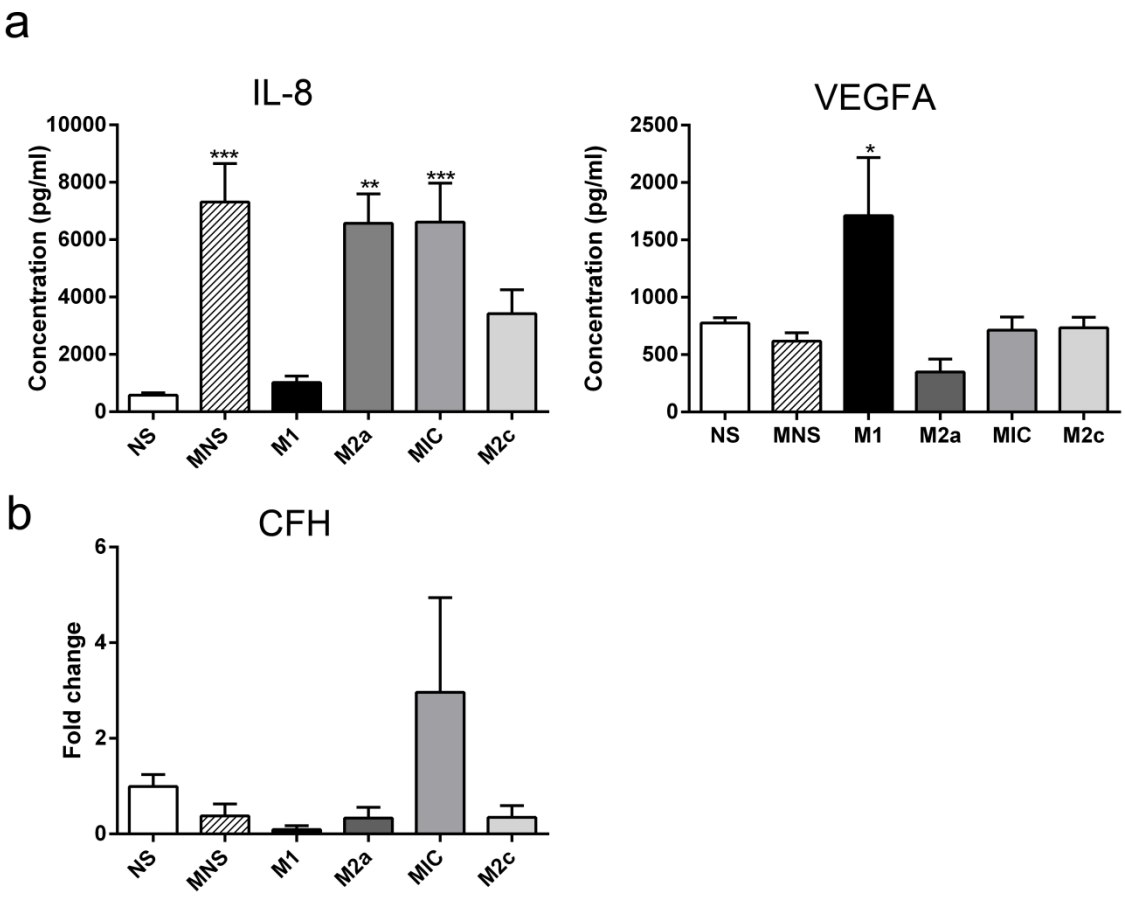

Figure 6.11. The effect of stimulation of ARPE19 monolayers with polarised macrophage conditioned media on factors associated with AMD.

(a) Measurement of IL-8 and VEGF 24 hours after stimulation of ARPE19 monolayers with MNS, M1, M2a, MIC and M2c conditioned media (n=9 per group). NS ARPE19 cells were used as a control (n=9). Data are pooled from three independent experiments and expressed as pg/ml+SEM. Data shown were analysed using RM one-way ANOVA followed by Bonferroni correction. *p<0.05, **p<0.01, ***p<0.001 vs NS control. **(b)** Changes in mRNA transcript levels of CFH were investigated at 8 hours after stimulation of ARPE19 monolayers with MNS, M1, M2a, MIC and M2c conditioned media (n=4 per group). NS ARPE19 cells were used as a control (n=4). Data shown are pooled from two independent experiments and expressed as fold change from NS controls +SEM. Data were analysed using RM one-way ANOVA followed by Bonferroni correction. *p<0.05, **p<0.01, ***p<0.001 vs NS control.

6.3.6 The effect of macrophage stimulation with Avastin or Lucentis on ARPE19 monolayers

The two drugs commonly used for the treatment of wet AMD, Avastin and Lucentis, are both targeted against VEGF and differ in that one (Avastin) is a whole IgG1 molecule and the other (Lucentis) is a Fab' fragment.[331] To investigate whether Avastin or Lucentis can induce macrophage activation and subsequently affect RPE function, CM from macrophages stimulated with plate-immobilised Avastin (Avastin CM) or Lucentis (Lucentis CM) was added to ARPE19 monolayers and barrier function and cytokine concentration in the apical chamber investigated.

6.3.6.1 The effect of CM from Avastin or Lucentis stimulated macrophages on ARPE19 barrier function

Stimulation of ARPE19 monolayers with MNS CM lead to a significant decrease in TEER to 90% of initial TEER, when compared to NS controls (p=0.01). Stimulation of ARPE19 monolayers with Avastin or Lucentis CM did not induce any changes in TEER (Figure 6.12.).

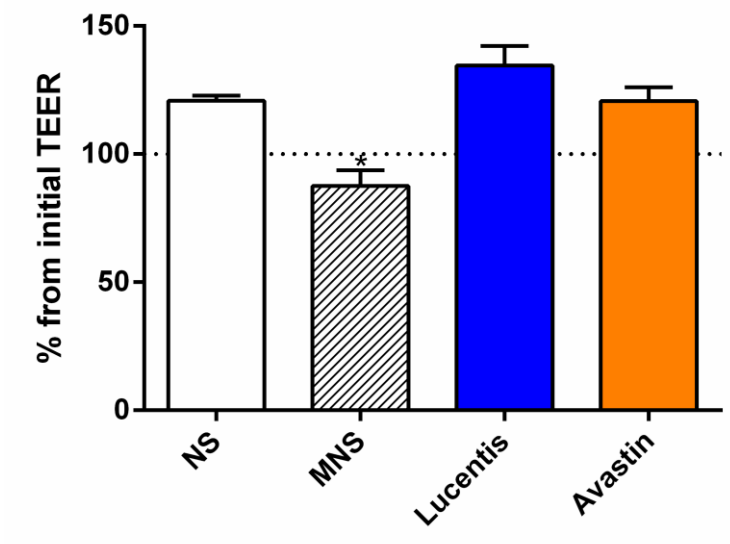

Figure 6.12. The effect of Avastin or Lucentis macrophage conditioned media on ARPE19 barrier function.

TEER measurements 24 hours after stimulation of ARPE19 monolayers with MNS, Lucentis and Avastin conditioned media (n=6 per group). NS ARPE19 cells were used as a control (n=6). Data shown are pooled from three independent experiments and expressed as percentage from initial TEER±SEM. Data were analysed using RM one-way ANOVA followed by Bonferroni correction. *p<0.05, **p<0.01, ***p<0.001vs NS control.

6.3.6.2 The effect of CM from Avastin or Lucentis stimulated macrophages on the concentration of cytokines in the apical chamber

The concentration of cytokines in the CM of polarised macrophages is shown in Table 6.2. There were detectable levels of all cytokines studied in all macrophage CM. Lucentis CM showed an increase in TNF-α when compared to MNS CM, from 21pg/ml to 704pg/ml. A much more pronounced increase in TNF-α was observed in Avastin CM, to 2000pg/ml. The concentration of IL-8 in Lucentis and Avastin CM was 2.5ng/ml and 3ng/ml, which was substantially lower than that observed in MNS CM at 8ng/ml.

Table 6.2. Mean concentration of cytokines (pg/ml) in macrophage conditioned medium.

	MNS n=3	Avastin n=3	Lucentis n=3
IFN-γ	38	26	24
IL-10	16	18	17
IL-12 (p70)	5	4	6
IL-1β	2	11	7
IL-6	22	54	89
IL-8	8014	3000	2500
TNF-α	21	2000	704
VEGFA	8	9	9

When compared to NS control, stimulation of ARPE19 monolayers with Lucentis CM led to a significant increase in IL-10 ($p<0.0001$), IL-6 ($p=0.0017$), IL-1β ($p=0.02$), IFN-γ ($p=0.04$) and IL-12 ($p=0.001$) to 8pg/ml IL-10, 530pg/ml IL-6, 6pg/ml IL-1β, 35pg/ml IFN-γ and 4pg/ml IL-12. However, only IL-6 was significantly increased when compared to monolayers stimulated with MNS CM ($p=0.05$). Stimulation of monolayers with Avastin supernatants led to a significant increase in all cytokines studied when compared to NS controls, IL-10 ($p=0.0002$), IL-6 ($p<0.0001$), IL-1β ($p<0.0001$), TNF-α ($p<0.0001$), IFN-γ ($p=0.0004$) and IL-12 ($p<0.0001$) to 10 pg/ml IL-10, 400 pg/ml IL-6, 8pg/ml IL-1β, 1ng/ml TNF-α, 35pg/ml IFN-γ and 4 pg/ml IL-12. The pro-inflammatory cytokines IL-6 ($p=0.001$), IL-1β ($p=0.0004$) and TNF-α ($p<0.0001$) were significantly increased in the apical chamber of monolayers stimulated with Avastin CM when compared to MNS stimulated monolayers (Figure 6.13.).

6.3.6.3 The effect of CM from Avastin or Lucentis stimulated macrophages on the concentration on factors associated with AMD

The concentration of IL-8 in the apical chamber was increased 24 hours after stimulation with Avastin ($p=0.001$) or Lucentis ($p=0.002$) CM to 2800pg/ml and 2700pg/ml, respectively. However, stimulation with MNS CM led to a higher increase in IL-8 concentration to 7500pg/ml. This was likely due to the high levels of IL-8 in all CM (Table 6.2.).The concentration of VEGF in the apical chamber was unaltered by stimulation with MNS or Lucentis CM. Stimulation with Avastin CM led to a significant two-fold increase in VEGF ($p=0.0008$) to 2300pg/ml (Figure 6.14.), despite the low levels of VEGF in Avastin CM.

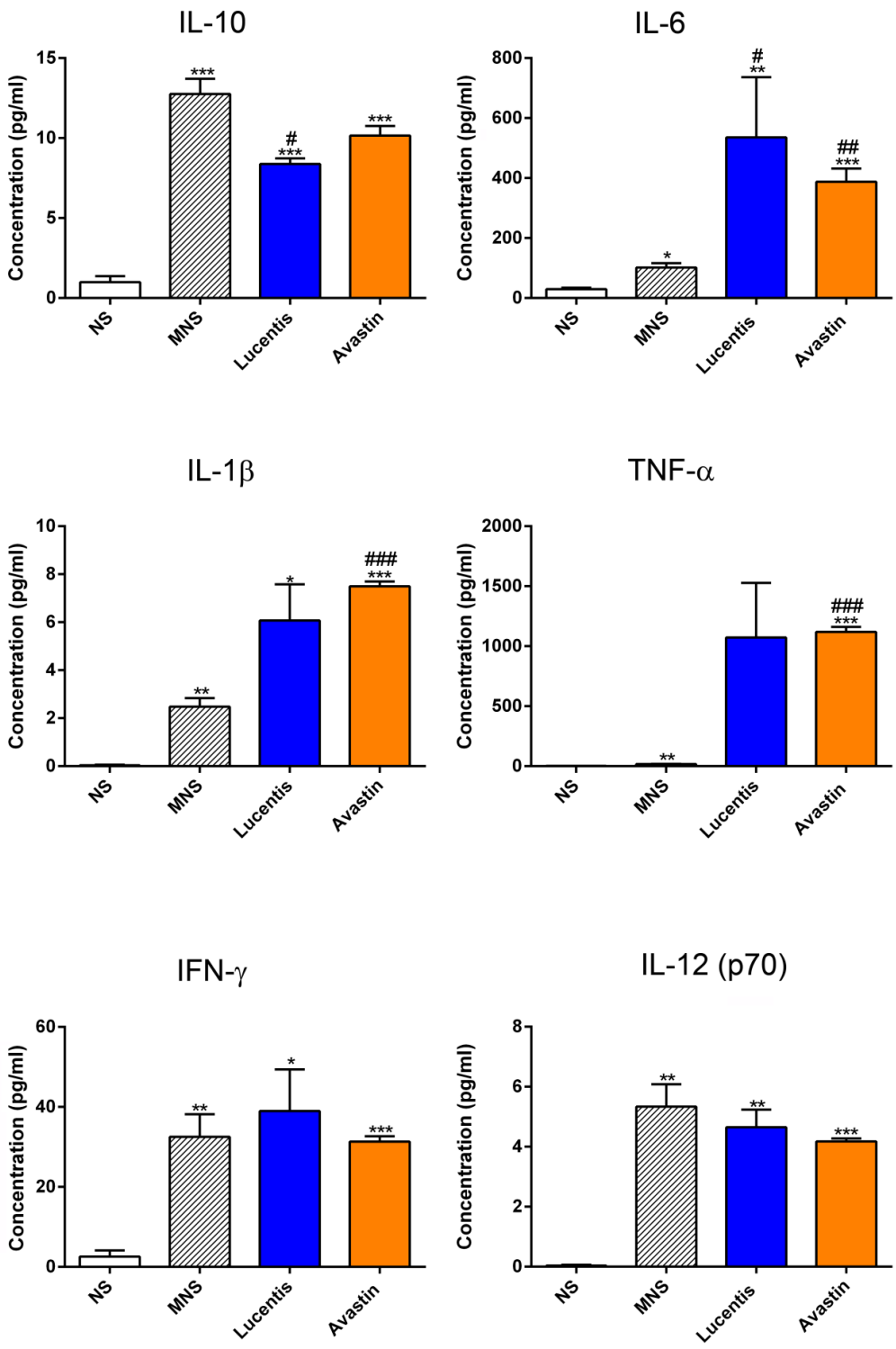

Figure 6.13. Concentration of pro-inflammatory cytokines in the apical chamber following addition of Lucentis and Avastin conditioned medium to ARPE19 monolayers.

Cytokine measurements 24 hours after stimulation of ARPE19 monolayers with MNS, Lucentis and Avastin conditioned media (n=6 per group). NS ARPE19 cells were used as a control (n=6). Data shown are pooled from three independent experiments and expressed as pg/ml+SEM. Data were analysed using

RM one-way ANOVA followed by Bonferroni correction. *p<0.05, **p<0.01, ***p<0.001 vs NS control.

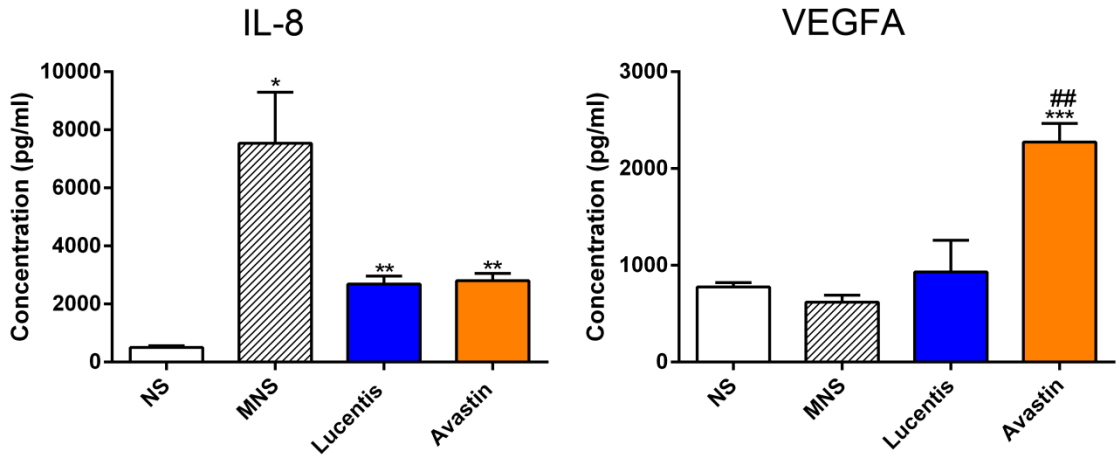

Figure 6.14. Concentration of factors linked to AMD in the apical chamber following addition of Lucentis and Avastin conditioned medium to ARPE19 monolayers.

Cytokine measurements 24 hours after stimulation of ARPE19 monolayers with MNS, Lucentis and Avastin conditioned media (n=6 per group). NS ARPE19 cells were used as a control (n=6). Data shown are pooled from three independent experiments and expressed as pg/ml+SEM. Data were analysed using RM one-way ANOVA followed by Bonferroni correction. *p<0.05, **p<0.01, ***p<0.001 vs NS control.

6.4 Discussion

The role of inflammation in AMD has generated much interest, with observations from human studies and several mouse models supporting a role for subretinal inflammation in the pathogenesis of AMD.[91, 143, 171] However, the mechanism by which subretinal inflammation could contribute to AMD have not yet been elucidated.[10] To investigate how subretinal inflammation could affect RPE function, ARPE19 monolayers were grown on transwell supports and inflammatory stimuli were added to the apical chamber (Figure 6.1.). These results show that addition of IL-4+IL-13 or CM from M2a macrophages led to substantial disruption of ARPE19 barrier function, as seen by decreased TEER. These changes were accompanied by altered distribution of the tight junction proteins ZO-1 and occludin and a significant increase in the cytokine IL-6. Direct stimulation with IFN-γ+LPS and, in particular, indirect stimulation with M1 CM led to significant increase in cytokine concentration in the apical chamber, including IL-6 and VEGF, without any detectable changes in TEER. In addition, stimulation with Avastin CM, but not Lucentis CM, led to a significant increase in the concentration of VEGF in the apical chamber. These results suggest that macrophage activation in the

subretinal space can lead to significant generation of pro-inflammatory cytokines and to changes in RPE barrier function, which could contribute to AMD pathology.

6.4.1 ARPE19 monolayers as a model of RPE physiology

ARPE19 monolayers have been widely used to study the effect of several stimuli on RPE barrier function and secretion of cytokines,[72, 342] but limited data exists on the effect of cytokines on ARPE19 TEER.[54, 343] To characterise the ARPE19 monolayers as a model of subretinal inflammation in our lab, recombinant cytokines and LPS were added to the apical chamber and TEER and concentration of cytokines in the apical chamber were measured at several time-points. Changes in TEER were more pronounced at 24 hours after stimulation and TEER seemed to decrease over time irrespective of treatment. This was likely due to repeated changes in temperature and CO_2 when removing the transwells containing the ARPE19 monolayers from the incubator at the several time points investigated. To avoid this effect, in subsequent experiments only two TEER measurements (baseline and 24 hour) were taken per well. Concentrations of pro-inflammatory cytokines in the apical chamber were elevated at 24 hours after stimulation for most cytokines studied. This was likely due to accumulation of secreted cytokines in the apical chamber over time. Finally, changes in transcript levels for CFH were only detected at 8 hours after stimulation. Based on these results, in subsequent experiments, TEER and cytokine changes were investigated 24 hours after stimulation, whilst changes in transcript levels were investigated 8 hours after stimulation.

ARPE19 monolayers grown in transwells polarise with the apical side facing the upper chamber and the basal side facing the lower chamber.[342] When grown in standard tissue culture wells, APRE19 cells polarise in a similar manner, with the basal side attached to the plastic well and the apical side facing upwards.[342] However, growing the ARPE19 cells in a transwell system allows for a more physiological representation of the RPE as it allows for the cells to feed from the basal side, as occurs *in vivo*, but also allows study of changes in secretion at both the apical and basal surfaces.[342] Nevertheless, there are several limitations of this model, in particular when studying the effect of inflammation on the RPE. Similar to the RPE *in vivo,* ARPE19 cells express anti-inflammatory cytokines such as pigmented epithelium derived factor (PEDF)[344] creating an immunosuppressant environment, which has been shown to modulate microglia and

macrophage activation.[47, 215] Ethical approval to co-culture human macrophages with the ARPE19 cells was not obtained during the time-frame of this thesis. Therefore, in our experiments, human macrophages were first polarised, separately from the ARPE19 cells and thus, in the absence of this immunosuppressant environment. Perhaps a way to circumvent this problem would have been to stimulate the macrophages in the presence of supernatant from NS ARPE19 cells. Secondly, as co-culture was not possible for these experiments no cell-to-cell contacts between macrophages and the ARPE19 cells could form, which is likely to introduce further differences between our model and what may happen *in vivo*. One must thus be careful when interpreting results from this model for translation into humans. Nevertheless, the results in this chapter show that ARPE19 monolayers are a useful, yet simple, model to study how diverse inflammatory mediators affect some aspects of RPE physiology.

6.4.2 Immune-complex and ARPE19 function

In the previous chapters, it was shown that immune complex formation in the retina leads to a strong inflammatory response, which is dependent on FcγRs. ARPE19 cells have been reported to express FcγRI, FcγRII and FcγRIII and thus to possess the ability to interact with IgG.[345] Unexpectedly, the results show that both large heat aggregated IgG (immune complexes) alone or conditioned medium from immune complex stimulated macrophages did not induce changes in TEER or cytokine secretion by ARPE19 cells or human macrophages. No expression of FcγRI or FcγRIIb by qPCR and immunocytochemistry, or of FcγRIIa and III by immunocytochemistry was detected in ARPE19 cells (Appendix II, A8). This could explain why direct application of immune complexes did not induce changes in TEER or cytokine concentration in the apical chamber, as ARPE19 cells would be unable to interact with the immune complexes. Similarly, stimulation of ARPE19 monolayers with MIC CM did not lead to any changes in TEER or cytokine levels in the apical chamber. With the exception of a small increase in IL-6 and a decrease in IL-8, analysis of the CM did not reveal any differences in cytokine levels between non-stimulated macrophages and macrophages stimulated with immune complexes. In addition, flow cytometry analysis of the polarised macrophages (performed by Lekh Dahal, Appendix II, A9) did not show any differences in the activation markers CD40 and CD11b or in FcγR expression between immune complex activated or non-stimulated macrophages, suggesting that the immune

complexes did not induce macrophage activation. This is consistent with previous reports, showing soluble immune complexes alone do not phenotypically polarise macrophages.[263] In contrast, stimulation of macrophages with immobilised Avastin (IgG1) induced macrophage activation, as seen by increased levels of IL-6, IL-1β and TNF-α when compared to non-stimulated macrophages. These results suggest that insoluble, but not soluble, immune complexes, may activate macrophages and subsequently induce functional changes to the RPE. It has been shown that Avastin-VEGF immune complexes form in the eyes of monkeys with AMD-like pathology.[346] It would be interesting to investigate if in humans VEGF-Avastin immune complexes form and whether these may be soluble or insoluble. This may prove helpful to guide further studies and thus contribute to understanding of the mechanisms behind side effects associated with Avastin.

6.4.3 The effect of inflammatory stimuli on barrier function of the ARPE

The outer blood retina barrier (BRB) is composed of the Bruch's membrane (BrM) and tight junctions between the RPE.[37] Therefore, integrity of the RPE is essential to regulate transport of substances from the blood stream across to the retina. [1] The results in this chapter show that specific inflammatory stimuli can significantly disrupt barrier function.

IFN-γ+LPS and M1 conditioned medium

The presence of TNF-α^+IL-12^+ macrophages in association with RPE degeneration in the mouse retina[209] and $CCL11^+$ or $iNOS^+$ macrophages in human AMD eyes,[174, 201] has led some authors to suggest the presence of M1-polarised macrophages could lead to damage of the RPE and contribute to AMD pathology.[201, 209] To investigate the biological effect of M1 stimulation on RPE function, ARPE19 monolayers were stimulated directly with IFN-γ+LPS or with CM from M1 polarised macrophages. Previous *in vitro* studies on RPE barrier function using rat RPE[55] and human foetal RPE (hfRPE) cells[54] and on endothelial barrier function (an important component of the inner BRB) using human umbilical vein endothelial (HUVEC) cells[53] have shown that LPS or IFN-γ+LPS stimulation leads to decreased TEER and, hence, compromised barrier function. Unexpectedly, addition of neither IFN-γ+LPS nor M1 CM led to

changes in RPE TEER. These contrasting results could possibly be explained by different degrees of stimulation. In the studies using RPE, the dose of IFN-γ added to the cells was twice as high as that used in this study and 50 times higher than the levels of IFN-γ present in M1 CM.[54] Similarly, the dose of LPS used was 5 times higher than that used in this study.[54] Additionally, differences in cell type may help explain these results. This would be of particular interest when comparing RPE and endothelial cells, as it may mean the outer and inner blood barriers respond differently to inflammatory stimuli. Supporting this idea, in one study it was shown that VEGF can differentially regulate expression of ZO-1 in human RPE and endothelial cells; resulting in increased TEER and ZO-1 transcript levels in primary human retinal pigmented epithelial cells and decreased TEER and ZO-1 transcript levels in HUVEC endothelial cells.[63]

Stimulation of retinal pigmented epithelial cells with LPS and IFN-γ has been previously shown to induce disruption of ZO-1 and occludin, which was accompanied by TEER changes.[54, 55] Surprisingly, despite the lack of effect on TEER, addition of IFN-γ+LPS or M1 CM to ARPE19 monolayers led to disturbed tight junctions, seen as fragmented staining of ZO-1 and occludin, which makes these results challenging to interpret. In a model of lung epithelium barrier, stimulation of cultured human airway epithelial cells (Calu3) with IFN-γ at a dose 10 times higher than that used in this chapter increases TEER, despite disrupted ZO-1 and occludin distribution.[347] Changes in phosphorylation state of tight junction proteins play an important role in regulation of tight junction function.[348-352] In particular, phosphorylation of serine/threonine residues in occludin and ZO-1 have been shown to correlate with increased tight junction resistance. These changes did, however, also correlate with increased tight junction assembly, detectable by immunohistochemistry.[348, 349, 351, 352] One study showed a correlation between increased phosphorylation of ZO-1 and increased TEER, without changes to tight junction protein expression levels or location.[350] It is thus possible that following stimulation with IFN-γ+LPS or M1 CM, the TEER could be rescued due to the phosphorylation state of tight junction proteins.

The claudin family of tight junction proteins, composed of 24 known different proteins, is thought to be key in allowing cell-specific regulation of tight junction function.[52] Interestingly, decreased protein levels of claudin-11 and claudin-12 have been shown to correlate with decreased TEER in ARPE19 cells following IL-1β stimulation.[51] It is possible that changes in tight junction proteins such as claudins could rescue TEER

following IFN-γ+LPS or M1 CM stimulation of ARPE19 monolayers. Thus, it would be interesting to investigate expression of these proteins in the model used in this chapter. Moreover, tight junction reorganisation in response to IFN-γ+LPS has been shown to develop from 10 to 72 hours after stimulation,[51, 52] and would require study at later time-points than was done here.

IL-4+IL-13 and M2a conditioned medium

The effect of IL-4 and IL-13 on RPE barrier function has not been previously reported. However, studies using Calu3[347] and HUVEC cells[353] have shown that IL-4+IL-13 stimulation can lead to increased barrier permeability and decreased TEER. Consistent with this, stimulation of ARPE19 monolayers directly with IL-4+IL-13 or with M2a CM led to a decrease in TEER of 15-20% and accompanying disruption of the tight junction proteins ZO-1 and occludin. Although changes in ZO-1 and occludin could potentially explain these results, changes in ZO-1 and occludin did not affect TEER following IFN-γ+LPS or M1 CM stimulation. It would thus be interesting to also investigate expression of claudins in these monolayers.

IL-10 and M2c conditioned medium

Despite an apparent increase in immunoreactivity for ZO-1 and occludin, IL-10 and M2c CM stimulation of ARPE19 monolayers did not have an effect in TEER. Similar to IL-4+IL-13, no reports on the effect of IL-10 stimulation on retinal pigmented epithelial cells exist. However, IL-10 has been reported to antagonise IFN-γ induced changes in TEER in HUVEC cells by inducing increased expression of occludin.[53] It would be interesting to investigate whether IL-10 stimulation could rescue the decrease in TEER observed following stimulation of monolayers with IL-4+IL-13 and M2a CM, as increased levels of IL-10 could potentially explain the lack of effect of IFN-γ+LPS and/or M1 stimulation on TEER. Altogether these results reinforce the need to understand the consequence of subretinal inflammation on the RPE. Secretion of inflammatory mediators by subretinal macrophages could affect RPE barrier function and thus contribute to AMD pathology.

6.4.4 The effect of inflammation on the microenvironment

Increased levels of the pro-inflammatory cytokines IL-6 and IL-8 are present in the aqueous humour of patients suffering from AMD, but it is not clear what the source of these cytokines or their impact is.[354, 355] Secretion of pro-inflammatory cytokines by the RPE, including TNF-α, IL-1β, IL-6 and IL-8 can be induced by inflammatory stimuli such as TNF-α, LPS, IFN-γ and IL-4.[72] In addition, macrophages and microglia are well known for their ability to secrete high levels of cytokines.[94, 96] Therefore, RPE and subretinal microglia and/or macrophages could both be contributing to the heighten levels of cytokines in AMD eyes. In this study it is shown that both direct and indirect (macrophage CM) stimulation of ARPE19 monolayers apically can lead to increased concentrations of pro-inflammatory cytokines in the apical chamber. The increased levels of cytokines following direct stimulation with inflammatory stimuli are due to secretion by the RPE, as no other cell type is present. With the exception of VEGF, CM from MNS and all polarised macrophages contained elevated levels of all cytokines studied when compared to supernatant from NS ARPE19 monolayers. The increased levels of cytokines in the apical chamber following addition of macrophage CM were likely due to the fact that these cytokines were already present in the CM.

The role of pro-inflammatory cytokines in orchestrating inflammatory responses and their impact on the brain has been well characterised, in particular in response to LPS stimulation.[356] However, their effect on the retina and, in particular, RPE cell function is not well understood. Changes in the microenvironment could lead to altered homeostasis of the retina either by altering RPE physiology or by direct action on the photoreceptors. Stimulation of retinal pigmented epithelial cells with inflammatory stimuli, including LPS+IFN-γ, TNF-α and IL-1β has been shown to decrease TEER[54, 55] and, hence, alter barrier function. As detailed in 6.4.3. IFN-γ +LPS or M1 stimulation did not lead to any changes in TEER, despite the increased levels of pro-inflammatory cytokines (IL-6, TNF-α, IL-1β, IL-12 and IFN-γ), whereas IL-4+IL-13 and M2a stimulation which led to milder increases in cytokines (IL-6 or IL-6 and TNF-α, respectively) resulted in a significant decrease in TEER. IL-6 stimulation of HUVEC endothelial cells leads to decreased TEER due to reorganisation of tight junction.[53] It is possible that IL-6 mediates the disturbed tight junction distribution observed in IL-4+IL-13, IFN-γ+LPS, M2a and M1 CM stimulated monolayers. Increased levels of IL-10, shown to have a protective effect on TEER, in IFN-γ+LPS and M1 CM stimulated

monolayers could potentially explain the lack of effect on TEER. Nevertheless, it is still puzzling that IFN-γ+LPS or M1 CM stimulation of ARPE19 monolayers, resulting in increased levels of pro-inflammatory cytokines, including TNF-α and IL-1β do not lead to changes in TEER. This chapter's results thus suggest that pro-inflammatory cytokine concentration is not related to barrier function. The contrast of these results with the literature could possibly be explained by the high doses of stimuli used in other studies. With the exception of IL-8, M1 CM contained the highest concentration of all cytokines studied with 4.7ng/ml of TNF-α and 26pg/ml of IL-1β. These values are 20 times and 380 times lower, respectively, than those used for stimulation in the literature.[54, 55] IL-10 and M2c stimulation did not lead to any changes in cytokine concentration, with the exception of increased concentrations of IL-10, potentially due to residual IL-10 used for stimulation. This did not have an effect on TEER in this chapter's studies. As discussed above, it may be interesting to investigate whether adding IL-10 or M2c CM can rescue TEER in M2a stimulated ARPE19 monolayers.

The presence of high concentrations of cytokines could affect other RPE functions such as phagocytosis of photoreceptor outer segments, which could greatly affect retina physiology. With the exception of the anti-inflammatory cytokine TGF-β,[357] limited data on the effect of cytokines on phagocytosis of photoreceptors is available. TGF-β has been shown to increase phagocytosis of photoreceptor outer segments by the RPE.[357] It would be interesting to investigate whether pro-inflammatory cytokines would have an opposing effect on phagocytic function of the RPE. Reduced ability to phagocytose photoreceptor outer segments could lead to debris build up, which could contribute to AMD. In addition, cytokines could act directly on photoreceptors and hence alter retina homeostasis.

6.4.5 The effect of inflammation on AMD factors

Although the mechanisms involved in the pathogenesis of AMD are still unclear, some factors have been associated with the disease. In particular, polymorphisms in CFH increase the risk of developing AMD.[127, 140] Decreased levels of CFH at the RPE have been associated with AMD[336] and C. Luo et al[335] have shown that CFH expression by mouse RPE *in vitro* can be regulated by stimulation with M1 and M2b conditioned media. In contrast, no significant changes in CFH mRNA transcript levels were detected in this chapter's results, possibly due to species differences. These results indicate apical

stimulation of RPE with inflammatory stimuli does not affect CFH expression. Dysregulation of the complement system in AMD could occur due to other factors, such as genetic background,[140, 189, 326] ageing[8] and/or oxidative stress.[194] Further studies are required to fully understand the regulation and contribution of CFH and other complement components to AMD.

IL-8 has also been associated with AMD. A polymorphism in (A251T, A/A) leading to increased expression of IL-8[358] has been associated with AMD[359] and increased levels of this cytokine can be detected in the aqueous humour of patients suffering from exudative AMD.[354, 355] In the present study, the levels of IL-8 in the apical chamber were increased following stimulation with IFNγ+LPS or MNS, M2a and MIC CM. Surprisingly, M1 stimulation did not lead to increased levels of IL-8 in the apical chamber. However, the concentration of IL-8 in the basal chamber was increased to similar levels to those in the apical chamber after stimulation with MNS, M2a and MIC supernatants (Appendix II, A7). It is possible that M1 stimulation of ARPE19 monolayers leads to basal secretion of IL-8. Also, the disturbances in tight junction distribution discussed in 6.4.3 could lead to permeability changes, allowing IL-8 to cross from the apical to basal chamber. However, the changes in tight junction distribution after addition of M1 or M2a CM were similar, which makes the role of tight junctions less likely. Although IL-8 has been associated with AMD, the exact role of this cytokine in pathology of the disease is unknown. Nevertheless, IL-8 is known to be a potent inducer of angiogenesis.[358] Together, these results suggest that the presence of macrophages in the subretinal space could contribute to the pathogenesis of exudative AMD by increasing the levels of the pro-angiogenic cytokine IL-8.

Finally, changes to the levels of VEGF, thought to be the main mediator of angiogenesis in AMD,[167] were investigated. Only stimulation of monolayers with IFN-γ+LPS or M1 led to significant changes in VEGF concentration in the apical chamber. Whilst IFN-γ+LPS led to a small but significant increase, stimulation with M1 supernatants led to a two-fold increase in VEGF concentration in the apical chamber. The levels of VEGF were low in the M1 CM, indicating that some factor in the M1 CM is inducing VEGF section by the RPE. These results support the hypothesis that M1-polarised macrophages in the subretinal space contribute to progression into wet AMD by inducing increased levels of VEGF, thus contributing to pathological angiogenesis.

6.4.6 The effect of Avastin vs Lucentis on ARPE19 monolayers

The use of Avastin for the treatment of wet AMD has been associated with a higher risk of hospitalisation due to systemic complications and with increased incidence of intraocular inflammation.[275-277] The causes for the different side-effects associated with the two drugs are yet unknown.[278] Avastin, as a full length IgG could form immune complexes, [346] interact with FcγRs on macrophages/microglia and induce inflammation, which could potentially lead to side effects. In the present experiments macrophages were stimulated with immobilised Avastin or Lucentis for 48 hours, their supernatants collected and added to the apical chamber of ARPE19 monolayers. The results show neither CM from macrophages exposed to Avastin nor Lucentis induce any changes in barrier function of ARPE19 monolayers, but result in increased levels of all cytokines when compared to NS monolayers. Stimulation of macrophages with plate-immobilised Avastin and Lucentis led to an increase in the concentration of IL-1β and TNF-α when compared to non-stimulated macrophages, but the increase in TNF-α was substantially higher following stimulation with Avastin, suggesting differential activation of the macrophages by the two drugs. Due to the lack of an Fcγ fragment, Lucentis lacks the ability to interact with FcγRs and hence, activate macrophages. Thus, the increased levels of cytokines following stimulation with Lucentis were unexpected. The Lucentis used in these experiments was surplus drug from the clinic. It is possible that there was endotoxin contamination of the vial used to collect the Lucentis surplus used in these experiments.

Interestingly, addition of macrophage conditioned medium from macrophages stimulated with Avastin, but not Lucentis, led to a significant increase in VEGF in the apical chamber, despite the low levels of this growth factor in the CM. This suggests that activation of macrophages by Avastin can induce secretion of VEGF by the RPE. Triggering of VEGF secretion by macrophages and/or the RPE could be counterproductive for therapy. Increased cardiovascular complications are associated with the use of Avastin vs. Lucentis.[277, 278] It has been postulated that this is due to leaking of anti-VEGF therapy into the circulation and alteration of circulating VEGF levels affecting endothelial cells physiology.[278] Activation of macrophages by Avastin-VEGF immune complexes could result in higher levels of VEGF following Avastin therapy, potentially explaining the increased systemic side effects associated with the use of VEGF. The results in this chapter are inconclusive as to whether Avastin

stimulation would lead to more inflammation, however, they support the idea that the two drugs can have different effects on macrophage and/or RPE function and that therefore could affect the retina differently. A more thorough analysis of the effect of Avastin and Lucentis on inflammation in the retina is thus necessary.

6.4.7 Conclusion

In this chapter RPE barrier function is shown to respond differently to diverse inflammatory stimuli, with IL-4+IL-13 and M2a CM stimulation resulting in a pronounced decrease in barrier function. In addition, both stimulation with cytokines or conditioned medium of polarised macrophages can greatly change the microenvironment of the apical chamber. Particularly, stimulation with IFN-γ+LPS or M1 CM results in increased levels of several pro-inflammatory cytokines including IL-6, TNF-α and IL-1β and VEGF, which is strongly implicated in the pathology of wet AMD. Finally, stimulation of macrophages with Avastin or Lucentis was shown to lead to differential secretion of TNF-α by macrophages and VEGF by the RPE. These results reinforce the need to understand the effect of different inflammatory stimuli on RPE function.

Chapter 7:

General Discussion

Inflammation is thought to have an important role in the pathogenesis of AMD[10] and historically, the research on AMD has focused on the involvement of the complement cascade.[76] In recent years, however, macrophages have been identified as possible important immune cells in the pathogenesis of this disease.[10] Macrophages have been found in association with drusen,[174] geographic atrophy[174] and neovascular membranes,[174, 185, 201] but it remains unclear how they could contribute to pathology.[10] Patients suffering from AMD have high titers of circulating autoantibodies against retinal antigens[11, 12, 15, 16] and although IgG accumulates in the eyes of these patients,[13] the involvement of autoantibodies in AMD pathology remains unresolved. Elucidating the biological effects and mechanisms of immune complex-mediated responses in the retina may contribute to the understanding of AMD pathology and provide insight how therapeutic antibodies used to treat this disease may impact retinal physiology. With this in mind, the main aim of this thesis was to investigate whether IgG immune complex-FcγR interactions may contribute to pathogenesis of AMD and impact on efficacy and/or safety of immunotherapy.

In this thesis it was shown that immune complex deposition in the mouse retina leads to a transient, yet robust inflammatory response that is dependent on the presence of activating FcγRs, particularly FcγRI and FcγRIII, but not on FcγRIV. It was also shown that C1q, and hence activation of the classical complement cascade, is not essential for initiating antibody mediated inflammation in the retina. Immune complex deposition and increased numbers of $CD45^+$ immune cells expressing FcγRIIa and FcγRIIb were found in the choroid of early AMD donors, suggesting a role for immune complex responses in the early stages of AMD pathology. Additionally in the retina of wet AMD donor eyes the microglia expressed FcγRI, FcγRIIa and FcγRIIb, which could interact with therapeutic antibodies and hence impact on efficacy and/or safety of therapy. Using a human cell culture system, it was shown that macrophage polarisation can differentially impact on ARPE19 TEER and VEGF secretion, suggesting macrophage activation could contribute to AMD pathology by altering RPE function. Finally, it was found that activation of macrophages by Avastin (bevacizumab), but not Lucentis (ranibizumab), leads to enhanced secretion of VEGF by ARPE19 cells, which may help explain the different side effects associated with the use of the two drugs.

7.1 Immune complex-mediated inflammation in the mouse retina

In Chapter 3 the reverse Arthus reaction was applied to the retina to investigate the effect of immune complex deposition and if it may lead to AMD-like pathology. In peripheral organs the Arthus reaction results in a rapid inflammatory response which is resolved by 24 hours and characterised by platelet, neutrophil and mast cell recruitment (peaking at 2-4 hours), oedema and haemorrhage (peaking at 6h-8h) and subsequent tissue necrosis.[279, 290, 293, 303, 312] Contrastingly, immune complex formation in the retina resulted in a delayed inflammatory response that resolved by 14 days after OVA challenge and was characterised by activation of microglia and recruitment of myeloid and lymphoid cells, including $CD11b^+$ cells with a macrophage morphology and $CD4^+$ T cells but not neutrophils, peaking at 3-7 days. This delay is possibly due to the presence of an intact BRB, restricting the access of IgG and/or immune cells to the retina. Supporting this, immune complex formation in the brain, protected by a BBB, leads to a similarly delayed response.[282] FcRn may also play a role. It is thought that FcRn expressed by endothelial cells in the blood vessels of the retina transports IgG from the retina into the blood stream.[240] An increase in OVA-specific IgG in the retina following intravitreal injection of OVA may lead to saturation of the FcRn and hence reduced drainage of the IgG and increased immune complex formation. Additionally, pro-inflammatory stimuli such as IFN-γ have been shown to induce reduced expression of FcRn.[360] Although expression of IFN-γ following immune complex formation was not investigated, immune complex-mediated inflammation in the retina could potentially lead to reduced expression of FcRn and hence, to accumulation of IgG.

In the lung Arthus reaction, the tissue resident macrophages, alveolar macrophages, are essential to induce neutrophil infiltration through FcγR-mediated secretion of C5a, and depletion of macrophages with clodronate liposomes results in inhibition of the lung inflammatory response.[303] In Chapter 3, no C5a or its receptor, C5R, were detected by qPCR but it was not clear whether this was due to a technical issue, as discussed in 3.4.2. Stimulation of FcγRs by immune complexes also leads to secretion of MCP-1[295] and MCP-1 mRNA transcript levels in the retina were increased by 18-fold 24 hours after OVA challenge. FcγR-mediated MCP-1 secretion by retinal microglia may mediate recruitment of the $CD11b^+$ cells observed by 3 and 7 days. Depletion of

peripheral macrophages with clodronate liposomes (Appendix I, A6) resulted in a non-significant, yet substantial reduction in the number of infiltrating $CD11b^+$ and $CD45^+$ cells in the retina 7 days after intravitreous OVA challenge. This suggests a role for infiltrating macrophages in potentiating further recruitment of myeloid cells. Although further studies are required to elucidate the mechanisms involved, the results from these experiments suggest that retinal microglia and macrophages recruited from the circulation are both important in immune complex responses in the retina. The role of the RPE in the recruitment of $CD11b^+$ and $CD45^+$ immune cells in this model remains to be studied.

Activation of retinal microglia has been implicated in AMD.[10] Immune complex formation in the retina resulted in increased expression of FcγRs and MHC II, suggesting activation of these cells, but it did not lead to any detectable functional changes to photoreceptors (studied by ERG) or to the development of AMD-like pathology (studied by fundoscopy and fluorescent angiography). Although further optimisation of these techniques may be required, this indicates that transient accumulation of immune complexes in the retina is not sufficient to induce functional changes. Hollyfield et al successfully induced AMD-like features such as RPE atrophy in mice by immunisation against oxidised protein adducts (i.e. CEP-MSA). These authors show that IgG and C3 accumulates in the choroid/RPE, but not retina, inducing pathology in ageing mice.[194, 196] Restriction of immune complex deposition in the retina by the presence of a BRB may be an important consideration when evaluating the role of retinal auto-antibodies in the pathology of AMD. In a pilot study (Appendix I, A5), the presence of autoantibodies against retinal antigens did not induce AMD-like changes such as drusen-like deposits and photoreceptor degeneration in 18-month old mice. This suggests the presence of circulating auto-antibodies alone is not sufficient to induce changes in the retina. It is likely that changes to the choroid/RPE (e.g. accumulation of debris and/or oxidised proteins) induced by aging and/or AMD-risk factors such as oxidative stress, may allow antibodies to gain access to their antigen at the choroid/RPE, as is the case in the CEP-MSA model.[194, 196] These would then mediate damage by inducing microglia activation and recruitment of myeloid cells.

Consistent with previous literature,[300, 301] the results in Chapter 4 show that while C1q is redundant for immune complex-induced activation of microglia and recruitment of myeloid cells, the presence of activating FcγRs is essential. The absence of activating

FcγRs in the microglia of $\gamma^{-/-}$ mice prevents FcγR-mediated activation of these cells by immune complexes, which could result in inhibition of MCP-1 expression by the microglia, possibly explaining the inhibition of myeloid cell recruitment.[288, 295] These studies are the first to show that immune complex formation in the retina results in a local inflammatory response that critically depends on the interaction with effector cells expressing Fcγ receptors.

Particularly, FcγRI and FcγRIII were shown to be necessary for the development of the immune complex-mediated responses in the retina. While the indispensable role of FcγRIII in most models of immune complex-mediated injury is well accepted,[228, 310, 361] FcγRI is generally thought to have limited contribution due to saturation by monomeric IgG.[224] There was a clear requirement for FcγRI in immune complex-induced inflammation in the retina, possibly due to this receptor not being saturated, as discussed in section 4.4.2. Aside from the potential to interact with immune complexes, FcγRI on microglia may potentially interact with monomeric IgG, which enhances endocytosis and TNF-α secretion.[102, 362] The human FcγRI resembles its mouse homologue in its high affinity for monomeric IgG (IgG1, IgG3 and IgG4 in humans).[363] This may be important in the context of AMD as human FcγRI, expressed by retinal microglia, could interact with monomeric IgG in exudative AMD or with monoclonal antibodies used for therapy (mostly of the IgG1 subclass) potentially inducing inflammation and, subsequently, retinal damage.

The collection of studies in these chapters argues against a role for immune complex formation in the retina in the pathogenesis of AMD. Instead accumulation of immune complexes at the choroid/RPE may be important in early AMD. However, understanding the kinetics and mechanisms of immune complex-mediated inflammation in the retina may be useful, as immune complexes may form in the retina in exudative AMD and following immunotherapy. Although tissue-specific mechanisms of immune complex-mediated inflammation have been previously reported in the lung[303, 312] and brain,[282] the studies in Chapters 3 and 4 are the first to show the retina responds to immune complexes in a tissue-specific manner, characterised by retinal microglia and macrophage activation, and dependent on FcγRI and FcγRIII.

7.2 Immune-complex and Fcγ receptors in the pathology of AMD

7.2.1 Early AMD

A similar immune system and ease of genetic manipulations have made mice an ideal model to study immune-related human diseases.[364] Although structurally similar, the mouse and human retina have several differences. Importantly, the mouse retina lacks a macula.[2] Therefore it is essential to validate findings from mouse models in human tissue. In Chapter 5 evidence for immune complex deposition and subsequent inflammation in early AMD was investigated by histology. While IgG or C1q deposits in the choroid of AMD patients have been previously described,[13, 14, 40] the studies in this thesis are the first to demonstrate co-localisation of IgG and C1q in the choroid of early AMD donor eyes but not age-matched healthy control eyes, suggesting the involvement of immune complex deposition in the choroid, but not retina, in early AMD pathology.

Immune complexes can induce inflammation both via activation of the classical complement cascade and through FcγR-mediated activation of effector function.[217] Expression of complement proteins in the choroid of AMD patients has been extensively studied, with evidence to support the presence of complement proteins specific to the alternative pathway (CFH)[78, 336] , the classical pathway (SERPING1, IgG, and C1q),[188, 336] and common to all pathways such as C3, C5 and MAC amongst others.[14, 149, 152, 188, 336] In Chapter 5, co-localisation of IgG and MAC at the choroid suggested activation of the complement cascade by the classical pathway. This could lead to damage of the choroid and contribute to AMD pathology. Interestingly, depletion of CFH in a mouse model of GMNP results in exacerbated immune complex deposition in the kidney glomeruli,[365] demonstrating the ability of CFH to regulate the classical arm of the complement cascade. In humans, the Y402H (H/H) polymorphism in CFH results in increased MAC deposition in the choroid of early AMD, when compared to early AMD eyes without this high risk polymorphism.[326] Whilst this may be due to overactivation of the alternative complement cascade,[74] it is tempting to speculate that the 420H/H CFH polymorphism could also contribute to AMD pathology by CFH-enhanced immune complex deposition and subsequent tissue damage.

In Chapter 5 a significant increase in the numbers of $CD45^+$ cells expressing FcγRIIa in the choroid was detected. Crosslinking of activating FcγRs, including FcγRIIa, leads to activation of a signalling cascade (Figure 1.14.) culminating with activation of transcription factors such as JNK, MAPK and p38, and, importantly with Ca^{2+} release from the endoplasmic reticulum (ER).[17] The latter enables activation of effector functions such as degranulation, ADDC and phagocytosis.[17] Using humanised $\gamma^{-/-}$ mice expressing FcγRIIa, it has been demonstrated that this receptor is sufficient to initiate the Arthus reaction in the skin,[366, 367] systemic anaphylaxis,[367] arthritis[368] and immune complex-mediated airway inflammation.[367] Additionally, in Chapter 4 it was shown that FcγRIII, the mouse equivalent of FcγRIIa,[363] is essential for the development of immune complex-mediated inflammation in the mouse retina. It is thus possible that activation of FcγRIIa by immune complexes in the human choroid could lead to inflammation and, hence, contribute to the pathogenesis of AMD.

Conflicting with this hypothesis, $CD45^+$ cells expressing FcγRIIb, the only inhibitory FcγR, were also significantly increased in the choroid of early AMD donor eyes. Crosslinking of FcγRIIb by immune complexes triggers activation of phosphatases, ultimately resulting in inhibition of Ca^{2+} release from the ER (Figure 1.14.).[17] Thus cross-linking of FcγRIIb by IC can counteract the effect of FcγRIIa crosslinking and hence result in inhibition of effector function.[17] Although there are significant differences between the mouse and human FcγR systems, findings from mouse models have been successfully translated into humans.[363] The results in Chapter 3 show an increase in the number of cells expressing all FcγRs, including FcγRII (equivalent of FcγRIIb in human) after immune complex deposition in the retina. Despite the high numbers of $FcγRIIb^+$ cells, a robust inflammatory response was still evident, likely due to upregulation of activating FcγRs overcoming the FcγRII-mediated inhibition.[224] In human AMD, immune complex-mediated inflammation could potentially occur through engagement of FcγRIIa, despite the increase in $FcγRIIb^+$ cells. However, more sensitive assays (e.g. flow cytometry) would have to be performed to determine the ratio of activating vs inhibitory FcγRs and thus confirm this hypothesis.[224] Together these novel findings suggest that immune complex mediated inflammation at the choroid could contribute to the pathology of early AMD through activation of the complement cascade and crosslinking of FcγRIIa on effector cells.

Degranulation of mast cells and neutrophils is a key event in immune complex-mediated tissue injury.[367, 368] In Chapter 5 no neutrophils were detected in human eye tissue, but mast cells were detected in the choroid of early AMD eyes and, surprisingly, in the choroid of healthy controls. P. McMenamin and E. Polla recently reported that mast cells are present in healthy choroid of most vertebrates, including fish, mice and humans,[369] suggesting a homeostatic role for these cells. Yet, A. Takeda et al have shown increased expression of CCR3 in the choroid of AMD eyes when compared to healthy controls. CCR3 is a receptor involved in eosinophil and mast cell chemotaxis,[327] supporting the idea that mast cells may be involved. Because mast cells constitutively express FcγRIIa,[370] they have the potential to interact with immune complexes deposited in the choroid of AMD patients. The antibody used to detect mast cells in Chapter 5 did not differentiate between "resting" and degranulating mast cells. Investigating whether there is mast cell degranulation in the choroid of early AMD patients, e.g. by staining with toluidine blue, may be an interesting future direction as release of proteases and reactive oxygen species by degranulating mast cells could be a mechanism of damage of the choroid in early AMD.

FcγRIIa expression by macrophages has been shown to be important in mediating immune complex-induced tissue injury[371] and $CD45^{+}Fc\gamma RIIa^{+}$ cells with macrophage-like morphology were observed in the choroid of early AMD donors. Activation of macrophages by immune complexes can lead to secretion of reactive oxygen species and pro-inflammatory cytokines such as IL-6 and IL-1β,[263] which are increased in the circulation and drusen of AMD patients.[372] In Chapter 6 stimulation of human macrophages with large heat aggregated gamma-globulins (HAGG), as a model of soluble immune complex, did not lead to changes in expression of activation markers (CD11b, CD40 ,FcγRI, IIa, IIb and III; Appendix II, A9), or in secretion of cytokines (IL-1β, TNF-α, IL-6, IL-12, IFN-γ and IL-10), suggesting failure to activate macrophages. C.A. Ambarus et al recently showed that stimulation of macrophages with HAGG is not sufficient to induce macrophage activation as measured by changes in expression of CD80, CD14, FcγRI, IIb and III, and secretion of TNF-α, IL-6 and IL-10,[263] which could explain the results in Chapter 6. Supporting this, stimulation with immobilised IgG1 (Avastin) as a model of insoluble immune complexes led to activation of macrophages as measured by increased levels of IL-6, IL-1β and TNF-α. Immobilised $F(ab)_2$ fragments (Lucentis) did not induce this response, providing

evidence for a role of FcγRs. Co-localisation of IgG and C1q in the lumen of choriocapillaris in Chapter 5 suggests immune complexes in early AMD may be immobilised. Activation of macrophages by immobilised immune complexes at the choroid could contribute to AMD pathology by damage of the choriocapillaris or by influence of pro-inflammatory cytokines on the RPE.

It is unclear whether AMD pathology starts at the RPE or the choroid, with most authors supporting the idea that age-related and/or oxidative damage to the RPE is an initiating event.[74] Consistent with this, conditional inhibition of VEGFA secretion by the RPE in mouse, leads to rapid death of the endothelial cells of the choriocapillaris and eventually to development of AMD-like RPE atrophy.[170] However, studies in human tissue favour the idea that pathology may start at the choroid. Mullins et al demonstrated that cell death of the choriocapillaris endothelium is associated with early AMD, before any RPE pathology is observed.[152] Moreover, analysis of transcriptional differences between healthy and early AMD donor eyes show that most transcriptional changes associated with early-AMD occur in genes associated with blood vessel homeostasis (including thrombomodulin, endothelial cell-specific chemotaxis regulator and $ICAM_2$), further supporting early pathological changes in AMD may occur at the choriocapillaris.[373] The results from Chapter 5 are consistent with the idea that pathology may start in the choroid. Immune complex deposits found in the choriocapillaris would initiate the complement cascade or interact with FcγRs expressed by immune cells in the choroid to mediate damage of the choriocapillaris. It is possible that initial damage to these blood vessels (e.g. immune complex-mediated necrosis of endothelial cells[279]) would result in altered function of the RPE (e.g. due to hypoxia), which could result in decreased VEGF secretion by the RPE and further damage to the choriocapillaris.

7.2.2 Late AMD

In contrast to early AMD where macrophages were predominantly present in the choroid, the presence of macrophages/microglia has been described in the retina of patients suffering from wet AMD by several research groups[174, 185, 201] and was confirmed in this thesis' results. Although much interest exists on the contribution of these cells to the pathology of AMD, only two studies have tried to phenotype macrophage/microglia associated with AMD lesions in humans. X. Cao et al detected an

increase in mRNA transcript and protein level of the M1 chemokine, CCL11 in the choroid and subretinal space of wet AMD, when compared to healthy controls[201] and S. Cherepanoff showed expression of iNOS by AMD-associated macrophages/microglia.[174] These results led both authors to suggest pro-inflammatory M1 macrophages are associated with wet AMD. The results in Chapter 5 show microglia in wet AMD express FcγRI, FcγRIIa and FcγRIIb, which are expressed by M1- and immune complex activated macrophages.[263] Although it is possible to speculate these cells may contribute to AMD pathology by inducing inflammation, further studies are necessary to fully understand how macrophage activation can affect retinal physiology.

The RPE performs a variety of important functions for retinal homeostasis, including maintenance of BRB function, secretion of growth factors (including VEGF) and regulation of immunity.[37] Surprisingly, despite previous reports in the literature, stimulation of retinal pigmented epithelial cells with pro-inflammatory stimuli (IFN-γ+LPS) or supernatants from M1 polarized macrophages did not lead to significant changes in TEER. However, it led to a significant increase in the concentration of pro-inflammatory cytokines in the apical chamber (present in the macrophage CM and ARPE19 cells) and interestingly to a significant increase in secretion of VEGF by ARPE19 cells. Increased VEGF secretion by the RPE due to a pro-inflammatory microenvironment could result in abnormal blood vessel formation. This is consistent with the hypothesis that a shift from M2 to M1 macrophages may contribute to progression into wet AMD.[201] Contrastingly, studies in a mouse model of laser-induced CNV show that M2a macrophages lead to more severe CNV lesions.[215] In Chapter 6, stimulation of ARPE19 cells with M2a supernatant did not lead to any changes in VEGF secretion by the RPE but it did lead to compromised barrier function. In the laser-induced model of CNV, a laser is used to introduce a break in the BRB, through which new blood vessels quickly grow. The laser lesion is an acute insult which leads to recruitment of macrophages and neutrophils from the periphery.[374] M2 macrophages could contribute to increased lesion size in this model by increasing BRB permeability, thus facilitating macrophage and neutrophil infiltration in response to laser injury. However, chemokines secreted in response to laser-induced tissue injury (e.g. MCP-1[203]) most likely are key in allowing immune cell infiltration.

There is little evidence from human studies that M2a macrophages could contribute to AMD pathology. Firstly, no histopathological data exists that shows evidence of M2a markers (e.g. Arg1, Ym1 and CCL22) in human AMD.[201] Secondly, no strong association between diseases such as asthma, where M2a macrophages predominate, has been found.[375] In fact, allergy, dominated by the presence of M2a macrophages in the affected tissue, has been shown to be protective against incidence and progression of AMD.[376] In contrast, a polymorphism in the IL-4 gene (T590C, T/T) resulting in increased serum levels of IL-4 has been shown to increase the risk of developing AMD in a small Taiwanese population.[377] In Chapter 6 it was shown IL-4 leads to a decrease in TEER of ARPE19 monolayers. Increased levels of IL-4 could lead to increased permeability of the BRB and hence be permissive to leukocyte infiltration in the retina, possibly contributing to AMD. These observations are interesting as macrophage polarisation could be a target for therapy. Immune modulators (i.e. TLR agonists) skewing macrophage activation are already in clinical trials or used for therapy in diseases such as asthma.[378] Reversing M1 polarisation in the choroid and/or subretinal space locally may be an interesting strategy for therapy in wet AMD.

7.3 Immune complex, Fcγ receptors and immunotherapy for AMD

An important aspect of this thesis is the potential for therapeutic antibodies, including those used to treat wet AMD, to interact with FcγRs in the retina. As a whole IgG1 molecule, Avastin, but not Lucentis, has the potential to interact with FcγRs. This could mediate the incidence of undesirable side effects. In line with this, the use of Avastin vs Lucentis for the treatment of AMD is associated with a significant higher risk of developing intraocular inflammation[275, 276] and other complications such as retinal bleed or detachment.[277] In Chapters 3 and 4 it was shown that immune complex formation in the mouse retina leads to a robust inflammatory response that is dependent on the presence of FcγRs, whilst in Chapter 5 we show that FcγRI and FcγRIIa are present in the retina of human wet AMD. It is plausible that Avastin-VEGF immune complex formation in the retina of wet AMD patients, could lead to intraocular inflammation, by interaction of these immune complexes with FcγRs expressed by microglia.

Because Avastin is a monoclonal antibody and VEGF a monomeric protein, it is unlikely that soluble Avastin-VEGF immune complexes form *in vivo*, which could be a limiting factor in induction of FcγR-mediated inflammation and/or other FcγR-mediated side effects.[17] The formation of Avastin-VEGF complexes with heparin expressed by platelets *in vivo* is sufficient to trigger FcγRIIa activation.[379] Endothelial cells express heparin sulphate, an endogenous heparin-like substance,[380] and hence, Avastin-VEGF complexes could similarly form on these cells. Supporting this, intravitreous injection of Avastin in monkeys results in immune complex formation in the choroid.[346] This could lead to activation of FcγRIIa on immune cells (e.g. microglia and macrophages), potentially mediating Avastin-associated side effects such as inflammation and vascular death.[275, 278] Recent studies have shown that both the mouse and human FcγRI are capable of mediating mAb-induced immunotherapy for experimental melanoma, indicating mAb interaction with FcγRI induces effector functions such as ADDC, phagocytosis and release of pro-inflammatory cytokines.[361, 381] FcγRI could thus also contribute to Avastin-associated side effects. Additionally, monomeric Avastin could bind to the high affinity FcγRI, leading to increased levels of TNF-α.[362] The increased incidence of side effects associated with Avastin vs Lucentis such as increased inflammation could thus be mediated by interaction with FcγRI and/or FcγRIIa expressed by retinal microglia.

Increased incidence of thromboembolic events and vascular death has also been associated with the use of Avastin vs Lucentis for treatment of wet AMD.[277, 278] Interestingly, in Chapter 6 it was demonstrated that conditioned media from macrophages stimulated with plate-immobilised Avastin, led to a two-fold increase in VEGF secretion by ARPE19 cells, an effect that was not observed following stimulation of macrophages with plate-immobilised Lucentis. These results suggest that activation of macrophages by Avastin immune complexes may indirectly lead to secretion of VEGF by ARPE19 cells, possibly by release of mediators such as IFN-γ and TNF-α. Dysregulation of VEGF secretion by the RPE has been show to greatly affect the physiology of the choriocapillaris,[170] hence, stimulation of VEGF secretion by Avastin activated macrophages, may partially explain the increased incidence of vascular side effects associated with the use of Avastin vs Lucentis. Collectively, these results highlight the urgency of understanding antibody mediated responses in the retina as it may greatly impact our understanding of immunotherapy in the eye.

7.4 Future directions

The results described in this thesis show that whilst immune complex formation in the mouse retina leads to robust neuroinflammation, it does not lead to AMD-like pathology and that in human early AMD, immune complexes are present in the choroid, but not in the retina. This poses the question: does immune complex mediated-inflammation initiated at the choroid lead to AMD-like pathology in mice? The choroid is a peripheral tissue and, therefore, the response to immune complex deposition will likely be different to that of the retina. For example, neutrophils would be able to access immune complexes in the choroid, while it was shown in Chapter 3 that they do not do so in the retina. Additionally, the presence of mast cells, macrophages expressing activating receptors (in contrast to the downregulated microglia) and complement proteins would likely lead to a more typical peripheral inflammatory response to immune complex formation. This could subsequently lead to damage of the choroid and RPE and contribute to pathogenesis of AMD. Investigating this hypothesis is an important future direction that may clarify the involvement of immune complex and FcγRs found in the choroid of early AMD in pathology of the disease.

In view of this a pilot experiment was performed where OVA was injected at the back of the eye, to target the choroid of OVA-sensitised mice. Eyes were collected 3 days after challenge and examined histologically for immune complex formation and inflammation. This protocol resulted in immune complex deposition in the choroid and in a local inflammatory response that did not propagate to the inner layers of the retina but did involve the RPE and the outer segments of the photoreceptors, similar to early AMD (Figure 7.1.). Characterising the kinetics of immune complex formation in the choroid and associated inflammation, the cell type involved and functional consequence may advance our understanding of the pathological mechanisms involved in early AMD.

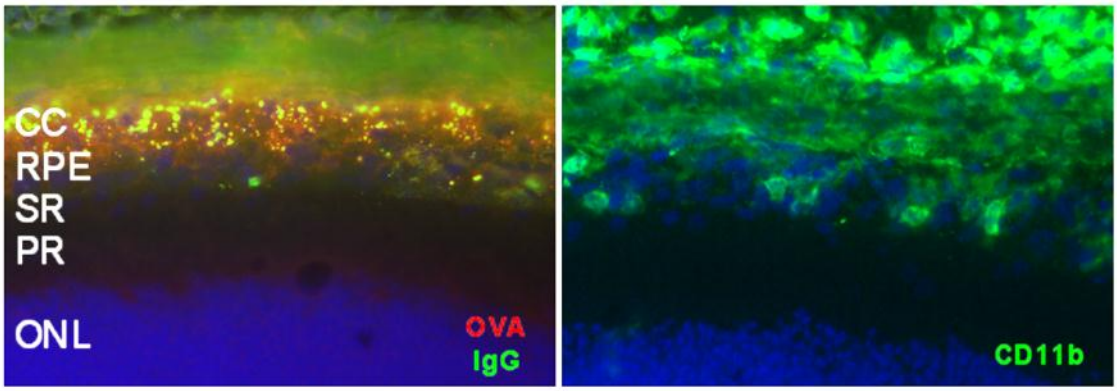

Figure 7.1. Immune complex formation at the choroid leads to a localised inflammatory response that does not affect the inner retina.

CC – choriocapillaris, RPE – retinal pigmented epithelium, SR- subretinal space, PR – photoreceptors, ONL – outer nuclear layer.

Further, it would be interesting to investigate if and how immune complex formation in the choroid and outer retina may induce functional changes to the retina. As the mouse retina is predominantly composed of rods, rather than cones, scotopic ERGs were performed following immune complex formation in the retina, but no reliable results were obtained (Appendix I, A4). Behavioural tests such as the vision augmented locomotion[382] and the optokinetic head-tracking[383] could be used to assess retinal function following immune complex formation. The former consists of leaving mice in a running wheel where they will move to baseline levels, a behaviour that is increased by 15% in the presence of dim light. This increase is inhibited in the presence of visual deficits.[382] The optokinetic tracking measures acuity and sensitivity to contrast in mice. Briefly, mice are placed in an arena in the presence of a moving panel with sine wave gratings of various spacial frequencies and/or contrasts; as long as they can see, mice will move their heads to track the gratings. Thus head movement can be taken as a measurement of acuity and/or contrast.[383] Assessing functional changes in response to immune complex formation in the choroid and/or outer retina could clarify how immune complex deposition in AMD may lead to retinal degeneration.

Another important aspect to keep in mind for future experiments is the importance of chronicity for the development of AMD-like features in animal models. In the model developed in Chapter 3, no functional alterations were detected despite the severe inflammatory response. The techniques used for functional analysis (fundoscopy, fluorescein angiography and ERG) had only recently been introduced in our lab, thus the lack of detectable functional alterations was possibly due to technical problems as

previously mentioned. However, the transient nature of the immune complex responses in this model may also provide an explanation for this. For example, the CEP-MSA immunisation model (section 1.5.2.) can take up to 12-24 months after immunisation before any pathological changes are observed. [196, 209] Similarly, in the *CCL2*$^{-/-}$,*CCR2*$^{-/-}$ and *CX3CR1*$^{-/-}$ mice AMD-like pathology, measured as RPE atrophy and formation of drusen-like deposits is only observed from 12 to 18 months of age,[143, 171, 203, 210] highlighting the importance of chronic immune stimulation for the development of AMD-like pathology. Intravitreous delivery of OVA was only performed once per mouse. Introducing a slow-release device in the choroid of OVA sensitised mice, will deliver OVA at the back of the eye in a prolonged manner. This will result in a chronic presence of immune complex responses which may subsequently lead to more prolonged changes in the retina.

The results from this thesis also highlighted the importance of FcγRs in mediating immune complex responses. Studying the involvement of FcγRs in immune complex-mediated inflammation initiated in the choroid using *γ*$^{-/-}$, *FcγRI*$^{-/-}$, *FcγRIII*$^{-/-}$ and *FcγRIV*$^{-/-}$ mice will also be important. Additionally, studying human AMD tissue will be essential to understand the involvement of FcγRs in AMD. An important aspect of this will be to investigate the predominance of IgG subclasses in early AMD eyes. Due to the differential affinity of IgG subclass for particular FcγRs and/or complement this will be important to understand the involvement of specific FcγRs and C1q in AMD pathology. In Chapter 5 high levels of IgG were present in the choroid of healthy and early AMD donors, but C1q deposition only occurred in early AMD eyes. Interestingly, a single study has shown that in a group of 17 patients with early AMD, 12 had anti-retinal IgG3 autoantibodies, which have high affinity for C1q.[17, 384] A change in subclass ratio in early AMD vs healthy controls may explain the differences in C1q deposition between the two groups.

Further, polymorphism in the genes coding for FcγRIIa (H131R, H/H) and FcγRIIIa (V158F, V/V) have been associated with incidence and progression of immune complex-mediated diseases, including rheumatoid arthritis and SLE.[271] It would thus be interesting to investigate whether these polymorphisms are associated with incidence of AMD or progression into dry or wet late AMD. The FcγRIIa H131R and FcγRIIIa V158F polymorphisms result in increased ADDC and phagocytosis of mAb-coated cancer cells and have also been implicated in the efficacy of anti-cancer mAb

therapy.[272] Avastin may potentially interact with FcγRs to mediate unwanted side effects such as intraocular inflammation. Hence, it would be interesting to investigate whether increased incidence of side-effects associated with Avastin may co-relate with FcγR polymorphisms.

Finally, in Chapter 4 it was demonstrated that FcγRI has a prominent role in immune complex-mediated inflammation in the retina. Due to the ability of this receptor to bind to monomeric IgG, this could impact on immunotherapy. It would be interesting to investigate whether intravitreous injection of monomeric IgG would be sufficient to induce microglia activation and myeloid cell recruitment, as seen following immune complex deposition, and whether this may be abrogated in *FcγRI*$^{-/-}$. Moreover, using humanised $\gamma^{-/-}$ mice, expressing only human FcγRI, Avastin or Lucentis could be injected intravitreously to study whether the two may lead to differential biological effects *in vivo*, similar to *in vitro* as was observed in Chapter 6. A good understanding of the role of individual FcγRs in immune complex-mediated inflammation in the retina may help to better tailor antibody therapies for retinal diseases.

7.5 Summary

Ageing is the biggest risk factor associated with incidence of AMD. Several age-related changes to the eye occur, including thickening of the BrM, thinning of the choroid and drusen formation.[6] In addition to ageing, dysregulation of the innate immune system (particularly complement)[40, 171] and oxidative stress[127, 132] have also been associated with AMD. In this thesis, the role of immune complex-mediated inflammation on AMD pathology was investigated. It remains unclear whether antibodies have a causative role in AMD or are merely a consequence of the disease. Nevertheless, the results in this thesis clearly show that immune complex deposition in the mouse retina can lead to a severe inflammatory response characterised by microglia activation and recruitment of macrophages and that components of this response are present in the choroid of human early AMD. Immune complex deposition was apparent in the lumens of the choriocapillaris with accompanied increase in the number of immune cells expressing FcγRs (FcγRIIa and FcγRIIb), which were shown to be essential for mediating immune complex responses in the mouse retina. Evidence for immune complex-mediated inflammation in the choroid, but not retina, of early AMD patients is indicative of the disease starting at the choroid. Compromised oxygen supply due to age-related changes

to the choroid and BrM combined with damage of the aged choroid by immune complex-mediated inflammation or oxidative stress could lead to hypoxia and hence damage and/or degeneration of the RPE, contributing to pathology of AMD (Figure 7.2). The work in this thesis shows for the first time that immune complex-mediated inflammation may contribute to pathogenesis of AMD.

The work of this thesis also resulted in the novel description of the role of individual activating FcγRs in immune complex-mediated responses in the mouse retina. Particularly, evidence was provided that FcγRI may play a more predominant role in antibody-mediated responses in the retina than what has been previously described for organs such as the skin, lung and kidney.[224, 227] Although further studies are needed to confirm this, this is an exciting finding that may greatly impact on our understanding not only of immune complex-mediated pathology in the retina but also immunotherapy in ocular disease. FcγRIII was also important in mediating immune complex-induced inflammation in the retina. The human homologues for these receptors, FcγRI and FcγRIIa, respectively, were abundantly present in the retinae of wet AMD patients, where they could interact with autoantibodies in areas of haemorrhage or with monoclonal antibodies used for therapy to induce inflammation.

Collectively the results in this thesis support the hypothesis that immune complex-mediated inflammation and FcγRs may contribute to the pathology of AMD and that interaction of monoclonal antibodies with FcγRs may impact on efficacy and/or safety of immunotherapy. Further studies will be essential to understand the consequence of immune complex deposition in the choroid in early AMD.

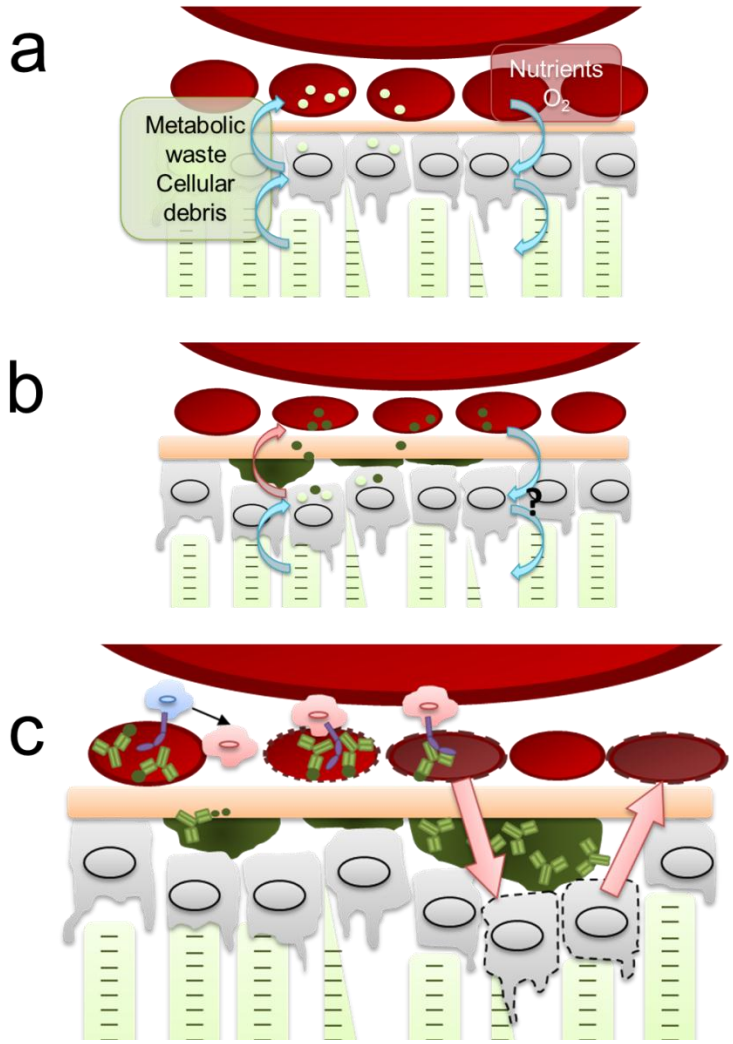

Figure 7.2. An integrated model of the contribution of immune complex-mediated inflammation in the choroid to the pathogenesis of AMD.

(a) The choroid supplies most of the oxygen needed for the outer retina. In a healthy eye, the RPE mediates transport of nutrients from the choroid to the retina and of debris from the retina to the choroid. **(b)** Age-related changes to the retina such as decrease of choroidal density and increase in the thickness of BrM likely compromise transport of debris out of the retina, leading to build up of debris in the subretinal space and RPE/choroid. These changes might also compromise nutrient and oxygen supply to the retina, which could potentially lead to dysfunction of the RPE. **(c)** In early AMD antibodies deposit in the lumens of the choriocapillaris and cells expressing FcγRIIa can be seen in close proximity to these blood vessels. Activation of effector function via cross linking of antibodies with FcγRs on these cells may lead to damage of the blood vessels. This could subsequently lead to damage of the RPE due to hypoxia. In turn, damage to the RPE could result in further damage to the choriocapillaris due to decreased levels of VEGF, which could eventually lead to progression into late stage AMD.

Appendices

Appendix 1

A1. Modelling immune complex-mediated responses in the retina

To develop the model of immune complex-mediated inflammation in the retina C57BL/6 mice were first used. Mice were immunised against OVA as described in section 2.1.2. To induce immune complex deposition in the retina, following immunisation with OVA, 10μg of OVA were injected intravitreously. Mice were culled 3 days after injection and the tissue analysed for immune complex formation (Figure 0.1). Immune complexes were difficult to detect in C57BL/6 mice after OVA challenge, therefore the protocol was repeated using BALB/c mice, known to mount stronger humoral responses.[385]

Immune complex formation was assessed by immunohistochemical detection of OVA (red) and IgG (green) (Figure A1). Where OVA and IgG co-localised (yellow) was considered to be an immune complex (Figure 0.1.a arrows). Challenge with 10μg of OVA using C57BL/6 mice resulted in a small amount of immune complexes forming in the subretinal space (Figure A1 a arrows). Using BALB/c mice, intravitreous challenge with 10μg of OVA resulted in more pronounced immune complex formation (Figure A1 a arrows). To investigate whether this could be due to differences in the humoral response to OVA, the titers of anti-OVA IgG were measured in the serum of immunised mice from the two different strains. BALB/c mice had 10 times higher levels of anti-OVA IgG when compared to C57BL/6. (Figure A1 b)

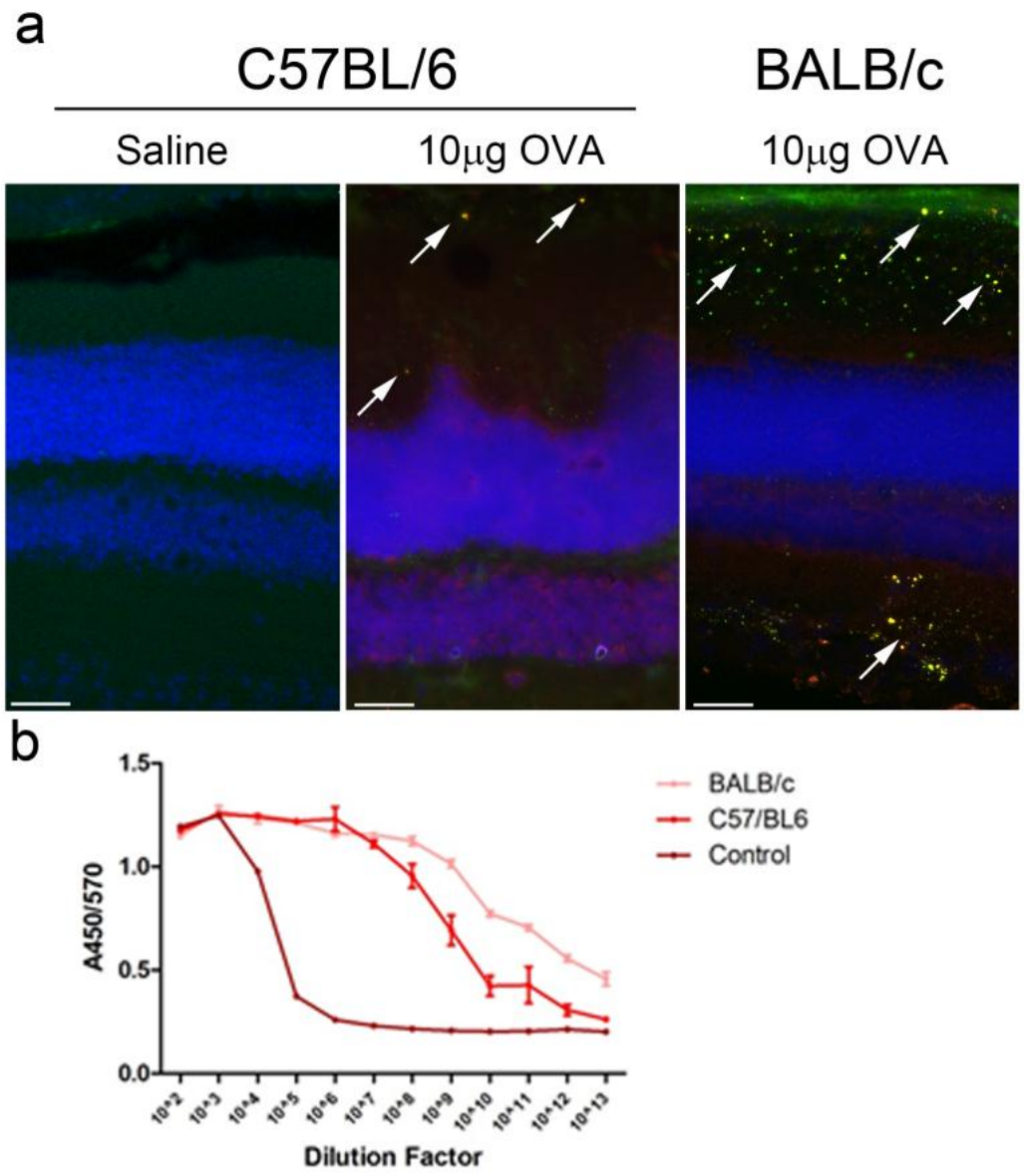

Figure A1 Immune complex formation in the mouse retina following OVA challenge.
(a) Immunohistochemical detection of OVA (red) and IgG (green) 3 days after intravitreous saline injection or intravitreous injection of 10μg OVA in C57BL/6 or 10μg OVA in BALB/c mice (n=3-6 mice per group). Immune complexes (co-localisation, yellow) are indicated by arrows. **(b)** Anti-OVA serum antibody titers are 10 fold higher in BALB/c (n=4) than in C57BL/6 (n=3) mice immunised with the same protocol. Control BALB/c mice (n=1) immunised against retina homogenate did not show any detectable levels of anti-OVA antibodies. Scale bars - 50μm.

A2. The inflammatory response to OVA in non-immunised mice

To determine whether intravitreous injection of OVA alone could induce an inflammatory response, non-immunised mice were injected intravitreously with OVA, culled 3 days after injection and their eyes collected for immunohistochemical analysis. Intravitreous injection of OVA in non-immunised mice did not result in an increase in the number of $CD11b^+$ or $CD45^+$ cells or cells expressing any of the inflammatory markers analysed in Chapter 3 (Figure A2)

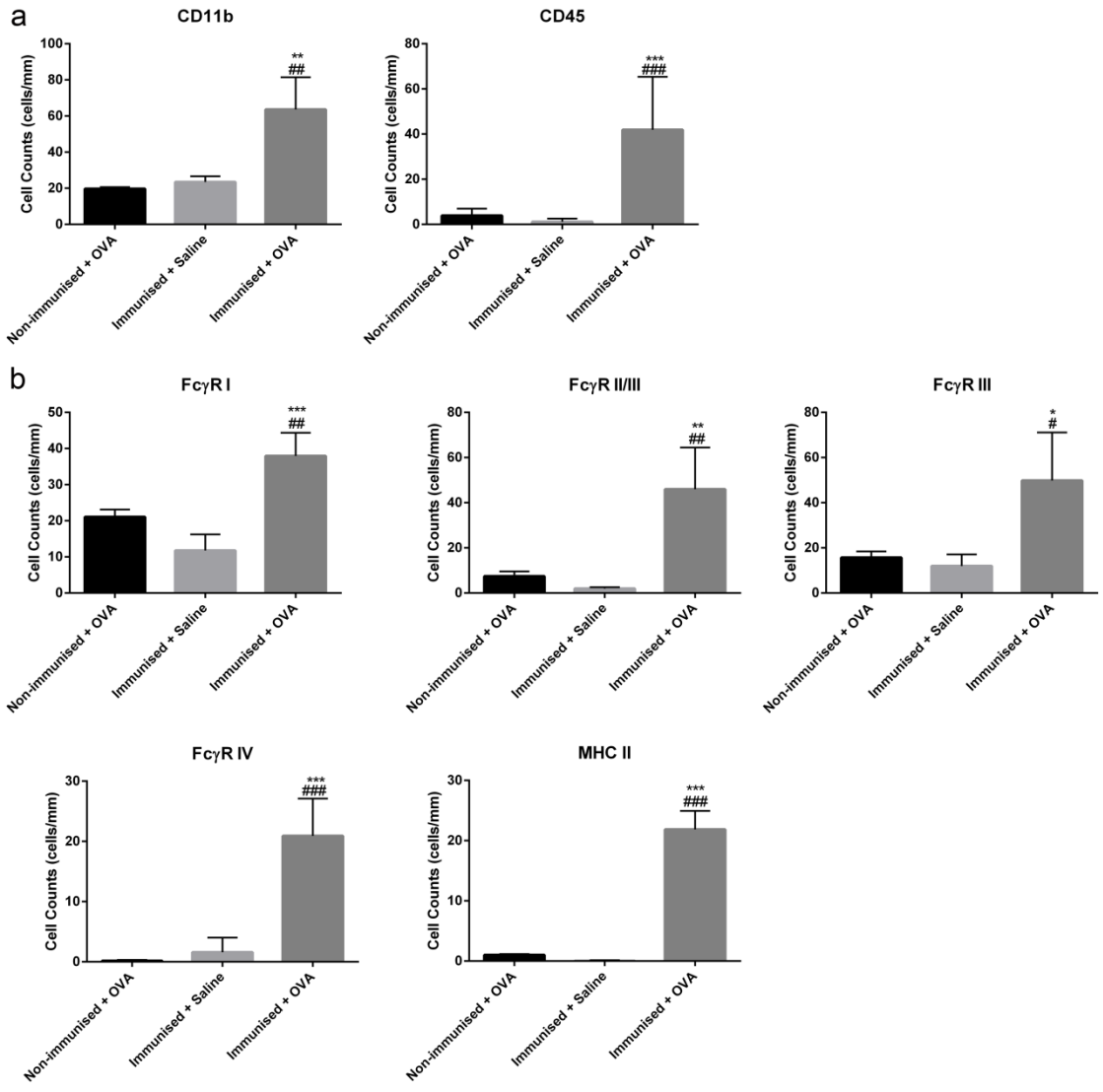

Figure A2 Quantification of number of cells expressing inflammatory markers following intravitreous injection of OVA in OVA-immunised and non-immunised mice.

(a) Quantification of $CD11b^+$ or $CD45^+$ cell number/mm of retina. **(b)** Quantification of cell number/mm of retina expressing FcγR I, II/III, III, IV and MHC II.. Data are expressed as number of cells/mm of retina +SEM and were analysed using two-way ANOVA followed by Bonferroni post-hoc (n=3-6 mice per group). *p<0.05, **p<0.01, ***p<0.001 immunised + saline vs immunised + OVA; #p<0.05, ##p<0.01, ###p<0.001 non-immunised + OVA vs immunised + OVA.

A3. Immunohistochemical detection of CD8

The results in Chapter 3 show that immune complex formation in the retina results in infiltration of $CD3^+$ T cells. To further characterise the nature of these T cells, stains for CD4 and CD8 were performed. Immunohistochemistry for CD8, revealed what appeared to be unspecific staining in the retina, in particular in the outer plexiform layer (Figure A3). At 3 and 7 days after OVA challenge $CD8^+$ cells were observed in the subretinal space and choroid (Figure A3. insets). Based on their morphology and location these appeared to be T cells. However, due to the immunoreactivity in the ONL it is difficult to ascertain this. It would be important to perform the same stain on CD8 knock-out retinae, in order to establish whether the immunoreactivity seen is due to unspecific staining or CD8 expression by T lymphocytes or other retinal cell type.

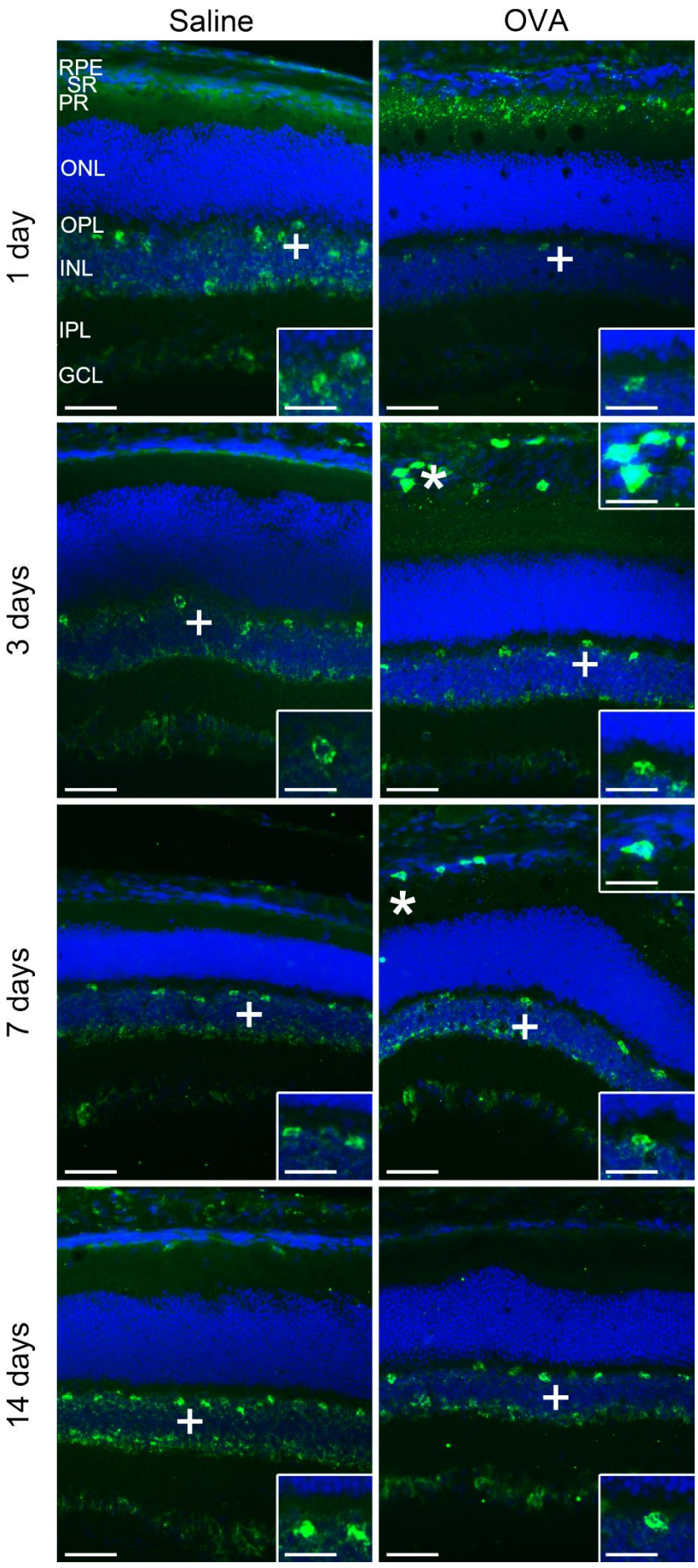
Saline
OVA
RPE
SR
PR
ONL
OPL
INL
IPL
GCL
1 day
3 days
7 days
14 days

Figure A3 Immunohistochemical detection of CD8.
Immunohistochemistry for CD8 24 hours (1 day), 3, 7 and 14 days after saline or OVA injection. Immunoreactivity was detected in the OPL in all conditions. CD8+ cells with morphology resembling that of T cells were observed 3 and 7 days after OVA challenge (*). + indicates origin of bottom left right, * indicates origin of top right insets (n=4-6 mice per group). RPE, retinal pigmented epithelium; SR, subretinal space; PR, photoreceptors; ONL, outer nuclear layer; OPL, outer plexiform layer; INL, inner nuclear layer; IPL, inner plexiform layer; GCL, ganglion cell layer. Scale bars - 50μm, inset scale bars - 25μm.

A4. Electroretinogram

Scotopic ERGs were measured 3 days after saline or OVA challenge and no differences between the two groups were detected. A small group size (n=3 per group) could explain the lack of effect. In addition, there was a lot of "background noise" detected by the ERG set up, which could also affect the results obtained (Figure A4). This technical problem had not been resolved by the end of the experiments. Further optimisation of the set up and protocol are required before ERG function can be appropriately assessed.

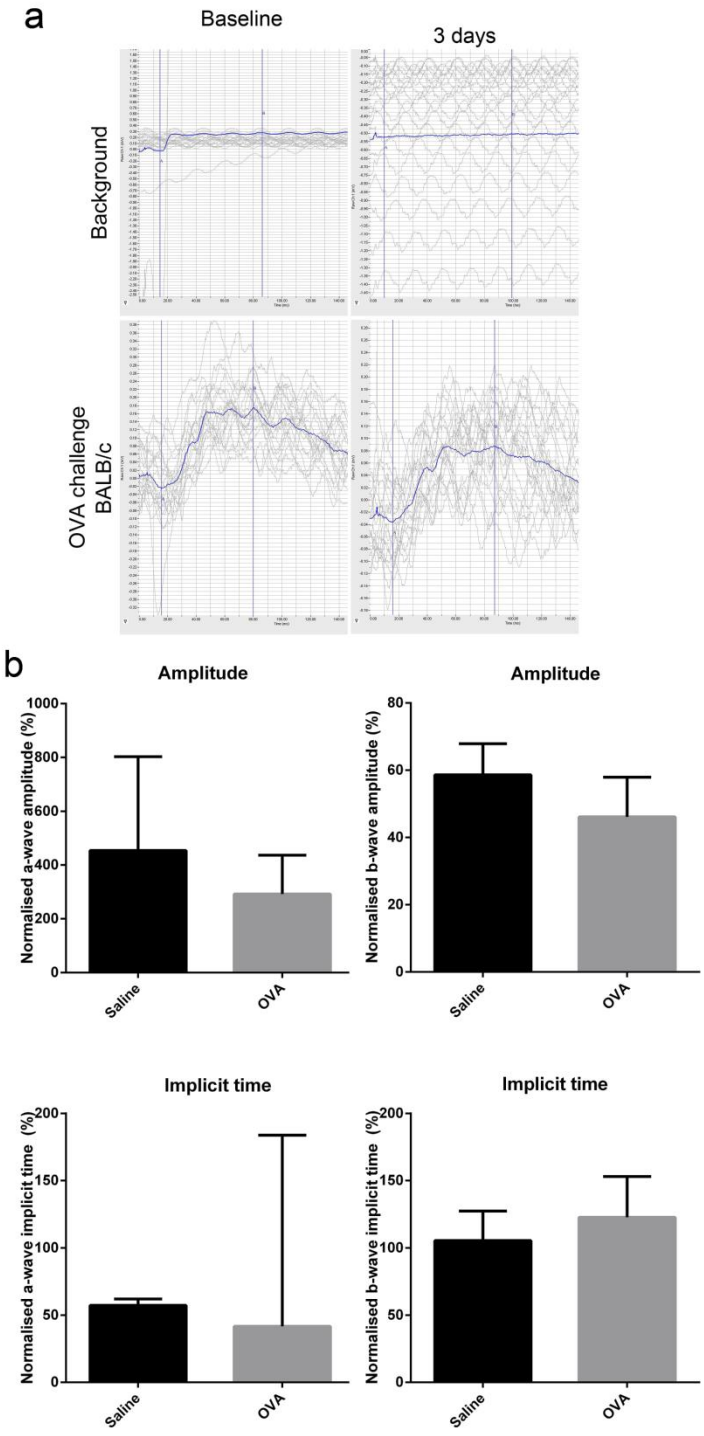

Figure A4 Scotopic ERG analysis.

(a) ERG recordings. Each individual recording is showed in a gray line; the blue line represents the average recording. The top panel shows the recording for electromagnetic background (obtained by placing the two electrodes, reference and ground together). On the day baseline readings were taken electromagnetic background was low. This was greatly increased on the day experimental measurements were taken. The bottom panel shows ERG recordings from anaesthetised mice. **(b)** Quantification of the amplitude and time taken to reach a and b waves.

A5. Circulating retinal autoantibodies and retinal degeneration

Because patients suffering from AMD have high titers of circulating retinal autoantibodies,[15, 16, 48] a pilot experiment was performed to investigate whether the presence of circulating autoantibodies may lead to the formation of drusen-like deposits and/or photoreceptor degeneration. 10 six-week old BALB/c mice were immunised against retina homogenates. Briefly retinae from 10 healthy BALB/c mice were collected and homogenised in 4ml of sterile saline using a Griffiths tube tissue grinder. Mice were immunised with retina homogenates by intraperitoneal (i.p.) injection of 100µl of retina homogenate and Alum (1:1 ratio). 3 months after initial immunisation and 2 weeks before the end of the experiment, mice were injected i.p. with 100µl of retina homogenate. Mice were sacrificed 18 months after the initial immunisation.

The presence of autoantibodies was confirmed by incubating fresh frozen 20µm retinal sections with serum from mice immunised with retina homogenates and detecting IgG binding with a sheep anti-mouse IgG FITC-labelled $F(ab')_2$. Serum from OVA-immunised mice was used as a control (Figure A5 a). Autoantibodies with affinity for retinal antigens were present in 6 of the 10 immunised mice and appeared to bind astrocytes (Figure A5 a, inset). Interestingly, the astrocyte marker GFAP is one of the targets of autoantibodies present in human AMD.[16] The presence of drusen and photoreceptor degeneration has been previously detected in mouse with haematoxylin and eosin staining (H&E).[207] The presence of circulating retinal autoantibodies did not lead to the formation of drusen-like deposits or to retinal degeneration in this study, as seen by H&E (Figure A5 b), suggesting circulating autoantibodies alone are not sufficient to induce changes in the retina. These results are a starting point for further experiments. Optimisation of the immunisation protocol and control normal aged mice will need to be obtained for future experiments. Techniques such as electron microscopy may be required to detect small changes such as RPE atrophy.

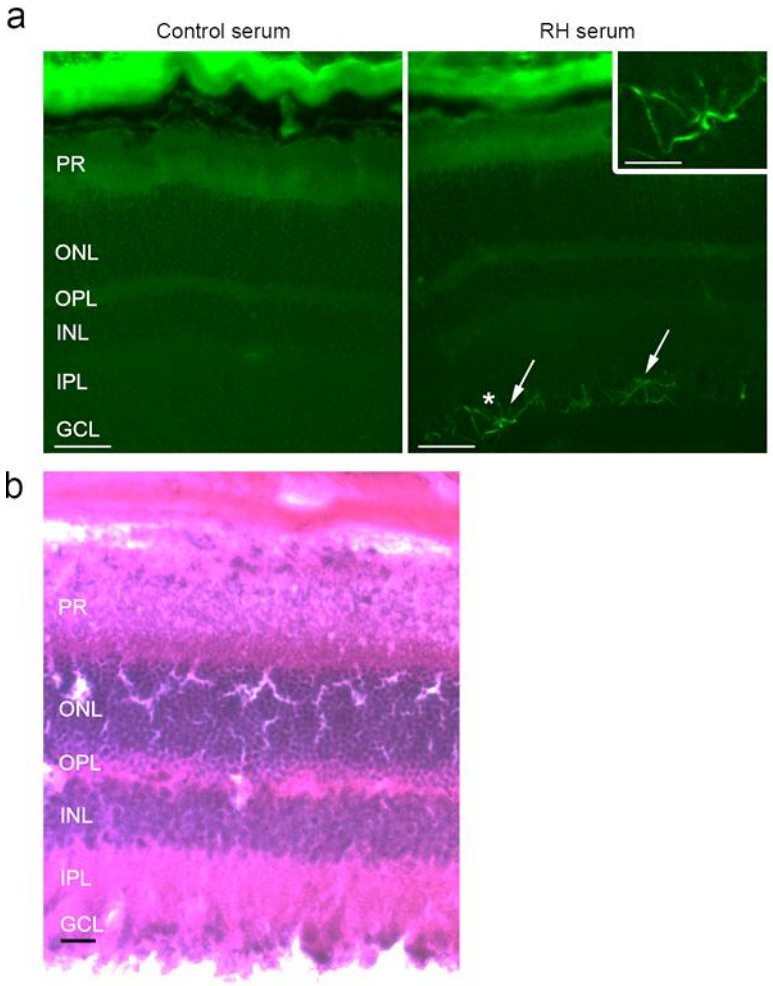

Figure A5 Immunisation of mice with retina homogenates leads to circulating antibodies against retinal antigens but not to retinal degeneration.
(a) Serum from mice immunised against retinal homogenates, or against OVA as a control, was incubated on retinal sections from BALB/c mice and the presence of autoantibodies was detected with sheep anti-mouse IgG FITC-labelled F(ab')2. Immunisation with retina homogenates resulted in antibodies with affinity for cells with astrocyte morphology (inset). Scale bars - 50µm, inset - 25µm. **(b)** H&E staining did not reveal any morphological abnormalities in mice immunised with retina homogenates. Scale bar - 20µm

A6. The effect of macrophage depletion on the inflammatory response to immune complex formation in the retina

To study the role of recruited macrophages in the response to immune complex formation in the retina, liposomes containing clodronate, or PBS as a control, were administered twice intraperitoneally to OVA immunised mice. 1 day after injection of

liposomes, mice were injected intravitreously with 10µg of OVA in saline to induce immune complex formation in the retina and their eyes and spleen collected 3 and 7 days after injection, as detailed in section 2.1.3.

Macrophage depletion was confirmed by immunohistochemical staining of CD68, CD11b and CD64 (FcγRI) in the spleen (Figure A6). Immunoreactivity for the general myeloid markers CD68 and CD11b revealed that while CD68 staining was decreased, there was an apparent increase in the number of CD11b cells in the spleen of mice treated with liposomes containing clodronate, possibly due to increased numbers of other CD11b+ myeloid cells such as neutrophils. Staining for CD64, expressed mainly by macrophages, revealed that the spleens of mice treated with clodronate-filled liposomes had a much reduced number of $CD64^+$ cells, suggesting successful macrophage depletion.[172] However, a better way to confirm peripheral macrophage depletion would have been to analyse the presence of monocytes/macrophages in white blood cells isolated from whole blood e.g. by flow cytometry.

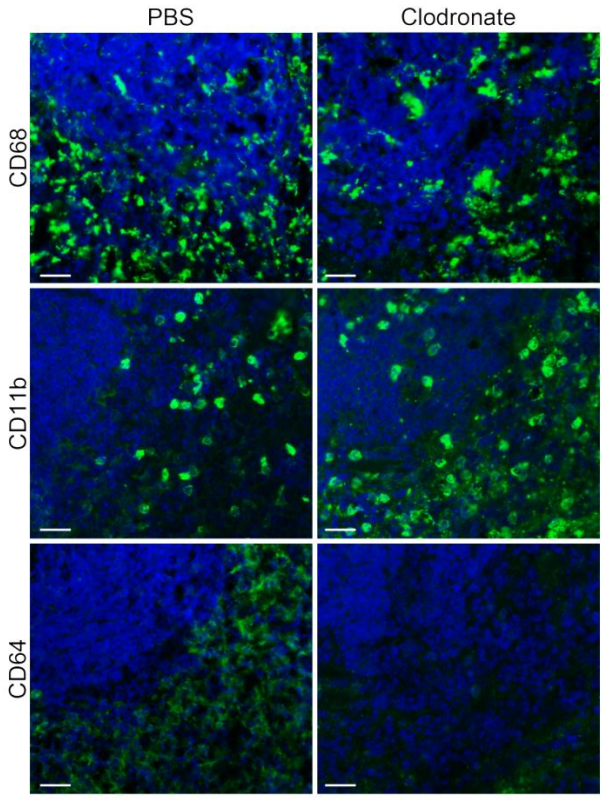

Figure A6 Immunohistochemical detection of CD68, CD11b and CD64.
Immunohistochemistry for CD68, CD11b and CD64 was performed in the spleens of mice treated with liposomes containing PBS or clodronate 7 days after intravitreous injection of OVA (n=3-5). Scale bars - 25µm.

Macrophage depletion with liposomes containing clodronate did not lead to any significant changes in microglia activation or leukocyte recruitment 3 days after intravitreous injection of OVA, as seen by CD11b, CD45 and MHC II immunoreactivity. This could have been due to incomplete depletion of macrophages or due to the small sample size (n=3 mice per group). Treatment with clodronate 7 days after intravitreous injection with OVA resulted in a non-significant decrease in the number of recruited leukocytes when compared to control mice treated with PBS-filled liposomes, suggesting recruited macrophages may further contribute to leukocyte recruitment in response to immune complex formation in the retina (Figure A7.).

These results were a starting point for future experiments. Larger sample sizes and studying the impact of macrophage depletion on control OVA-immunised mice injected with saline intravitreously are important issues to be taken into consideration in future experiments.

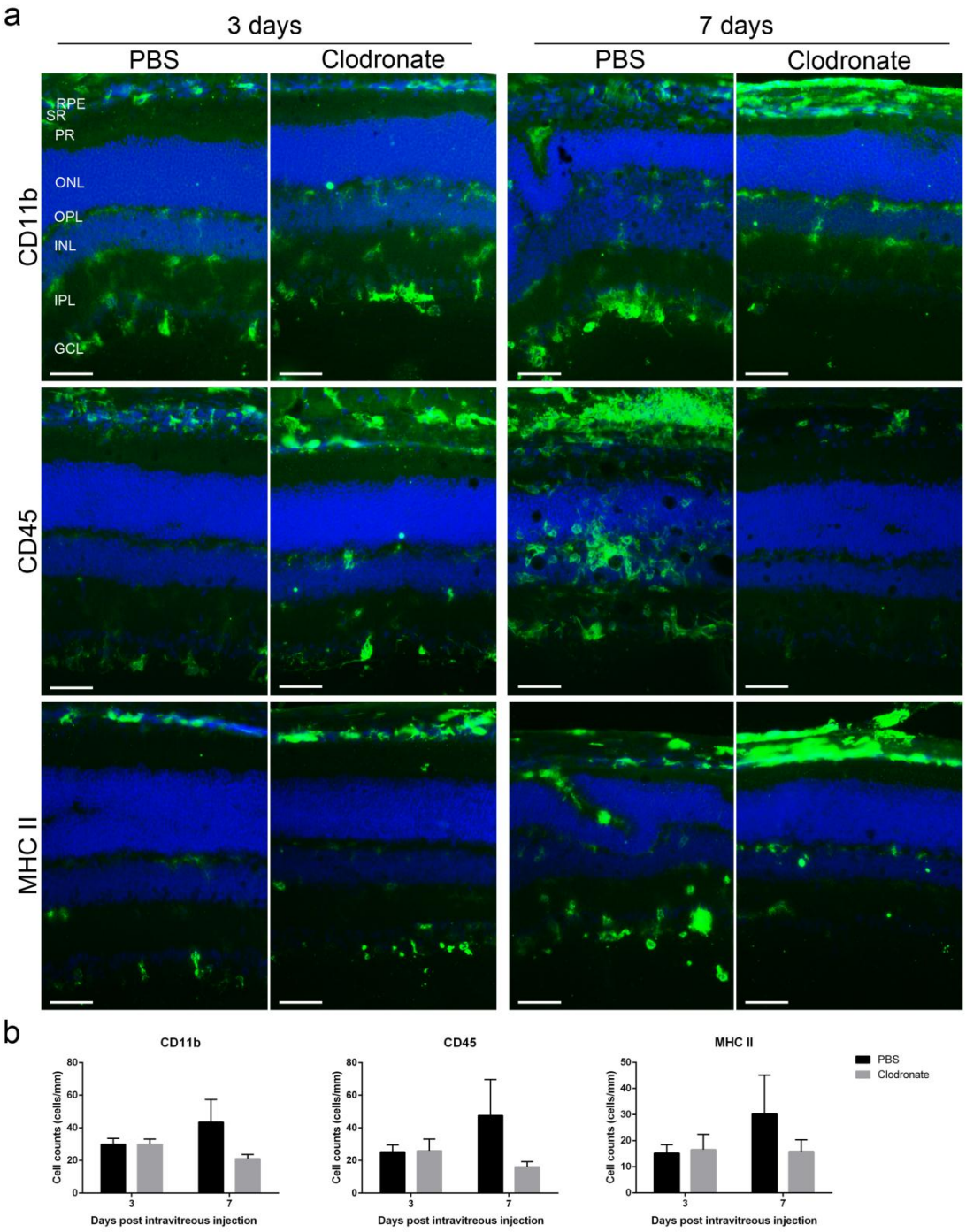

Figure A7 The effect of depletion of macrophages on the response to immune complex formation in the retina.

(a) Immunohistochemistry for CD11b, CD45 and MHC II in the retina of mice treated with PBS- or clodronate-filled liposomes, 3 and 7 days after intravitreous injection with saline. RPE, retinal pigmented epithelium; SR, subretinal space; PR, photoreceptors; ONL, outer nuclear layer; OPL, outer plexiform layer; INL, inner nuclear layer; IPL, inner plexiform layer; GCL, ganglion cell layer. Scale bars - 50µm. **(b)** Quantification of cell number/mm of retina expressing CD11b, CD45 and MHC II. Data are expressed as number of cells/mm of retina +SEM and were analysed using two-way ANOVA followed by Bonferroni post-hoc (n=3-5 mice per group).

Appendix 2

A7. The effect of immune stimulation on the inflammatory milleu in the basal chamber

As described in chapter 6 ARPE19 monolayers were stimulated apically with 50ng/ml LPS + 2ng/ml IFN-γ,10ng/ml IL-4 + 10ng/ml IL-13, 20ng/ml IL-10 or 10μg/ml of large heat-aggregated human IgG (immune complex, IC), or indirectly with conditioned medium of macrophages polarised with the same stimuli for 48 hours; M1 (50ng/ml LPS + 2ng/ml IFN-γ), M2a (10ng/ml IL-4 + 10ng/ml IL-13), M2c (20ng/ml IL-10) and MIC (10μg/ml of large heat-aggregated human IgG) on the apical side. Non-stimulated ARPE19 cells or ARPE19 stimulation with conditioned media from non-stimulated macrophages (MNS) were used as controls. The concentration of cytokines in the basal chamber was measured 24 hours after stimulation.

- **The effect of direct stimulation on apical secretion of cytokines by ARPE19 monolayers**

The levels of IL-6 in the basal chamber were significantly increased following stimulation of ARPE19 monolayers with IL-4+IL-13 from 7.904pg/ml to 27.96pg/ml (p=0.0115), whilst the concentration of IL-10 in the basal chamber was significantly increased following stimulation with IFN-γ+LPS, IL-4+IL-13 and IL-10 from 0.015pg/ml to 1.310pg/ml (p=0.0024), 0.156pg/ml (p=0.0147) and 5.180pg/ml (p=0.0019), respectively (Figure A8).

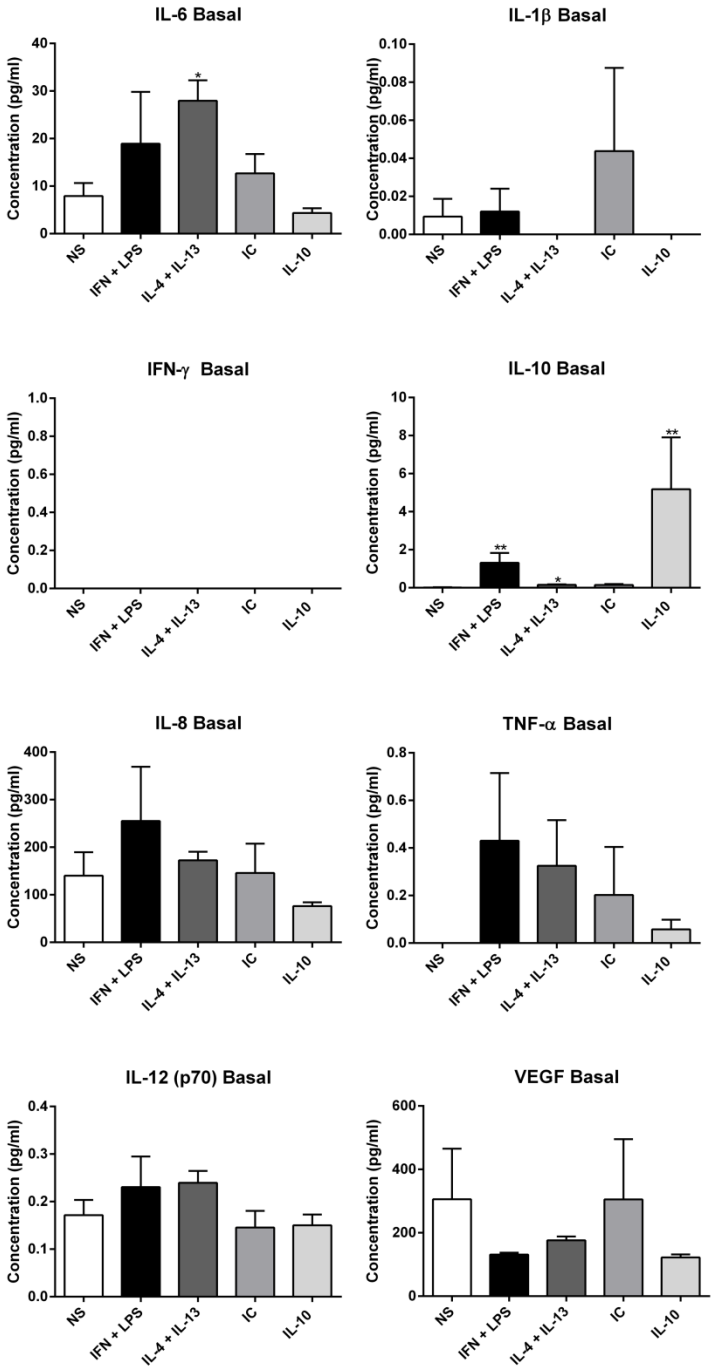

Figure A8 Concentration of pro-inflammatory cytokines in the basal chamber following direct stimulation of ARPE19 monolayers.

Cytokine measurements 24 hours after stimulation of ARPE19 monolayers with IFN-γ+LPS, IL-4+IL-13, IC and IL-10 (n=9 per group). NS ARPE19 cells were used as a control (n=9). Data shown are pooled from three independent experiments and expressed as pg/ml+SEM. Data were analysed using a non-parametric RM Friedman test followed by Dunn's correction. *p<0.05, **p<0.01, ***p<0.001 vs NS control.

- **The effect of indirect stimulation of ARPE19 monolayers with polarised macrophage CM on the concentration of in the apical chamber**

Stimulation of ARPE19 monolayers with conditioned media (CM) from polarised macrophages resulted in increased levels of cytokines in the basal chamber. At 24 hours basal levels of cytokines in the basal chamber of NS RPE monolayers were 0.015pg/ml IL-10, 7.904pg/ml IL-6, 0.009pg/ml IL-1β, 1.94pg/ml IL-8 and 0.171pg/ml IL-12 (p70) with no detectable levels of TNF-α or IFN-γ. Stimulation with CM from non-stimulated macrophages (MNS) did not change the levels of cytokines in the basal chamber. Addition of M1 CM led to a significant increase in Il-10 ($p=0.0008$), IL-6 ($p=0.0003$), IL-1β ($p=0.0339$), TNF-α ($p=0.0011$), IL-12 ($p=0.0024$) and IL-8 ($p=0.0034$) to 6.14pg/ml IL-10, 217.6pg/ml IL-6, 2.09pg/ml IL-1β, 21.45pg/ml TNF-α, 3.69pg/ml IL-12 and 5.4ng/ml IL-8 and a non-significant increase in IFN-γ ($p<0.059$) to 18.09pg/ml IFN-γ. Stimulation with M2a CM led to a significant increase in IL-10 ($p=0.0003$), IL-6 ($p=0.0008$), IL-1β ($p=0.0154$), TNF-α ($p=0.0002$), IL-12 (p70; $p=0.0125$) and IL-8 ($p=0.028$) to 2pg/ml IL-10, 58.21pg/ml IL-6, 0.59pg/ml IL-1β, 6.11pg/ml TNF-α, 2.23pg/ml IL-12 and 1.4ng/ml IL-8, and a non-significant increase in IFN-γ ($p=0.028$) to 5.10pg/ml. Addition of M2c supernatant to ARPE19 monolayers led to a significant increase in IL-10 ($p<0.0001$) to 1.3ng/ml IL-10. Addition of supernatant from immune-complex stimulated macrophages MIC did not lead to any significant changes in the pro-inflammatory cytokines investigated. None of the stimuli induced changes in the basal concentration of VEGF (Figure A9).

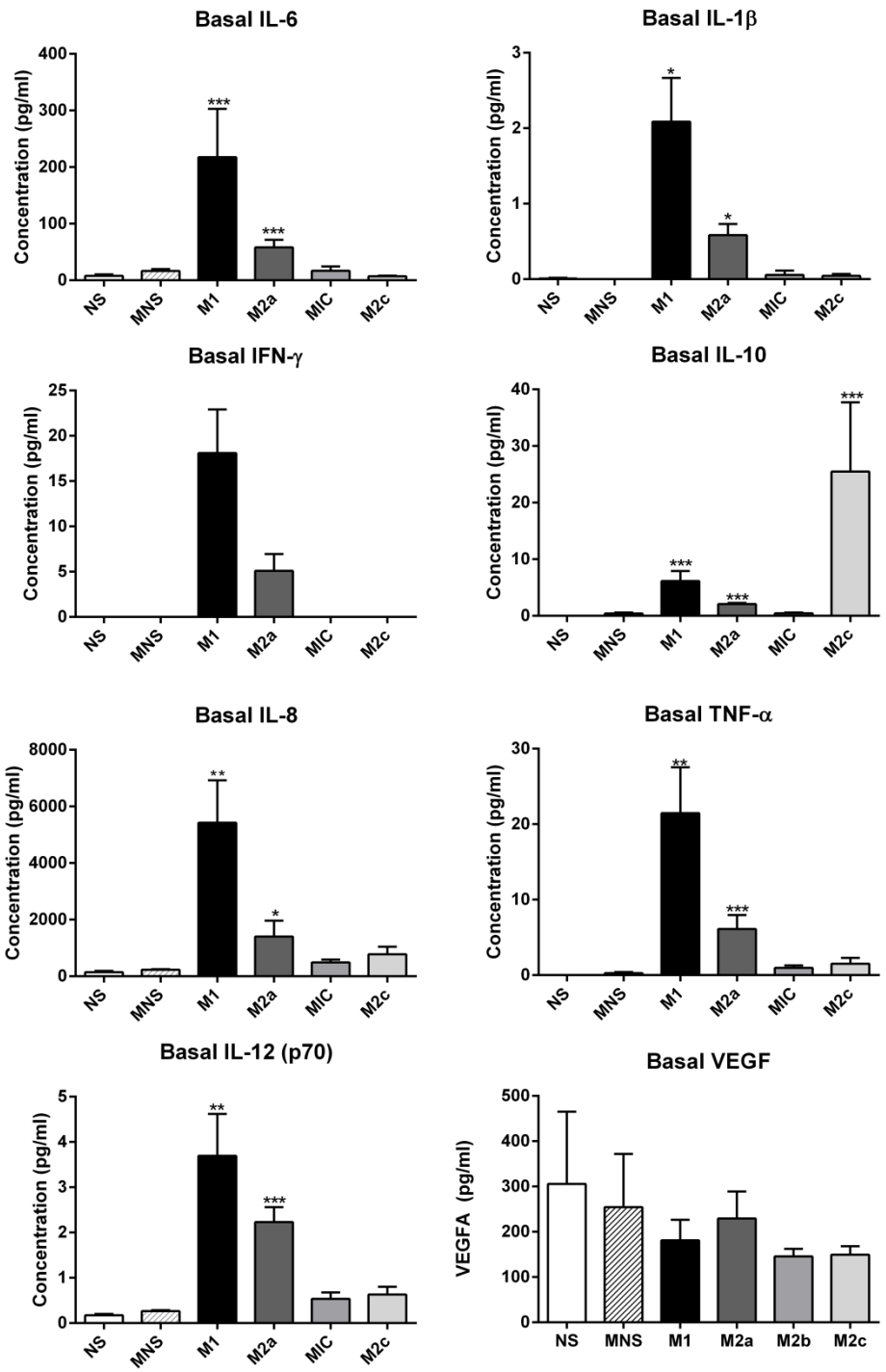

Figure A9 Concentration of cytokines in the basal chamber following addition of macrophage conditioned medium to ARPE19 monolayers. Cytokine measurements 24 hours after stimulation of ARPE19 monolayers with MNS, M1, M2a, MIC and M2c conditioned media (n=9 per group). NS ARPE19 cells were used as a control (n=9). Data are pooled from three independent experiments and expressed as pg/ml+SEM. Data were analysed using non-parametric RM Friedman test followed by Dunn's correction. *p<0.05, **p<0.01, ***p<0.001 vs NS control.

- **The effect of indirect stimulation with CM from macrophages stimulated with Avastin or Lucentis on the concentration of cytokines in the basal chamber**

Apart from a significant increase in the levels of IL-6 in the basal chamber, stimulation of ARPE19 monolayers with conditioned media from macrophages stimulated with plate-immobilised Avastin or Lucentis did not lead to any significant changes in the concentration of cytokines in the basal chamber (Figure A10).

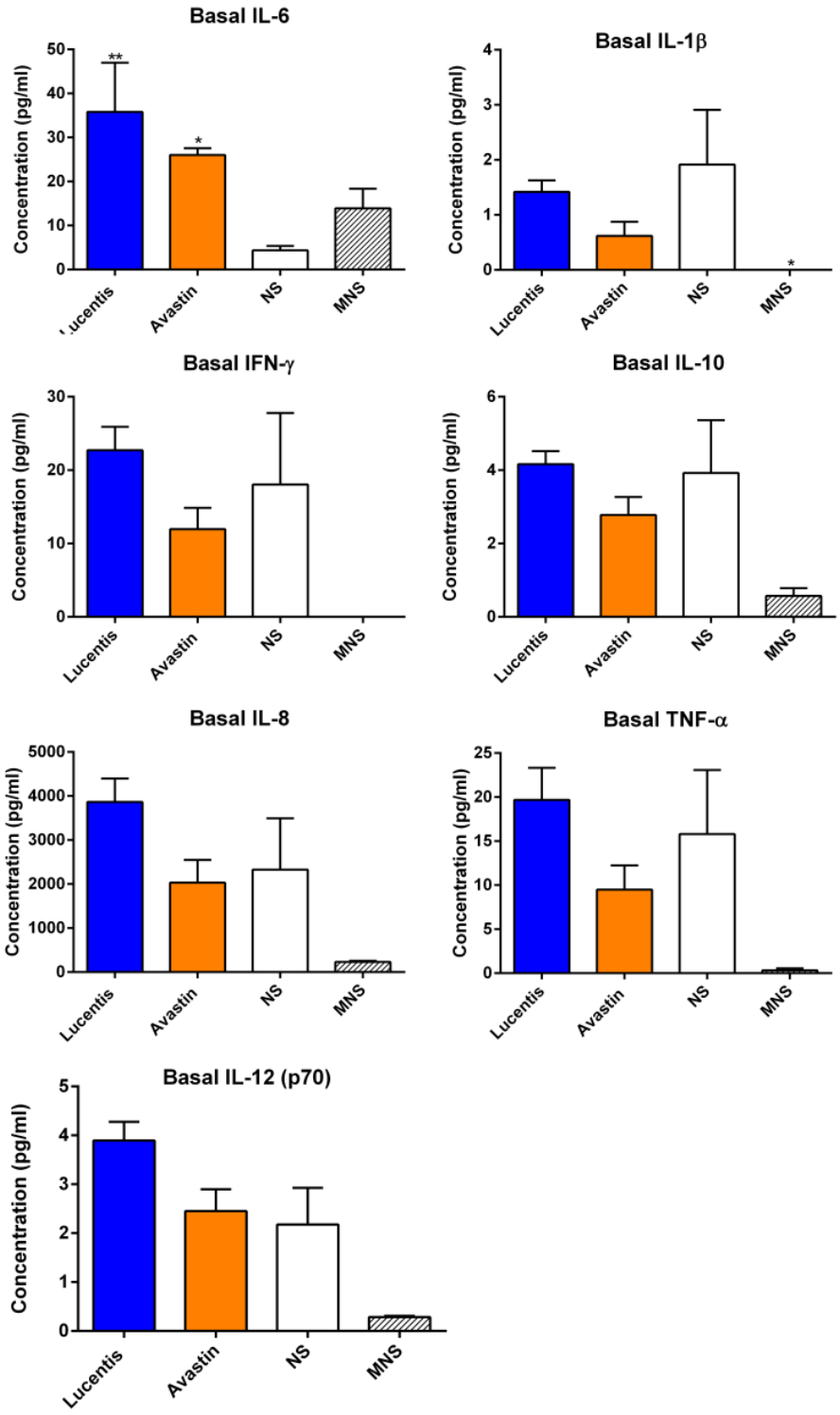

Figure A10 Concentration of cytokines in the basal chamber following addition of Avastin or Lucentis stimulated macrophage conditioned medium to ARPE19 monolayers.

Cytokine measurements 24 hours after stimulation of ARPE19 monolayers with MNS, Avastin and Lucentis conditioned media (n=6 per group). NS ARPE19 cells were used as a control (n=6). Data are pooled from three independent experiments and expressed as pg/ml+SEM. Data were analysed using non-

parametric RM Friedman test followed by Dunn's correction. *p<0.05, **p<0.01, ***p<0.001 vs NS control.

A8. FcγR expression by ARPE19 monolayers

Expression of FcγRI and FcγRIIb by ARPE19 monolayers was investigated by qPCR 8h following stimulation with IFN-γ+LPS, IL-4+IL-13, IL-10 and immune complex (n=6). Non-stimulated ARPE19 cells were used as a control (n=6). Analysis of melting curves from the qPCR reactions revealed multiple peaks, suggesting unspecific amplification of product for both FcγRI and FcγRIIb primers. No positive control tissue (e.g. mRNA from M1 human macrophages) was available at the time of these experiments. Expression of FcγRI, FcγRIIa, FcγRIIb and FcγRIII was then investigated by immunocytochemistry. No immunoreactivity for FcγRI, FcγRIIa, FcγRIIb and FcγRIII was detected. The antibodies for FcγRI, FcγRIIa and FcγRIIb had been successfully used in 4% P.F.A-frozen human retinal section, however no positive control for immunocytochemistry was available. Together these results suggest ARPE19 cells do not express FcγRs. However, further experiments are required to confirm this (Figure A11).

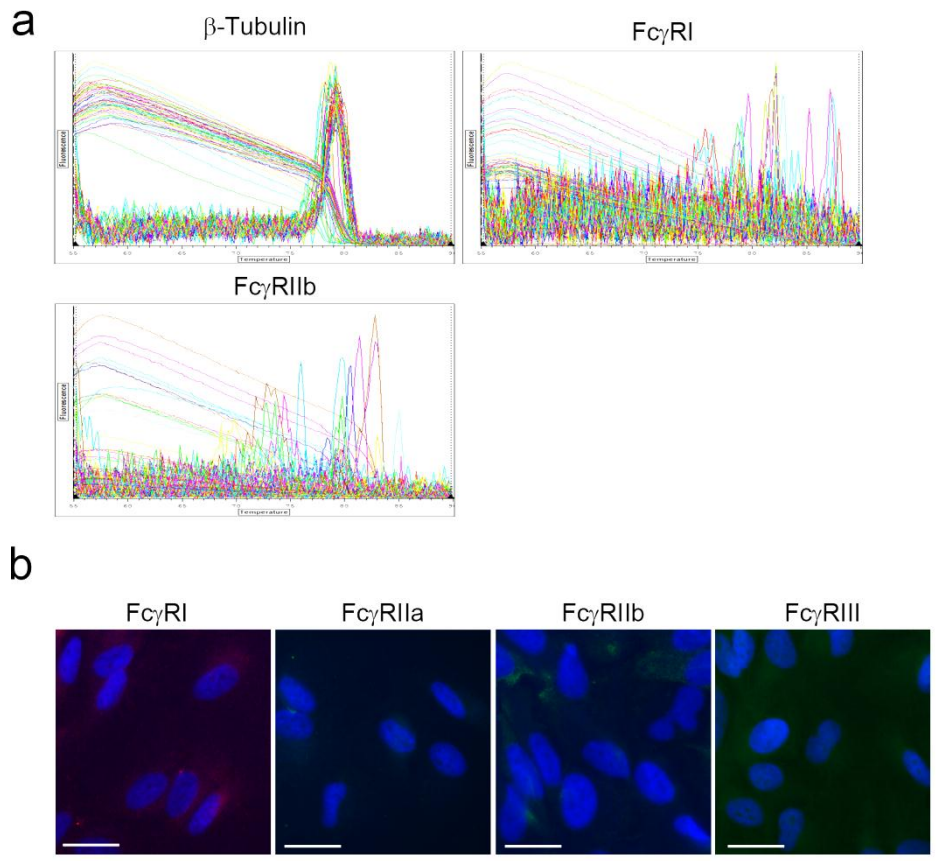

Figure A11 ARPE19 cells do not appear to express FcγRs.
(a) Melting curves from qPCR reactions with FcγRI- and FcγRIIb-primers. **(b)** Immunocytochemistry for FcγRI, FcγRIIa, FcγRIIb and FcγRIII in ARPE19 monolayers. Scale bar -25µm.

A9. Macrophage phenotype following stimulation

Human macrophages were isolated from whole blood and polarised by Lekh Dahal. Following polarisation macrophages conditioned medium was collected and macrophage phenotype characterised by flow cytometry. Flow cytometry experiments, data collection, analysis and plotting was performed by Lekh Dahal. Macrophage polarisation with IFN-γ+LPS (M1) resulted in increased levels of CD40 and FcγRIIb when compared to non-stimulated macrophages (NS). IL-4+IL-13 (M2a) stimulation resulted only in increased levels of CD11b, whilst stimulation with IL-10 resulted in increased levels of FcγRI in all donors and FcγRIIb in donor 2. Stimulation with immune complex (IC) did not result in changes in levels of any of the markers investigated when compared to non-stimulated macrophages, suggesting IC failed to activate the macrophages (Figure A12).

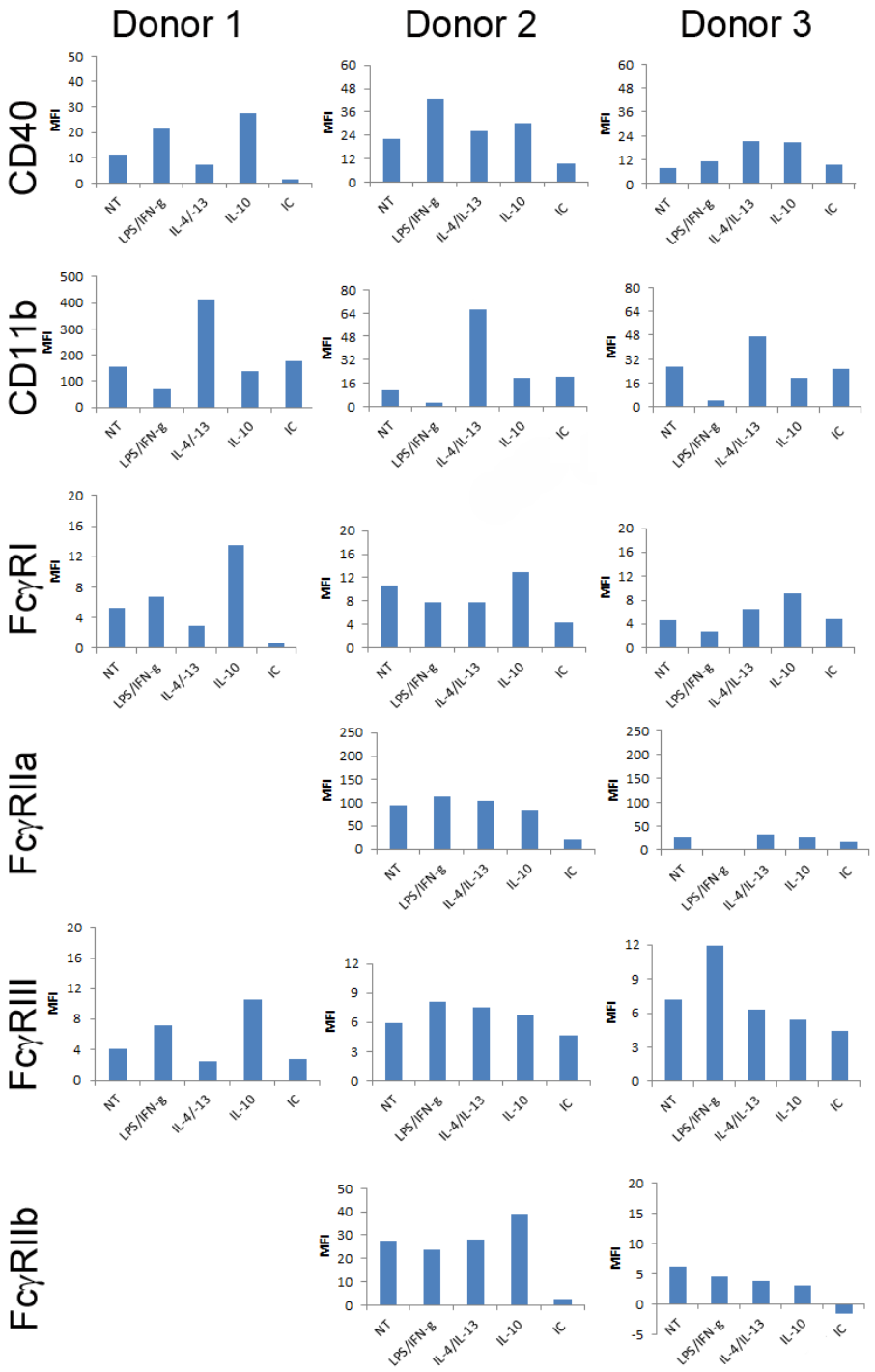

Figure A12 Macrophage phenotype following polarisation. Macrophage phenotype was investigated by flow cytometry.

Data are expressed in mean fluorescence intensity (MFI). All data was collected and plotted by Lekh Dahal.

Appendix 3

To perform an *a priori* power analysis data from immunohistochemistry quantification was used.

The effect size (Cohen's d) and effect-size correlation were calculated using the following means and standard deviations (StDev) for the percentage of CD45 and FcγRIIa or FcγRIIb double positive cells in the retina or choroid:

	CD45+ FcγRIIa				CD45+ FcγRIIb			
	Control		AMD		Control		AMD	
	Mean	StDev	Mean	StDev	Mean	StDev	Mean	StDev
Retina	71.06	33.36	88.48	14.85	36.60	13.75	73.03	4.18
Choroid	41.55	8.99	66.57	15.22	39.07	9.55	56.05	18.64

Effect-size correlation (r) and Cohen's d (d) were calculated at http://www.uccs.edu/~lbecker/ using the following equations:

Calculate *d* and *r* using means and standard deviations

Calculate the value of Cohen's *d* and the effect-size correlation, r_{YA}, using the means and standard deviations of two groups (treatment and control).

Cohen's $d = M_1 - M_2 / \sigma_{pooled}$
where $\sigma_{pooled} = \sqrt{[(\sigma_1^2 + \sigma_2^2) / 2]}$

$r_{YA} = d / \sqrt{(d^2 + 4)}$

Note: d and r_{YA} are positive if the mean difference is in the predicted direction.

Group 1		Group 2	
M_1	36.60	M_2	73.03
SD_1	13.75	SD_2	4.18

Compute Reset

Cohen's *d*	effect-size *r*
-3.584903	-0.873288

So that:

	CD45+ FcγRIIa		CD45+ FcγRIIb	
	r	d	r	d
Retina	-0.31963	-0.6747	-0.87329	-3.5849
Choroid	-0.70741	-2.0017	-0.49735	-1.1465

Finally, sample size calculations were made using anticipated effect size (Cohen's d calculated above), desired statistical power level = 0.8, probability level = 0.05 for a two-tailed hypothesis t-test using the website: http://www.uccs.edu/~lbecker/ so that expected minimum sample size per group is:

	CD45+ FcγRIIa (n)	CD45+ FcγRIIb (n)
Retina	36	3
Choroid	6	14

List of References

1. Kolb H. Photoreceptors. In: *Webvision: The organization of the retina and visual system. http://webvision.med.utah.edu/*; 1995.

2. Kolb H. Simple Anatomy of the Retina. In: *Webvision: The organization of the retina and visual system. http://webvision.med.utah.edu/*; 1995.

3. Gehrs KM, Anderson DH, Johnson LV, Hageman GS. Age-related macular degeneration--emerging pathogenetic and therapeutic concepts. *Ann Med*. 2006;38:450-471.

4. Prasad PS, Schwartz SD, Hubschman JP. Age-related macular degeneration: Current and novel therapies. *Maturitas*. 2010;66:46-50.

5. Jager RD, Mieler WF, Miller JW. Age-related macular degeneration. *N Engl J Med*. 2008;358:2606-2617.

6. Ardeljan D, Chan CC. Aging is not a disease: Distinguishing age-related macular degeneration from aging. *Prog Retin Eye Res*. 2013;37:68-89.

7. Krabbe KS, Pedersen M, Bruunsgaard H. Inflammatory mediators in the elderly. *Experimental Gerontology*. 2004;39:687-699.

8. Ma W, Cojocaru R, Gotoh N, et al. Gene expression changes in aging retinal microglia: relationship to microglial support functions and regulation of activation. *Neurobiol Aging*. 2013;34:2310-2321.

9. Ogawa T, Kitagawa M, Hirokawa K. Age-related changes of human bone marrow: a histometric estimation of proliferative cells, apoptotic cells, T cells, B cells and macrophages. *Mech Ageing Dev*. 2000;117:57-68.

10. Ambati J, Atkinson JP, Gelfand BD. Immunology of age-related macular degeneration. *Nat Rev Immunol*. 2013;13:438-451.

11. Morohoshi K, Patel N, Ohbayashi M, et al. Serum autoantibody biomarkers for age-related macular degeneration and possible regulators of neovascularization. *Exp Mol Pathol*. 2012;92:64-73.

12. Morohoshi K, Ohbayashi M, Patel N, Chong V, Bird AC, Ono SJ. Identification of anti-retinal antibodies in patients with age-related macular degeneration. *Exp Mol Pathol*. 2012;93:193-199.

13. Mullins RF, Russell SR, Anderson DH, Hageman GS. Drusen associated with aging and age-related macular degeneration contain proteins common to extracellular deposits associated with atherosclerosis, elastosis, amyloidosis, and dense deposit disease. *FASEB J*. 2000;14:835-846.

14. Mullins RF, Aptsiauri N, Hageman GS. Structure and composition of drusen associated with glomerulonephritis: implications for the role of

complement activation in drusen biogenesis. *Eye (Lond)*. 2001;15:390-395.

15. Patel N, Ohbayashi M, Nugent AK, et al. Circulating anti-retinal antibodies as immune markers in age-related macular degeneration. *Immunology*. 2005;115:422-430.

16. Penfold PL, Provis JM, Furby JH, Gatenby PA, Billson FA. Autoantibodies to retinal astrocytes associated with age-related macular degeneration. *Graefes Arch Clin Exp Ophthalmol*. 1990;228:270-274.

17. Nimmerjahn F, Ravetch JV. Fcgamma receptors as regulators of immune responses. *Nat Rev Immunol*. 2008;8:34-47.

18. Pham VT, Wen L, McCluskey P, Madigan MC, Penfold PL. Human retinal microglia express candidate receptors for HIV-1 infection. *Br J Ophthalmol*. 2005;89:753-757.

19. Kolb H. Gross Anatomy of the Eye. In: *Webvision: The organization of the retina and visual system. http://webvision.med.utah.edu/*; 1995.

20. Pasternak T, Bisley JW, Calkins D. Visual Information Processing in the Primate Brain. In: Gallagher M, Nelson RJ (eds), *Handbook of Psychology* New York: John Wyley & Sons; 200:139-185.

21. Caspi RR. Ocular autoimmunity: the price of privilege? *Immunol Rev*. 2006;213:23-35.

22. Streilein JW. Immunoregulatory mechanisms of the eye. *Prog Retin Eye Res*. 1999;18:357-370.

23. Tomi M, Hosoya K. The role of blood-ocular barrier transporters in retinal drug disposition: an overview. *Expert Opinion on Drug Metabolism & Toxicology*. 2010;6:1111-1124.

24. Zhou R, Caspi RR. Ocular immune privilege. *F1000 Biol Rep*. 2010;2.

25. Sakamoto T, Ishibashi T. Hyalocytes: essential cells of the vitreous cavity in vitreoretinal pathophysiology? *Retina*. 2011;31:222-228.

26. Caspi RR. A look at autoimmunity and inflammation in the eye. *J Clin Invest*. 2010;120:3073-3083.

27. Berger JF, Fine SL, Maguire MG. Macular Biology. In: *Age-Related Macular Degeneration*. 1st ed. Philadelphia: Mosby; 1999:1-16.

28. Kolb H. Glial Cells of the Retina. In: *Webvision: The organization of the retina and visual system. http://webvision.med.utah.edu/*; 1995.

29. Kolb H. Outer Plexiform Layer. In: *Webvision: The organization of the retina and visual system. http://webvision.med.utah.edu/*; 1995.

30. Kolb H. Inner Plexiform Layer. In: *Webvision: The organization of the retina and visual system. http://webvision.med.utah.edu/*; 1995.

31. Shechter R, London A, Schwartz M. Orchestrated leukocyte recruitment to immune-privileged sites: absolute barriers versus educational gates. *Nat Rev Immunol*. 2013;13:206-218.

32. Mendes-Jorge L, Ramos D, Luppo M, et al. Scavenger function of resident autofluorescent perivascular macrophages and their contribution to the maintenance of the blood-retinal barrier. *Invest Ophthalmol Vis Sci*. 2009;50:5997-6005.

33. Xu H, Dawson R, Forrester JV, Liversidge J. Identification of novel dendritic cell populations in normal mouse retina. *Invest Ophthalmol Vis Sci*. 2007;48:1701-1710.

34. Lehmann U, Heuss ND, McPherson SW, Roehrich H, Gregerson DS. Dendritic cells are early responders to retinal injury. *Neurobiol Dis*. 2010;40:177-184.

35. Ransohoff RM, Perry VH. Microglial physiology: unique stimuli, specialized responses. *Annu Rev Immunol*. 2009;27:119-145.

36. Perry VH, Teeling J. Microglia and macrophages of the central nervous system: the contribution of microglia priming and systemic inflammation to chronic neurodegeneration. *Semin Immunopathol*. 2013;35:601-612.

37. Strauss O. The retinal pigment epithelium in visual function. *Physiol Rev*. 2005;85:845-881.

38. Kevany BM, Palczewski K. Phagocytosis of Retinal Rod and Cone Photoreceptors. *Physiology*. 2010;25:8-15.

39. Kaylor JJ, Yuan Q, Cook J, et al. Identification of DES1 as a vitamin A isomerase in Muller glial cells of the retina. *Nat Chem Biol*. 2013;9:30-36.

40. Anderson DH, Mullins RF, Hageman GS, Johnson LV. Perspective - A role for local inflammation in the formation of drusen in the aging eye. *American Journal of Ophthalmology*. 2002;134:411-431.

41. Bird AEC, Bressler NM, Bressler SB, et al. An International Classification and Grading System for Age-Related Maculopathy and Age-Related Macular Degeneration. *Survey of Ophthalmology*. 1995;39:367-374.

42. Streilein JW. Ocular immune privilege: the eye takes a dim but practical view of immunity and inflammation. *J Leukoc Biol*. 2003;74:179-185.

43. Streilein JW. Immune regulation and the eye: a dangerous compromise. *FASEB J*. 1987;1:199-208.

44. Streilein JW. Anterior chamber associated immune deviation: the privilege of immunity in the eye. *Surv Ophthalmol*. 1990;35:67-73.

45. Streilein JW, Ksander BR, Taylor AW. Immune deviation in relation to ocular immune privilege. *J Immunol*. 1997;158:3557-3560.

46. Streilein JW, Ma N, Wenkel H, Ng TF, Zamiri P. Immunobiology and privilege of neuronal retina and pigment epithelium transplants. *Vision Res*. 2002;42:487-495.

47. Zamiri P, Sugita S, Streilein JW. Immunosuppressive properties of the pigmented epithelial cells and the subretinal space. *Chem Immunol Allergy*. 2007;92:86-93.

48. Morohoshi K, Goodwin AM, Ohbayashi M, Ono SJ. Autoimmunity in retinal degeneration: autoimmune retinopathy and age-related macular degeneration. *J Autoimmun*. 2009;33:247-254.

49. Kaur C, Foulds WS, Ling EA. Blood-retinal barrier in hypoxic ischaemic conditions: basic concepts, clinical features and management. *Prog Retin Eye Res*. 2008;27:622-647.

50. Klaassen I, van Noorden CJ, Schlingemann RO. Molecular basis of the inner blood-retinal barrier and its breakdown in diabetic macular edema and other pathological conditions. *Prog Retin Eye Res*. 2013;34:19-48.

51. Abe T, Sugano E, Saigo Y, Tamai M. Interleukin-1beta and barrier function of retinal pigment epithelial cells (ARPE-19): aberrant expression of junctional complex molecules. *Invest Ophthalmol Vis Sci*. 2003;44:4097-4104.

52. Rizzolo LJ, Peng S, Luo Y, Xiao W. Integration of tight junctions and claudins with the barrier functions of the retinal pigment epithelium. *Prog Retin Eye Res*. 2011;30:296-323.

53. Capaldo CT, Nusrat A. Cytokine regulation of tight junctions. *Biochim Biophys Acta*. 2009;1788:864-871.

54. Peng S, Gan G, Rao VS, Adelman RA, Rizzolo LJ. Effects of proinflammatory cytokines on the claudin-19 rich tight junctions of human retinal pigment epithelium. *Invest Ophthalmol Vis Sci*. 2012;53:5016-5028.

55. Zech JC, Pouvreau I, Cotinet A, Goureau O, Le VB, de KY. Effect of cytokines and nitric oxide on tight junctions in cultured rat retinal pigment epithelium. *Invest Ophthalmol Vis Sci*. 1998;39:1600-1608.

56. Stewart PA, Tuor UI. Blood-eye barriers in the rat: correlation of ultrastructure with function. *J Comp Neurol*. 1994;340:566-576.

57. Sa-Pereira I, Brites D, Brito MA. Neurovascular unit: a focus on pericytes. *Mol Neurobiol*. 2012;45:327-347.

58. Sakagami K, Wu DM, Puro DG. Physiology of rat retinal pericytes: modulation of ion channel activity by serum-derived molecules. *J Physiol*. 1999;521 Pt 3:637-650.

59. Hughes S, Gardiner T, Hu P, Baxter L, Rosinova E, Chan-Ling T. Altered pericyte-endothelial relations in the rat retina during aging: implications for vessel stability. *Neurobiol Aging*. 2006;27:1838-1847.

60. Bell RD, Winkler EA, Sagare AP, et al. Pericytes control key neurovascular functions and neuronal phenotype in the adult brain and during brain aging. *Neuron*. 2010;68:409-427.

61. Augustin AJ, Kirchhof J. Inflammation and the pathogenesis of age-related macular degeneration. *Expert Opin Ther Targets*. 2009;13:641-651.

62. Penfold PL, Madigan MC, Gillies MC, Provis JM. Immunological and aetiological aspects of macular degeneration. *Prog Retin Eye Res*. 2001;20:385-414.

63. Ghassemifar R, Lai CM, Rakoczy PE. VEGF differentially regulates transcription and translation of ZO-1alpha+ and ZO-1alpha- and mediates trans-epithelial resistance in cultured endothelial and epithelial cells. *Cell Tissue Res*. 2006;323:117-125.

64. Hori J. Mechanisms of immune privilege in the anterior segment of the eye: what we learn from corneal transplantation. *J Ocul Biol Dis Infor*. 2008;1:94-100.

65. Jiang LQ, Streilein JW. Immune privilege extended to allogeneic tumor cells in the vitreous cavity. *Invest Ophthalmol Vis Sci*. 1991;32:224-228.

66. Wenkel H, Streilein JW. Analysis of immune deviation elicited by antigens injected into the subretinal space. *Invest Ophthalmol Vis Sci*. 1998;39:1823-1834.

67. Wenkel H, Chen PW, Ksander BR, Streilein JW. Immune privilege is extended, then withdrawn, from allogeneic tumor cell grafts placed in the subretinal space. *Invest Ophthalmol Vis Sci*. 1999;40:3202-3208.

68. Sonoda KH, Sakamoto T, Qiao H, et al. The analysis of systemic tolerance elicited by antigen inoculation into the vitreous cavity: vitreous cavity-associated immune deviation. *Immunology*. 2005;116:390-399.

69. Detrick B, Hooks JJ. Immune regulation in the retina. *Immunol Res*. 2010;47:153-161.

70. Streilein JW, Wilbanks GA, Taylor A, Cousins S. Eye-derived cytokines and the immunosuppressive intraocular microenvironment: a review. *Curr Eye Res*. 1992;11 Suppl:41-47.

71. Zamiri P, Masli S, Streilein JW, Taylor AW. Pigment epithelial growth factor suppresses inflammation by modulating macrophage activation. *Invest Ophthalmol Vis Sci*. 2006;47:3912-3918.

72. Holtkamp GM, Kijlstra A, Peek R, de Vos AF. Retinal pigment epithelium-immune system interactions: cytokine production and cytokine-induced changes. *Prog Retin Eye Res*. 2001;20:29-48.

73. Xu H, Chen M, Forrester JV. Para-inflammation in the aging retina. *Prog Retin Eye Res*. 2009;28:348-368.

74. Anderson DH, Radeke MJ, Gallo NB, et al. The pivotal role of the complement system in aging and age-related macular degeneration: hypothesis re-visited. *Prog Retin Eye Res*. 2010;29:95-112.

75. Dunkelberger JR, Song WC. Complement and its role in innate and adaptive immune responses. *Cell Research*. 2010;20:34-50.

76. Issa PC, Scholl HPN, Holz FG, Knolle P, Kurts C. The complement system and its possible role in the pathogenesis of age-related macular degeneration (AMD). *Ophthalmologe*. 2005;102:1036-+.

77. Cruvinel WM, Mesquita D, Jr., Araujo JA, et al. Immune system - part I. Fundamentals of innate immunity with emphasis on molecular and cellular mechanisms of inflammatory response. *Rev Bras Reumatol*. 2010;50:434-461.

78. Fett AL, Hermann MM, Muether PS, Kirchhof B, Fauser S. Immunohistochemical localization of complement regulatory proteins in the human retina. *Histol Histopathol*. 2012;27:357-364.

79. Singh A, Faber C, Falk M, Nissen MH, Hviid TV, Sorensen TL. Altered Expression of CD46 and CD59 on Leukocytes in Neovascular Age-Related Macular Degeneration. *Am J Ophthalmol*. 2012;154:193-199.

80. Ransohoff RM, Cardona AE. The myeloid cells of the central nervous system parenchyma. *Nature*. 2010;468:253-262.

81. Ginhoux F, Greter M, Leboeuf M, et al. Fate mapping analysis reveals that adult microglia derive from primitive macrophages. *Science*. 2010;330:841-845.

82. Ginhoux F, Lim S, Hoeffel G, Low D, Huber T. Origin and differentiation of microglia. *Front Cell Neurosci*. 2013;7:45.

83. Kaneko H, Nishiguchi KM, Nakamura M, Kachi S, Terasaki H. Characteristics of bone marrow-derived microglia in the normal and injured retina. *Invest Ophthalmol Vis Sci*. 2008;49:4162-4168.

84. Kezic J, Xu H, Chinnery HR, Murphy CC, McMenamin PG. Retinal microglia and uveal tract dendritic cells and macrophages are not CX3CR1 dependent in their recruitment and distribution in the young mouse eye. *Invest Ophthalmol Vis Sci*. 2008;49:1599-1608.

85. Kezic JM, McMenamin PG. The effects of CX3CR1 deficiency and irradiation on the homing of monocyte-derived cell populations in the mouse eye. *PLoS One*. 2013;8:e68570.

86. Karlstetter M, Ebert S, Langmann T. Microglia in the healthy and degenerating retina: insights from novel mouse models. *Immunobiology*. 2010;215:685-691.

87. Harada T, Harada C, Kohsaka S, et al. Microglia-Muller glia cell interactions control neurotrophic factor production during light-induced retinal degeneration. *J Neurosci*. 2002;22:9228-9236.

88. Srinivasan B, Roque CH, Hempstead BL, Al-Ubaidi MR, Roque RS. Microglia-derived pronerve growth factor promotes photoreceptor cell death via p75 neurotrophin receptor. *J Biol Chem*. 2004;279:41839-41845.

89. Ritter MR, Banin E, Moreno SK, Aguilar E, Dorrell MI, Friedlander M. Myeloid progenitors differentiate into microglia and promote vascular repair in a model of ischemic retinopathy. *J Clin Invest*. 2006;116:3266-3276.

90. Nimmerjahn A, Kirchhoff F, Helmchen F. Resting microglial cells are highly dynamic surveillants of brain parenchyma in vivo. *Science*. 2005;308:1314-1318.

91. Langmann T. Microglia activation in retinal degeneration. *J Leukoc Biol*. 2007;81:1345-1351.

92. Sugita S. Role of ocular pigment epithelial cells in immune privilege. *Arch Immunol Ther Exp (Warsz)*. 2009;57:263-268.

93. Kierdorf K, Prinz M. Factors regulating microglia activation. *Front Cell Neurosci*. 2013;7:44.

94. Perry VH, Nicoll JA, Holmes C. Microglia in neurodegenerative disease. *Nat Rev Neurol*. 2010;6:193-201.

95. Mantovani A, Locati M, Uguccioni M. Chemokines in immunopathology: From dark sides to clinical translation. *Immunol Lett*. 2012;145:1.

96. Mosser DM, Edwards JP. Exploring the full spectrum of macrophage activation. *Nat Rev Immunol*. 2008;8:958-969.

97. Mantovani A, Biswas SK, Galdiero MR, Sica A, Locati M. Macrophage plasticity and polarization in tissue repair and remodelling. *J Pathol*. 2013;229:176-185.

98. Mantovani A, Sica A, Sozzani S, Allavena P, Vecchi A, Locati M. The chemokine system in diverse forms of macrophage activation and polarization. *Trends Immunol*. 2004;25:677-686.

99. Ferrante CJ, Pinhal-Enfield G, Elson G, et al. The adenosine-dependent angiogenic switch of macrophages to an M2-like phenotype is independent of interleukin-4 receptor alpha (IL-4Ralpha) signaling. *Inflammation*. 2013;36:921-931.

100. Kadl A, Meher AK, Sharma PR, et al. Identification of a novel macrophage phenotype that develops in response to atherogenic phospholipids via Nrf2. *Circ Res*. 2010;107:737-746.

101. Gleissner CA. Macrophage Phenotype Modulation by CXCL4 in Atherosclerosis. *Front Physiol*. 2012;3:1.

102. Gomez CR, Boehmer ED, Kovacs EJ. The aging innate immune system. *Curr Opin Immunol*. 2005;17:457-462.

103. Zealley B, de Grey AD. Commentary on Some Recent Theses Relevant to Combating Aging: December 2013. *Rejuvenation Res*. 2013.

104. Ramrattan RS, van der Schaft TL, Mooy CM, de Bruijn WC, Mulder PG, de Jong PT. Morphometric analysis of Bruch's membrane, the choriocapillaris, and the choroid in aging. *Invest Ophthalmol Vis Sci*. 1994;35:2857-2864.

105. Bhutto I, Lutty G. Understanding age-related macular degeneration (AMD): relationships between the photoreceptor/retinal pigment epithelium/Bruch's membrane/choriocapillaris complex. *Mol Aspects Med*. 2012;33:295-317.

106. Dollery CT, Bulpitt CJ, Kohner EM. Oxygen supply to the retina from the retinal and choroidal circulations at normal and increased arterial oxygen tensions. *Invest Ophthalmol*. 1969;8:588-594.

107. Hussain AA, Starita C, Hodgetts A, Marshall J. Macromolecular diffusion characteristics of ageing human Bruch's membrane: implications for age-related macular degeneration (AMD). *Exp Eye Res*. 2010;90:703-710.

108. Feeney-Burns L, Ellersieck MR. Age-related changes in the ultrastructure of Bruch's membrane. *Am J Ophthalmol*. 1985;100:686-697.

109. Pauleikhoff D, Sheraidah G, Marshall J, Bird AC, Wessing A. [Biochemical and histochemical analysis of age related lipid deposits in Bruch's membrane]. *Ophthalmologe*. 1994;91:730-734.

110. Kamei M, Hollyfield JG. TIMP-3 in Bruch's membrane: changes during aging and in age-related macular degeneration. *Invest Ophthalmol Vis Sci*. 1999;40:2367-2375.

111. Beattie JR, Pawlak AM, Boulton ME, et al. Multiplex analysis of age-related protein and lipid modifications in human Bruch's membrane. *FASEB J*. 2010;24:4816-4824.

112. Berger JF, Fine SL, Maguire MG. Natural History. In: *Age-Related Macular Degeneration*. 1st ed. Philadelphia: Mosby; 1999:1-16.

113. Bjornsson OM, Syrdalen P, Bird AC, Peto T, Kinge B. The prevalence of age-related maculopathy (ARM) in an urban Norwegian population: the Oslo Macular Study. *Acta Ophthalmologica Scandinavica*. 2006;84:636-641.

114. Klaver CCW, Assink JJM, van Leeuwen R, et al. Incidence and progression rates of age-related maculopathy: The Rotterdam study. *Investigative Ophthalmology & Visual Science*. 2001;42:2237-2241.

115. Klein R. Overview of progress in the epidemiology of age-related macular degeneration. *Ophthalmic Epidemiol*. 2007;14:184-187.

116. Franceschi C, Bonafe M, Valensin S, et al. Inflamm-aging - An evolutionary perspective on immunosenescence. *Molecular and Cellular Gerontology*. 2000;908:244-254.

117. Min H, Montecino-Rodriguez E, Dorshkind K. Effects of aging on early B- and T-cell development. *Immunol Rev*. 2005;205:7-17.

118. Haynes L, Swain SL. Why aging T cells fail: implications for vaccination. *Immunity*. 2006;24:663-666.

119. Dorshkind K, Montecino-Rodriguez E, Signer RA. The ageing immune system: is it ever too old to become young again? *Nat Rev Immunol*. 2009;9:57-62.

120. Xu H, Chen M, Manivannan A, Lois N, Forrester JV. Age-dependent accumulation of lipofuscin in perivascular and subretinal microglia in experimental mice. *Aging Cell*. 2008;7:58-68.

121. Hart AD, Wyttenbach A, Perry VH, Teeling JL. Age related changes in microglial phenotype vary between CNS regions: grey versus white matter differences. *Brain Behav Immun*. 2012;26:754-765.

122. Damani MR, Zhao L, Fontainhas AM, Amaral J, Fariss RN, Wong WT. Age-related alterations in the dynamic behavior of microglia. *Aging Cell*. 2011;10:263-276.

123. Medzhitov R. Origin and physiological roles of inflammation. *Nature*. 2008;454:428-435.

124. Andersen N. Prevalence of age-related maculopathy and age-related macular degeneration among the Inuit in Greenland. The Greenland Inuit Eye Study. *Acta Ophthalmologica*. 2008;86:44.

125. Casaroli-Marano R, Pinero A, Adan A, et al. Prevalence of age-related macular degeneration in Spain. *British Journal of Ophthalmology*. 2011;95:931-936.

126. Friedman DS, O'Colmain B, Tomany SC, et al. Prevalence of age-related macular degeneration in the United States. *Archives of Ophthalmology*. 2004;122:564-572.

127. Ding X, Patel M, Chan CC. Molecular pathology of age-related macular degeneration. *Prog Retin Eye Res*. 2009;28:1-18.

128. Lotery A. Progress in understanding and treating age-related macular degeneration. *Eye (Lond)*. 2008;22:739-741.

129. Hammond CJ, Webster AR, Snieder H, Bird AC, Gilbert CE, Spector TD. Genetic influence on early age-related macular degeneration: a population-based twin study. *Investigative Ophthalmology & Visual Science*. 2001;42:S310.

130. Coleman HR, Chan CC, Ferris FL, III, Chew EY. Age-related macular degeneration. *Lancet*. 2008;372:1835-1845.

131. Coleman AL, Yu F. Eye-related medicare costs for patients with age-related macular degeneration from 1995 to 1999. *Ophthalmology*. 2008;115:18-25.

132. Pons M, Marin-Castano ME. Cigarette Smoke-Related Hydroquinone Dysregulates MCP-1, VEGF and PEDF Expression in Retinal Pigment Epithelium in Vitro and in Vivo. *Plos One*. 2011;6.

133. Chakravarthy U, Augood C, Bentham GC, et al. Cigarette smoking and age-related macular degeneration in the EUREYE study. *Ophthalmology*. 2007;114:1157-1163.

134. Dhubhghaill SSN, Cahill MT, Campbell M, Cassidy L, Humphries MM, Humphries P. The Pathophysiology of Cigarette Smoking and Age-Related Macular Degeneration. *Retinal Degenerative Diseases: Laboratory and Therapeutic Investigations*. 2010;664:437-446.

135. Khan JC, Thurlby DA, Shahid H, et al. Smoking and age related macular degeneration: the number of pack years of cigarette smoking is a major determinant of risk for both geographic atrophy and choroidal neovascularisation. *British Journal of Ophthalmology*. 2006;90:75-80.

136. Bertram KM, Baglole CJ, Phipps RP, Libby RT. Molecular regulation of cigarette smoke induced-oxidative stress in human retinal pigment epithelial cells: implications for age-related macular degeneration. *American Journal of Physiology-Cell Physiology*. 2009;297:C1200-C1210.

137. Seddon JM, Chew EY, Klein R, Clemons TE. Is cholesterol a risk factor for progression to advanced AMD? *Investigative Ophthalmology & Visual Science*. 2002;43:U437.

138. Seddon JM, Cote J, Rosner B. Progression of age-related macular degeneration - Association with dietary fat, transunsaturated fat, nuts, and fish intake. *Archives of Ophthalmology*. 2003;121:1728-1737.

139. Krishnadev N, Meleth AD, Chew EY. Nutritional supplements for age-related macular degeneration. *Current Opinion in Ophthalmology*. 2010;21:184-189.

140. Klein RJ, Zeiss C, Chew EY, et al. Complement factor H polymorphism in age-related macular degeneration. *Science*. 2005;308:385-389.

141. Lotery A, Trump D. Progress in defining the molecular biology of age related macular degeneration. *Hum Genet*. 2007;122:219-236.

142. Pei XT, Li XX, Bao YZ, et al. Association of c3 gene polymorphisms with neovascular age-related macular degeneration in a chinese population. *Curr Eye Res*. 2009;34:615-622.

143. Combadiere C, Feumi C, Raoul W, et al. CX3CR1-dependent subretinal microglia cell accumulation is associated with cardinal features of age-related macular degeneration. *J Clin Invest*. 2007;117:2920-2928.

144. Despriet DD, Bergen AA, Merriam JE, et al. Comprehensive analysis of the candidate genes CCL2, CCR2, and TLR4 in age-related macular degeneration. *Invest Ophthalmol Vis Sci*. 2008;49:364-371.

145. Goverdhan SV, Howell MW, Mullins RF, et al. Association of HLA class I and class II polymorphisms with age-related macular degeneration. *Invest Ophthalmol Vis Sci*. 2005;46:1726-1734.

146. Curcio CA, Millican CL. Basal linear deposit and large drusen are specific for early age-related maculopathy. *Archives of Ophthalmology*. 1999;117:329-339.

147. Sarks JP, Sarks SH, Killingsworth MC. Evolution of Soft Drusen in Age-Related Macular Degeneration. *Eye*. 1994;8:269-283.

148. Kliffen M, VanderSchaft TL, Mooy CM, Dejong PTVM. Morphologic changes in age-related maculopathy. *Microscopy Research and Technique*. 1997;36:106-122.

149. Hageman GS, Mullins RF. Molecular composition of drusen as related to substructural phenotype. *Molecular Vision*. 1999;5.

150. Kochounian H, Johnson LV, Fong HK. Accumulation of extracellular RGR-d in Bruch's membrane and close association with drusen at intercapillary regions. *Exp Eye Res*. 2009;88:1129-1136.

151. Lengyel I, Tufail A, Hosaini HA, Luthert P, Bird AC, Jeffery G. Association of drusen deposition with choroidal intercapillary pillars in the aging human eye. *Invest Ophthalmol Vis Sci*. 2004;45:2886-2892.

152. Mullins RF, Johnson MN, Faidley EA, Skeie JM, Huang J. Choriocapillaris vascular dropout related to density of drusen in human eyes with early age-related macular degeneration. *Invest Ophthalmol Vis Sci*. 2011;52:1606-1612.

153. Bressler NM, Silva JC, Bressler SB, Fine SL, Green WR. Clinicopathological Correlation of Drusen and Retinal-Pigment Epithelial Abnormalities in Age-Related Macular Degeneration. *Retina-the Journal of Retinal and Vitreous Diseases*. 1994;14:130-142.

154. Midena E, Segato T, Blarzino MC, Angeli CD. Macular Drusen and the Sensitivity of the Central Visual-Field. *Documenta Ophthalmologica*. 1994;88:179-185.

155. Curcio CA, Johnson M, Huang JD, Rudolf M. Aging, age-related macular degeneration, and the response-to-retention of apolipoprotein B-containing lipoproteins. *Prog Retin Eye Res*. 2009;28:393-422.

156. Johnson LV, Ozaki S, Staples MK, Erickson PA, Anderson DH. A potential role for immune complex pathogenesis in drusen formation. *Experimental Eye Research*. 2000;70:441-449.

157. Grossniklaus HE, Ling JX, Wallace TM, et al. Macrophage and retinal pigment epithelium expression of angiogenic cytokines in choroidal neovascularization. *Molecular Vision*. 2002;8:119-126.

158. Tomany SC, Wang HJ, van Leeuwen R, et al. Risk factors for incident age-related macular degeneration - Pooled findings from 3 continents. *Ophthalmology*. 2004;111:1280-1287.

159. Lewis H, Straatsma BR, Foos RY, Lightfoot DO. Reticular Degeneration of the Pigment-Epithelium. *Ophthalmology*. 1985;92:1485-1495.

160. Sallo FB, Rechtman E, Peto T, et al. Functional aspects of drusen regression in age-related macular degeneration. *British Journal of Ophthalmology*. 2009;93:1345-1350.

161. Gass JDM. Drusen and Disciform Macular Detachment and Degeneration. *Archives of Ophthalmology*. 1973;90:206-217.

162. Sunness JS, Bressler NM, Maguire MG. Scanning Laser Ophthalmoscopic Analysis of the Pattern of Visual-Loss in Age-Related Geographic Atrophy of the Macula. *American Journal of Ophthalmology*. 1995;119:143-151.

163. Elman MJ, Fine SL, Murphy RP, Patz A, Auer C. The Natural-History of Serous Retinal-Pigment Epithelium Detachment in Patients with Age-Related Macular Degeneration. *Ophthalmology*. 1986;93:224-230.

164. Killingsworth MC, Sarks SH. Giant-Cells in Disciform Macular Degeneration of the Human-Eye. *Micron*. 1982;13:359-360.

165. Killingsworth MC, Sarks JP, Sarks SH. Macrophages Related to Bruchs Membrane in Age-Related Macular Degeneration. *Eye*. 1990;4:613-621.

166. Berger JF, Fine SL, Maguire MG. Geographic Atrophy. In: *Age-Related Macular Degeneration*. 1st ed. Philadelphia: Mosby; 1999:1-16.

167. Spilsbury K, Garrett KL, Shen WY, Constable IJ, Rakoczy PE. Overexpression of vascular endothelial growth factor (VEGF) in the retinal pigment epithelium leads to the development of choroidal neovascularization. *Am J Pathol*. 2000;157:135-144.

168. Ma W, Zhao L, Fontainhas AM, Fariss RN, Wong WT. Microglia in the mouse retina alter the structure and function of retinal pigmented epithelial cells: a potential cellular interaction relevant to AMD. *PLoS One*. 2009;4:e7945.

169. Grunwald JE, Daniel E, Ying GS, et al. Photographic assessment of baseline fundus morphologic features in the Comparison of Age-Related Macular Degeneration Treatments Trials. *Ophthalmology*. 2012;119:1634-1641.

170. Kurihara T, Westenskow PD, Bravo S, Aguilar E, Friedlander M. Targeted deletion of Vegfa in adult mice induces vision loss. *J Clin Invest*. 2012;122:4213-4217.

171. Ambati J, Anand A, Fernandez S, et al. An animal model of age-related macular degeneration in senescent Ccl-2- or Ccr-2-deficient mice. *Nat Med*. 2003;9:1390-1397.

172. Espinosa-Heidmann DG, Suner IJ, Hernandez EP, Monroy D, Csaky KG, Cousins SW. Macrophage depletion diminishes lesion size and severity in experimental choroidal neovascularization. *Invest Ophthalmol Vis Sci*. 2003;44:3586-3592.

173. Sakurai E, Anand A, Ambati BK, van RN, Ambati J. Macrophage depletion inhibits experimental choroidal neovascularization. *Invest Ophthalmol Vis Sci*. 2003;44:3578-3585.

174. Cherepanoff S, McMenamin P, Gillies MC, Kettle E, Sarks SH. Bruch's membrane and choroidal macrophages in early and advanced age-related macular degeneration. *Br J Ophthalmol*. 2010;94:918-925.

175. Penfold PL, Killingsworth MC, Sarks SH. Senile Macular Degeneration - the Involvement of Giant-Cells in Atrophy of the Retinal-Pigment Epithelium. *Investigative Ophthalmology & Visual Science*. 1986;27:364-371.

176. Wang Y, Wang VM, Chan CC. The role of anti-inflammatory agents in age-related macular degeneration (AMD) treatment. *Eye (Lond)*. 2011;25:127-139.

177. Landa G, Amde W, Doshi V, et al. Comparative Study of Intravitreal Bevacizumab (Avastin) versus Ranibizumab (Lucentis) in the Treatment of Neovascular Age-Related Macular Degeneration. *Ophthalmologica*. 2009;223:370-375.

178. Miller JW. Treatment of age-related macular degeneration: beyond VEGF. *Jpn J Ophthalmol*. 2010;54:523-528.

179. Brouzas D, Koutsandrea C, Moschos M, Papadimitriou S, Ladas I, Apostolopoulos M. Massive choroidal hemorrhage after intravitreal administration of bevacizumab (Avastin) for AMD followed by controlateral sympathetic ophthalmia. *Clin Ophthalmol*. 2009;3:457-459.

180. Shima C, Sakaguchi H, Gomi F, et al. Complications in patients after intravitreal injection of bevacizumab. *Acta Ophthalmol*. 2008;86:372-376.

181. Mitchell P. A systematic review of the efficacy and safety outcomes of anti-VEGF agents used for treating neovascular age-related macular degeneration: comparison of ranibizumab and bevacizumab. *Current Medical Research and Opinion*. 2011;27:1465-1475.

182. Barzelay A, Lowenstein A, George J, Barak A. Influence of Non-Toxic Doses of Bevacizumab and Ranibizumab on Endothelial Functions and Inhibition of Angiogenesis. *Current Eye Research*. 2010;35:835-841.

183. Biswas P, Sengupta S, Choudhary R, Home S, Paul A, Sinha S. Comparative role of intravitreal ranibizumab versus bevacizumab in choroidal neovascular membrane in age-related macular degeneration. *Indian Journal of Ophthalmology*. 2011;59:191-196.

184. Donoso LA, Kim D, Frost A, Callahan A, Hageman G. The role of inflammation in the pathogenesis of age-related macular degeneration. *Surv Ophthalmol*. 2006;51:137-152.

185. Penfold PL, Killingsworth MC, Sarks SH. Senile Macular Degeneration - the Involvement of Immunocompetent Cells. *Graefes Archive for Clinical and Experimental Ophthalmology*. 1985;223:69-76.

186. Penfold PL, Provis JM, Billson FA. Age-related macular degeneration: ultrastructural studies of the relationship of leucocytes to angiogenesis. *Graefes Arch Clin Exp Ophthalmol*. 1987;225:70-76.

187. Tuo J, Grob S, Zhang K, Chan CC. Genetics of immunological and inflammatory components in age-related macular degeneration. *Ocul Immunol Inflamm*. 2012;20:27-36.

188. Mullins RF, Faidley EA, Daggett HT, Jomary C, Lotery AJ, Stone EM. Localization of complement 1 inhibitor (C1INH/SERPING1) in human eyes with age-related macular degeneration. *Exp Eye Res*. 2009;89:767-773.

189. Gibson J, Hakobyan S, Cree AJ, et al. Variation in complement component C1 inhibitor in age-related macular degeneration. *Immunobiology*. 2012;217:251-255.

190. Fukumoto M, Nakaizumi A, Zhang T, Lentz SI, Shibata M, Puro DG. Vulnerability of the retinal microvasculature to oxidative stress: ion channel-dependent mechanisms. *Am J Physiol Cell Physiol*. 2012;302:C1413-C1420.

191. Pennesi ME, Neuringer M, Courtney RJ. Animal models of age related macular degeneration. *Mol Aspects Med*. 2012;33:487-509.

192. Crabb JW, Miyagi M, Gu X, et al. Drusen proteome analysis: an approach to the etiology of age-related macular degeneration. *Proc Natl Acad Sci U S A*. 2002;99:14682-14687.

193. Gu X, Meer SG, Miyagi M, et al. Carboxyethylpyrrole protein adducts and autoantibodies, biomarkers for age-related macular degeneration. *J Biol Chem*. 2003;278:42027-42035.

194. Hollyfield JG, Bonilha VL, Rayborn ME, et al. Oxidative damage-induced inflammation initiates age-related macular degeneration. *Nat Med*. 2008;14:194-198.

195. Hollyfield JG. Age-related macular degeneration: the molecular link between oxidative damage, tissue-specific inflammation and outer retinal disease: the Proctor lecture. *Invest Ophthalmol Vis Sci*. 2010;51:1275-1281.

196. Hollyfield JG, Perez VL, Salomon RG. A hapten generated from an oxidation fragment of docosahexaenoic acid is sufficient to initiate age-related macular degeneration. *Mol Neurobiol*. 2010;41:290-298.

197. Ebrahem Q, Renganathan K, Sears J, et al. Carboxyethylpyrrole oxidative protein modifications stimulate neovascularization: Implications for age-related macular degeneration. *Proc Natl Acad Sci U S A*. 2006;103:13480-13484.

198. West XZ, Malinin NL, Merkulova AA, et al. Oxidative stress induces angiogenesis by activating TLR2 with novel endogenous ligands. *Nature*. 2010;467:972-976.

199. Sarks SH. Drusen and Their Relationship to Senile Macular Degeneration. *Australian Journal of Ophthalmology*. 1980;8:117-130.

200. Luhmann UF, Lange CA, Robbie S, et al. Differential modulation of retinal degeneration by Ccl2 and Cx3cr1 chemokine signalling. *PLoS One*. 2012;7:e35551.

201. Cao X, Shen D, Patel MM, et al. Macrophage polarization in the maculae of age-related macular degeneration: a pilot study. *Pathol Int*. 2011;61:528-535.

202. Sparrow JR, Boulton M. RPE lipofuscin and its role in retinal pathobiology. *Exp Eye Res*. 2005;80:595-606.

203. Luhmann UF, Robbie S, Munro PM, et al. The drusenlike phenotype in aging Ccl2-knockout mice is caused by an accelerated accumulation of swollen autofluorescent subretinal macrophages. *Invest Ophthalmol Vis Sci*. 2009;50:5934-5943.

204. Tuo J, Smith BC, Bojanowski CM, et al. The involvement of sequence variation and expression of CX3CR1 in the pathogenesis of age-related macular degeneration. *FASEB J*. 2004;18:1297-1299.

205. Lu X, Kang YB. Chemokine (C-C Motif) Ligand 2 Engages CCR2(+) Stromal Cells of Monocytic Origin to Promote Breast Cancer Metastasis to Lung and Bone. *Journal of Biological Chemistry*. 2009;284:29087-29096.

206. Prinz M, Priller J. Tickets to the brain: Role of CCR2 and CX(3)CR1 in myeloid cell entry in the CNS. *Journal of Neuroimmunology*. 2010;224:80-84.

207. Tuo J, Bojanowski CM, Zhou M, et al. Murine ccl2/cx3cr1 deficiency results in retinal lesions mimicking human age-related macular degeneration. *Invest Ophthalmol Vis Sci*. 2007;48:3827-3836.

208. Ross RJ, Zhou M, Shen D, et al. Immunological protein expression profile in Ccl2/Cx3cr1 deficient mice with lesions similar to age-related macular degeneration. *Exp Eye Res*. 2008;86:675-683.

209. Cruz-Guilloty F, Saeed AM, Echegaray JJ, et al. Infiltration of proinflammatory m1 macrophages into the outer retina precedes damage in a mouse model of age-related macular degeneration. *Int J Inflam*. 2013;2013:503725.

210. Luhmann UF, Carvalho LS, Robbie SJ, et al. Ccl2, Cx3cr1 and Ccl2/Cx3cr1 chemokine deficiencies are not sufficient to cause age-related retinal degeneration. *Exp Eye Res*. 2013;107:80-87.

211. Mattapallil MJ, Wawrousek EF, Chan CC, et al. The Rd8 mutation of the Crb1 gene is present in vendor lines of C57BL/6N mice and embryonic stem cells, and confounds ocular induced mutant phenotypes. *Invest Ophthalmol Vis Sci*. 2012;53:2921-2927.

212. Dace DS, Khan AA, Kelly J, Apte RS. Interleukin-10 promotes pathological angiogenesis by regulating macrophage response to hypoxia during development. *PLoS One*. 2008;3:e3381.

213. Jawad S, Liu B, Li Z, et al. The role of macrophage class a scavenger receptors in a laser-induced murine choroidal neovascularization model. *Invest Ophthalmol Vis Sci*. 2013;54:5959-5970.

214. Horie S, Robbie SJ, Liu J, et al. CD200R signaling inhibits pro-angiogenic gene expression by macrophages and suppresses choroidal neovascularization. *Sci Rep*. 2013;3:3072.

215. Zhao H, Roychoudhury J, Doggett TA, Apte RS, Ferguson TA. Age-dependent changes in FasL (CD95L) modulate macrophage function in a model of age-related macular degeneration. *Invest Ophthalmol Vis Sci*. 2013;54:5321-5331.

216. Dumonde DC, Kaspgrochowska E, Banga JP, et al. Autoimmune Mechanisms in Inflammatory Eye Disease. *Transactions of the Ophthalmological Societies of the United Kingdom*. 1985;104:232-238.

217. Nimmerjahn F, Ravetch JV. Antibody-mediated modulation of immune responses. *Immunol Rev*. 2010;236:265-275.

218. Oakey RJ, Howard TA, Hogarth PM, Tani K, Seldin MF. Chromosomal mapping of the high affinity Fc gamma receptor gene. *Immunogenetics*. 1992;35:279-282.

219. Nimmerjahn F, Bruhns P, Horiuchi K, Ravetch JV. FcgammaRIV: a novel FcR with distinct IgG subclass specificity. *Immunity*. 2005;23:41-51.

220. Ravetch JV, Bolland S. IgG Fc receptors. *Annu Rev Immunol*. 2001;19:275-290.

221. Allen JM, Seed B. Isolation and expression of functional high-affinity Fc receptor complementary DNAs. *Science*. 1989;243:378-381.

222. Radaev S, Sun P. Recognition of immunoglobulins by Fcgamma receptors. *Mol Immunol*. 2002;38:1073-1083.

223. Zhang Z, Goldschmidt T, Salter H. Possible allelic structure of IgG2a and IgG2c in mice. *Mol Immunol*. 2012;50:169-171.

224. Nimmerjahn F, Ravetch JV. Divergent immunoglobulin g subclass activity through selective Fc receptor binding. *Science*. 2005;310:1510-1512.

225. Baudino L, Nimmerjahn F, Azeredo da SS, et al. Differential contribution of three activating IgG Fc receptors (FcgammaRI, FcgammaRIII, and FcgammaRIV) to IgG2a- and IgG2b-induced autoimmune hemolytic anemia in mice. *J Immunol*. 2008;180:1948-1953.

226. Ioan-Facsinay A, de Kimpe SJ, Hellwig SM, et al. FcgammaRI (CD64) contributes substantially to severity of arthritis, hypersensitivity responses, and protection from bacterial infection. *Immunity*. 2002;16:391-402.

227. Nimmerjahn F, Lux A, Albert H, et al. FcgammaRIV deletion reveals its central role for IgG2a and IgG2b activity in vivo. *Proc Natl Acad Sci U S A*. 2010;107:19396-19401.

228. Hazenbos WL, Heijnen IA, Meyer D, et al. Murine IgG1 complexes trigger immune effector functions predominantly via Fc gamma RIII (CD16). *J Immunol*. 1998;161:3026-3032.

229. Niederer HA, Willcocks LC, Rayner TF, et al. Copy number, linkage disequilibrium and disease association in the FCGR locus. *Hum Mol Genet*. 2010;19:3282-3294.

230. Dijstelbloem HM, van de Winkel JG, Kallenberg CG. Inflammation in autoimmunity: receptors for IgG revisited. *Trends Immunol*. 2001;22:510-516.

231. Pricop L, Redecha P, Teillaud JL, et al. Differential modulation of stimulatory and inhibitory Fc gamma receptors on human monocytes by Th1 and Th2 cytokines. *J Immunol*. 2001;166:531-537.

232. Tridandapani S, Wardrop R, Baran CP, et al. TGF-beta 1 suppresses myeloid Fc gamma receptor function by regulating the expression and function of the common gamma-subunit. *J Immunol*. 2003;170:4572-4577.

233. Bolland S, Ravetch JV. Spontaneous autoimmune disease in Fc(gamma)RIIB-deficient mice results from strain-specific epistasis. *Immunity*. 2000;13:277-285.

234. Takai T, Ono M, Hikida M, Ohmori H, Ravetch JV. Augmented humoral and anaphylactic responses in Fc gamma RII-deficient mice. *Nature*. 1996;379:346-349.

235. Takai T, Li M, Sylvestre D, Clynes R, Ravetch JV. FcR gamma chain deletion results in pleiotrophic effector cell defects. *Cell*. 1994;76:519-529.

236. Billadeau DD, Leibson PJ. ITAMs versus ITIMs: striking a balance during cell regulation. *J Clin Invest*. 2002;109:161-168.

237. Ghosh S, Hayden MS. New regulators of NF-kappaB in inflammation. *Nat Rev Immunol*. 2008;8:837-848.

238. Loegering DJ, Lennartz MR. Signaling pathways for Fc gamma receptor-stimulated tumor necrosis factor-alpha secretion and respiratory burst in RAW 264.7 macrophages. *Inflammation*. 2004;28:23-31.

239. Baker K, Qiao SW, Kuo T, et al. Immune and non-immune functions of the (not so) neonatal Fc receptor, FcRn. *Semin Immunopathol*. 2009;31:223-236.

240. Rath T, Kuo TT, Baker K, et al. The immunologic functions of the neonatal Fc receptor for IgG. *J Clin Immunol*. 2013;33 Suppl 1:S9-17.

241. Bruhns P. Properties of mouse and human IgG receptors and their contribution to disease models. *Blood*. 2012;119:5640-5649.

242. Kim H, Robinson SB, Csaky KG. FcRn receptor-mediated pharmacokinetics of therapeutic IgG in the eye. *Mol Vis*. 2009;15:2803-2812.

243. Powner MB, McKenzie JA, Christianson GJ, Roopenian DC, Fruttiger M. Expression of neonatal fc receptor in the eye. *Invest Ophthalmol Vis Sci*. 2014;55:1607-1615.

244. Hageman GS, Mullins RF, Russell SR, Johnson LV, Anderson DH. Vitronectin is a constituent of ocular drusen and the vitronectin gene is expressed in human retinal pigmented epithelial cells. *Faseb Journal*. 1999;13:477-484.

245. Russell SR, Mullins RF, Schneider BL, Hageman GS. Location, substructure, and composition of basal laminar drusen compared with drusen associated with aging and age-related macular degeneration. *American Journal of Ophthalmology*. 2000;129:205-214.

246. VanderSchaft TL, Mooy CM, Debruijn WC, Dejong PTVM. Early Stages of Age-Related Macular Degeneration - An Immunofluorescence and Electron-Microscopy Study. *British Journal of Ophthalmology*. 1993;77:657-661.

247. Umeda S, Suzuki MT, Okamoto H, et al. Molecular composition of drusen and possible involvement of anti-retinal autoimmunity in two different forms of macular degeneration in cynomolgus monkey (Macaca fascicularis). *FASEB J*. 2005;19:1683-1685.

248. Klejnberg T, Moraes Junior HV. [Ophthalmological alterations in outpatients with systemic lupus erythematosus]. *Arq Bras Oftalmol*. 2006;69:233-237.

249. Han DP, Sievers S. Extensive drusen in type I membranoproliferative glomerulonephritis. *Arch Ophthalmol*. 2009;127:577-579.

250. Baglio V, Gharbiya M, Balacco-Gabrieli C, et al. Choroidopathy in patients with systemic lupus erythematosus with or without nephropathy. *J Nephrol*. 2011;24:522-529.

251. Kerjaschki D, Schulze M, Binder S, et al. Trans-Cellular Transport and Membrane Insertion of the C5B-9 Membrane Attack Complex of

Complement by Glomerular Epithelial-Cells in Experimental Membranous Nephropathy. *Journal of Immunology*. 1989;143:546-552.

252. Anderson CF, Mosser DM. A novel phenotype for an activated macrophage: the type 2 activated macrophage. *J Leukoc Biol*. 2002;72:101-106.

253. Anderson CF, Gerber JS, Mosser DM. Modulating macrophage function with IgG immune complexes. *J Endotoxin Res*. 2002;8:477-481.

254. Zhang Y, Liu S, Liu J, et al. Immune complex/Ig negatively regulate TLR4-triggered inflammatory response in macrophages through Fc gamma RIIb-dependent PGE2 production. *J Immunol*. 2009;182:554-562.

255. Debets JM, van de Winkel JG, Ceuppens JL, Dieteren IE, Buurman WA. Cross-linking of both Fc gamma RI and Fc gamma RII induces secretion of tumor necrosis factor by human monocytes, requiring high affinity Fc-Fc gamma R interactions. Functional activation of Fc gamma RII by treatment with proteases or neuraminidase. *J Immunol*. 1990;144:1304-1310.

256. Clavel C, Nogueira L, Laurent L, et al. Induction of macrophage secretion of tumor necrosis factor alpha through Fcgamma receptor IIa engagement by rheumatoid arthritis-specific autoantibodies to citrullinated proteins complexed with fibrinogen. *Arthritis Rheum*. 2008;58:678-688.

257. Mathsson L, Lampa J, Mullazehi M, Ronnelid J. Immune complexes from rheumatoid arthritis synovial fluid induce FcgammaRIIa dependent and rheumatoid factor correlated production of tumour necrosis factor-alpha by peripheral blood mononuclear cells. *Arthritis Res Ther*. 2006;8:R64.

258. Radstake TR, van Lent PL, Pesman GJ, et al. High production of proinflammatory and Th1 cytokines by dendritic cells from patients with rheumatoid arthritis, and down regulation upon FcgammaR triggering. *Ann Rheum Dis*. 2004;63:696-702.

259. Pricop L, Gokhale J, Redecha P, Ng SC, Salmon JE. Reactive oxygen intermediates enhance Fc gamma receptor signaling and amplify phagocytic capacity. *J Immunol*. 1999;162:7041-7048.

260. Stuart LM, Ezekowitz RA. Phagocytosis: elegant complexity. *Immunity*. 2005;22:539-550.

261. Swanson JA, Hoppe AD. The coordination of signaling during Fc receptor-mediated phagocytosis. *J Leukoc Biol*. 2004;76:1093-1103.

262. Huang Z, Hoffmann FW, Fay JD, et al. Stimulation of unprimed macrophages with immune complexes triggers a low output of nitric oxide by calcium-dependent neuronal nitric-oxide synthase. *J Biol Chem*. 2012;287:4492-4502.

263. Ambarus CA, Santegoets KC, van BL, et al. Soluble immune complexes shift the TLR-induced cytokine production of distinct polarized human macrophage subsets towards IL-10. *PLoS One*. 2012;7:e35994.

264. Boross P, Arandhara VL, Martin-Ramirez J, et al. The inhibiting Fc receptor for IgG, FcgammaRIIB, is a modifier of autoimmune susceptibility. *J Immunol*. 2011;187:1304-1313.

265. Clynes R, Dumitru C, Ravetch JV. Uncoupling of immune complex formation and kidney damage in autoimmune glomerulonephritis. *Science*. 1998;279:1052-1054.

266. Niederer HA, Clatworthy MR, Willcocks LC, Smith KGC. Fc gamma RIIB, Fc gamma RIIIB, and systemic lupus erythematosus. *Year in Immunology 2*. 2010;1183:69-88.

267. Joachim SC, Bruns K, Lackner KJ, Pfeiffer N, Grus FH. Analysis of IgG antibody patterns against retinal antigens and antibodies to alpha-crystallin, GFAP, and alpha-enolase in sera of patients with "wet" age-related macular degeneration. *Graefes Arch Clin Exp Ophthalmol*. 2007;245:619-626.

268. Vedeler CA, Fitzpatrick-Klove L. Receptors for immunoglobulin G demonstrated on human peripheral nerve fibres by electron microscopy. *Neurosci Lett*. 1990;115:167-170.

269. Cribbs DH, Berchtold NC, Perreau V, et al. Extensive innate immune gene activation accompanies brain aging, increasing vulnerability to cognitive decline and neurodegeneration: a microarray study. *J Neuroinflammation*. 2012;9:179.

270. Kaneko E, Niwa R. Optimizing Therapeutic Antibody Function Progress with Fc Domain Engineering. *Biodrugs*. 2011;25:1-11.

271. van Sorge NM, van der Pol WL, van de Winkel JG. FcgammaR polymorphisms: Implications for function, disease susceptibility and immunotherapy. *Tissue Antigens*. 2003;61:189-202.

272. Mellor JD, Brown MP, Irving HR, Zalcberg JR, Dobrovic A. A critical review of the role of Fc gamma receptor polymorphisms in the response to monoclonal antibodies in cancer. *J Hematol Oncol*. 2013;6:1.

273. Pander J, Gelderblom H, Antonini NF, et al. Correlation of FCGR3A and EGFR germline polymorphisms with the efficacy of cetuximab in KRAS wild-type metastatic colorectal cancer. *Eur J Cancer*. 2010;46:1829-1834.

274. Rodrigues EB, Farah ME, Maia M, et al. Therapeutic monoclonal antibodies in ophthalmology. *Progress in Retinal and Eye Research*. 2009;28:117-144.

275. Johnson D, Sharma S. Ocular and systemic safety of bevacizumab and ranibizumab in patients with neovascular age-related macular degeneration. *Curr Opin Ophthalmol*. 2013;24:205-212.

276. Sharma S, Johnson D, Abouammoh M, Hollands S, Brissette A. Rate of serious adverse effects in a series of bevacizumab and ranibizumab injections. *Can J Ophthalmol*. 2012;47:275-279.

277. Nuzzi R, Tridico F. Local and Systemic Complications after Intravitreal Administration of Anti-Vascular Endothelial Growth Factor Agents in the Treatment of Different Ocular Diseases: A Five-Year Retrospective Study. *Semin Ophthalmol*. 2013.

278. Chakravarthy U, Harding SP, Rogers CA, et al. Alternative treatments to inhibit VEGF in age-related choroidal neovascularisation: 2-year findings of the IVAN randomised controlled trial. *Lancet*. 2013;382:1258-1267.

279. Carter PM. Immune complex disease. *Ann Rheum Dis*. 1973;32:265-271.

280. Edwards AO, Ritter R, III, Abel KJ, Manning A, Panhuysen C, Farrer LA. Complement factor H polymorphism and age-related macular degeneration. *Science*. 2005;308:421-424.

281. Ennis S, Jomary C, Mullins R, et al. Association between the SERPING1 gene and age-related macular degeneration: a two-stage case-control study. *Lancet*. 2008;372:1828-1834.

282. Teeling JL, Carare RO, Glennie MJ, Perry VH. Intracerebral immune complex formation induces inflammation in the brain that depends on Fc receptor interaction. *Acta Neuropathol*. 2012;124:479-490.

283. Lunnon K, Teeling JL, Tutt AL, Cragg MS, Glennie MJ, Perry VH. Systemic inflammation modulates Fc receptor expression on microglia during chronic neurodegeneration. *J Immunol*. 2011;186:7215-7224.

284. De Haas AH, Boddeke HW, Biber K. Region-specific expression of immunoregulatory proteins on microglia in the healthy CNS. *Glia*. 2008;56:888-894.

285. Ramos BF, Zhang Y, Jakschik BA. Neutrophil elicitation in the reverse passive Arthus reaction. Complement-dependent and -independent mast cell involvement. *J Immunol*. 1994;152:1380-1384.

286. Szalai AJ, Digerness SB, Agrawal A, et al. The Arthus reaction in rodents: species-specific requirement of complement. *J Immunol*. 2000;164:463-468.

287. van Dinther-Janssen AC, van Maarsseveen AC, de GJ, Scheper RJ. Comparative migration of T- and B-lymphocyte subpopulations into skin inflammatory sites. *Immunology*. 1983;48:519-527.

288. Anders HJ, Vielhauer V, Kretzler M, et al. Chemokine and chemokine receptor expression during initiation and resolution of immune complex glomerulonephritis. *J Am Soc Nephrol*. 2001;12:919-931.

289. Banks WA, Terrell B, Farr SA, Robinson SM, Nonaka N, Morley JE. Passage of amyloid beta protein antibody across the blood-brain barrier in a mouse model of Alzheimer's disease. *Peptides*. 2002;23:2223-2226.

290. Crawford JP, Movat HZ, Minta JO, Opas M. Acute inflammation induced by immune complexes in the microcirculation. *Exp Mol Pathol*. 1985;42:175-193.

291. Okada M, Shimada K. Effects of various pharmacologic agents on allergic inflammation of the eye. The roles of chemical mediators in ocular inflammation. *Invest Ophthalmol Vis Sci*. 1980;19:176-181.

292. Okada M, Shimada K. The continuous and quantitative observation of permeability changes of the blood-aqueous barrier in allergic inflammation of the eye. *Invest Ophthalmol Vis Sci*. 1980;19:169-175.

293. Hopken UE, Lu B, Gerard NP, Gerard C. Impaired inflammatory responses in the reverse arthus reaction through genetic deletion of the C5a receptor. *J Exp Med*. 1997;186:749-756.

294. Strachan AJ, Woodruff TM, Haaima G, Fairlie DP, Taylor SM. A new small molecule C5a receptor antagonist inhibits the reverse-passive Arthus reaction and endotoxic shock in rats. *J Immunol*. 2000;164:6560-6565.

295. Alonso A, Bayon Y, Renedo M, Crespo MS. Stimulation of Fc gamma R receptors induces monocyte chemoattractant protein-1 in the human monocytic cell line THP-1 by a mechanism involving I kappa B-alpha degradation and formation of p50/p65 NF-kappa B/Rel complexes. *Int Immunol*. 2000;12:547-554.

296. Perego C, Fumagalli S, De Simoni MG. Temporal pattern of expression and colocalization of microglia/macrophage phenotype markers following brain ischemic injury in mice. *J Neuroinflammation*. 2011;8:174.

297. Faber C, Singh A, Kruger FM, Juel HB, Sorensen TL, Nissen MH. Age-related Macular Degeneration Is Associated with Increased Proportion of CD56(+) T Cells in Peripheral Blood. *Ophthalmology*. 2013;120:2310-2316.

298. Ezzat MK, Hann CR, Vuk-Pavlovic S, Pulido JS. Immune cells in the human choroid. *Br J Ophthalmol*. 2008;92:976-980.

299. Appay V, van Lier RA, Sallusto F, Roederer M. Phenotype and function of human T lymphocyte subsets: consensus and issues. *Cytometry A*. 2008;73:975-983.

300. Sylvestre D, Clynes R, Ma M, Warren H, Carroll MC, Ravetch JV. Immunoglobulin G-mediated inflammatory responses develop normally in complement-deficient mice. *J Exp Med*. 1996;184:2385-2392.

301. Sylvestre DL, Ravetch JV. Fc receptors initiate the Arthus reaction: redefining the inflammatory cascade. *Science*. 1994;265:1095-1098.

302. Shushakova N, Skokowa J, Schulman J, et al. C5a anaphylatoxin is a major regulator of activating versus inhibitory FcgammaRs in immune complex-induced lung disease. *J Clin Invest*. 2002;110:1823-1830.

303. Skokowa J, Ali SR, Felda O, et al. Macrophages induce the inflammatory response in the pulmonary Arthus reaction through G alpha i2 activation that controls C5aR and Fc receptor cooperation. *J Immunol*. 2005;174:3041-3050.

304. Baumann U, Kohl J, Tschernig T, et al. A codominant role of Fc gamma RI/III and C5aR in the reverse Arthus reaction. *J Immunol*. 2000;164:1065-1070.

305. Mihai S, Nimmerjahn F. The role of Fc receptors and complement in autoimmunity. *Autoimmun Rev*. 2013;12:657-660.

306. Kasperkiewicz M, Nimmerjahn F, Wende S, et al. Genetic identification and functional validation of FcgammaRIV as key molecule in autoantibody-induced tissue injury. *J Pathol*. 2012;228:8-19.

307. Syed SN, Konrad S, Wiege K, et al. Both FcgammaRIV and FcgammaRIII are essential receptors mediating type II and type III autoimmune responses via FcRgamma-LAT-dependent generation of C5a. *Eur J Immunol*. 2009;39:3343-3356.

308. Bevaart L, Jansen MJ, van Vugt MJ, Verbeek JS, van de Winkel JG, Leusen JH. The high-affinity IgG receptor, FcgammaRI, plays a central role in antibody therapy of experimental melanoma. *Cancer Res*. 2006;66:1261-1264.

309. Otten MA, van der Bij GJ, Verbeek SJ, et al. Experimental antibody therapy of liver metastases reveals functional redundancy between Fc gammaRI and Fc gammaRIV. *J Immunol*. 2008;181:6829-6836.

310. Hazenbos WL, Gessner JE, Hofhuis FM, et al. Impaired IgG-dependent anaphylaxis and Arthus reaction in Fc gamma RIII (CD16) deficient mice. *Immunity*. 1996;5:181-188.

311. Mancardi DA, Jonsson F, Iannascoli B, et al. Cutting Edge: The murine high-affinity IgG receptor FcgammaRIV is sufficient for autoantibody-induced arthritis. *J Immunol*. 2011;186:1899-1903.

312. Baumann U, Chouchakova N, Gewecke B, et al. Distinct tissue site-specific requirements of mast cells and complement components C3/C5a receptor in IgG immune complex-induced injury of skin and lung. *J Immunol*. 2001;167:1022-1027.

313. Fossati-Jimack L, Ioan-Facsinay A, Reininger L, et al. Markedly different pathogenicity of four immunoglobulin G isotype-switch variants of an antierythrocyte autoantibody is based on their capacity to interact in vivo with the low-affinity Fcgamma receptor III. *J Exp Med*. 2000;191:1293-1302.

314. Park SY, Ueda S, Ohno H, et al. Resistance of Fc receptor- deficient mice to fatal glomerulonephritis. *J Clin Invest*. 1998;102:1229-1238.

315. Huugen D, van EA, Xiao H, et al. Inhibition of complement factor C5 protects against anti-myeloperoxidase antibody-mediated glomerulonephritis in mice. *Kidney Int*. 2007;71:646-654.

316. Kumar V, Ali SR, Konrad S, et al. Cell-derived anaphylatoxins as key mediators of antibody-dependent type II autoimmunity in mice. *J Clin Invest*. 2006;116:512-520.

317. Barnes N, Gavin AL, Tan PS, Mottram P, Koentgen F, Hogarth PM. FcgammaRI-deficient mice show multiple alterations to inflammatory and immune responses. *Immunity*. 2002;16:379-389.

318. Giorgini A, Brown HJ, Lock HR, et al. Fc gamma RIII and Fc gamma RIV are indispensable for acute glomerular inflammation induced by switch variant monoclonal antibodies. *J Immunol*. 2008;181:8745-8752.

319. Chouchakova N, Skokowa J, Baumann U, et al. Fc gamma RIII-mediated production of TNF-alpha induces immune complex alveolitis independently of CXC chemokine generation. *J Immunol*. 2001;166:5193-5200.

320. Meyer D, Schiller C, Westermann J, et al. FcgammaRIII (CD16)-deficient mice show IgG isotype-dependent protection to experimental autoimmune hemolytic anemia. *Blood*. 1998;92:3997-4002.

321. Jakus Z, Nemeth T, Verbeek JS, Mocsai A. Critical but overlapping role of FcgammaRIII and FcgammaRIV in activation of murine neutrophils by immobilized immune complexes. *J Immunol*. 2008;180:618-629.

322. Shankar A, Mitchell P, Rochtchina E, Tan J, Wang JJ. Association between circulating white blood cell count and long-term incidence of age-related macular degeneration: the Blue Mountains Eye Study. *Am J Epidemiol*. 2007;165:375-382.

323. Margolis R, Spaide RF. A pilot study of enhanced depth imaging optical coherence tomography of the choroid in normal eyes. *Am J Ophthalmol*. 2009;147:811-815.

324. D'souza Y, Short CD, McLeod D, Bonshek RE. Long-term follow-up of drusen-like lesions in patients with type II mesangiocapillary glomerulonephritis. *Br J Ophthalmol*. 2008;92:950-953.

325. Sofat R, Casas JP, Webster AR, et al. Complement factor H genetic variant and age-related macular degeneration: effect size, modifiers and relationship to disease subtype. *Int J Epidemiol*. 2012;41:250-262.

326. Mullins RF, Dewald AD, Streb LM, Wang K, Kuehn MH, Stone EM. Elevated membrane attack complex in human choroid with high risk complement factor H genotypes. *Exp Eye Res*. 2011;93:565-567.

327. Takeda A, Baffi JZ, Kleinman ME, et al. CCR3 is a target for age-related macular degeneration diagnosis and therapy. *Nature*. 2009;460:225-230.

328. Berger JF, Fine SL, Maguire MG. Histopathological features. In: *Age-Related Macular Degeneration*. 1st ed. Philadelphia: Mosby; 1999:1-16.

329. Heier JS, Antoszyk AN, Pavan PR, et al. Ranibizumab for treatment of neovascular age-related macular degeneration: a phase I/II multicenter, controlled, multidose study. *Ophthalmology*. 2006;113:633-634.

330. Spaide RF, Laud K, Fine HF, et al. Intravitreal bevacizumab treatment of choroidal neovascularization secondary to age-related macular degeneration. *Retina*. 2006;26:383-390.

331. Chakravarthy U, Harding SP, Rogers CA, et al. Ranibizumab versus bevacizumab to treat neovascular age-related macular degeneration: one-year findings from the IVAN randomized trial. *Ophthalmology*. 2012;119:1399-1411.

332. Martin DF, Maguire MG, Fine SL, et al. Ranibizumab and bevacizumab for treatment of neovascular age-related macular degeneration: two-year results. *Ophthalmology*. 2012;119:1388-1398.

333. Heier JS, Brown DM, Chong V, et al. Intravitreal aflibercept (VEGF trap-eye) in wet age-related macular degeneration. *Ophthalmology*. 2012;119:2537-2548.

334. Liu J, Copland DA, Horie S, et al. Myeloid cells expressing VEGF and arginase-1 following uptake of damaged retinal pigment epithelium suggests potential mechanism that drives the onset of choroidal angiogenesis in mice. *PLoS One*. 2013;8:e72935.

335. Luo C, Zhao J, Madden A, Chen M, Xu H. Complement expression in retinal pigment epithelial cells is modulated by activated macrophages. *Exp Eye Res*. 2013;112:93-101.

336. Bhutto IA, Baba T, Merges C, Juriasinghani V, McLeod DS, Lutty GA. C-reactive protein and complement factor H in aged human eyes and eyes with age-related macular degeneration. *Br J Ophthalmol*. 2011;95:1323-1330.

337. Leung KW, Barnstable CJ, Tombran-Tink J. Bacterial endotoxin activates retinal pigment epithelial cells and induces their degeneration through IL-6 and IL-8 autocrine signaling. *Mol Immunol*. 2009;46:1374-1386.

338. Dunn KC, Aotaki-Keen AE, Putkey FR, Hjelmeland LM. ARPE-19, a human retinal pigment epithelial cell line with differentiated properties. *Exp Eye Res*. 1996;62:155-169.

339. Kendig DM, Tarloff JB. Inactivation of lactate dehydrogenase by several chemicals: implications for in vitro toxicology studies. *Toxicol In Vitro*. 2007;21:125-132.

340. Merin S, Blair NP, Tso MO. Vitreous fluorophotometry in patients with senile macular degeneration. *Invest Ophthalmol Vis Sci*. 1987;28:756-759.

341. Whitcup SM, Sodhi A, Atkinson JP, et al. The role of the immune response in age-related macular degeneration. *Int J Inflam*. 2013;2013:348092.

342. Hornof M, Toropainen E, Urtti A. Cell culture models of the ocular barriers. *Eur J Pharm Biopharm*. 2005;60:207-225.

343. Chen Y, Kijlstra A, Chen Y, Yang P. IL-17A stimulates the production of inflammatory mediators via Erk1/2, p38 MAPK, PI3K/Akt, and NF-kappaB pathways in ARPE-19 cells. *Mol Vis*. 2011;17:3072-3077.

344. Ablonczy Z, Dahrouj M, Tang PH, et al. Human retinal pigment epithelium cells as functional models for the RPE in vivo. *Invest Ophthalmol Vis Sci*. 2011;52:8614-8620.

345. Wang Y, Bian ZM, Yu WZ, Yan Z, Chen WC, Li XX. Induction of interleukin-8 gene expression and protein secretion by C-reactive protein in ARPE-19 cells. *Exp Eye Res*. 2010;91:135-142.

346. Schraermeyer U, Julien S. Formation of immune complexes and thrombotic microangiopathy after intravitreal injection of bevacizumab in the primate eye. *Graefes Arch Clin Exp Ophthalmol*. 2012;250:1303-1313.

347. Ahdieh M, Vandenbos T, Youakim A. Lung epithelial barrier function and wound healing are decreased by IL-4 and IL-13 and enhanced by IFN-gamma. *Am J Physiol Cell Physiol*. 2001;281:C2029-C2038.

348. Raleigh DR, Boe DM, Yu D, et al. Occludin S408 phosphorylation regulates tight junction protein interactions and barrier function. *J Cell Biol*. 2011;193:565-582.

349. Rincon-Choles H, Vasylyeva TL, Pergola PE, et al. ZO-1 expression and phosphorylation in diabetic nephropathy. *Diabetes*. 2006;55:894-900.

350. Stevenson BR, Anderson JM, Braun ID, Mooseker MS. Phosphorylation of the tight-junction protein ZO-1 in two strains of Madin-Darby canine kidney cells which differ in transepithelial resistance. *Biochem J*. 1989;263:597-599.

351. Suzuki T, Elias BC, Seth A, et al. PKC eta regulates occludin phosphorylation and epithelial tight junction integrity. *Proc Natl Acad Sci U S A*. 2009;106:61-66.

352. Rao R. Occludin phosphorylation in regulation of epithelial tight junctions. *Ann N Y Acad Sci*. 2009;1165:62-68.

353. Kotowicz K, Callard RE, Klein NJ, Jacobs MG. Interleukin-4 increases the permeability of human endothelial cells in culture. *Clin Exp Allergy*. 2004;34:445-449.

354. Jonas JB, Tao Y, Neumaier M, Findeisen P. Cytokine concentration in aqueous humour of eyes with exudative age-related macular degeneration. *Acta Ophthalmol*. 2012;90:e381-e388.

355. Miao H, Tao Y, Li XX. Inflammatory cytokines in aqueous humor of patients with choroidal neovascularization. *Mol Vis*. 2012;18:574-580.

356. Dantzer R, O'Connor JC, Freund GG, Johnson RW, Kelley KW. From inflammation to sickness and depression: when the immune system subjugates the brain. *Nat Rev Neurosci*. 2008;9:46-56.

357. Hayashi A, Nakae K, Naka H, Ohji M, Tano Y. Cytokine effects on phagocytosis of rod outer segments by retinal pigment epithelial cells of normal and dystrophic rats. *Curr Eye Res*. 1996;15:487-499.

358. Hull J, Ackerman H, Isles K, et al. Unusual haplotypic structure of IL8, a susceptibility locus for a common respiratory virus. *Am J Hum Genet*. 2001;69:413-419.

359. Goverdhan SV, Ennis S, Hannan SR, et al. Interleukin-8 promoter polymorphism -251A/T is a risk factor for age-related macular degeneration. *Br J Ophthalmol*. 2008;92:537-540.

360. Liu X, Ye L, Christianson GJ, Yang JQ, Roopenian DC, Zhu X. NF-kappaB signaling regulates functional expression of the MHC class I-related neonatal Fc receptor for IgG via intronic binding sequences. *J Immunol*. 2007;179:2999-3011.

361. Albanesi M, Mancardi DA, Macdonald LE, et al. Cutting edge: FcgammaRIII (CD16) and FcgammaRI (CD64) are responsible for anti-glycoprotein 75 monoclonal antibody TA99 therapy for experimental metastatic B16 melanoma. *J Immunol*. 2012;189:5513-5517.

362. Hulse RE, Swenson WG, Kunkler PE, White DM, Kraig RP. Monomeric IgG is neuroprotective via enhancing microglial recycling endocytosis and TNF-alpha. *J Neurosci*. 2008;28:12199-12211.

363. Lux A, Nimmerjahn F. Of mice and men: the need for humanized mouse models to study human IgG activity in vivo. *J Clin Immunol*. 2013;33 Suppl 1:S4-S8.

364. Mestas J, Hughes CC. Of mice and not men: differences between mouse and human immunology. *J Immunol*. 2004;172:2731-2738.

365. Alexander JJ, Hack BK, Jacob A, et al. Abnormal immune complex processing and spontaneous glomerulonephritis in complement factor H-deficient mice with human complement receptor 1 on erythrocytes. *J Immunol*. 2010;185:3759-3767.

366. Tsuboi N, Asano K, Lauterbach M, Mayadas TN. Human neutrophil Fcgamma receptors initiate and play specialized nonredundant roles in antibody-mediated inflammatory diseases. *Immunity*. 2008;28:833-846.

367. Jonsson F, Mancardi DA, Zhao W, et al. Human FcgammaRIIA induces anaphylactic and allergic reactions. *Blood*. 2012;119:2533-2544.

368. Tsuboi N, Ernandez T, Li X, et al. Regulation of human neutrophil Fcgamma receptor IIa by C5a receptor promotes inflammatory arthritis in mice. *Arthritis Rheum*. 2011;63:467-478.

369. McMenamin PG, Polla E. Mast cells are present in the choroid of the normal eye in most vertebrate classes. *Vet Ophthalmol*. 2013;16 Suppl 1:73-78.

370. Zhao W, Kepley CL, Morel PA, Okumoto LM, Fukuoka Y, Schwartz LB. Fc gamma RIIa, not Fc gamma RIIb, is constitutively and functionally expressed on skin-derived human mast cells. *J Immunol*. 2006;177:694-701.

371. McKenzie SE, Taylor SM, Malladi P, et al. The role of the human Fc receptor Fc gamma RIIA in the immune clearance of platelets: a transgenic mouse model. *J Immunol*. 1999;162:4311-4318.

372. Seddon JM, George S, Rosner B, Rifai N. Progression of age-related macular degeneration: prospective assessment of C-reactive protein, interleukin 6, and other cardiovascular biomarkers. *Arch Ophthalmol*. 2005;123:774-782.

373. Whitmore SS, Braun TA, Skeie JM, et al. Altered gene expression in dry age-related macular degeneration suggests early loss of choroidal endothelial cells. *Mol Vis*. 2013;19:2274-2297.

374. Tsutsumi-Miyahara C, Sonoda KH, Egashira K, et al. The relative contributions of each subset of ocular infiltrated cells in experimental choroidal neovascularisation. *Br J Ophthalmol*. 2004;88:1217-1222.

375. Moorthy S, Cheung N, Klein R, Shahar E, Wong TY. Are lung disease and function related to age-related macular degeneration? *Am J Ophthalmol*. 2011;151:375-379.

376. Ristau T, Ersoy L, Lechanteur YT, et al. Allergy is a protective factor against age-related macular degeneration. *Invest Ophthalmol Vis Sci*. 2013.

377. Sheu SJ, Ger LP, Kuo NW, Liu NC, Wu TT, Lin MC. Association of IL-4 gene polymorphism and age-related macular degeneration in Taiwanese adults. *Taiwan Journal of Ophthalmology*. 2012;2:51-55.

378. Dimov VV, Casale TB. Immunomodulators for asthma. *Allergy Asthma Immunol Res*. 2010;2:228-234.

379. Meyer T, Robles-Carrillo L, Robson T, et al. Bevacizumab immune complexes activate platelets and induce thrombosis in FCGR2A transgenic mice. *J Thromb Haemost*. 2009;7:171-181.

380. Zhao B, Zhang C, Forsten-Williams K, Zhang J, Fannon M. Endothelial cell capture of heparin-binding growth factors under flow. *PLoS Comput Biol*. 2010;6:e1000971.

381. Mancardi DA, Albanesi M, Jonsson F, et al. The high-affinity human IgG receptor FcgammaRI (CD64) promotes IgG-mediated inflammation, anaphylaxis, and antitumor immunotherapy. *Blood*. 2013;121:1563-1573.

382. Thompson S, Mullins RF, Philp AR, Stone EM, Mrosovsky N. Divergent phenotypes of vision and accessory visual function in mice with visual cycle dysfunction (Rpe65 rd12) or retinal degeneration (rd/rd). *Invest Ophthalmol Vis Sci*. 2008;49:2737-2742.

383. Puk O, Dalke C, Hrabe de AM, Graw J. Variation of the response to the optokinetic drum among various strains of mice. *Front Biosci*. 2008;13:6269-6275.

384. Cherepanoff S, Mitchell P, Wang JJ, Gillies MC. Retinal autoantibody profile in early age-related macular degeneration: preliminary findings from the Blue Mountains Eye Study. *Clin Experiment Ophthalmol*. 2006;34:590-595.

385. Heinzel FP, Sadick MD, Holaday BJ, Coffman RL, Locksley RM. Reciprocal expression of interferon gamma or interleukin 4 during the resolution or progression of murine leishmaniasis. Evidence for expansion of distinct helper T cell subsets. *J Exp Med*. 1989;169:59-72.